OPERATION KOMOREBI

REALIZATION CALCULUS



RESEARCH LIBRARY

# Stratified Universality for Resolved Representations

Profiled lane transport, semantic quotients, carrier change, and certified descent

Traditional paper

**Komorebi P.**

Standardized publication edition / 8 October 2026

REALIZATION CALCULUS

## Reading scope

**Mathematical base: version 2.0.0 (23 September 2026).** This edition retains the finite atlas and finite profiled and holonomy-twisted lane theorems, with the local corrections recorded in the publication note. The mathematical base adds a formal calculus of task-relative semantic quotients, exact bridge loss, carrier factorization, observer base change, admissibility-relative obstruction, and enrichment lifting. Inherited claims retain their original proof boundaries. New claims are separated in Part IV and in the expanded theorem concordance.

Universality is asserted only relative to declared grammars, strata, bridges, preservation profiles, normalization targets, and descent doctrines.


**Abstract**

Komorebi Math is formulated as a relative classifying and transport theory of resolved representations. A resolved theory records typed operations, packet decompositions, refinement laws, residuals, certificates, and only those analytic, tensor, metric, or arithmetic structures included in a declared preservation profile. Its realizations are organized into normalized strata. Reversible changes of presentation form representation groupoids, while quotients, completions, reductions, and other information-losing constructions remain in a directed category with explicit loss passports.

The first theorem layer establishes the additive–Karoubi resolved envelope, finite profiled atlas assembly, and componentwise invariant descent. The finite profiled Universal Lane Transport Theorem identifies every morphism between complete finite split packet systems with its full lane matrix. Composition becomes block contraction, refinement is functorial, and selectors split retained transport from a named residual. Under finite address holonomy, the same calculus descends as sections of a matrix local system. Monodromy orbits give the finest ordinary global lane coarsening, and pair orbits carry the compatible selector algebra.

The second theorem layer formalizes task-relative semantics. For a declared continuation grammar and observation family, the behavioral quotient is the coarsest exact representation preserving every future observation. In module-valued slices, task combination, common coarsening, relative residuals, bridge loss, essential-image failure, and task weakening fit into canonical exact sequences. Carrier replacement is possible exactly on a kernel-factorization locus. Set-valued residual equality and linear residual span are separated by an explicit relation module. Convex value packets, provenance states, additive route packets, and weighted-linear states therefore remain distinct unless certified comparison maps are supplied.

Finally, obstruction is indexed by the admissible realization class. Enlarging that class can reduce an optimized defect, while zero infimum may still fail to be attained. Rich structure descends under forgetting, but reconstructing it from a bare bridge is a typed lifting problem. The resulting theory is finite, profiled, task-relative, and auditable. It does not assert one global coordinate system, one observer-independent minimum, equivalence of all carriers, or effectivity of an unrestricted heterogeneous stack.



**Keywords:** resolved representation, stratified universality, lane transport, semantic quotient, behavioral core, carrier change, observer base change, exact loss, address holonomy, admissibility-relative obstruction, certified descent.


**Central claim.** Komorebi Math is a stratified classifying and transport theory of resolved representations. Within a declared profile, it separates exact representation change from directional information loss. Within a declared semantic slice, it constructs the coarsest representation preserving all future

task observations. Changes of carrier, observer, geometry, completion, or enrichment are legal only through certified comparison or lifting data.

**Claim boundary.** The paper does not assert that every mathematical object has a finite Komorebi presentation, that all strata or carriers are equivalent, that every bridge is reversible, that arbitrary presentations admit one observer-independent minimum, or that the unrestricted heterogeneous atlas is an effective stack. Internal proof status, exact computation, classical import, historical novelty, and independent peer validation remain distinct classifications.

**Publication edition and source availability.** This publication edition preserves the theorem labels, concordance component identities, and claim boundaries of the 23 September 2026 version 2.0.0, with five local amendments recorded explicitly: orbit supports are distinguished from nonzero selector action; observer updates have finite branching, finite raw-history aggregation, and declared empty-fiber conventions; the compactness proof of escape uses an attained positive minimum; the coinduction and finite-certification proofs make their fixed-point implications explicit; and metric statements declare positive dimension, determinant normalization, and inverse edge traversal. The original sources and inherited records remain included unchanged. Its companion visual guide and Lean guide are reading and evidence guides to that mathematical base.

The complete release includes the Markdown (`.md`) files, LaTeX sources, figure generators, data, exact validators, and inherited validation reports. Inherited reports retain their original dates and scope. Written formal mathematics, exact finite computation, publication checks, and Lean certification are separate forms of evidence. No Lean source files or Lean build project are present in the supplied version 2.0.0 source tree. Separate related Lean developments, where identified, require their own source and theorem correspondence. This publication edition does not claim a fresh Lean build or a new independent proof audit of the complete manuscript.

# Contents

**1 Introduction** **1**
1.1 The assembly problem . . . 1
1.2 Main theorem and classification domain . . . 1
1.3 Contributions . . . 1
1.4 Proof status and organization . . . 2

**2 Main theorem suite and proof architecture** **2**

**I Common foundations and finite assembly** **4**

**3 Resolved theories, packet coordinates, and preservation profiles** **4**
3.1 Typed resolved signatures . . . 4
3.2 Packet objects, analysis, and exact transfer coordinates . . . 8
3.3 Refinement, selected support, and named residuals . . . 10
3.4 Preservation profiles and proof-support certificates . . . 11
3.5 The finite additive-Karoubi resolved envelope . . . 13
3.6 Profile-indexed extensions and the exact boundary of Foundation layer . . . 15

**4 Strata, normalized charts, typed bridges, and obstruction objects** **17**
4.1 Stratum passports and normalized model categories . . . 17
4.2 Representation groupoids, gauge levels, and the directed transformation category . . . 20
4.3 Bridge passports, bridge classes, and information-loss profiles . . . 21
4.4 Overlap categories and bridge-law certificates . . . 23
4.5 Reversible cores inside directional bridges . . . 25
4.6 Finite holonomy and the maximal path-flat core . . . 26
4.7 Relative cokernel obstructions and loss under coarsening . . . 26
4.8 Semilinear effectivity, projective descent, and the Brauer class . . . 29
4.9 Higher coherence defects and typed obstruction comparison . . . 30

**5 The theorem concordance and edition control** **33**
5.1 Audit result . . . 33
5.2 Material supersession decisions . . . 33
5.3 Existing bridges and exact invariant slices . . . 34

**6 Finite profiled resolved atlas assembly** **34**

6.1 Finite atlases and descent data . . . 36
6.2 The assembly theorem . . . 36

**II Certified native strata 37**

**7 Verified finite Mahler atlas models 38**
7.1 Affine-Mahler chart groupoid . . . 38
7.2 Integral split packet descent . . . 38

**8 The normalized C-finite three-chart atlas 39**
8.1 Persistent C-finite semantics . . . 39
8.2 The recurrence chart . . . 39
8.3 The rational OGF chart . . . 39
8.4 The minimal state chart . . . 40
8.5 Effective descent across the three charts . . . 40
8.6 Descent of the minimality and torsion-Fourier invariants . . . 42
8.7 Exact examples . . . 42

**9 A first heterogeneous effective-descent atlas 42**
9.1 The restricted semantic doctrine . . . 43
9.2 Four normalized charts . . . 44
9.3 Explicit bridge passports . . . 47
9.4 Triple-overlap and quadruple coherence . . . 50
9.5 Effective descent for objects and morphisms . . . 52
9.6 A compatible complete invariant family . . . 53
9.7 Exact examples and a normalization boundary . . . 53
9.8 Exact finite verification . . . 55

**10 Rational-mask digital descent beyond pure periodicity 55**
10.1 Frobenius-radical characterization . . . 56
10.2 The rational-collapse obstruction . . . 57
10.3 Denominator stabilization and the canonical Cartier module . . . 59
10.4 The exact reachable compiler core . . . 60
10.5 Three normalized charts . . . 61
10.6 Coherence and effective descent . . . 63
10.7 Compatible invariants and collapse stratification . . . 64
10.8 Exact examples and strict boundaries . . . 64

10.9 Exact finite verification . . . . . 67

**11 Fixed-radix regular normalization and the automatic finite-orbit boundary 67**

11.1 Section operators and the canonical kernel module . . . . . 68
11.2 Word-Hankel rank and minimal digit-linear dimension . . . . . 70
11.3 Strict shortlex normalization . . . . . 71
11.4 The automatic finite-orbit subatlas . . . . . 73
11.5 Exact regular examples beyond automaticity . . . . . 74
11.6 Exact finite verification . . . . . 75

**12 Integral saturation, Smith–Fitting defects, and prime-power effectivity 77**

12.1 The raw section lattice and its canonical saturation . . . . . 78
12.2 The exact reduction sequence . . . . . 80
12.3 Digit equivariance and the prime-power tower . . . . . 81
12.4 p-adic completion and the disappearance of finite ghosts . . . . . 83
12.5 Orbit closure and three levels of effectivity . . . . . 84
12.6 All-moduli completion and the integral effectivity obstruction . . . . . 86
12.7 Canonical integral record and directional reduction atlas . . . . . 87

**13 Filtered Euler products, prime-power seeds, and the divisor–ghost bridge 88**

13.1 Filtered products and coefficient stabilization . . . . . 88
13.2 Canonical Euler coordinates . . . . . 89
13.3 Ghost coordinates and logarithmic-derivative recurrence . . . . . 90
13.4 Multiplicative arithmetic functions as prime-power descent . . . . . 92
13.5 Prime-Euler and local ghost coordinates . . . . . 93
13.6 The divisor–ghost cross-stratum bridge . . . . . 96
13.7 A restricted product–multiplicative atlas . . . . . 97
13.8 Why the bridge is restricted . . . . . 98
13.9 Exact finite verification . . . . . 99

**14 Local Newton–Mahler coordinates, affine polyphase descent, and precision ladders 100**

14.1 Two Mahler languages and the declared local doctrine . . . . . 100
14.2 Complete clopen packets and effective local descent . . . . . 101
14.3 The affine Mahler kernel and mixed-radix coherence . . . . . 103
14.4 Finite-degree bridge ladder and collective recovery . . . . . 104
14.5 Valuation ledgers and Frobenius sparsity . . . . . 107
14.6 Carmichael–Mahler state constructors and precision amplification . . . . . 107

14.7 The exact boundary with functional-Mahler masks . . . 109
14.8 Exact examples and finite verification . . . 110

**15 Holonomic Ore charts, multisection modules, and a Fuchsian packet theorem 111**
15.1 Ore annihilators and normalized holonomic charts . . . 112
15.2 The exact coefficient bridge . . . 113
15.3 The ordinary-point holonomic atlas . . . 114
15.4 General arithmetic multisection . . . 115
15.5 Operator singularities and local exponent packets . . . 117
15.6 An exact binomial–Fuchsian packet family . . . 118
15.7 Orbit aliasing and address cancellation . . . 120
15.8 Local exponent and monodromy packet . . . 121
15.9 Marked normalized packet atlas . . . 122
15.10 Examples and exact verification . . . 124

**16 Selected algebraic branches, packet Weil restriction, and collision invariants 125**
16.1 Minimal polynomials and finite branch selectors . . . 126
16.2 The normalized selected-branch atlas . . . 127
16.3 The exact residue-packet polynomial compiler . . . 127
16.4 Weil-restricted packet degree . . . 129
16.5 Tuple collision and selected-orbit loss . . . 130
16.6 A sharp Catalan parity theorem . . . 131
16.7 A quadratic-radical collision phase diagram . . . 132
16.8 The directional algebraic-to-holonomic bridge . . . 134
16.9 Exact examples and finite verification . . . 135

**17 Nonlinear polynomial fixed points, compressed packet composition, and finite tree signatures 136**
17.1 Marked polynomial fixed-point systems . . . 136
17.2 Packet jets, hypergraphs, and the marked nonlinear atlas . . . 138
17.3 Exact diagonal packet Faà di Bruno compression . . . 139
17.4 The cyclic nonlinear core of a packet system . . . 140
17.5 A finite residue signature for simply generated trees . . . 142
17.6 Dominant singularity orbits . . . 144
17.7 The sharp full $q$-ary family . . . 145
17.8 Verification, status, and exact boundary . . . 147

**18 Finite Galois, profinite, and Tannakian resolved symmetry 148**

18.1 Finite subgroup, fixed-field, and Reynolds-projector charts . . . 148
18.2 Compatibility, normality, and conjugate atlases . . . 149
18.3 Double cosets as exact transition packets . . . 151
18.4 Ramification as a nested resolution . . . 153
18.5 Profinite completion and finite quotient effectivity . . . 154
18.6 Semilinear vector descent and Hilbert 90 . . . 155
18.7 Projective descent and the Brauer obstruction . . . 156
18.8 Finite étale and neutral Tannakian symmetry . . . 157
18.9 The assembled finite Galois resolved atlas . . . 158
18.10 Exact finite verification . . . 160

**III Certified global synthesis and scope 160**

**19 Global invariant descent on the certified finite atlas 161**
19.1 The authoritative bridge matrix . . . 161
19.2 Certified connected components . . . 163
19.3 Normalizer-induced higher coherence . . . 165
19.4 Invariant descent theorem . . . 165
19.5 Digital–regular–linear–functional-Mahler component . . . 167
19.6 Continuous Newton–Mahler component . . . 168
19.7 A genuine nonlinear–algebraic–holonomic overlap . . . 169
19.8 Euler–multiplicative component . . . 171
19.9 Finite Galois component . . . 172
19.10 The global tagged invariant . . . 172
19.11 Directional satellites and exact loss records . . . 173
19.12 Exact finite verification . . . 174

**20 Universal lane transport at finite profile 176**
20.1 Finite profiled lane systems . . . 176
20.2 The universal finite transport theorem . . . 177
20.3 Certified change of resolution and exact loss sequences . . . 180
20.4 The matrix category carried by a lane system . . . 181
20.5 Multilinear and specified-polynomial transport . . . 182
20.6 Factorial lanes and residue packets . . . 183
20.7 Typed native specializations . . . 184
20.8 Descent of lane systems through a finite atlas . . . 188

20.9 Sharp boundaries and a finite counterexample . . . 190
20.10 Exact finite validation and interpretation . . . 191

**21 Holonomy-twisted lane transport and orbit descent 192**
21.1 Holonomy-profiled lane data . . . 192
21.2 The holonomy-twisted transport theorem . . . 193
21.3 Monodromy orbits and the finest untwisted coarsening . . . 195
21.4 Permutation modules and the orbital path algebra . . . 197
21.5 Cyclotomic orbit lanes over the rational field . . . 198
21.6 Exact finite validation and scope . . . 199

**IV Relative semantic quotients and changes of doctrine 200**

**22 Relative semantic quotients and behavioral cores 200**
22.1 Semantic slices and resolved observational systems . . . 200
22.2 The maximal stable invisible core . . . 202
22.3 Greatest-fixed-point construction and finite recognition . . . 203
22.4 The task–congruence Galois connection . . . 203
22.5 Semantic quotient lattice . . . 204
22.6 The two-view semantic diamond . . . 204
22.7 Exact change of task . . . 206

**23 Carrier change, observer base change, and provenance 207**
23.1 Carrier factorization and joint semantic completion . . . 207
23.2 Behavioral bridges and exact loss . . . 208
23.3 Carrier-indexed observer packets . . . 209
23.4 Carrier no-go mechanisms . . . 209
23.5 Observer base change and the relation module . . . 210
23.6 Observer-conditioned convex packets . . . 211

**24 Admissibility change, geometric obstruction, and doctrine lifting 212**
24.1 Admissible realization classes and optimized defect . . . 212
24.2 Metric packets and intrinsic distortion . . . 213
24.3 Exact convex-versus-quadratic separation . . . 214
24.4 Escape without positive gap . . . 215
24.5 Forgetful descent and enrichment lifting . . . 216
24.6 Two variances and the indexed architecture . . . 216

**25 Scope, classification targets, and open boundaries** **218**
25.1 Directional satellites . . . 220
25.2 Open mathematical obligations . . . 220

**26 Conclusion** **221**

**A Theorem concordance and proof-status index** **222**

**B Edition-control ledger** **228**

**C Publication audit and development provenance** **231**

**D Detailed open-obligation ledger** **233**
D.1 Correct dependency order . . . 233
D.2 What this manuscript closes . . . 233
D.3 What remains . . . 235
D.4 Finite completion criterion . . . 241

**E Detailed claim-boundary ledger** **243**
E.1 Claims supported at manuscript level . . . 243
E.2 Claims not established . . . 245

**F Validation record** **248**

# 1 Introduction

## 1.1 The assembly problem

The source manuscripts already contain typed quiver and module semantics, seed presentations, exact packet coordinates, refinement and residual calculus, nonlinear packet composition, finite holonomy, relative obstruction objects, operator-algebraic recognition, Galois descent, and several exact sequence and arithmetic realizations [1, 2, 3, 6, 7]. The central problem is therefore no longer to reconstruct these foundations independently. It is to determine when they assemble into one finite, typed, coherent classifying object.

The proposed architecture has six layers:

$$\boxed{\begin{array}{c}\text{resolved syntax} \longrightarrow \text{normalized strata} \longrightarrow \text{typed overlaps} \longrightarrow \text{coherence} \\ \longrightarrow \text{effective descent} \longrightarrow \text{compatible complete invariants.}\end{array}}$$

Each arrow carries a proof obligation. A semantic analogy is not a bridge. A bridge is not reversible merely because formulas exist in both directions. Local completeness is not global completeness until the local isomorphisms themselves satisfy descent.

## 1.2 Main theorem and classification domain

Three theorem levels are kept distinct. First, the finite profiled Universal Lane Transport Theorem is an internal theorem about complete finite split packet systems in an additive idempotent-complete category. Its holonomy-twisted extension retains exact analysis, synthesis, composition, refinement, selectors, and residuals when chart loops permute lane addresses. The global coordinate object is then a matrix local system, and ordinary lane projectors descend at the monodromy-orbit resolution.

Second, the finite atlas assembly theorem is conditional in general. Given profile-preserving normalized strata, typed reversible overlaps, coherent comparison cells, effective descent, and compatible native invariants, the descended invariant reflects isomorphism. The manuscript verifies these hypotheses on a finite certified atlas whose reversible core has five connected semantic components.

Third, the semantic quotient theorem works inside a fixed doctrine and declared observation category. It constructs the maximal continuation-stable invisible core and the associated task-relative quotient. In module-valued slices, semantic combination and bridge transport admit canonical exact sequences. Carrier and observer changes are separate factorization problems, while changes of admissible geometry or enrichment are typed lifting problems.

The statements are strongest precisely because their targets are explicit. Lane transport concerns declared finite resolutions. Atlas classification concerns the declared normalized finite atlas. Behavioral minimality concerns one semantic slice. None of these statements classifies arbitrary presentations, identifies all carrier algebras, or promotes unverified doctrine changes to equivalences.

## 1.3 Contributions

The paper makes fourteen consolidated contributions.

1. It provides a source-controlled theorem concordance and an explicit profile-indexed additive–Karoubi resolved envelope.

2. It separates representation groupoids from the directed transformation category and assigns every certified bridge a preservation and information-loss passport.
3. It proves a finite profiled atlas assembly theorem and distinguishes holonomy, relative cokernel, Brauer, and higher-coherence defects.
4. It establishes normalized effective-descent atlases and complete native invariants on the five-component certified semantic union.
5. It proves exact bridge comparison and higher coherence, including the nonlinear–algebraic–holonomic Fuss–Catalan triangle.
6. It proves the finite profiled Universal Lane Transport Theorem with exact block transport, refinement, selectors, residuals, and separately typed fold and kernel clauses.
7. It removes the trivial-address-holonomy restriction from transport by proving matrix-local-system descent, orbit coarsening, pair-orbit selectors, and orbital path composition.
8. It defines the task-relative behavioral quotient as the coarsest exact representation preserving all declared future observations.
9. It identifies the behavioral kernel as the maximal continuation-stable invisible core and gives a greatest-fixed-point computation with finite-dimensional termination.
10. It proves the semantic diamond, relative semantic residual, task-change exact sequence, bridge-loss exact sequence, and extension law for composite loss in module-valued slices.
11. It proves the carrier factorization gate and the universal joint completion preserving two incomparable carrier semantics.
12. It separates Set-valued continuation minimization from linear residual minimization by an exact relation-module sequence and an explicit polyphase family with infinite discrete state and finite Hankel rank.
13. It proves carrier-indexed observer aggregation and observer-conditioned convex packet transport, while isolating cancellation, idempotence, singular-resurrection, and provenance boundaries.
14. It formalizes admissibility monotonicity, completion/gap/escape stratification, a sharp convex-versus-quadratic example, and the forgetful-descent versus enrichment-lifting principle.

### 1.4 Proof status and organization

Classical inputs, internally proved theorems, exact finite verification, conditional statements, framework definitions, and conjectures are separately marked. The theorem concordance is source control for this distinction. Part I gives the common resolved foundation and finite assembly theorem. Part II develops the certified native strata. Part III gives global synthesis and finite profiled and holonomy-twisted lane transport. Part IV develops task-relative semantic quotients, carrier and observer change, exact loss, admissibility-relative obstruction, and doctrine lifting. The final sections state scope and conclusion. Detailed development, claim-boundary, and validation records are retained in the appendices.

## 2 Main theorem suite and proof architecture

Let

$$\mathfrak{A}_{\mathrm{cert}} := \mathfrak{A}_{13}$$

denote the finite certified atlas constructed in Section 19. Its reversible core is the disjoint union of five connected semantic components, while its directional satellites retain explicit loss or obstruction passports.

**Theorem 2.1** (Stratified resolved representation, descent, and complete invariant theorem)**.** *Let $\mathbb{K}$ be the resolved theory used in this manuscript and let $\mathfrak{A}_{\mathrm{cert}}$ be the declared finite atlas. Then the following statements hold.*

1. *Every chart is a profile-preserving realization of the common resolved syntax, and every reversible edge is an equivalence on its named overlap category.*
2. *The descent category exists as the finite pseudolimit of the atlas and decomposes as the coproduct of its five connected semantic components.*
3. *Every proof whose constructor support lies in the common verified preservation profile transports to compatible local theorems and hence to the corresponding global resolved object.*
4. *The semantic normalizers induce the comparison 2-cells on all nonempty triple overlaps and force the quadruple-overlap coherence equation.*
5. *The compatible native invariant family descends to a tagged global invariant*

$$\mathcal{J}_{\mathrm{cert}} : \mathrm{Desc}(\mathfrak{A}_{\mathrm{cert}}) \longrightarrow \mathrm{Desc}(\mathcal{V}_{\mathrm{cert}}).$$

6. *The descended invariant is complete on the declared normalized global category:*

$$\mathcal{J}_{\mathrm{cert}}(X) \cong \mathcal{J}_{\mathrm{cert}}(Y) \quad \Longleftrightarrow \quad X \cong Y.$$

7. *Every noninvertible construction remains outside the reversible core and carries a typed record of its preserved structure, forgotten information, named residual, or obstruction class.*

*Proof.* The common resolved syntax and preservation-profile transport are established in Section 3. The finite atlas and its pseudolimit are supplied by theorem 6.3. The normalizer comparison cells and their higher coherence are theorem 19.2. Descent of compatible invariant families is theorem 19.4. Completeness is theorem 19.11; its hypotheses are verified component by component in Section 19. The bridge passports and obstruction taxonomy in Section 4 keep every directional construction outside the maximal subgroupoid. Combining these results proves all seven assertions. □

**Corollary 2.2** (Relative universality)**.** *The certified atlas is universal for profile-preserving models of the declared resolved grammar on its five normalized semantic components. This universality is relative to the chosen grammar, strata, bridges, preservation profiles, normalization targets, and descent doctrine.*

**Theorem 2.3** (Relative semantic quotient and typed contract-change theorem)**.** *Fix a declared semantic slice in a stratum of the resolved theory. Assume the required effective quotients exist. Then:*

1. *the behavioral quotient is the coarsest exact representation preserving all declared future observations;*
2. *its kernel or congruence is the maximal continuation-stable invisible core;*
3. *strengthening the task induces a canonical map from the stronger quotient to the weaker quotient;*
4. *in module-valued slices, joint semantics, shared semantics, relative residuals, bridge loss, essential-image failure, and task weakening fit into canonical exact sequences;*

5. *one carrier semantics replaces another exactly on the corresponding kernel-factorization locus;*
6. *observer base change may introduce an independent relation object and therefore does not follow from carrier compatibility;*
7. *enlarging an admissible realization class can only decrease optimized defect, but zero infimum need not be attained;*
8. *lifting a bare bridge to richer metric, tensor, topological, projective, or completed structure requires a separate enhancement certificate.*

*Proof.* The universal quotient and maximal-core statements are theorems 22.4 and 22.6. Task change and the module exact sequences are theorems 22.16, 22.20, 23.5 and 23.7. Carrier and observer change are theorems 23.1 and 23.13. Admissibility monotonicity is theorem 24.2, and the enrichment statement is proposition 24.9. Each assertion retains its printed doctrine and existence hypotheses. □

**Corollary 2.4** (No absolute minimal representation)**.** *There is no observer-independent or doctrine-independent minimum asserted by this manuscript. Minimality is relative to the carrier, continuation grammar, observation category, query family, and admissible enrichment class.*

*Boundary* 2.5 (Publication boundary). Theorem 2.1 does not imply a global canonical normal form for arbitrary mathematical objects, equivalence of all broad strata, decidability of arbitrary presentation equivalence, or effectivity of an unrestricted heterogeneous stack. It also does not identify functional-Mahler equations with Newton-Mahler interpolation, forget branch data in the algebraic-to-holonomic direction, or infer Tannakian symmetry from a merely faithful additive realization.

# Part I

# Common foundations and finite assembly

## 3 Resolved theories, packet coordinates, and preservation profiles

This section expands the common formal core used by every later atlas construction. The purpose is not to force every domain into one category. It is to separate four layers that are often conflated:

$$\boxed{\text{typed syntax} \longrightarrow \text{resolved coordinates} \longrightarrow \text{profile-preserving realization} \longrightarrow \text{domain semantics.}}$$

The first two layers are algebraic. The third records which algebraic or universal constructions survive a realization. The fourth supplies domain-specific hypotheses such as completeness, positivity, convergence, integrality, measurability, or analytic continuation. A cross-domain statement is a theorem only when all four layers are present.

### 3.1 Typed resolved signatures

**Definition 3.1** (Finite resolved signature)**.** Fix a commutative coefficient ring $\mathbb{k}$. A finite resolved signature is a tuple

$$\mathbb{K}_{\mathrm{fin}} = (Q, I, \mathsf{P}, \mathsf{Ref}, \mathsf{Comp}, \mathsf{Cert})$$

with the following data.

**Table 1:** The publication theorem spine. Section numbers are resolved by the final build; the logical order, rather than the numbering, is authoritative.

| Stage | Principal result | Exact role in the proof | Location |
|---|---|---|---|
| Resolved source | Additive-Karoubi envelope | Literal finite packet objects and profile-indexed realization source | theorem 3.36 |
| Typed atlas | Bridge passports and obstruction separation | Reversible overlaps are separated from directional loss | Section 4 |
| Finite assembly | Profiled atlas assembly | Bilimit, theorem transport, groupoid core, and global directional functors | theorem 6.3 |
| Native normalization | Certified stratum atlases | Complete local coordinates on declared semantic slices | Part II |
| Higher coherence | Normalizer-induced coherence | Unique semantic normalizers force all certified overlap cycles to commute | theorem 19.2 |
| Invariant descent | Certified invariant-descent theorem | Coherent local invariants descend through effective object and morphism gluing | theorem 19.4 |
| Global completeness | Tagged componentwise invariant | The descended invariant reflects isomorphism on the five-component union | theorems 2.1 and 19.11 |
| Lane transport | Finite profiled Universal Lane Transport Theorem | Exact block transport, refinement, selection, residuals, conditional fold loss, and certified descent | theorems 20.3 and 20.24 |
| Twisted transport | Holonomy-Twisted Universal Lane Transport Theorem | Matrix-local-system synthesis, base-fiber invariant normal form, orbit coarsening, and orbital path algebra | theorems 21.3, 21.6 and 21.8 and corollary 21.4 |
| Task semantics | Relative semantic quotient theorem | Behavioral cores, task quotients, semantic diamonds, and exact task loss | theorems 2.3, 22.16 and 22.20 |
| Carrier and observer change | Factorization and base-change theorems | Joint semantic completion, exact bridge loss, relation modules, and carrier-indexed aggregation | theorems 23.1, 23.5, 23.9 and 23.13 |
| Admissibility and lifting | Class-relative defect and enhancement gates | Completion/gap/escape, geometry-class separation, and typed enrichment lifting | theorems 24.2 and 24.7 and proposition 24.9 |

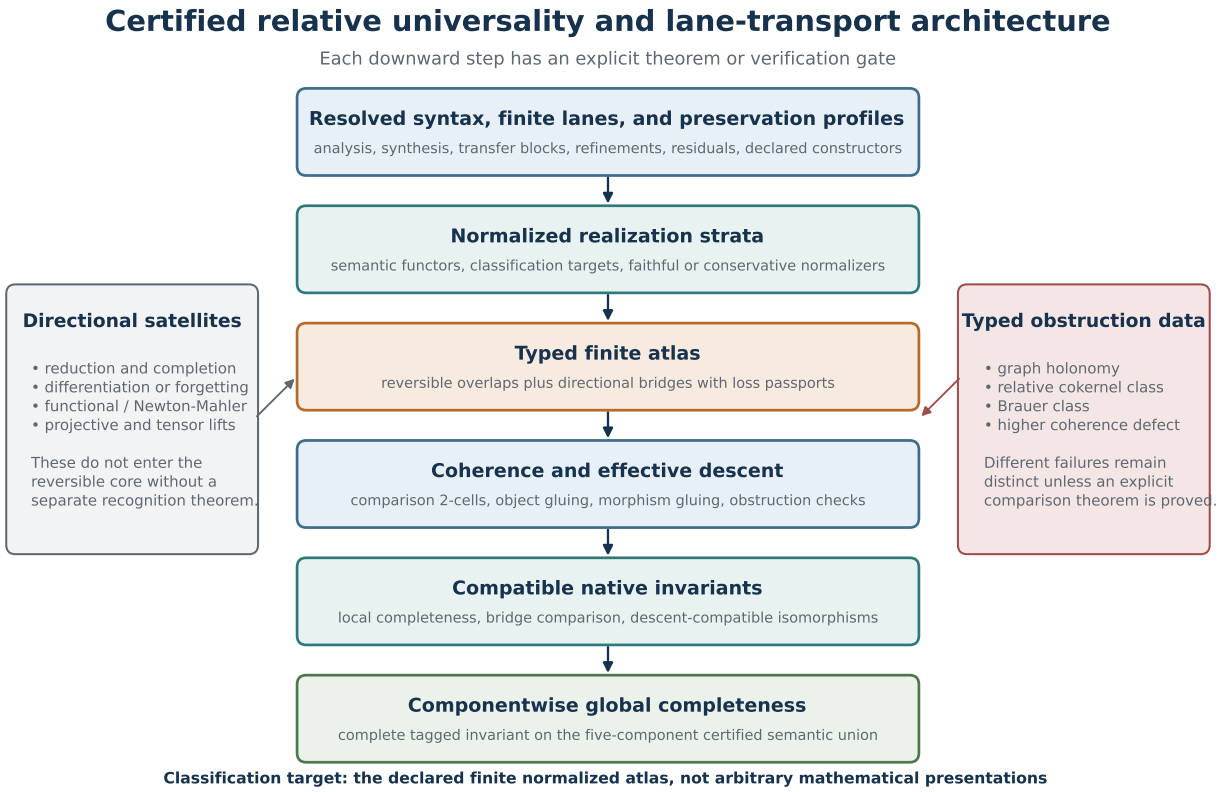



**Figure 1:** Proof architecture of the journal-facing theorem. The vertical spine contains the reversible construction and descent argument. Directional satellites and obstruction data remain typed external inputs rather than silent equivalences.

(i) $Q = (Q_0, Q_1, s, t)$ is a finite quiver. Its vertices are sorts and its arrows are typed primitive operations.

(ii) $I \triangleleft \Bbbk Q$ is a finitely generated two-sided ideal generated by $\Bbbk$-linear combinations of paths with common source and common target.

(iii) P is a finite list of packet declarations. A declaration on a sort $X$ consists of endomorphism words $p_{X,r,i}$ and the relations

$$p_{X,r,i}p_{X,r,j} = \delta_{ij}p_{X,r,i}, \qquad \sum_i p_{X,r,i} = 1_X.$$

(iv) Ref is a finite list of refinement declarations. For $s \succeq r$, an address map

$$\rho_{sr} : I_{X,s} \twoheadrightarrow I_{X,r}$$

is accompanied by the equations

$$p_{X,r,i} = \sum_{\rho_{sr}(j)=i} p_{X,s,j}.$$

(v) Comp is a list of optional completion tags. A tag names a doctrine to be added later, such as Banach completion, a $C^*$-involution, a multiplier completion, or a monoidal structure. A tag is not itself an existence theorem.

(vi) Cert is a list of named residual and certificate types. Each certificate type specifies its source object, target object, and the equations or inequalities it is intended to record.

The finite signature is the presentation-level object. It records legal words and declared equations. It does not identify a preferred realization, a preferred coordinate basis, or a preferred semantic domain.

**Definition 3.2** (Realization of a finite resolved signature)**.** Let $\mathcal{C}$ be a $\Bbbk$-linear category. A realization of $\mathbb{K}_{\mathrm{fin}}$ in $\mathcal{C}$ assigns an object $M_X$ to every vertex $X \in Q_0$ and a morphism

$$M_a : M_{s(a)} \longrightarrow M_{t(a)}$$

to every arrow $a \in Q_1$, such that all relations in $I$, all packet equations, and all declared refinement equations hold. Completion and certificate tags are interpreted only when the realization profile explicitly includes them.

**Theorem 3.3** (Typed realization and module equivalence, imported)**.** *Let*

$$\Lambda_{\mathbb{K}} := \Bbbk Q / I.$$

*In $\Bbbk$-modules, the category of typed realizations of the linear grammar $(Q, I)$ is equivalent to the category of unital left $\Lambda_{\mathbb{K}}$-modules. Under the equivalence, the vertex idempotent $e_X$ acts as the projector onto the component of sort $X$, and each arrow acts in its declared source-target block.*

*Proof.* A typed realization defines the action of a path by composition and then extends $\Bbbk$-linearly. Every element of $I$ acts by zero, so the action factors through $\Lambda_{\mathbb{K}}$. Conversely, for a unital module $M$, the pairwise orthogonal vertex idempotents give

$$M = \bigoplus_{X \in Q_0} e_X M,$$

and an arrow $a : X \to Y$ maps $e_X M$ into $e_Y M$. These constructions are inverse up to their canonical natural isomorphisms. This is the typed-module theorem of Paper I [1]. □

*Remark* 3.4 (Presentation is not classification). The theorem fixes the semantics of one declared grammar. It does not say that the grammar is unique, minimal, or recoverable from a finite list of observations. Distinct quivers with relations can present equivalent module categories, and one realization can annihilate additional syntax through the kernel of its action.

**Example 3.5** (Two-sort transfer grammar)**.** Take two sorts $X, Y$, one arrow $a : X \to Y$, and no nontrivial relation. A realization is a single typed map

$$M_X \xrightarrow{M_a} M_Y.$$

After collapsing to $M_X \oplus M_Y$, the vertex idempotents are coordinate packets and $M_a$ is one off-diagonal transfer block. The smallest typed grammar therefore already contains the distinction between object packets and transfer channels.

### 3.2 Packet objects, analysis, and exact transfer coordinates

**Definition 3.6** (Finite packet system)**.** Let $X$ be an object of a preadditive category. A finite packet system on $X$ is a family

$$\mathcal{P} = (p_i)_{i \in I} \subseteq \mathrm{End}(X)$$

satisfying

$$p_i^2 = p_i, \qquad p_i p_j = 0 \quad (i \neq j), \qquad \sum_{i \in I} p_i = 1_X.$$

No self-adjointness or metric orthogonality is assumed unless stated separately.

Assume now that $\mathcal{C}$ is additive and idempotent complete. Choose a splitting

$$X_i \xrightarrow{\iota_i} X \xrightarrow{\pi_i} X_i, \qquad \iota_i \pi_i = p_i, \qquad \pi_i \iota_i = 1_{X_i}.$$

The packet equations imply

$$\pi_i \iota_j = 0 \quad (i \neq j).$$

**Definition 3.7** (Packet analysis and synthesis)**.** The packet analysis and synthesis maps are

$$\mathcal{A}_{\mathcal{P}} := (\pi_i)_{i \in I} : X \longrightarrow \bigoplus_{i \in I} X_i,$$

$$\mathcal{S}_{\mathcal{P}} := (\iota_i)_{i \in I} : \bigoplus_{i \in I} X_i \longrightarrow X.$$

**Theorem 3.8** (Exact packet-coordinate isomorphism, imported)**.** *For every finite packet system in an additive idempotent-complete category,*

$$\boxed{\mathcal{S}_{\mathcal{P}} \mathcal{A}_{\mathcal{P}} = 1_X, \qquad \mathcal{A}_{\mathcal{P}} \mathcal{S}_{\mathcal{P}} = 1_{\oplus_i X_i}.}$$

*Consequently,*

$$X \cong \bigoplus_{i \in I} X_i.$$

*Proof.* The first identity is

$$\mathcal{S}_{\mathcal{P}} \mathcal{A}_{\mathcal{P}} = \sum_i \iota_i \pi_i = \sum_i p_i = 1_X.$$

The $(i, j)$-entry of the second composite is $\pi_i \iota_j$, which equals $1_{X_i}$ for $i = j$ and zero otherwise. This is the exact packet-coordinate theorem of Paper I [1]. □

**Corollary 3.9** (Packetwise equality)**.** *For parallel morphisms $f, g : Z \to X$,*

$$f = g \quad \Longleftrightarrow \quad \pi_i f = \pi_i g \text{ for every } i.$$

*For parallel morphisms $f, g : X \to Z$,*

$$f = g \quad \Longleftrightarrow \quad f\iota_i = g\iota_i \text{ for every } i.$$

*Proof.* One direction is immediate. In the other direction, insert the reconstruction identity on the appropriate side and sum the packetwise equalities. □

**Corollary 3.10** (Universal mapping property of packet coordinates)**.** *For every object $Z$, restriction to the packet objects gives natural bijections*

$$\mathrm{Hom}(X, Z) \cong \prod_i \mathrm{Hom}(X_i, Z), \qquad \mathrm{Hom}(Z, X) \cong \prod_i \mathrm{Hom}(Z, X_i),$$

*where the products are finite. Packetwise maps therefore assemble uniquely into a global map.*

**Definition 3.11** (Mixed transfer blocks)**.** Let $\mathcal{P} = (p_i)$ be a packet system on $X$, let $\mathcal{Q} = (q_a)$ be a packet system on $Y$, and choose splittings $(\iota_i, \pi_i)$ and $(\jmath_a, \varpi_a)$. For $f : X \to Y$, define the packet-to-packet map

$$f_{ai} := \varpi_a f \iota_i : X_i \longrightarrow Y_a.$$

Its ambient corner is

$$q_a f p_i = \jmath_a f_{ai} \pi_i.$$

**Theorem 3.12** (Exact transfer reconstruction and block composition, imported)**.** *Every morphism $f : X \to Y$ has the exact expansion*

$$\boxed{f = \sum_{a,i} q_a f p_i = \sum_{a,i} \jmath_a f_{ai} \pi_i.}$$

*If $g : Y \to Z$ is resolved by a packet system $\mathcal{R} = (r_c)$, then*

$$\boxed{(gf)_{ci} = \sum_a g_{ca} f_{ai}.}$$

*Proof.* Insert the finite packet identities on both sides of $f$:

$$f = \left( \sum_a q_a \right) f \left( \sum_i p_i \right).$$

For composition, insert $1_Y = \sum_a q_a$ between $g$ and $f$. This is the transfer-block reconstruction and multiplication law of Paper I [1]. □

**Corollary 3.13** (Path expansion)**.** *For a composable string*

$$X_0 \xrightarrow{f_1} X_1 \xrightarrow{f_2} \cdots \xrightarrow{f_m} X_m$$

*with packet systems on every $X_j$, each source-target block of $f_m \cdots f_1$ is the sum over all compatible intermediate packet paths of the corresponding block products.*

**Example 3.14** (Exact oblique packets)**.** Over any field, set

$$p_1 = \begin{pmatrix} 1 & 1 \\ 0 & 0 \end{pmatrix}, \qquad p_2 = \begin{pmatrix} 0 & -1 \\ 0 & 1 \end{pmatrix}.$$

Then $p_1^2 = p_1$, $p_2^2 = p_2$, $p_1 p_2 = p_2 p_1 = 0$, and $p_1 + p_2 = I$. The decomposition of $\mathbb{k}^2$ is exact, although the packets are not orthogonal for the standard inner product. This separates the algebraic reconstruction theorem from later metric statements about energy or best approximation.

### 3.3 Refinement, selected support, and named residuals

**Definition 3.15** (Finite refinement)**.** A packet system $\mathcal{P}^s = (p_j^s)_{j\in I_s}$ refines $\mathcal{P}^r = (p_i^r)_{i\in I_r}$ when there is a surjection

$$\rho_{sr} : I_s \twoheadrightarrow I_r$$

such that

$$p_i^r = \sum_{\rho_{sr}(j)=i} p_j^s.$$

The map $\rho_{sr}$ records the address of each fine packet inside its coarse ancestor.

**Proposition 3.16** (Aggregation and transitivity)**.** *A finite aggregation of pairwise annihilating packets is again a packet system. If $t \succeq s \succeq r$, then refinement is transitive with address map*

$$\rho_{tr} = \rho_{sr} \circ \rho_{ts}.$$

*Proof.* For an aggregated packet, idempotence follows because all cross terms vanish. Distinct aggregates annihilate each other, and the total sum remains the identity. Substituting the $t$-level expansion into the $s$-level expansion gives the composite address law. □

**Theorem 3.17** (Exact refinement law, imported)**.** *Let $p_i^r = \sum_{\rho_{sr}(j)=i} p_j^s$ and $q_a^u = \sum_{\sigma_{vu}(b)=a} q_b^v$. For every morphism $f : X \to Y$,*

$$\boxed{q_a^u f p_i^r = \sum_{\sigma_{vu}(b)=a} \sum_{\rho_{sr}(j)=i} q_b^v f p_j^s.}$$

*Coarsening the fine block product of two composable maps gives the coarse block product.*

*Proof.* Insert the two refinement identities on the left and right of $f$. For composition, expand both maps at the fine level, multiply, and sum over descendant intermediate packets. The fine intermediate projectors sum to the coarse intermediate projector. This is the exact refinement law of Resolution Theory [2]. □

**Definition 3.18** (Support compression and residual)**.** For packet systems $\mathcal{P}$ on $X$ and $\mathcal{Q}$ on $Y$, let $E \subseteq I_{\mathcal{Q}} \times I_{\mathcal{P}}$. Define

$$C_E(f) := \sum_{(a,i)\in E} q_a f p_i, \qquad R_E(f) := f - C_E(f).$$

The first term is the retained transfer support and the second is its named residual.

**Proposition 3.19** (Boolean algebra of block selectors)**.** *As endomorphisms of the $\Bbbk$-module $\mathrm{Hom}(X, Y)$, the selectors satisfy*

$$C_E^2 = C_E, \qquad C_E C_F = C_{E\cap F}, \qquad R_E = I - C_E.$$

*In particular,*

$$C_E R_E = R_E C_E = 0, \qquad f = C_E(f) + R_E(f).$$

*Proof.* Applying $C_E$ to a block $q_b f p_j$ retains it exactly when $(b, j) \in E$. Pairwise annihilation removes every mismatched source or target index. The formulas follow block by block. □

**Definition 3.20** (Relational support product)**.** For $E \subseteq I_Y \times I_X$ and $F \subseteq I_Z \times I_Y$, define

$$F \circ E := \{(c, i) : \text{there exists } a \in I_Y \text{ with } (c, a) \in F \text{ and } (a, i) \in E\}.$$

**Proposition 3.21** (Support propagation under composition)**.** *If $f = C_E(f)$ and $g = C_F(g)$, then*

$$gf = C_{F\circ E}(gf).$$

*Thus exact zero patterns propagate by relational composition.*

*Proof.* Every block of $gf$ is a sum $\sum_a g_{ca} f_{ai}$. A nonzero summand can occur only along an intermediate address $a$ belonging to the relational product. □

**Proposition 3.22** (Exact residual product identity)**.** *Let*

$$f_E = C_E(f), \quad r_f = R_E(f), \qquad g_F = C_F(g), \quad r_g = R_F(g).$$

*Then*

$$\boxed{gf - g_F f_E = r_g f_E + g_F r_f + r_g r_f.}$$

*If the morphisms lie in a normed operator algebra with a submultiplicative norm, then*

$$\|gf - g_F f_E\| \le \|r_g\|\,\|f_E\| + \|g_F\|\,\|r_f\| + \|r_g\|\,\|r_f\|.$$

*Proof.* Substitute $g = g_F + r_g$ and $f = f_E + r_f$ and expand. The norm estimate is immediate from the triangle inequality and submultiplicativity. □

The identity is a basic certificate-propagation law. It explains exactly which residual terms enter after composing two compressed transfers. No asymptotic claim is required.

**Theorem 3.23** (Hilbert–Schmidt optimality, imported)**.** *Assume $X, Y$ are Hilbert spaces, the packet idempotents are orthogonal projectors, and $f : X \to Y$ is Hilbert–Schmidt. Then $C_E$ is the Hilbert–Schmidt orthogonal projection onto the selected block subspace and*

$$\|R_E(f)\|_{\mathrm{HS}}^2 = \sum_{(a,i)\notin E} \|q_a f p_i\|_{\mathrm{HS}}^2.$$

*Consequently, $C_E(f)$ is the unique best Hilbert–Schmidt approximation to $f$ among operators supported on $E$.*

*Boundary* 3.24 (Algebraic exactness is not metric optimality). For arbitrary idempotent packets, reconstruction and residual decomposition remain exact. Orthogonal energy identities and best-approximation statements require a Hilbert structure, orthogonal projectors, and the stated operator class. Those hypotheses are part of the theorem rather than consequences of the packet notation.

## 3.4 Preservation profiles and proof-support certificates

A realization can preserve one part of the resolved calculus and forget another. The preservation profile is therefore a mathematical interface, not informal metadata.

**Definition 3.25** (Constructor universe)**.** Fix a declared universe $\mathfrak{C}$ of constructors and universal properties. Typical entries are

$$0,\ 1,\ \text{finite sums},\ \text{composition},\ \text{scalar action},\ \text{biproducts},$$
$$\text{kernels},\ \text{cokernels},\ \text{quotients},\ \text{tensor products},$$
$$\text{packet idempotents},\ \text{transfer blocks},\ \text{refinements},\ \text{named residuals},$$
$$\text{finite limits},\ \text{finite colimits},\ \text{topological completions},\ \text{adjoints}.$$

The list may be enlarged, but every new entry must specify the exact identity or universal property to be preserved.

**Definition 3.26** (Verified preservation profile)**.** A verified preservation profile $\Pi_F$ for a functor $F : \mathcal{C} \to \mathcal{D}$ consists of a subset of $\mathfrak{C}$ together with a proof or declared comparison isomorphism showing that $F$ preserves each listed constructor. We write $c \in \Pi_F$ only after the corresponding preservation claim has been verified.

**Definition 3.27** (Proof-support certificate)**.** A proof-support certificate for a finite proof $\mathcal{P}$ is a finite subset

$$\mathrm{csupp}(\mathcal{P}) \subseteq \mathfrak{C}$$

containing every constructor and universal property used in the proof. The certificate need not be minimal. It must be sufficient and auditable.

**Proposition 3.28** (Common profile and composition)**.** *Let $F : \mathcal{C} \to \mathcal{D}$ and $G : \mathcal{D} \to \mathcal{E}$. Every constructor preserved by both functors, with compatible chosen comparison data, is preserved by $GF$. For a finite diagram of realizations and bridges, the intersection*

$$\Pi_{\mathrm{common}} := \bigcap_F \Pi_F$$

*is therefore a valid common profile for every proof transported through the whole diagram.*

*Proof.* Preservation equations and comparison isomorphisms compose. Universal properties remain universal after applying the second functor whenever both preservation witnesses are present. Intersecting the verified lists retains only constructors supported at every stage. □

**Theorem 3.29** (Equational realization principle, imported)**.** *Let $F : \mathcal{C} \to \mathcal{D}$ be additive between preadditive categories. Every equality of morphism expressions built from declared generators by finite sums, additive inverses, identities, zero maps, and composition is preserved by $F$. Scalar multiplication is preserved when the categories are enriched over the same coefficient ring and $F$ is linear. If a proof additionally invokes a chosen biproduct, kernel, cokernel, quotient, tensor product, completion, or another universal construction, the proof transports only when that constructor belongs to $\Pi_F$.*

*Proof.* Functoriality preserves identities and composition. Additivity preserves zero, sums, and additive inverses. Linearity preserves the declared scalar action. Structural induction on the morphism expression transports every equational step. When a step is characterized by a universal property, the verified profile witness identifies the image construction with the corresponding target construction. This is the equational realization principle of Paper I [1]. □

**Proposition 3.30** (Profile-safe theorem transport)**.** *Let $\mathcal{P}$ prove a statement $T$ in the resolved syntax, and let $F$ be a realization or bridge. Suppose*

$$\mathrm{csupp}(\mathcal{P}) \subseteq \Pi_F.$$

*After every additional domain hypothesis used by $T$ has been verified in the target, $F(T)$ is a valid target theorem. If the inclusion fails, the source proof does not by itself establish the target statement.*

*Proof.* Apply theorem 3.29 to every equational and universal-construction step in the proof certificate. The remaining assumptions are precisely the domain-specific hypotheses, which are checked separately. □

**Definition 3.31** (Semantic realization certificate)**.** A semantic realization certificate for transporting a theorem consists of four fields:

(C1) an explicit functor or intertwining construction;

(C2) its verified preservation profile;

(C3) a proof-support certificate for the source theorem together with the inclusion into the profile;

(C4) verification of every target-specific hypothesis and a restatement of the conclusion in native target objects.

**Table 2:** Typical preservation gates. The right column names the extra obligation rather than asserting it automatically.

| Proof step | Required profile entry | Additional target obligation |
|---|---|---|
| Finite block identity | finite sums, composition, packet idempotents | verify that the declared packet equations hold |
| Kernel or cokernel argument | the corresponding universal property | check the target category has the selected construction |
| Quotient descent | quotient preservation | identify the target quotient and, topologically, its quotient topology |
| Infinite reconstruction | declared convergence/completion doctrine | specify norm, strong, weak, or unconditional convergence |
| Tensor reconstruction | tensor preservation and coherence | verify associativity, unit, and any symmetry or dagger structure used |
| Positivity or best approximation | adjoint, positivity, Hilbert structure | verify orthogonality and the relevant operator ideal |
| Arithmetic congruence | integral or local realization data | verify valuation, denominator, and reduction hypotheses |

*Boundary* 3.32 (Terminology is not semantic transport). Calling a frequency band, residue class, ramification sector, or latent channel a "packet" is only terminological reuse until the packet idempotents, reconstruction law, transfer blocks, and required preservation maps are supplied. Failure of a profile gate is an explicit open obligation, not permission to infer the desired theorem by analogy.

### 3.5 The finite additive-Karoubi resolved envelope

The full profile-indexed envelope remains a multi-doctrine problem. The finite linear, additive, and split-idempotent core can be constructed exactly.

**Definition 3.33** (Linear grammar category)**.** For a finite linear resolved presentation $\mathbb{K}_{\mathrm{lin}} = (Q, I, \mathsf{P}, \mathsf{Ref})$, let

$$\mathcal{A}_{\mathbb{K}} := \Bbbk Q / I.$$

This is the $\Bbbk$-linear category whose objects are the vertices of $Q$ and whose morphisms are $\Bbbk$-linear combinations of typed paths modulo the declared relations.

**Definition 3.34** (Finite additive hull)**.** The category $\mathrm{Add}(\mathcal{A}_{\mathbb{K}})$ has finite tuples

$$A = (A_1, \dots, A_m)$$

as objects. A morphism $A \to B = (B_1, \dots, B_n)$ is an $n \times m$ matrix with entries in $\mathcal{A}_{\mathbb{K}}(A_j, B_i)$. Composition is matrix multiplication using composition and addition in $\mathcal{A}_{\mathbb{K}}$.

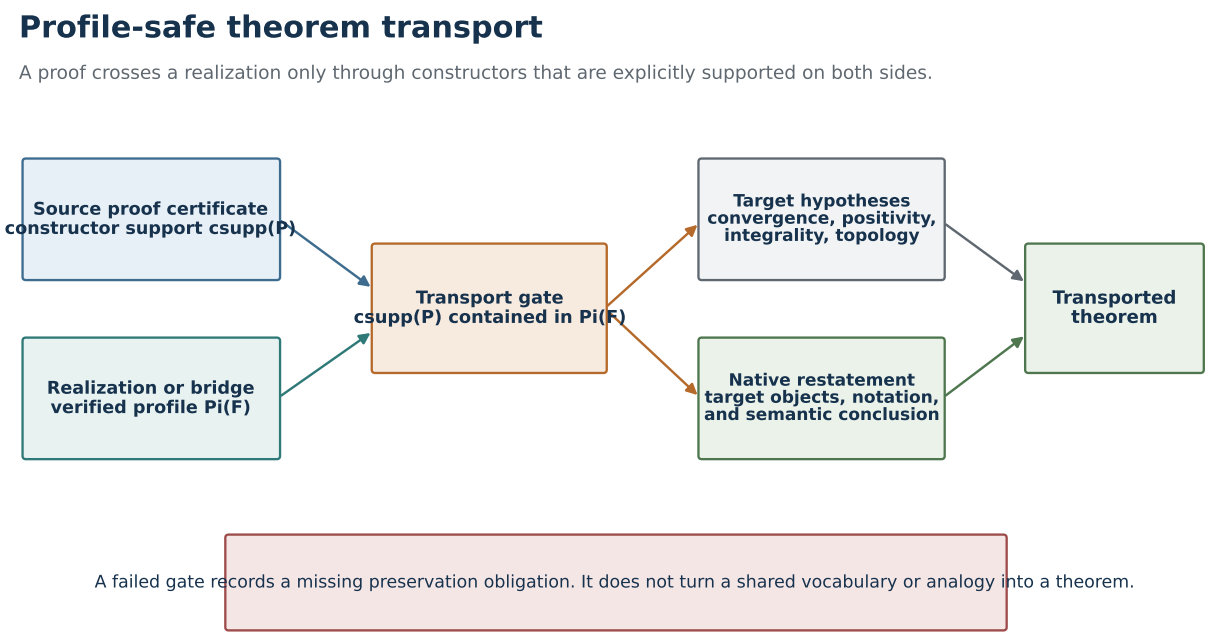



**Figure 2:** The theorem-transport gate. A shared vocabulary is not enough: the constructors used by the proof must lie inside the verified profile, and target-specific hypotheses must still be checked.

**Definition 3.35** (Karoubi envelope)**.** The Karoubi envelope $\mathrm{Kar}(\mathrm{Add}(\mathcal{A}_{\mathbb{K}}))$ has pairs $(A,e)$, where $e : A \to A$ is idempotent, as objects. A morphism

$$f : (A,e) \longrightarrow (B,d)$$

is a morphism $f : A \to B$ satisfying

$$f = dfe.$$

The identity on $(A,e)$ is $e$.

**Theorem 3.36** (Finite additive-Karoubi resolved envelope)**.** *The category*

$$\boxed{\mathrm{Syn}_{\mathrm{ak}}(\mathbb{K}_{\mathrm{lin}}) := \mathrm{Kar}\big(\mathrm{Add}(\Bbbk Q/I)\big)}$$

*is small, additive, idempotent complete, and $\Bbbk$-linear. For every additive idempotent-complete $\Bbbk$-linear category $\mathcal{C}$, restriction to the generating quiver induces an equivalence*

$$\mathrm{Fun}^{\oplus}_{\Bbbk}\big(\mathrm{Syn}_{\mathrm{ak}}(\mathbb{K}_{\mathrm{lin}}),\mathcal{C}\big) \simeq \mathrm{Mod}_{\mathrm{ak}}(\mathbb{K}_{\mathrm{lin}},\mathcal{C}),$$

*where the right side is the category of typed realizations satisfying all declared relations and carrying every declared packet idempotent to a split idempotent.*

*Proof.* There are four universal stages.

*Free typed stage.* The free $\Bbbk$-linear category on $Q$ is universal for assigning objects to vertices and morphisms to arrows.

*Relation stage.* Quotienting by $I$ imposes exactly the declared linear, packet, and refinement equations. A functor out of $\Bbbk Q/I$ is therefore the same as a typed realization satisfying those equations.

*Additive stage.* Every $\Bbbk$-linear functor from $\Bbbk Q/I$ into an additive category extends, uniquely up to canonical natural isomorphism, to an additive functor from the finite additive hull by sending a tuple to the corresponding biproduct and a matrix to its induced biproduct map.

*Idempotent-splitting stage.* Every additive functor into an idempotent-complete category extends, again uniquely up to canonical natural isomorphism, across the Karoubi envelope by sending $(A, e)$ to the chosen image of the split idempotent $F(e)$. Morphisms satisfying $f = dfe$ descend to the corresponding split summands.

Composing these universal properties yields the displayed equivalence. Smallness is preserved because only finite tuples and idempotents in hom sets of a small category are adjoined. □

**Proposition 3.37** (Fully faithful grammar embedding)**.** *The canonical composite*

$$\mathcal{A}_{\mathbb{K}} \longrightarrow \mathrm{Add}(\mathcal{A}_{\mathbb{K}}) \longrightarrow \mathrm{Kar}(\mathrm{Add}(\mathcal{A}_{\mathbb{K}}))$$

*is fully faithful. Thus the envelope adds finite biproducts and split summands without identifying two previously distinct grammar morphisms.*

*Proof.* The first functor sends an object to the one-term tuple and preserves its hom set exactly. The second sends $A$ to $(A, 1_A)$; its morphism condition is $f = 1_B f 1_A$, which imposes no additional relation. □

**Corollary 3.38** (Declared packets become literal objects)**.** *Every declared idempotent $p : X \to X$ defines an object $(X, p)$ of $\mathrm{Syn}_{\mathrm{ak}}(\mathbb{K}_{\mathrm{lin}})$. A complete packet family $(p_i)$ gives the canonical isomorphism*

$$(X, 1_X) \cong \bigoplus_i (X, p_i).$$

**Corollary 3.39** (Linear resolved strata as model categories)**.** *Every additive split-idempotent realization stratum of $\mathbb{K}_{\mathrm{lin}}$ is a category of profile-preserving functors out of $\mathrm{Syn}_{\mathrm{ak}}(\mathbb{K}_{\mathrm{lin}})$.*

**Example 3.40** (One operator and primary packets)**.** Take one sort, one endomorphism $T$, and one relation $\mu(T) = 0$. The linear grammar algebra is $\Bbbk[x]/(\mu)$. When

$$\mu = \mu_1 \cdots \mu_r$$

is a product of pairwise comaximal factors, the Chinese remainder idempotents define packet objects for the primary summands. The envelope splits those idempotents formally. Over a realization where the same factorization remains valid, the packet objects become the corresponding invariant primary sectors.

*Remark* 3.41 (Universal does not mean presentation-minimal)*.* The envelope is universal for realizations of the declared presentation. It does not provide a canonical smallest quiver, decide equivalence of arbitrary presentations, or identify a globally minimal packet system. Those are recognition or minimization problems inside particular strata.

### 3.6 Profile-indexed extensions and the exact boundary of Foundation layer

**Definition 3.42** (Profile-indexed resolved envelope)**.** For a preservation profile $\Pi$, a profile-indexed resolved envelope $\mathrm{Syn}_{\Pi}(\mathbb{K})$, when it exists, is a universal source satisfying

$$\mathrm{Mod}_{\Pi}(\mathbb{K}, \mathcal{C}) \simeq \mathrm{Fun}_{\Pi}(\mathrm{Syn}_{\Pi}(\mathbb{K}), \mathcal{C})$$

for every target category $\mathcal{C}$ carrying the structures named by $\Pi$. The equivalence must preserve the chosen comparison data, not only the underlying functors.

**Table 3:** Profile extensions beyond the proved additive-Karoubi core.

| Doctrine | Additional data required | Boundary |
|---|---|---|
| Nonlinear / operadic | colored finite-arity operations, symmetric actions, substitution, coherence | available locally in the nonlinear packet calculus, not freely present in every stratum |
| Banach / topological | topology, boundedness, convergence mode, completion and quotient-topology rules | algebraic packet sums do not choose a topology |
| $C^*$ / $W^*$ | involution, norm, positivity, closure, multiplier or weak completion | faithful corner realization does not automatically preserve an independent tensor product |
| Countable packets | strong, norm, weak, or unconditional convergence with boundedness controls | finite identities do not determine the infinite convergence doctrine |
| Monoidal / Tannakian | tensor product, unit, coherence, exact faithful fiber functor when reconstruction is claimed | ordinary faithful representation is weaker than monoidal reconstruction |
| Arithmetic / local | integral models, reductions, valuations, completeness, residue and lift data | denominator and reduction hypotheses remain domain-specific |

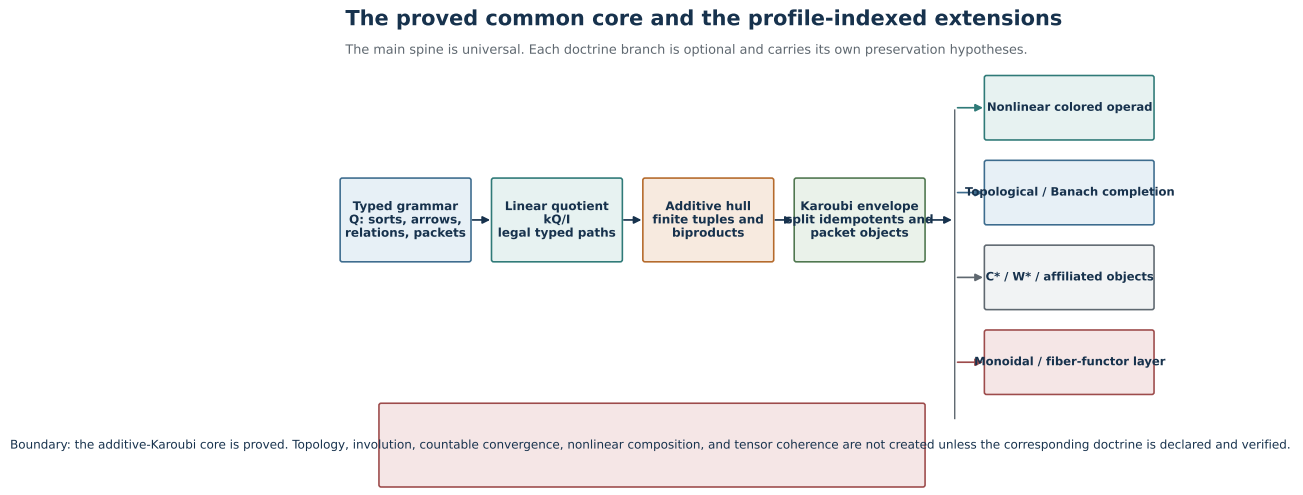



**Figure 3:** The proved common envelope and the optional profile branches. The branches should be added only for the strata that actually preserve them.

*Boundary* 3.43 (No single overpowered envelope). The existence of $\mathrm{Syn}_{\mathrm{ak}}$ does not prove the existence of one universal category simultaneously free, complete, $C^*$, $W^*$, nonlinear-operadic, monoidal, and arithmetically integral in a way preserved by every target. The mathematically safer target is a family of profile-indexed envelopes or a doctrine-valued construction with explicit forgetful and comparison maps.

**Section result.** The foundational language is now explicit at four levels: typed grammar semantics, exact finite packet and residual calculus, proof-support-controlled theorem transport, and the universal additive-Karoubi envelope. The nonlinear, analytic, operator-algebraic, monoidal, and arithmetic envelopes remain separate profile obligations rather than hidden assumptions.

# 4 Strata, normalized charts, typed bridges, and obstruction objects

The common envelope developed in Section 3 is deliberately weaker than most concrete mathematical domains. The next layer records how that envelope is realized, normalized, compared, and sometimes only partially remembered. The central organizing rule is that a chart is not specified by a list of examples. It is specified by a category of models, a preservation profile, a semantic functor, a normalized classification target, and explicit overlap data.

## 4.1 Stratum passports and normalized model categories

**Definition 4.1** (Profiled stratum passport)**.** A profiled Komorebi stratum is a record

$$\mathbf{S}_\alpha = (\mathcal{C}_\alpha, \Pi_\alpha, \mathcal{M}_\alpha, \mathcal{N}_\alpha, \mathrm{Sem}_\alpha, \mathcal{I}_\alpha),$$

with the following fields.

(i) $\mathcal{C}_\alpha$ is the ambient semantic category in which the realized objects live.

(ii) $\Pi_\alpha$ is the verified preservation profile of the realization.

(iii) $\mathcal{M}_\alpha$ is a full replete category of admissible models of the declared resolved syntax.

(iv) $\mathcal{N}_\alpha \subseteq \mathcal{M}_\alpha$ is a full replete normalized subcategory on which the intended inverse or classification theorem is stated.

(v)
$$\mathrm{Sem}_\alpha : \mathcal{M}_\alpha \longrightarrow \mathcal{O}_\alpha$$
is the native semantics functor.

(vi)
$$\mathcal{I}_\alpha : \mathrm{Core}(\mathcal{N}_\alpha) \longrightarrow \mathcal{D}_\alpha$$
is a declared invariant functor, when one has been constructed. Its codomain $\mathcal{D}_\alpha$ and classification target are part of the record.

The original four-field stratum $(\mathcal{C}_\alpha, \Pi_\alpha, \mathcal{M}_\alpha, \mathrm{Sem}_\alpha)$ remains the underlying realization datum. The normalized and invariant fields are additional assembly data rather than automatic consequences.

**Definition 4.2** (Normalization witness)**.** A normalization witness on a full subcategory $\mathcal{U}_\alpha \subseteq \mathcal{M}_\alpha$ consists of a functor

$$N_\alpha : \mathcal{U}_\alpha \longrightarrow \mathcal{N}_\alpha$$

and a natural isomorphism

$$\nu_\alpha : \mathrm{Sem}_\alpha N_\alpha \Longrightarrow \mathrm{Sem}_\alpha |_{\mathcal{U}_\alpha}.$$

It is *classification-normalizing* when every object of $\mathcal{U}_\alpha$ is semantically isomorphic to its image, and two normalized objects with isomorphic semantics are isomorphic in $\mathcal{N}_\alpha$. A normalization may be partial, domain-restricted, or defined only after auxiliary choices. Those restrictions belong to the passport.

**Definition 4.3** (Complete invariant on a declared target)**.** An invariant $\mathcal{I}_\alpha$ is complete on $\mathcal{N}_\alpha$ when

$$\mathcal{I}_\alpha(X) \cong \mathcal{I}_\alpha(Y) \quad \Longleftrightarrow \quad X \cong Y$$

for all $X, Y \in \mathcal{N}_\alpha$. This statement classifies the objects of $\mathcal{N}_\alpha$ up to the isomorphisms allowed there. It does not classify arbitrary presentations outside that subcategory.

**Proposition 4.4** (Semantic conservativity of a normalized chart)**.** *If $N_\alpha$ is classification-normalizing, then*

$$\mathrm{Sem}_\alpha |_{\mathcal{N}_\alpha}$$

*reflects isomorphisms. Consequently, a complete invariant on $\mathcal{N}_\alpha$ can be transported through a reversible overlap only after the overlap is shown to preserve the normalization and reflect the relevant isomorphisms.*

*Proof.* Let $X, Y \in \mathcal{N}_\alpha$ and suppose their semantic objects are isomorphic. The second clause of definition 4.2 gives $X \cong Y$. The final statement follows because completeness is an assertion about isomorphism classes, not merely about equality of numerical outputs. □

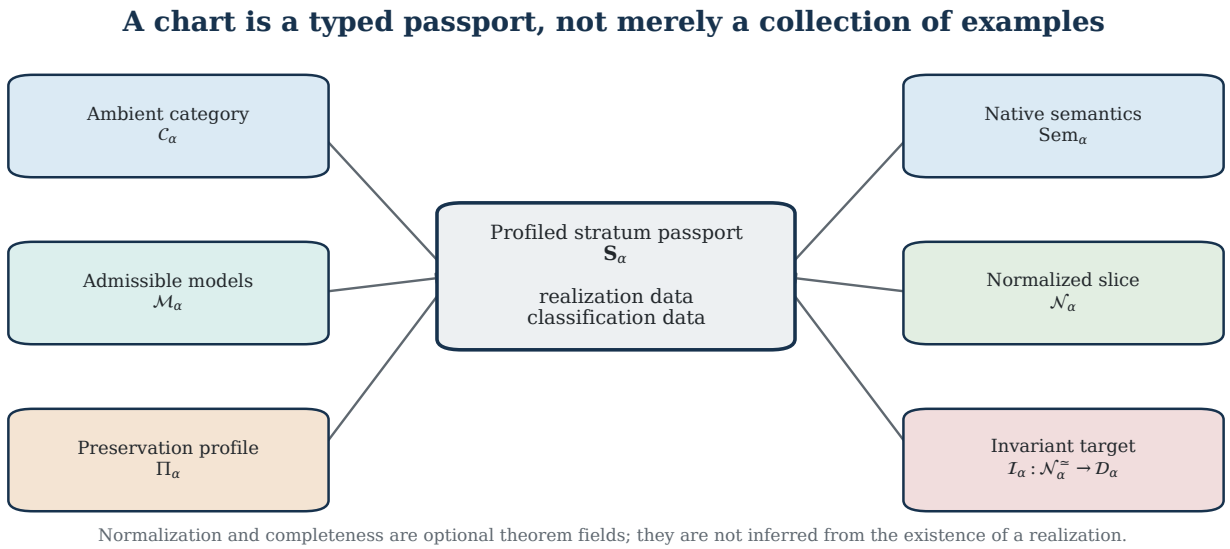



**Figure 4:** A stratum passport separates the ambient category, admissible models, preservation profile, semantics, normalization, and invariant target. Omitting any one of these fields makes cross-stratum classification claims ambiguous.

The present program uses the following principal strata. The normalized fields are intentionally narrower than the ambient strata. Several rows have exact slices but no canonical normalization for the whole broad class [7, 6, 8, 9].

**Table 4:** Current stratum passports at the level supported by the audited Library. A dash means that no whole-stratum normalization theorem is asserted.

| Stratum | Native objects | Native morphisms | Normalized or exact slice | Exact coordinate or invariant already available | Remaining boundary |
|---|---|---|---|---|---|
| Finite linear and C-finite | finite recurrences, rational OGFs, finite linear states | intertwiners, recurrence changes, similarity | minimal recurrence, reduced OGF, reachable-observable state | Hankel rank, reduced denominator degree, minimal state dimension, torsion–Fourier subsequence profile | no classification of arbitrary nonminimal or mixed-grammar presentations |
| Holonomic | P-recursive sequences, D-finite functions, differential modules | coefficient/differential intertwiners | fixed operator convention and selected local data | effective P-recursive–D-finite translation; finite annihilator modules | minimal multisection operators, singularity orbits, monodromy aliasing, and cancellation signatures |
| Digital | DFAO, finite digit kernels, regular linear representations | state maps and radix-compatible intertwiners | minimal DFAO for fixed radix and reading direction | unique minimal DFAO up to state renaming; exact finite $k$-kernel compilation | no all-moduli packet profile or general linear-state minimality for $k$-regular systems |
| Algebraic | selected algebraic branches and packet polynomial systems | branch-preserving polynomial maps | a declared branch with a fixed defining system | exact packet polynomial realization and synthesis | minimal system dimension, branch-collision data, and effective packet-degree bounds |
| Nonlinear/tree | packet jets, colored operations, rooted-tree systems | operadic substitutions and smooth intertwiners | marked polynomial fixed points; positive simply generated tree families | packet Faà di Bruno law, diagonal profile compression, SCC cyclic core, arity-gcd support and dominant-orbit signature | no global nonlinear normal form, mixed-direction universal compression, or coordinate-free minimal system dimension |
| Product and multiplicative | filtered Euler products, prime-power seed systems | exponent and local-factor maps | fixed Euler basis or declared multiplicative class | unique Euler exponents in the fixed basis; exact reconstruction from prime-power seeds | no canonical factorization across arbitrary product grammars and no general additive–multiplicative equivalence |
| Local, Mahler, and polyphase | Newton–Mahler coordinates, affine branches, functional masks, local states | affine restriction, refinement, Cartier and polyphase maps | fixed local chart and fixed modulus/radix conventions | unique Mahler coordinates, exact affine-polyphase transfer, exact Cartier automata for rational masks | no canonical global local normal form and no unrestricted bridge between functional and Newton–Mahler theories |
| Galois and Tannakian | semilinear packets, fixed-field charts, tensor representations | equivariant maps, induction/restriction, tensor morphisms | finite separable semisimple descent or neutral Tannakian fiber functor | Hilbert 90 descent, Brauer obstruction, subgroup/fixed-field classification, tensor reconstruction | modular and wild cases, and monoidal reconstruction without a verified fiber functor |

*Boundary* 4.5 (Multiple valid placements). A semantic object may occur in several strata. Catalan numbers, for example, may be algebraic, hypergeometric, P-recursive, and tree-generated. The atlas records these as distinct presentations with certified bridges. It does not force one placement to erase the others.

### 4.2 Representation groupoids, gauge levels, and the directed transformation category

For every stratum, the invertible part is the maximal subgroupoid

$$\mathfrak{Rep}_\alpha(\mathbb{K}) = \mathrm{Core}(\mathcal{M}_\alpha).$$

This core records changes of presentation that preserve all structure required by the overlap. Quotients, truncations, completions, specializations, differential annihilator maps, and compression maps generally remain outside it.

**Definition 4.6** (Finite coordinate action groupoid)**.** Fix a dimension vector $\mathbf{d} = (d_X)_{X\in\mathsf{S}}$. Let

$$G_{\mathbf{d}} = \prod_{X\in\mathsf{S}} GL_{d_X}(\mathbb{k})$$

act on the finite-dimensional representation space $\mathrm{Rep}_{\mathbf{d}}(\mathbb{K})$ by base change. The action groupoid

$$[\mathrm{Rep}_{\mathbf{d}}(\mathbb{K})/G_{\mathbf{d}}]$$

has representations as objects and coordinate changes carrying one representation to another as morphisms.

**Proposition 4.7** (Coordinate groupoid realizes isomorphism)**.** *Two objects of* $\mathrm{Rep}_{\mathbf{d}}(\mathbb{K})$ *are isomorphic as typed realizations exactly when they lie in the same* $G_{\mathbf{d}}$*-orbit. The stabilizer of a point is its coordinate automorphism group.*

*Proof.* A typed isomorphism is a family of invertible linear maps on the sort spaces intertwining every generating operation. This is precisely an element of $G_{\mathbf{d}}$ carrying one coordinate tuple to the other. Elements fixing the tuple are exactly the typed automorphisms. □

Three symmetry levels must remain separate.

**Table 5:** Three noninterchangeable symmetry notions.

| Symmetry level | Acting object | What it changes or preserves | Extra hypothesis |
|---|---|---|---|
| Gauge symmetry | coordinate-change group $G_{\mathbf{d}}$ or a local gauge family | changes presentation coordinates while preserving the represented object | an explicitly typed action on the chart |
| Intrinsic symmetry | $\mathrm{Aut}_{\mathcal{M}_\alpha}(M)$ | automorphisms of one resolved object inside the stratum | none beyond the native category |
| Reconstructed symmetry | $\mathrm{Aut}^{\otimes}(\omega)$ | tensor automorphisms of a fiber functor and the corresponding affine group scheme | faithful exact tensor fiber functor |

**Definition 4.8** (Typed directed transformation category)**.** The directed transformation category $\mathfrak{Dir}(\mathbb{K})$ has pairs $(\alpha, M)$, with $M \in \mathcal{M}_\alpha$, as objects. A morphism

$$(\alpha, M) \longrightarrow (\beta, N)$$

is an admitted bridge instance equipped with a bridge passport as in definition 4.10. Composition is defined only when the codomain profile of the first bridge satisfies the domain requirements of the second. The union of the representation groupoids embeds as the wide invertible subcategory.

*Boundary* 4.9 (Invertibility is evidence, not typography). Drawing a two-headed arrow does not make a bridge reversible. A bridge enters the representation groupoid only after an inverse, quasi-inverse, or recognition theorem has been proved on a named overlap category.

### 4.3 Bridge passports, bridge classes, and information-loss profiles

**Definition 4.10** (Bridge passport)**.** A certified bridge from stratum $\alpha$ to stratum $\beta$ is a record

$$\mathfrak{b} = (\mathcal{U}_\mathfrak{b}, \mathcal{V}_\mathfrak{b}, B_\mathfrak{b}, \tau_\mathfrak{b}, \Pi^{\mathrm{pres}}_\mathfrak{b}, \Pi^{\mathrm{refl}}_\mathfrak{b}, \Lambda_\mathfrak{b}, \nu_\mathfrak{b}, \chi_\mathfrak{b}),$$

where:

(i) $\mathcal{U}_\mathfrak{b} \subseteq \mathcal{M}_\alpha$ and $\mathcal{V}_\mathfrak{b} \subseteq \mathcal{M}_\beta$ are the declared domain and codomain subcategories;

(ii) $B_\mathfrak{b} : \mathcal{U}_\mathfrak{b} \to \mathcal{V}_\mathfrak{b}$ is the functor;

(iii) $\tau_\mathfrak{b}$ is its bridge class;

(iv) $\Pi^{\mathrm{pres}}_\mathfrak{b}$ records preserved constructors and universal properties;

(v) $\Pi^{\mathrm{refl}}_\mathfrak{b}$ records properties or isomorphisms reflected by the bridge;

(vi) $\Lambda_\mathfrak{b}$ is the information-loss profile;

(vii) $\nu_\mathfrak{b}$ is the semantic comparison map;

(viii) $\chi_\mathfrak{b}$ records normalization, residual, and certificate compatibility.

A passport may state that no inverse or no certificate transport is known. Missing data remain missing rather than being inferred from analogy.

The permitted bridge classes follow the work program in the controlling handoff.

**Definition 4.11** (Information-loss profile)**.** For a functor $B : \mathcal{U} \to \mathcal{V}$, its information-loss profile contains at least:

$$\begin{aligned} \mathrm{MorKer}_B(X, Y) &= \{(f, g) \in \mathrm{Hom}_\mathcal{U}(X, Y)^2 : Bf = Bg\}, \\ \mathrm{Coll}_B &= \{(X, Y) \in \mathrm{Ob}(\mathcal{U})^2 : BX \cong BY\}, \\ \mathrm{EssIm}(B) &\subseteq \mathcal{V}, \end{aligned}$$

together with the declared constructors, packet labels, residuals, certificates, branch data, topology, or arithmetic structure not preserved by $B$. The first component records morphism collapse, the second object collapse, and the third which target objects actually arise.

**Definition 4.12** (Faithfulness, conservativity, and reversibility)**.** A bridge is:

**Table 6:** Bridge classes used by the concrete atlas.

| Class | Required evidence | Interpretation |
|---|---|---|
| Equivalence | quasi-inverse and coherent unit/counit | reversible overlap of presentation groupoids |
| Fully faithful inclusion | bijections on hom-sets and full image description | no morphism loss inside the image, but possibly a smaller chart |
| Conservative forgetful functor | reflected isomorphisms | object equivalence remains detectable although structure may be forgotten |
| Information-losing directional functor | explicit semantic and loss statement | quotient, projection, annihilator, reduction, or compression |
| Constructor | proof that source data generate a target object | one-way realization, often with nonunique inverse data |
| Completion | topology and universal completion property | adds limits or closes a domain; reversibility requires a recognition theorem |
| Partially defined bridge | exact domain predicate | valid only on a named locus, branch, modulus, or regularity class |
| No certified bridge | none | no arrow is inserted into the trusted atlas |

(i) *morphism-faithful* when every $\mathrm{MorKer}_B(X, Y)$ is diagonal;

(ii) *conservative* when $Bf$ invertible implies that $f$ is invertible;

(iii) *classification-faithful* or *essentially injective on objects* when $BX \cong BY$ implies $X \cong Y$ on the declared domain;

(iv) *lossless on its image* when it is fully faithful;

(v) *reversible* when it is an equivalence onto the declared overlap.

These conditions answer different questions and should not be conflated.

**Proposition 4.13** (Composition law for bridge loss)**.** *Let*

$$\mathcal{U} \xrightarrow{B} \mathcal{V} \xrightarrow{C} \mathcal{W}$$

*be certified bridges.*

(i) *Every constructor or universal property preserved by both $B$ and $C$ is preserved by $CB$.*

(ii)
$$\mathrm{MorKer}_B(X, Y) \subseteq \mathrm{MorKer}_{CB}(X, Y).$$

(iii)
$$\mathrm{Coll}_B \subseteq \mathrm{Coll}_{CB}\,.$$

(iv)
$$\mathrm{EssIm}(CB) \subseteq \mathrm{EssIm}(C).$$

(v) *If both bridges are conservative, then their composite is conservative. If both are classification-faithful, then their composite is classification-faithful. If both are equivalences, then their composite is an equivalence.*

*Thus information forgotten at an earlier stage cannot be recovered by merely composing more forgetful bridges, although a later bridge may attach auxiliary data through a separate constructor.*

*Proof.* Functoriality proves the preservation claim. If $Bf = Bg$, then $CBf = CBg$, proving the second inclusion. If $BX \cong BY$, applying $C$ gives $CBX \cong CBY$, proving the third. Every object in the essential image of $CB$ is visibly in the essential image of $C$. For conservativity, if $CBf$ is invertible then $Bf$ is invertible because $C$ is conservative, and then $f$ is invertible because $B$ is conservative. For classification-faithfulness, $CBX \cong CBY$ implies $BX \cong BY$ and then $X \cong Y$. Composition of equivalences is standard. □

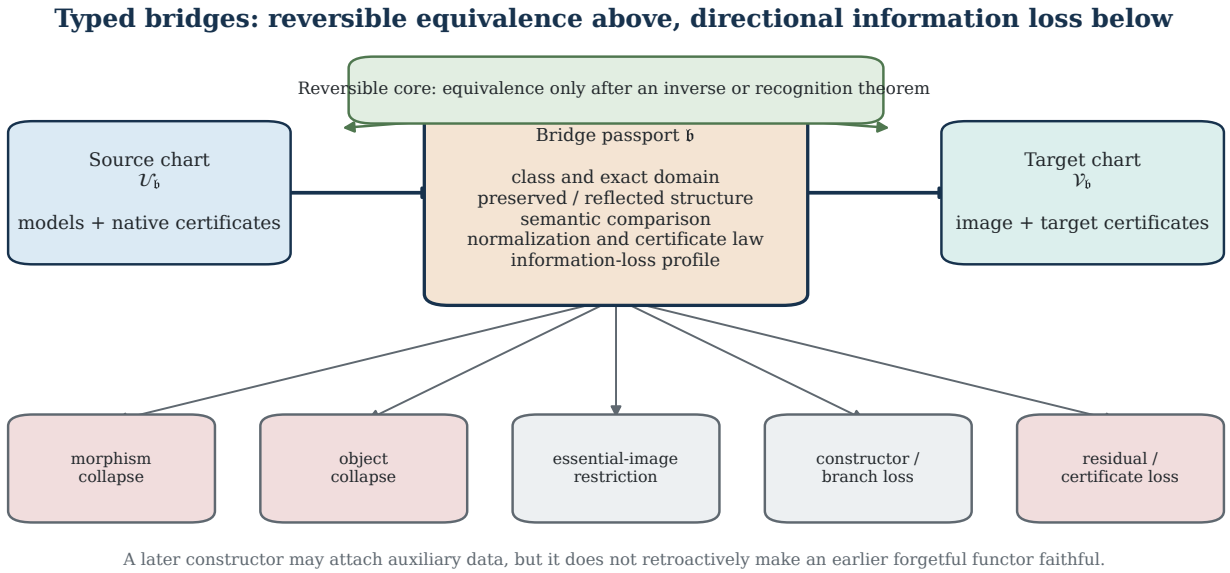



**Figure 5:** A bridge passport separates reversible equivalence from directional transformation and records the dimensions of information loss. The reversible core is a theorem-level subcategory, not an informal interpretation of the whole bridge.

Three typing cautions are especially important.

1. A selected algebraic branch can produce a D-finite annihilator, but the operator may forget the selected branch and its minimal polynomial. The bridge is directional unless that data are retained.
2. A rational functional-Mahler mask over $\mathbf{F}_p$ produces a Cartier representation and finite automaton under the stated hypotheses, but this does not identify it with a Newton–Mahler interpolation chart [8, 7].
3. A faithful Hilbert-space corner representation realizes packet projectors and transfers, but it does not automatically preserve a tensor product strongly enough for Tannakian reconstruction [2, 6].

### 4.4 Overlap categories and bridge-law certificates

**Definition 4.14** (Typed overlap)**.** A reversible overlap between strata $\alpha$ and $\beta$ consists of full replete subcategories

$$\mathcal{M}_{\alpha\beta} \subseteq \mathcal{M}_\alpha, \qquad \mathcal{M}_{\beta\alpha} \subseteq \mathcal{M}_\beta,$$

an equivalence

$$\Phi_{\alpha\beta} : \mathcal{M}_{\alpha\beta} \xrightarrow{\sim} \mathcal{M}_{\beta\alpha},$$

and a semantic natural isomorphism

$$\sigma_{\alpha\beta} : J_{\alpha\beta}\,\mathrm{Sem}_\alpha \Longrightarrow \mathrm{Sem}_\beta\,\Phi_{\alpha\beta}$$

for an explicitly declared comparison functor $J_{\alpha\beta}$ between the observable doctrines. An overlap is *normalized* when the equivalence restricts to the selected normalized subcategories.

**Definition 4.15** (Bridge-law certificate)**.** A bridge-law certificate for $B : \mathcal{U} \to \mathcal{V}$ records commuting or naturally commuting diagrams for each structure used downstream:

(i) native semantics;

(ii) packet analysis and synthesis;

(iii) refinement and coarsening maps;

(iv) selected-support compression and named residuals;

(v) proof or computation certificates;

(vi) normalization and invariant comparison maps.

For example, packet naturality requires comparison maps under which

$$B(p_{Y,b} f p_{X,a}) \cong p'_{B(Y),b}\,B(f)\,p'_{B(X),a},$$

and refinement naturality requires the image of each coarse packet to equal the declared sum of its refined descendants.

**Proposition 4.16** (Bridge-law transport)**.** *Let $\mathcal{P}$ be a proof whose constructor support lies in the preserved part of a bridge-law certificate. Then the image proof is valid in the target chart. If the proof concludes equality of normalized invariants, that equality descends across the bridge only when the normalization and invariant comparison maps are also included in the certificate.*

*Proof.* The first statement is the equational realization principle of Paper I applied with the bridge-specific preservation profile. The second statement follows because normalization and invariant functors are additional constructors in the proof diagram; they cannot be transported when their comparison cells are absent [1]. □

On triple overlaps, pairwise equivalences are not enough. One needs comparison cells

$$\eta_{\alpha\beta\gamma} : \Phi_{\beta\gamma}\Phi_{\alpha\beta} \Longrightarrow \Phi_{\alpha\gamma}.$$

For four charts, there are two composites from $\Phi_{\gamma\delta}\Phi_{\beta\gamma}\Phi_{\alpha\beta}$ to $\Phi_{\alpha\delta}$. Their ratio is the higher coherence defect.

**Definition 4.17** (Quadruple-overlap coherence defect)**.** Write horizontal composition of natural transformations as $*$. Define

$$\Omega_{\alpha\beta\gamma\delta} = \Big[\eta_{\alpha\gamma\delta} \circ (\mathrm{id} * \eta_{\alpha\beta\gamma})\Big] \circ \Big[\eta_{\alpha\beta\delta} \circ (\eta_{\beta\gamma\delta} * \mathrm{id})\Big]^{-1}.$$

It is a natural automorphism of $\Phi_{\alpha\delta}$ on the quadruple overlap. The atlas is coherent there exactly when

$$\Omega_{\alpha\beta\gamma\delta} = \mathrm{id}.$$

**Proposition 4.18** (Two elementary coherence mechanisms)**.** *The coherence defect vanishes in either of the following situations.*

(i) *All overlap functors compose strictly and every comparison cell is the identity.*

(ii) *Between each pair of relevant normalized objects there is at most one admissible comparison isomorphism compatible with semantics.*

*Proof.* The first case is immediate. In the second case, the two sides of the coherence equation are admissible comparison isomorphisms with the same source and target. Uniqueness forces them to agree. This is the mechanism used later in the normalized C-finite three-chart atlas. □

*Boundary* 4.19 (Prestack versus stack). Typed overlap functors and coherent comparison cells define atlas or prestack data. The word *stack* additionally requires effective descent: compatible local objects and morphisms must arise from global ones in the declared category.

### 4.5 Reversible cores inside directional bridges

Directional maps can contain a canonical reversible overlap without being globally invertible. Split packet analysis is the basic model.

**Theorem 4.20** (Split bridge rectification)**.** *Let $\mathcal{A}$ be an additive idempotent-complete category and suppose*

$$X \xrightarrow{A} Y \xrightarrow{L} X$$

*satisfies $LA = \mathrm{id}_X$. Put $E = AL$. Then:*

(i) $E^2 = E$;

(ii) $Y \cong \operatorname{im} E \oplus \operatorname{im}(1 - E)$;

(iii) $A : X \to \operatorname{im} E$ *is an isomorphism with inverse induced by* $L$;

(iv) $L(1 - E) = 0$, *so* $\operatorname{im}(1 - E)$ *is a named residual invisible to the decoder;*

(v) *the directional two-chart system becomes reversible after restricting the packet chart to the consistent core* $\operatorname{im} E$.

*In a module or vector-space realization,* $\operatorname{im}(1 - E) = \ker L$.

*Proof.* The identity $E^2 = A(LA)L = AL = E$ proves the first statement. Idempotent completeness splits $E$, producing the direct sum. The image of $A$ lies in $\operatorname{im} E$, and $LA = \mathrm{id}_X$ while $AL = E$ acts as the identity on $\operatorname{im} E$, so the restricted maps are inverse. Finally,

$$L(1 - E) = L - LAL = L - L = 0.$$

For modules, every $y \in \ker L$ satisfies $(1 - E)y = y$, while every vector in $\operatorname{im}(1 - E)$ is killed by $L$. □

**Corollary 4.21** (Exact meaning of a decoded packet core)**.** *A left inverse proves exact recovery on the consistent packet core. It does not prove that every ambient packet vector is consistent, that the residual is small, or that the packet representation is compressed. Those are separate geometric, analytic, or coding claims.*

The integral Mahler packet theorem is a concrete instance: the analysis matrix has an integer left inverse, the consistency projector is $AL$, and the residual is the complementary packet component. The same decoder survives every base change, while rank loss of individual residue channels remains visible after reduction [5].

### 4.6 Finite holonomy and the maximal path-flat core

Finite graph transport gives the sharpest reversible gluing model in the Library. Let $\Gamma = (V, E)$ be a finite connected graph. Attach a finite-dimensional $\Bbbk$-vector space $F_v$ to each vertex and an isomorphism $T_e : F_u \to F_v$ to each oriented edge $e : u \to v$, with $T_{\bar{e}} = T_e^{-1}$. Choose a root $o$ and spanning tree $S$. If $G_v : F_o \to F_v$ is tree transport, then every non-tree edge $e : u \to v$ has fundamental holonomy

$$H_e = G_v^{-1} T_e G_u \in GL(F_o).$$

Define

$$C_o = \bigcap_{e \notin S} \ker(H_e - I) = \mathrm{Fix}\langle H_e : e \notin S \rangle, \qquad C_v = G_v C_o.$$

**Theorem 4.22** (Maximal flat core and global sections)**.** *Under the preceding hypotheses [3, 5]:*

(i) *evaluation at the root identifies the space of global parallel sections with $C_o$;*

(ii) *$(C_v)_v$ is path-flat, meaning that all path transports with the same endpoints agree on the core;*

(iii) *it is the unique greatest path-flat subfamily;*

(iv) *it is independent of the chosen spanning tree and equals the common fixed space of all closed-path holonomies;*

(v) *for*

$$\Delta_S : F_o \longrightarrow \bigoplus_{e \notin S} F_o, \qquad \Delta_S x = ((H_e - I)x)_{e \notin S},$$

*one has*

$$C_o = \ker \Delta_S, \qquad \dim C_o = \dim F_o - \operatorname{rank} \Delta_S;$$

(vi) *the full fibers glue to one global frame exactly when every fundamental holonomy is the identity;*

(vii) *a gauge change conjugates the holonomies and transports the core, so $\dim C_o$ is gauge-invariant.*

*Proof.* For $x \in C_o$, set $x_v = G_v x$. Tree edges satisfy the parallel relation by construction, and a non-tree edge satisfies it because $H_e x = x$. Conversely, any global section is determined along the tree by its root value; every remaining edge forces that value to be fixed by the corresponding $H_e$. This proves the section classification. Closed paths are words in fundamental cycles, which gives path-flatness and tree independence. Any path-flat family must be fixed by every fundamental cycle and is therefore contained in $(C_v)_v$. The rank formula is rank–nullity. Full flatness and gauge covariance follow from spanning-tree normalization and conjugation of loop products. □

**Corollary 4.23** (Global section versus global frame)**.** *Nonidentity holonomy can leave a nonzero maximal core. Therefore the existence of some global compatible vectors is weaker than the existence of one global frame on the full fibers. The former is measured by $\dim C_o$; the latter requires $C_o = F_o$.*

### 4.7 Relative cokernel obstructions and loss under coarsening

Holonomy addresses compatibility of invertible transports. Correction problems have a different canonical object.

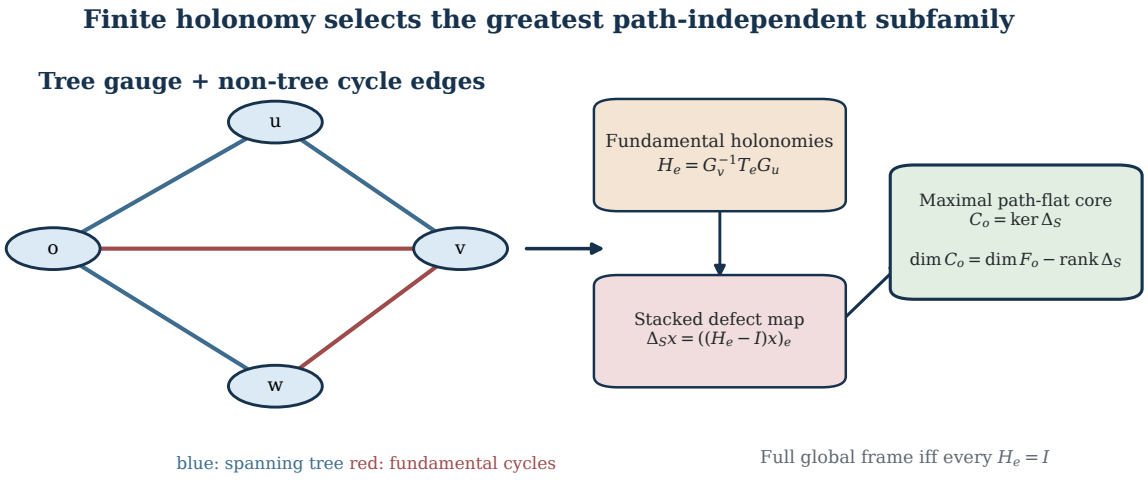



**Figure 6:** A spanning tree removes local gauge redundancy. Each remaining edge contributes a fundamental holonomy. Their common fixed space is the maximal path-flat core; the stacked defect map $\Delta_S$ measures the lost dimension.

**Definition 4.24** (Linear correction datum)**.** A linear correction datum is a map

$$D : U \longrightarrow V$$

and a defect $r \in V$. A correction is $u \in U$ satisfying $Du = -r$. The relative obstruction class is

$$\mathrm{Ob}_D(r) = [r] \in \operatorname{coker} D = V / \operatorname{im} D.$$

**Theorem 4.25** (Cokernel criterion, universality, and naturality)**.** *For a correction datum $(D, r)$ [3]:*

(i) *a correction exists if and only if* $\mathrm{Ob}_D(r) = 0$*;*

(ii) *every linear obstruction test $\varphi : V \to W$ satisfying $\varphi D = 0$ factors uniquely through $V \to \operatorname{coker} D$;*

(iii) *for every commuting square*

$$\begin{array}{ccc} U & \xrightarrow{D} & V \\ \downarrow a & & \downarrow b \\ U' & \xrightarrow{D'} & V', \end{array} \qquad bD = D'a,$$

*there is a unique induced map*

$$\overline{b} : \operatorname{coker} D \longrightarrow \operatorname{coker} D'$$

*with*

$$\overline{b}\ \mathrm{Ob}_D(r) = \mathrm{Ob}_{D'}(br).$$

*Proof.* The class vanishes exactly when $r \in \operatorname{im} D$, which is equivalent to solvability of $Du = -r$. A map annihilating $\operatorname{im} D$ factors uniquely through the quotient. In the square, the quotient map for $D'$, composed with $b$, vanishes on $\operatorname{im} D$, so the same universal property produces $\overline{b}$. □

**Proposition 4.26** (Packet coordinates on the obstruction quotient)**.** *Suppose $(Q_a)$ is a complete finite family of pairwise annihilating idempotents on $V$ and*

$$Q_a(\operatorname{im} D) \subseteq \operatorname{im} D$$

*for every $a$. Then the $Q_a$ descend to quotient idempotents $\overline{Q}_a$ on* coker $D$*,*

$$\operatorname{coker} D \cong \bigoplus_a \overline{Q}_a(\operatorname{coker} D), \qquad \overline{Q}_a \operatorname{Ob}_D(r) = [Q_a r].$$

*If $U$ and $V$ already split into matching packet summands and $D$ is block diagonal, this becomes*

$$\operatorname{coker} D \cong \bigoplus_a \operatorname{coker} D_a.$$

*Off-diagonal correction blocks can couple packet defects, so the block-diagonal hypothesis cannot be omitted.*

*Proof.* The invariance of $\operatorname{im} D$ makes $[v] \mapsto [Q_a v]$ well defined. Idempotence, annihilation, and reconstruction descend to the quotient. In the block-diagonal case the image of $D$ is the direct sum of the images of the restrictions. □

A coarse representation can erase a nonzero fine obstruction. The strengthened Paper III gives the exact bookkeeping device.

**Theorem 4.27** (Relative obstruction exact sequence)**.** *Suppose the diagram*

$$\begin{array}{ccccccccc} 0 & \to & U_0 & \to & U_f & \to & U_c & \to & 0 \\ & & \downarrow D_0 & & \downarrow D_f & & \downarrow D_c & & \\ 0 & \to & V_0 & \to & V_f & \to & V_c & \to & 0 \end{array}$$

*commutes and has exact rows. Then there is a natural exact sequence*

$$\begin{aligned} 0 \longrightarrow \ker D_0 \longrightarrow \ker D_f \longrightarrow \ker D_c \xrightarrow{\delta} \operatorname{coker} D_0 \\ \longrightarrow \operatorname{coker} D_f \longrightarrow \operatorname{coker} D_c \longrightarrow 0. \end{aligned}$$

*If a fine obstruction maps to zero in* coker $D_c$*, then it comes from* coker $D_0$*, the obstruction sector removed by coarsening. Coarse vanishing therefore does not imply fine vanishing.*

*Proof.* This is the direct kernel–cokernel sequence proved in the strengthened Paper III. The connecting map lifts an element of $\ker D_c$ to $U_f$, applies $D_f$, identifies the result in $V_0$, and takes its class modulo $\operatorname{im} D_0$. Exactness verifies independence of the lift and identifies each successive kernel with the preceding image [3, 4]. □

**Example 4.28** (A fine obstruction erased by summation)**.** Take all correction spaces to be zero,

$$V_f = \mathbb{k}^2, \qquad V_c = \mathbb{k}, \qquad p(x, y) = x + y.$$

The fine defect $(1, -1)$ is nonzero in $\operatorname{coker} D_f = V_f$, but its coarse image is zero. It lies entirely in

$$V_0 = \ker p = \operatorname{span}\{(1, -1)\}.$$

This is cancellation by coarsening, not correction of the fine defect.

**Definition 4.29** (Mapping cone)**.** For a cochain map $D : C^\bullet \to E^\bullet$, define

$$\mathrm{Cone}(D)^n = E^n \oplus C^{n+1}, \qquad d_{\mathrm{Cone}}(e,c) = (d_E e + Dc, -d_C c).$$

**Proposition 4.30** (Cohomological correction criterion)**.** *For a cocycle $e \in E^n$, the class of $(e,0)$ in $H^n(\mathrm{Cone}(D))$ vanishes exactly when $[e]$ lies in the image of $H^n(D)$. When the complexes are concentrated in degree zero,*

$$H^0(\mathrm{Cone}(D)) \cong \operatorname{coker} D.$$

*Proof.* The class of $(e,0)$ is a boundary exactly when there are $e' \in E^{n-1}$ and $c \in C^n$ with

$$e = d_E e' + Dc, \qquad d_C c = 0.$$

This is equivalent to $[e] = H^n(D)[c]$. Concentration in degree zero reduces the cone quotient to $E^0/\operatorname{im} D$. □

*Boundary* 4.31 (The correction map is problem data). The cokernel is canonical relative to $D$. The theory does not yet supply one choice-free rule that constructs the correct $D$ for every mathematical problem and every stratum. Calling $[r] \in \operatorname{coker} D$ canonical must not hide this dependence.

## 4.8 Semilinear effectivity, projective descent, and the Brauer class

Galois descent gives a second exact local-to-global model. Its linear and projective cases separate effectivity from obstruction sharply.

**Theorem 4.32** (Effective vector descent by Hilbert 90)**.** *Let $L/K$ be finite Galois with group $G$. Suppose*

$$a_{\sigma\tau} = a_\sigma\, \sigma(a_\tau), \qquad a_\sigma \in GL_n(L),$$

*defines a semilinear packet cocycle. Then there is $B \in GL_n(L)$ such that*

$$a_\sigma = B^{-1}\sigma(B).$$

*The twisted fixed packet*

$$W = (L^n)^{G,\star}$$

*is an $n$-dimensional $K$-vector space and*

$$W \otimes_K L \xrightarrow{\sim} L^n.$$

*Thus every finite linear semilinear atlas of this form is effective [6].*

**Theorem 4.33** (Brauer obstruction to projective packet descent)**.** *Projective semilinear descent data define a class*

$$\alpha \in H^1(G, PGL_n(L)).$$

*The connecting map for*

$$1 \longrightarrow L^\times \longrightarrow GL_n(L) \longrightarrow PGL_n(L) \longrightarrow 1$$

*produces*

$$\delta(\alpha) \in H^2(G, L^\times) = \mathrm{Br}(L/K).$$

*The projective atlas lifts to linear semilinear descent data exactly when $\delta(\alpha) = 0$. When the class is nonzero, the descended object is naturally a module over a central simple $K$-algebra split by $L$, rather than an ordinary $K$-vector space [6].*

*Proof.* This is the nonabelian cohomology exact sequence together with nonabelian Hilbert 90. Vanishing of the connecting class gives a $GL_n(L)$-valued cocycle; theorem 4.32 then trivializes it and constructs the descended vector space. A nonzero class is the classical relative Brauer obstruction. □

**Corollary 4.34** (Projective compatibility is not linear effectivity)**.** *A projective atlas may satisfy every visible overlap equation in $PGL_n$ and still have no global vector-space realization. Projective cocycle coherence and vanishing Brauer class are distinct conditions.*

The tensor reconstruction problem lies beyond ordinary corner realization.

**Theorem 4.35** (Tannakian boundary)**.** *Let $\mathcal{T}$ be a neutral Tannakian category over k and*

$$\omega : \mathcal{T} \longrightarrow \mathrm{Vect}_k$$

*a faithful exact tensor fiber functor. Then*

$$\mathcal{G} = \mathrm{Aut}^{\otimes}(\omega)$$

*is an affine group scheme and*

$$\mathcal{T} \simeq \mathrm{Rep}_k(\mathcal{G})$$

*as tensor categories. A faithful projector-corner representation without verified exact strong monoidal structure does not cross this boundary [6, 2].*

### 4.9 Higher coherence defects and typed obstruction comparison

The four obstruction families now admit a precise comparison. Each starts from different data and answers a different vanishing question.

**Table 7:** Typed obstruction comparison.

| Failure mode | Required datum | Obstruction object | Vanishing consequence | Nonzero meaning |
|---|---|---|---|---|
| Finite transport holonomy | connected graph, invertible edge transports, chosen structure group | fundamental cycle holonomies or the conjugacy class of $\pi_1(\Gamma) \to G$ | one global frame on the full fibers; on a fixed subspace, path-independent transport | path dependence; possibly a smaller nonzero fixed core |
| Relative correction failure | correction map $D : U \to V$ and defect $r$ | $[r] \in \operatorname{coker} D$, or a mapping-cone cohomology class | an allowed correction exists | the defect is outside the declared correction image |
| Projective Galois descent | projective semilinear cocycle over $L/K$ | $\delta(\alpha) \in H^2(G, L^\times) = \mathrm{Br}(L/K)$ | lift to linear descent, then effective vector descent by Hilbert 90 | descent to a twisted central-simple-algebra object rather than an ordinary vector space |
| Higher atlas coherence | pairwise equivalences and comparison 2-cells | $\Omega_{\alpha\beta\gamma\delta}$, a natural automorphism on a quadruple overlap | pseudofunctor coherence of the atlas | pairwise bridges use incompatible conventions or incomplete comparison data |

**Proposition 4.36** (Typed comparison principle for obstruction objects)**.** *An obstruction object transports from one problem to another only after a compatibility morphism for the underlying data has been supplied:*

(i) *commuting squares of correction maps induce maps on cokernels;*

(ii) *group homomorphisms or intertwiners compatible with edge transports induce maps on holonomy data and fixed cores;*

(iii) *morphisms of the relevant central extensions induce maps on cohomological descent obstructions;*

(iv) *modifications of atlas pseudofunctors transport higher coherence defects.*

*Absent such typed data, there is no canonical reduction of one obstruction family to another.*

*Proof.* Each item follows by applying the functorial construction defining the obstruction: quotient universality for cokernels, conjugation or intertwining for path products, functoriality of cohomology for Brauer classes, and naturality of horizontal and vertical composition for coherence cells. Since the input categories and codomains differ, no comparison exists without an explicit map between the inputs. □

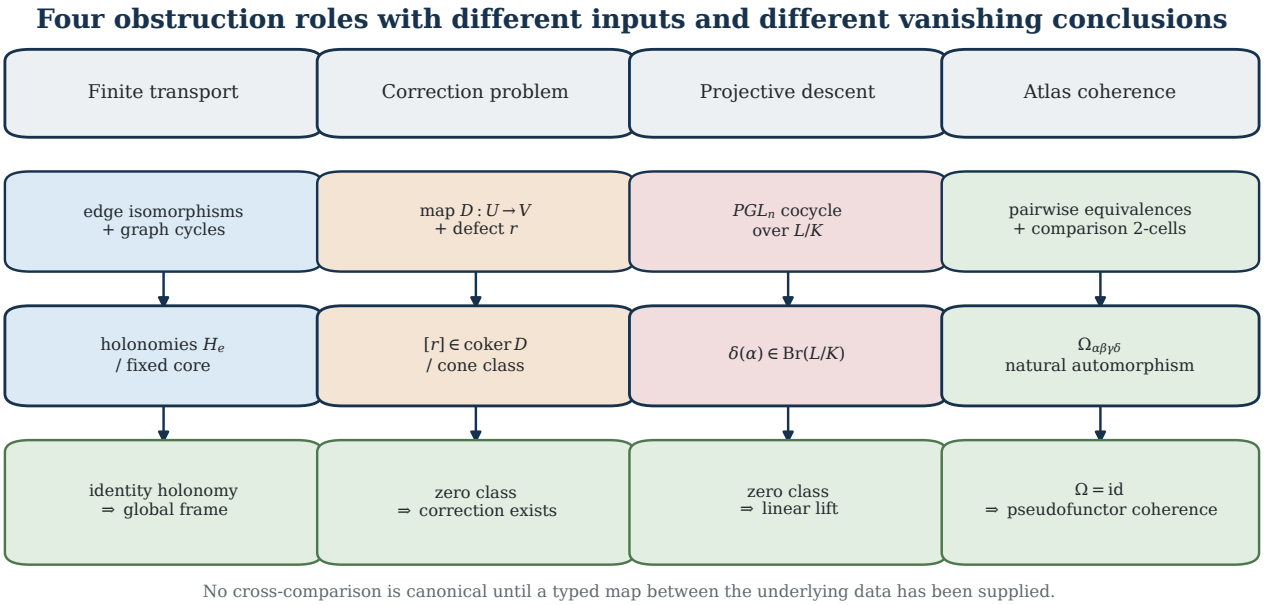



**Figure 7:** Four obstruction pipelines. The word *obstruction* names a role, not one universal scalar. The required input datum determines both the obstruction object and the exact consequence of vanishing.

**Section result.** The atlas layer now has explicit stratum passports, normalized subcategories, representation groupoids, a directed transformation category, bridge classes, information-loss profiles, overlap and bridge-law certificates, and a concrete higher-coherence defect. The four obstruction theories are stated with their own data and vanishing criteria. Finite holonomy supplies a maximal path-flat core, split bridges expose reversible consistent cores inside directional maps, relative cokernels separate correction from coarsening loss, and Galois theory separates Hilbert-90 effectivity from Brauer and Tannakian boundaries. The general heterogeneous atlas is still not declared effective until its actual bridge passports and coherence cells are verified.

**Table 8:** Status distribution in the 75-component theorem concordance.

| Classification | Components |
|---|---|
| proved internally | 52 |
| classical input | 12 |
| proved conditionally | 2 |
| framework only | 3 |
| conjectural | 6 |
| **Total** | **75** |

**Table 9:** Concordance coverage by mathematical domain.

| Domain | Components |
|---|---|
| Foundations | 17 |
| Groupoids and descent | 7 |
| Obstruction theory | 4 |
| Galois stratum | 4 |
| Linear stratum | 3 |
| Holonomic stratum | 1 |
| Digital stratum | 2 |
| Algebraic stratum | 1 |
| Transform stratum | 1 |
| Product stratum | 1 |
| Multiplicative stratum | 1 |
| Local stratum | 3 |
| Functional Mahler stratum | 3 |
| Assembly | 9 |
| Semantic quotient calculus | 7 |
| Bridge loss calculus | 2 |
| Carrier and observer change | 5 |
| Convex and admissibility change | 3 |
| Doctrine comparison | 1 |

# 5 The theorem concordance and edition control

## 5.1 Audit result

The concordance contains 56 components. Thirty-eight are proved internally, eight are classical theorems imported and reinterpreted, two are proved conditionally, two are definition or framework rows, and six remain conjectural. The new foundations row records the finite profiled Universal Lane Transport Theorem. The conjectural entries remain concentrated in the cross-stratum assembly layer. The local packet, obstruction, Galois, sequence, and Mahler components are substantially more complete than an older open-question ledger suggests.

## 5.2 Material supersession decisions

Three corrections are mathematically consequential.

**Relative obstruction theory.** Older Paper III editions leave a broad universal packet-obstruction principle conjectural. The strengthened edition replaces the finite-projector formulation by the relative class $[r] \in \operatorname{coker} D$, with vanishing, naturality, packet decomposition, quotient projectors, relative exact sequences, and mapping-cone formulations proved for declared correction data [3, 4]. The unresolved problem is not the quotient construction itself. It is a choice-free mechanism assigning the appropriate correction datum to arbitrary problems and strata.

**Paper I edition policy.** The complete symbolic core remains the theorem-ID and proof-status spine. The expanded clarified edition strengthens exposition and hypotheses without replacing the stable record identifiers [1].

**Core-Transfer status.** Addendum 04 replaces the isolated $m = 6, d = 3$ boundary by the exact composite-modulus rank law, sharp integral packet minimum, universal decoder, and all-degree stabilization [5]. The former example is now a sharp negative control inside a general theorem.

### 5.3 Existing bridges and exact invariant slices

The strongest source edition already contains the following exact or effective bridges on declared domains:

- constant recurrence $\leftrightarrow$ rational ordinary generating function $\leftrightarrow$ finite linear state;
- P-recursive $\leftrightarrow$ D-finite coefficient translation;
- finite digit realization $\leftrightarrow$ finite $k$-kernel;
- rational functional-Mahler mask $\rightarrow$ Cartier representation $\rightarrow$ finite automaton;
- finite-mask Cartier transitions $\leftrightarrow$ carry matrices;
- selected algebraic branch $\rightarrow$ packet polynomial system;
- invertible transform $\leftrightarrow$ transported packet resolution;
- Euler-product exponent coordinates $\leftrightarrow$ logarithmic-derivative recurrence data;
- finite modular state $\rightarrow$ local Newton-Mahler interpolation;
- local Mahler coordinates $\leftrightarrow$ affine polyphase branches;
- finite resolved $C^*$-system $\rightarrow$ faithful Hilbert packet realization.

The persistent C-finite stratum has the strongest complete transfer invariant. Active spectral and torsion-phase data determine the exact minimal recurrence, reduced denominator, Hankel rank, state dimension, rank drops, and periodic packet profile of every arithmetic subsequence [7]. Restricted exact coordinate systems also exist for fixed-radix automata, filtered Euler products, multiplicative prime-power seeds, local Mahler charts, finite semisimple Galois descent, and finite seed lattices. None of these restricted results is a single all-stratum classifier.

## 6 Finite profiled resolved atlas assembly

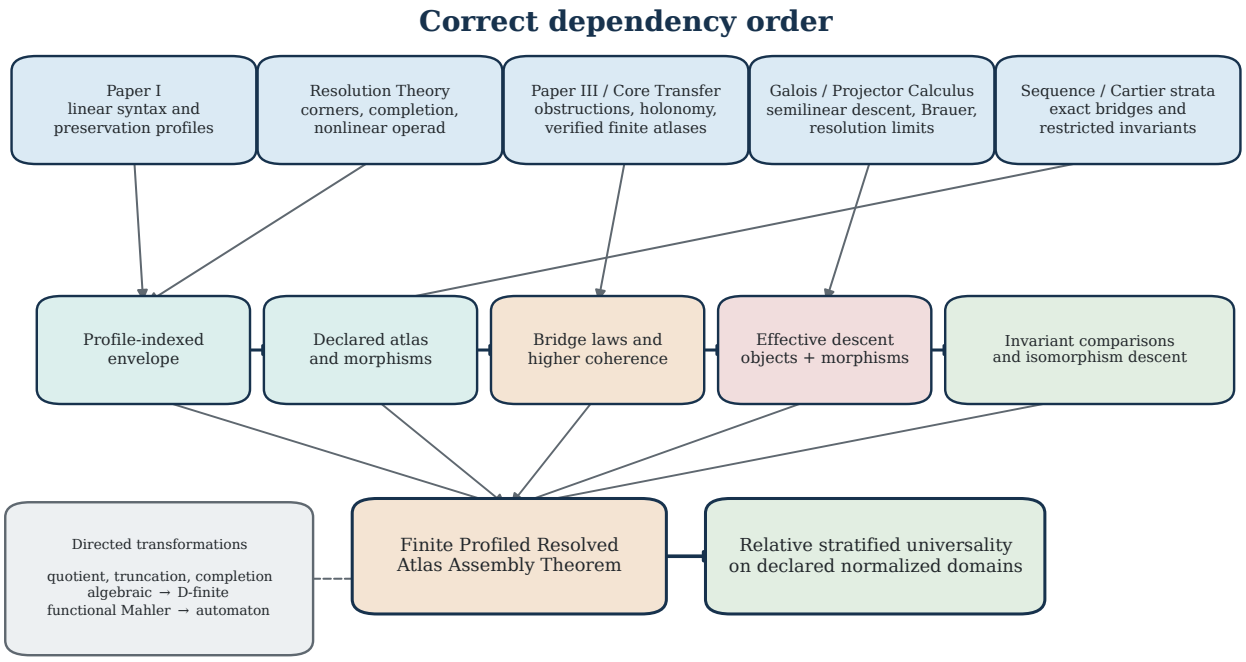



**Figure 8:** The corrected dependency graph. The theorem concordance and local results feed the assembly theorem, but the heterogeneous conclusion still depends on explicit atlas construction, coherence, effectivity, and isomorphism descent.

### 6.1 Finite atlases and descent data

**Definition 6.1** (Finite profiled resolved atlas)**.** Fix a small resolved theory $\mathbb{K}$. A finite profiled resolved atlas consists of:

(A1) a finite indexing category $\check{\mathcal{A}}$, retained through the overlap degrees needed for the cocycle law;

(A2) a pseudofunctor
$$\mathfrak{R} : \check{\mathcal{A}}^{\mathrm{op}} \to \mathbf{Cat};$$

(A3) a declared preservation profile $\Pi_U$ on every chart and overlap category $\mathfrak{R}(U)$;

(A4) coherent equivalences on the reversible overlaps and separately typed directional transformations;

(A5) a pseudonatural semantics
$$\mathrm{Sem} : \mathfrak{R} \Rightarrow \mathfrak{O}$$
into a common observable doctrine;

(A6) optional pseudonatural invariant families with explicitly typed comparison cells.

**Definition 6.2** (Descent category)**.** The category $\mathrm{Desc}(\mathfrak{R})$ has pseudocones over $\mathfrak{R}$ as objects and modifications as morphisms. Concretely, an object is a compatible family
$$(M_\alpha, \theta_{\alpha\beta})$$
with invertible overlap comparisons satisfying the cocycle law. A morphism is a compatible family of chart morphisms.

### 6.2 The assembly theorem

**Theorem 6.3** (Finite profiled resolved atlas assembly)**.** *Let*
$$\mathfrak{R} : \check{\mathcal{A}}^{\mathrm{op}} \to \mathbf{Cat}$$
*be a finite profiled resolved atlas. Assume the chart and overlap categories are small, or locally small in one fixed universe, the reversible transitions and comparison cells satisfy the pseudofunctor coherence equations, and every construction used below belongs to the verified profile of every participating chart and bridge. Then:*

(i) $\mathrm{Desc}(\mathfrak{R})$ *exists and has the universal property of the finite pseudolimit of* $\mathfrak{R}$*.*

(ii) *There is a canonical equivalence*
$$\mathrm{Core}\big(\mathrm{Desc}(\mathfrak{R})\big) \simeq \mathrm{Desc}\big(\mathfrak{R}^{\simeq}\big).$$

(iii) *Every pseudonatural transformation* $T : \mathfrak{R} \Rightarrow \mathfrak{S}$ *induces a functor*
$$\mathrm{Desc}(T) : \mathrm{Desc}(\mathfrak{R}) \to \mathrm{Desc}(\mathfrak{S}).$$
*If every* $T_U$ *is an equivalence, then* $\mathrm{Desc}(T)$ *is an equivalence. A pointwise noninvertible* $T$ *remains directional.*

(iv) *If two global morphism expressions use only constructors in the common verified preservation profile and their equality is proved in the resolved syntax, then, after every domain-specific hypothesis is verified locally, their realizations are equal in* $\mathrm{Desc}(\mathfrak{R})$*.*

(v) *A coherent pseudonatural invariant family* $I : \mathfrak{R} \Rightarrow \mathfrak{V}$ *induces*

$$\mathrm{Desc}(I) : \mathrm{Desc}(\mathfrak{R}) \to \mathrm{Desc}(\mathfrak{V}).$$

(vi) *If every local invariant is complete on its normalized chart and the groupoid of local invariant-compatible isomorphisms has effective descent, then* $\mathrm{Desc}(I)$ *is complete on the corresponding global normalized category.*

*If the semantic pseudonatural transformation is effective for objects and morphisms, then* $\mathrm{Desc}(\mathrm{Sem})$ *identifies descent data with the declared global semantic objects.*

*Proof.* Objects and morphisms of $\mathrm{Desc}(\mathfrak{R})$ are finite compatible families. Identities and composition are defined componentwise. The pseudofunctor coherence equations ensure that componentwise composition remains compatible. This explicit construction has the universal property of pseudocones, proving (i).

A descent morphism is invertible exactly when each component is invertible. The componentwise inverses satisfy the overlap equations obtained by inverting the original equations. This proves (ii).

A pseudonatural transformation acts on chart objects, overlap comparisons, and chart morphisms componentwise. Its coherence cells supply the target cocycle law. Pointwise quasi-inverses and their modifications descend, proving (iii).

For (iv), the equational realization principle transports the proof to each chart because every constructor used by the proof is preserved. Bridge naturality makes the local equalities compatible on overlaps. Equality in the descent category is componentwise. The argument creates no missing analytic or arithmetic hypotheses.

Statement (v) is the same pseudonatural-transformation construction applied to the invariant family. For (vi), an isomorphism between descended invariants gives local invariant matches. Local completeness supplies local object isomorphisms. The added isomorphism-effectivity hypothesis is exactly what glues those local isomorphisms to a global one. Without it, a holonomy class, a relative cokernel class, a Brauer class, or a higher coherence defect may obstruct the gluing.

The final assertion is the definition of semantic effectivity applied to the induced descent functor. □

**Corollary 6.4** (No automatic promotion of directional bridges)**.** *A directional bridge contributes a global functor only when it is pseudonatural with respect to the chosen atlas. It contributes an equivalence only when the chartwise bridge is an equivalence on the named overlap. No quotient, completion, or compression becomes reversible merely because it appears in the same diagram.*

**Corollary 6.5** (Global theorem transport)**.** *A theorem proved from packet reconstruction, refinement, residual calculus, or another preserved constructor descends globally only when every chart and bridge used by the proof carries that constructor in its verified preservation profile.*

*Remark* 6.6 (Exact status). Theorem 6.3 is a proved conditional theorem. It does not prove that the full proposed Komorebi atlas satisfies the hypotheses. The remaining work is the verification of the actual profiles, overlap categories, naturality cells, higher coherence, and effectivity.

## Part II

# Certified native strata

# 7 Verified finite Mahler atlas models

Two exact finite models already realize substantial pieces of the assembly theorem. They remain inside the affine-Mahler and packet-analysis setting, but they verify nontrivial coherence and effectivity mechanisms.

## 7.1 Affine-Mahler chart groupoid

Fix $d \geq 0$. Over characteristic zero, the affine Mahler coefficient maps $A_{m,s}^{(d)}$ are invertible and satisfy

$$A_{n,t}^{(d)} A_{m,s}^{(d)} = A_{mn,mt+s}^{(d)}.$$

For coprime $m, n$, the two paths around every declared Chinese-remainder diamond are equal [5]. Hence every finite subdiagram generated by these charts is a coherent finite chart groupoid with trivial holonomy on those diamonds.

**Proposition 7.1** (Rational affine-Mahler chart groupoid)**.** *Every finite characteristic-zero diagram generated by the invertible affine Mahler charts and the declared CRT comparison cells defines a strict finite groupoid atlas. Its path transport depends only on the represented affine substitution, and every declared CRT cycle has identity holonomy.*

## 7.2 Integral split packet descent

Let

$$A = P_{m,S}^{(d)} : \mathbb{Z}^{d+1} \to \mathbb{Z}^{|S|(d+1)}$$

be a stacked affine-Mahler packet analysis map. Whenever an integer left inverse $L$ exists,

$$LA = I, \qquad \Pi = AL, \qquad \Pi^2 = \Pi,$$

and

$$\mathbb{Z}^{|S|(d+1)} = \operatorname{im} A \oplus \ker L.$$

Thus the source chart and the normalized packet core $\operatorname{im} A$ are equivalent, while $\ker L$ is a named residual rather than discarded information.

Addendum 04 proves that the prefix

$$S_* = \{0, 1, \ldots, L_{\mathbb{Z}}(m, d) - 1\}$$

with

$$L_{\mathbb{Z}}(m, d) = \min(d + 1, B(m)), \qquad B(m) = \max\big(\{1\} \cup \{p^{v_p(m)} : p \mid m\}\big),$$

always admits an integer decoder and is cardinality-minimal [5].

**Proposition 7.2** (Integral split Mahler packet descent)**.** *The analysis-decoder pair above gives effective object and morphism descent between the source chart and the normalized packet-core chart. The split identity survives every base change. The residual summand* $\ker L$ *is functorial under maps intertwining both* $A$ *and* $L$*.*

*Proof.* The identities $LA = I$ and $\Pi = AL$ show that $A$ identifies the source with $\operatorname{im} A$, with inverse $L|_{\operatorname{im} A}$. For any packet vector $y$,

$$y = ALy + (y - ALy),$$

where $ALy \in \operatorname{im} A$ and $y - ALy \in \ker L$. The intersection is zero because $Ax \in \ker L$ implies $x = LAx = 0$. Tensoring $LA = I$ with any coefficient ring preserves the split identity. Intertwining maps preserve the image and kernel decompositions. □

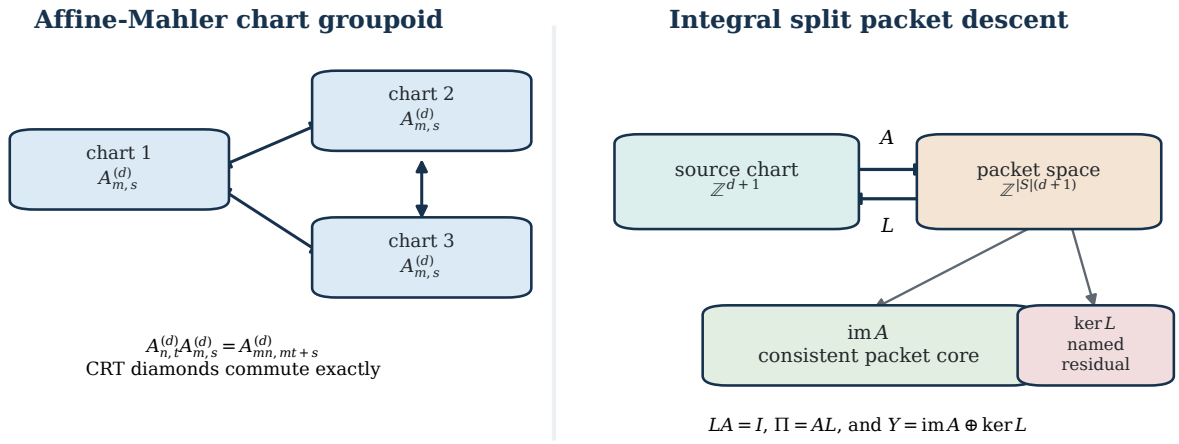



**Figure 9:** Two verified finite atlas mechanisms. The first is reversible and coherent. The second is split analysis-synthesis with a retained residual.

## 8 The normalized C-finite three-chart atlas

This section completes the first cross-presentation model in the theorem dependency graph. It does not combine unrelated broad strata, but it does prove a genuine three-chart effective descent theorem with nontrivial morphisms on the state side.

### 8.1 Persistent C-finite semantics

Fix a field $K$. A nonzero C-finite sequence $a = (a_n)_{n\geq 0}$ is *persistent* when its minimal characteristic polynomial has nonzero constant term. Equivalently, its active characteristic roots are nonzero, or its minimal state transition is invertible [7].

Let $\mathbf{Seq}_K^{\mathrm{pers}}$ be the discrete groupoid of persistent C-finite sequences over $K$.

### 8.2 The recurrence chart

An object of $\mathbf{Rec}_K^{\min}$ is a pair

$$(\chi, \mathbf{a}_0),$$

where

$$\chi(x) = x^d - c_{d-1}x^{d-1} - \cdots - c_1 x - c_0, \qquad c_0 \neq 0,$$

is the monic minimal recurrence polynomial and $\mathbf{a}_0 = (a_0, \ldots, a_{d-1})$ is the initial vector. It generates the sequence

$$a_{n+d} = c_{d-1}a_{n+d-1} + \cdots + c_1 a_{n+1} + c_0 a_n.$$

Because the recurrence is normalized and minimal, two objects representing the same sequence are equal. Thus $\mathbf{Rec}_K^{\min}$ is a discrete groupoid.

### 8.3 The rational OGF chart

An object of $\mathbf{Rat}_K^{\mathrm{red}}$ is a reduced rational power series

$$A(z) = \frac{P(z)}{Q(z)}, \qquad Q(0) = 1, \qquad \gcd(P, Q) = 1, \qquad \deg P < \deg Q,$$

whose reciprocal characteristic polynomial has nonzero constant term. Again the normalized reduced form is unique, so $\mathbf{Rat}_K^{\mathrm{red}}$ is discrete.

The recurrence-to-OGF bridge is explicit. From

$$\chi(x) = x^d - c_{d-1}x^{d-1} - \cdots - c_0$$

set

$$Q(z) = z^d\chi(z^{-1}) = 1 - c_{d-1}z - \cdots - c_0z^d.$$

The numerator is the degree-$< d$ truncation of $Q(z)\sum_{n\geq 0} a_n z^n$. Conversely, clearing $Q$ recovers the recurrence and the initial vector. Minimality is equivalent to reducedness.

### 8.4 The minimal state chart

An object of $\mathbf{State}_K^{\mathrm{min}}$ is a triple

$$(C, v, \lambda), \qquad C \in M_d(K), \quad v \in K^d, \quad \lambda \in (K^d)^*,$$

with $C$ invertible, producing

$$a_n = \lambda C^n v,$$

and satisfying reachability and observability. A morphism

$$S : (C, v, \lambda) \longrightarrow (C', v', \lambda')$$

is a similarity satisfying

$$C' = SCS^{-1}, \qquad v' = Sv, \qquad \lambda' = \lambda S^{-1}.$$

The semantic functor sends a state to its coefficient sequence.

The state-to-OGF bridge is the resolvent

$$A(z) = \lambda(I - zC)^{-1}v.$$

The reduced denominator has degree equal to the minimal state dimension, which equals the Hankel rank. Conversely, a reduced rational OGF has a companion realization. Reducedness makes the companion realization reachable, while the companion output is observable. Any two minimal realizations of the same sequence are uniquely similar through their common shift action on the Hankel column space [7].

### 8.5 Effective descent across the three charts

**Theorem 8.1** (Normalized C-finite three-chart atlas)**.** *For every field $K$, the semantic functors fit into equivalences of groupoids*

$$\mathbf{Rec}_K^{\mathrm{min}} \simeq \mathbf{Rat}_K^{\mathrm{red}} \simeq \mathbf{State}_K^{\mathrm{min}} \simeq \mathbf{Seq}_K^{\mathrm{pers}}.$$

*The recurrence-rational bridge is a strict inverse pair. The rational-state bridge is an equivalence with companion quasi-inverse. The comparison isomorphism on the state-side composite is the unique similarity between minimal realizations. Consequently:*

(i) *the three charts and their pairwise overlaps form a coherent finite profiled atlas;*

(ii) *the triple-overlap comparison satisfies the cocycle law by uniqueness of minimal similarity;*

(iii) *descent for objects and morphisms is effective;*

(iv) *the descent category is equivalent to* $\mathbf{Seq}_K^{\mathrm{pers}}$.

*Proof.* The equivalence between normalized minimal recurrences and reduced rational ordinary generating functions follows from the explicit reciprocal-denominator formula and clearing of the denominator. These constructions are mutually inverse.

A minimal state gives a rational resolvent. Conversely, a reduced rational series gives a companion state. Minimal linear dimension equals Hankel rank, and the reduced denominator degree has the same value. Hence the companion state is minimal. Any two minimal states representing the same sequence identify with the forward shift on the Hankel column space and are therefore similar. The similarity is unique because a reachable state is spanned by $C^n v$, so an intertwiner fixing the input vector is determined on a spanning set.

Choose the recurrence-to-state bridge to be the companion realization obtained through the rational chart. Then one triangular composite is strict. On the state side, the composite through the rational and recurrence charts returns the companion realization of the same sequence. The unique minimal similarity supplies the comparison isomorphism. Any two composites around a triple overlap are comparison isomorphisms between the same minimal realizations, so uniqueness forces the cocycle law.

Each semantic functor is an equivalence to the same discrete groupoid of persistent sequences. Compatible local objects and morphisms therefore descend uniquely up to the stated similarity, proving effectivity and the final equivalence. □

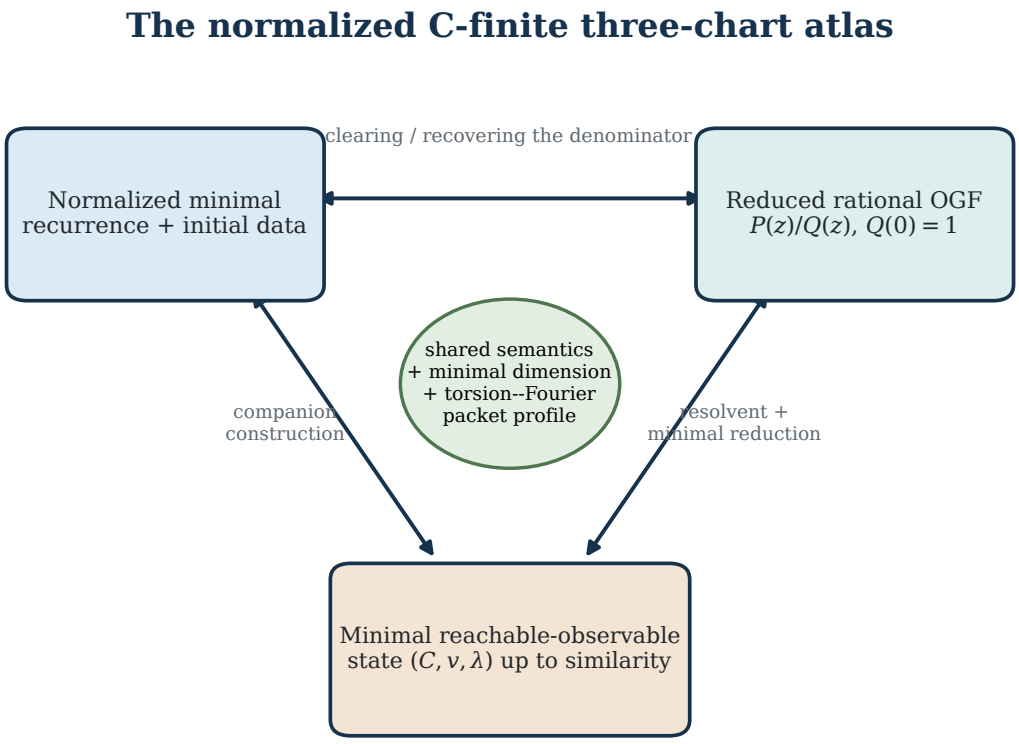



**Figure 10:** The normalized C-finite atlas. The recurrence and rational charts are canonical normal forms. The state chart has nontrivial presentation coordinates, but minimality makes every semantic identification unique up to similarity.

### 8.6 Descent of the minimality and torsion-Fourier invariants

For a persistent C-finite sequence, the minimal dimension

$$\rho(a) = \operatorname{linrank}(a) = \operatorname{rank} H(a)$$

is simultaneously the minimal recurrence order, the reduced denominator degree, and the dimension of a minimal reachable-observable state.

Over characteristic zero, write the unique active expansion over an algebraic closure as

$$a_n = \sum_{\lambda \in \Lambda} P_\lambda(n)\lambda^n.$$

For each sampling modulus $N$ and address $j$, the spectral torsion-Fourier theorem computes the exact minimal recurrence, reduced denominator, Hankel rank, state dimension, rank-drop mechanism, and finite periodic packet signature of $a_{Nm+j}$ [7].

**Corollary 8.2** (Cross-presentation torsion-Fourier descent)**.** *The minimal dimension and the complete arithmetic-subsequence packet-complexity profile are independent of whether the input is supplied as a normalized minimal recurrence, a reduced rational OGF, or a minimal state realization. The exact compiler outputs agree under every bridge in theorem 8.1.*

*Proof.* All three charts represent the same sequence. The compiler theorem accepts any of the three presentation types and computes quantities determined by the active modal decomposition or, equivalently, by exact reachable-observable reduction of the jump state. The bridge functors preserve the coefficient sequence, so the outputs agree. □

The phrase “complete invariant” here has a declared target. The torsion-Fourier signature is complete for the minimal recurrence and complexity profile of every arithmetic subsequence. It is not asserted to classify arbitrary sequence presentations or all sequence phenomena.

### 8.7 Exact examples

## 9 A first heterogeneous effective-descent atlas

The previous sections separated the formal assembly theorem from the nonformal work of declaring and verifying an actual atlas. This section discharges that burden for a deliberately restricted but genuinely heterogeneous example. The charts do not merely use different coordinates inside one linear category. They belong to three of the principal strata:

finite linear and C-finite  digital and automatic  functional-Mahler and Cartier.

The common semantic objects are unit purely periodic sequences over a prime field. The restriction is strong enough to make every bridge explicit, every normalized fiber rigid, every nonempty triple overlap coherent, and descent effective for both objects and morphisms. At the same time it is broad enough to contain repeated-root recurrences in characteristic $p$, nontrivial minimal automata, rational functional-Mahler masks, and redundant Cartier compiler presentations.

**Table 10:** Three exact C-finite examples across the normalized atlas.

| Sequence | Minimal recurrence | Reduced OGF | Minimal dimension | Packet behavior |
|---|---|---|---|---|
| Fibonacci $F_n$ | $x^2 - x - 1$ | $z/(1 - z - z^2)$ | 2 | The root ratio is not torsion. Every arithmetic subsequence retains rank 2. |
| $1 + (-1)^n$ | $x^2 - 1$ | $2/(1 - z^2)$ | 2 | At $N = 2$, the even packet is constant of rank 1 and the odd packet is zero. |
| $n + 1)$ | $(x - 1)^2$ | $1/(1 - z)^2$ | 2 | Every packet remains a nonzero affine polynomial in the packet index and retains rank 2. |

### 9.1 The restricted semantic doctrine

Fix a prime $p$. Let $\mathbf{Per}_p^{\times,\mathrm{per}}$ denote the discrete category whose objects are sequences

$$a = (a_n)_{n\geq 0} \in \mathbb{F}_p^{\mathbb{N}}$$

satisfying

$$a_0 = 1 \qquad \text{and} \qquad a_{n+T} = a_n \quad (n \geq 0)$$

for some $T \geq 1$. The least such positive integer is the *minimal period* $T(a)$. Write

$$w(a) = (a_0, \ldots, a_{T(a)-1})$$

for the primitive period word and

$$W_a(z) = \sum_{r=0}^{T(a)-1} a_r z^r.$$

Then

$$F_a(z) = \sum_{n\geq 0} a_n z^n = \frac{W_a(z)}{1 - z^{T(a)}}. \tag{1}$$

The fraction in Equation (1) need not be reduced. Cancellation is part of the normalized rational chart rather than an error. For example, over $\mathbb{F}_3$, the period word 12 has

$$\frac{1 + 2z}{1 - z^2} = \frac{1}{1 + z}.$$

*Boundary* 9.1 (Why the unit condition is retained). The functional-Mahler bridge uses the formal quotient

$$R_a(z) = \frac{F_a(z)}{F_a(z^p)}.$$

It is regular at the origin exactly when $F_a(0) \neq 0$. The normalization $a_0 = 1$ removes scalar ambiguity and gives $R_a(0) = 1$. Purely periodic sequences with $a_0 = 0$ remain valid C-finite and automatic objects, but they need not lie in this regular unit-mask overlap. They are not discarded; they lie outside the selected heterogeneous atlas.

**Proposition 9.2** (Finite-field persistence equals pure periodicity)**.** *For a sequence over $\mathbb{F}_p$, the following are equivalent.*

(i) *The sequence is C-finite and its minimal recurrence has nonzero constant term.*

(ii) *The sequence has a finite-dimensional state realization*

$$a_n = \lambda C^n v$$

*with $C \in GL_d(\mathbb{F}_p)$.*

(iii) *The sequence is purely periodic from $n = 0$.*

*If $m_a(x)$ is the monic minimal recurrence polynomial and $T = T(a)$, then*

$$m_a(x) \mid x^T - 1, \qquad T = \min\{N \geq 1 : m_a(x) \mid x^N - 1\}. \tag{2}$$

*Proof.* A recurrence with nonzero constant term has an invertible companion matrix, giving (i) $\Rightarrow$ (ii). The orbit of $v$ under an invertible map of the finite set $\mathbb{F}_p^d$ is a cycle containing its initial state, so (ii) $\Rightarrow$ (iii). A sequence of period $T$ is annihilated by $E^T - I$, where $E$ is the forward shift, giving (iii) $\Rightarrow$ (i). The minimal annihilator divides every annihilator, hence $m_a \mid x^T - 1$. Conversely, if $m_a \mid x^N - 1$, then $E^N - I$ annihilates the sequence. Minimality of $T$ proves Equation (2). □

Let

$$F_a(z) = \frac{P_a(z)}{Q_a(z)}$$

be reduced with

$$P_a(0) = Q_a(0) = 1.$$

If $d = \deg m_a$, then

$$Q_a(z) = z^d m_a(z^{-1}),$$

with the evident coefficient normalization. Taking reciprocal polynomials in Equation (2) gives

$$Q_a(z) \mid 1 - z^T, \qquad T = \min\{N \geq 1 : Q_a(z) \mid 1 - z^N\}. \tag{3}$$

Thus pure periodicity is visible both in the linear annihilator and in the reduced rational denominator.

## 9.2 Four normalized charts

The reversible core of the selected atlas has four charts. Each chart carries its own native objects and morphisms, but every normalized fiber over a fixed sequence will be shown to be contractible.

### 9.2.1 The minimal recurrence chart

An object of $\mathbf{Rec}_p^{\times,\mathrm{per}}$ is the normalized minimal recurrence polynomial

$$m(x) = x^d + c_1 x^{d-1} + \cdots + c_d, \qquad c_d \neq 0,$$

together with the initial vector $(a_0, \ldots, a_{d-1})$, subject to $a_0 = 1$ and the requirement that the generated sequence is purely periodic. Minimality means that no monic recurrence of lower degree annihilates the sequence. Morphisms are recurrence-presentation isomorphisms preserving the coefficient sequence. Because the minimal annihilator and initial data are unique, every endomorphism is the identity.

### 9.2.2 The reduced rational chart

An object of $\mathbf{Rat}_p^{\times,\mathrm{per}}$ is a reduced fraction

$$F(z) = \frac{P(z)}{Q(z)} \in \mathbb{F}_p(z), \qquad P(0) = Q(0) = 1,$$

whose coefficient sequence is purely periodic. Equivalently, $Q \mid 1 - z^T$ for some $T$ and the reduced coefficient sequence has no transient prefix. Morphisms preserve the rational function. Reducedness and the constant-term normalization make this chart rigid.

The recurrence-rational bridge is the strict inverse pair already used in the C-finite atlas: multiply the generating series by the reciprocal recurrence denominator, or recover the recurrence by clearing the reduced denominator. On the present finite-field subcategory, the additional condition $Q \mid 1 - z^T$ records pure periodicity.

### 9.2.3 The canonical digital chart

For $0 \le d < p$, define the Cartier section of a sequence by

$$(\Lambda_d a)_n = a_{pn+d}.$$

The $p$-kernel is

$$\mathcal{K}_p(a) = \left\{ \Lambda_{d_{\ell-1}} \cdots \Lambda_{d_0} a : \ell \ge 0,\ 0 \le d_i < p \right\}. \tag{4}$$

We use least-significant-digit-first words. Every finite digit word is allowed. Appending high zero digits may change the internal state but never changes the represented coefficient, because the output of a state $b$ is $b_0$ and $(\Lambda_0 b)_0 = b_0$.

The canonical Moore automaton has state set $\mathcal{K}_p(a)$, start state $a$, transition

$$\delta_d(b) = \Lambda_d b,$$

and output

$$o(b) = b_0.$$

After reading $d_0, \ldots, d_{\ell-1}$, its state is

$$\Lambda_{d_{\ell-1}} \cdots \Lambda_{d_0} a = \left(n \longmapsto a_{p^\ell n + r}\right), \qquad r = \sum_{j=0}^{\ell-1} d_j p^j.$$

**Proposition 9.3** (Finite periodic kernel and exact state model)**.** *Let $a \in \mathbf{Per}_p^{\times,\mathrm{per}}$ have minimal period $T$ and period word $w$. Every kernel state has the form*

$$b_{u,r}(n) = w_{un+r \bmod T}, \qquad u \in U_p(T), \quad r \in \mathbb{Z}/T\mathbb{Z}, \tag{5}$$

*where*

$$U_p(T) = \{p^e \bmod T : e \ge 0\}.$$

*The digit transition on pair representatives is*

$$(u, r) \xrightarrow{d} (pu, r + ud) \pmod T, \tag{6}$$

*and the output is $w_r$. Quotienting pair representatives by equality of the sequences in Equation (5) gives the canonical minimal least-significant-digit-first $p$-DFAO for $a$.*

*Proof.* After $\ell$ digits, the resulting subsequence is $n \mapsto a_{p^\ell n+r}$, which depends only on ($p^\ell \bmod T, r \bmod T$). Applying $\Lambda_d$ gives

$$\Lambda_d b_{u,r}(n) = b_{u,r}(pn+d) = w_{(pu)n+(r+ud)},$$

proving Equation (6). The pair set is finite, so the kernel is finite. Every kernel state is reachable by construction. If two kernel sequences differ, they differ at some $n$; reading the base-$p$ digits of that $n$ distinguishes the states by their outputs. Hence the kernel automaton is minimal. Any other reachable minimal automaton producing the same sequence is uniquely isomorphic to it by the usual behavioral quotient. □

The pair model gives a useful finite bound. Write

$$T = p^\nu M, \qquad \gcd(M, p) = 1,$$

and set $\mathrm{ord}_1(p) = 1$.

**Lemma 9.4** (Exact multiplier-orbit size)**.** *The set $U_p(T)$ has cardinality*

$$|U_p(T)| = \nu + \mathrm{ord}_M(p). \tag{7}$$

*Consequently,*

$$|\mathcal{K}_p(a)| \le T\big(\nu + \mathrm{ord}_M(p)\big). \tag{8}$$

*Proof.* For $0 \le e < \nu$, the residues $p^e \bmod p^\nu$ have distinct $p$-adic valuations. For $e \ge \nu$, the residue is zero modulo $p^\nu$, while modulo $M$ it runs through one multiplicative cycle of length $\mathrm{ord}_M(p)$. The early and eventual residues cannot coincide. This proves Equation (7). The kernel is a quotient of the pair set $U_p(T) \times \mathbb{Z}/T\mathbb{Z}$, giving Equation (8). □

Let $\mathrm{Aut}_p^{\times,\mathrm{per}}$ be the groupoid of reachable minimal least-significant-digit-first $p$-DFAOs whose output sequence lies in $\mathbf{Per}_p^{\times,\mathrm{per}}$. Morphisms are automaton isomorphisms preserving the start state, transitions, and outputs. Reachability forces every automorphism to be the identity.

### 9.2.4 The rational functional-Mahler mask chart

For a unit formal series $F(0) = 1$, define its local functional-Mahler mask by

$$\mathcal{M}_p(F)(z) = \frac{F(z)}{F(z^p)}. \tag{9}$$

Then

$$F(z) = \mathcal{M}_p(F)(z) F(z^p). \tag{10}$$

Iterating Equation (10) gives the coefficientwise product

$$F(z) = \prod_{j \ge 0} \mathcal{M}_p(F)(z^{p^j}). \tag{11}$$

Only finitely many factors contribute to each fixed coefficient.

If $F = P/Q$ is reduced and unit normalized, then

$$R_F(z) = \frac{P(z)Q(z^p)}{Q(z)P(z^p)}. \tag{12}$$

Thus every object of $\mathbf{Rat}_p^{\times,\mathrm{per}}$ has a rational mask. Reduce Equation (12) to

$$R_F(z) = \frac{A(z)}{B(z)}, \qquad A(0) = B(0) = 1, \qquad \gcd(A, B) = 1.$$

Define $\mathbf{Mask}_p^{\times,\mathrm{per}}$ to be the groupoid of such reduced rational masks whose normalized product solution Equation (11) has purely periodic coefficients. Morphisms preserve the reduced mask.

**Theorem 9.5** (Unit rational functional-Mahler equivalence)**.** *The assignments*

$$F \longmapsto \frac{F(z)}{F(z^p)} \qquad \textit{and} \qquad R \longmapsto \prod_{j\geq 0} R(z^{p^j})$$

*are inverse equivalences*

$$\mathbf{Rat}_p^{\times,\mathrm{per}} \simeq \mathbf{Mask}_p^{\times,\mathrm{per}}.$$

*The mask is unique for the represented series.*

*Proof.* Starting with $F$, the finite product through level $N$ telescopes:

$$\prod_{j=0}^{N} \frac{F(z^{p^j})}{F(z^{p^{j+1}})} = \frac{F(z)}{F(z^{p^{N+1}})}.$$

As $N \to \infty$, the denominator converges coefficientwise to $F(0) = 1$, proving that the product recovers $F$. Conversely, the product solution satisfies $F(z) = R(z)F(z^p)$, so $R = F/F(z^p)$. Reduced normalization makes the rational mask unique. □

*Boundary* 9.6 (Functional Mahler is not Newton-Mahler). The mask equation in this section is

$$F(z) = R(z)F(z^p).$$

It is a digit-section and automaton construction. It is not the Newton-Mahler interpolation expansion

$$f(x) = \sum_r c_r \binom{x}{r}.$$

Both occur elsewhere in the Library, but this atlas uses only the functional-Mahler meaning.

## 9.3 Explicit bridge passports

The reversible bridge core is generated by three explicit constructions:

$$\mathbf{Rec}_p^{\times,\mathrm{per}} \leftrightarrow \mathbf{Rat}_p^{\times,\mathrm{per}}, \qquad \mathbf{Rat}_p^{\times,\mathrm{per}} \leftrightarrow \mathrm{Aut}_p^{\times,\mathrm{per}}, \qquad \mathbf{Rat}_p^{\times,\mathrm{per}} \leftrightarrow \mathbf{Mask}_p^{\times,\mathrm{per}}.$$

The remaining reversible bridges are their normalized composites. A separate constructor and reachable-restriction lane connects masks to the digital normal form through the Cartier compiler.

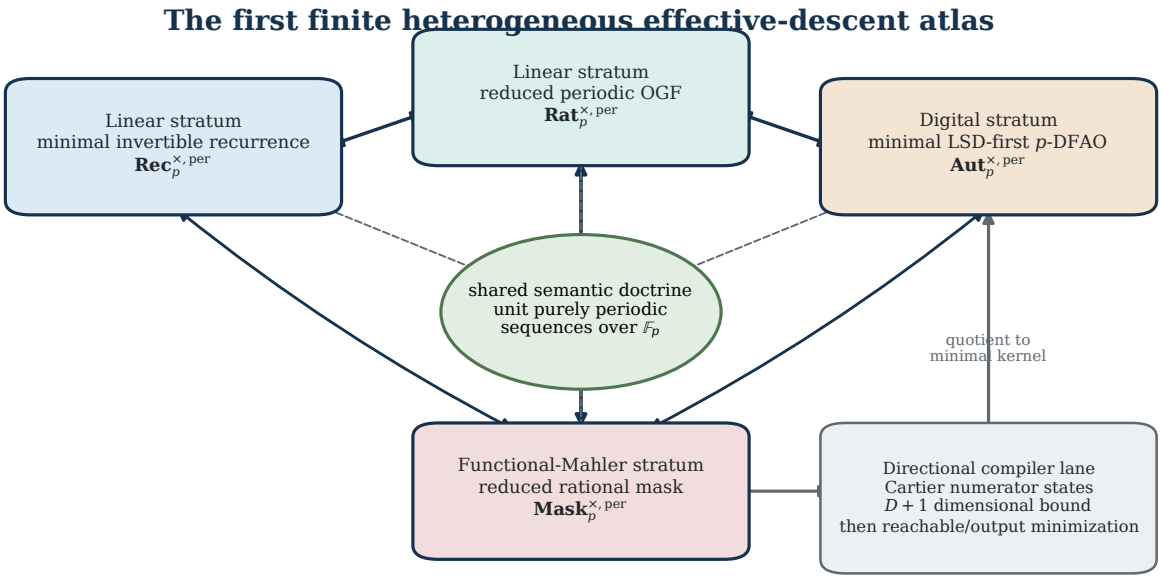



**Figure 11:** The first heterogeneous atlas proved effective in this manuscript. Four normalized reversible charts span three strata. The raw Cartier compiler is retained as a directional lane because its numerator coordinates need not be minimal.

**Table 11:** Bridge passports for the selected periodic atlas.

| Bridge | Exact class | Domain | Preserved data | Reflected data | Information loss or boundary |
|---|---|---|---|---|---|
| Recurrence $\leftrightarrow$ reduced OGF | equivalence | minimal invertible recurrence and reduced purely periodic rational series | coefficients, minimal annihilator, initial data, period, Hankel rank | equality and isomorphism | none after reduced normalization |
| Reduced OGF $\leftrightarrow$ minimal DFAO | equivalence on the periodic essential image | unit purely periodic series and reachable minimal LSD-first $p$-DFAOs | coefficient semantics, minimal period, canonical $p$-kernel, output behavior | equality of represented sequences | a nonminimal residue-pair automaton is quotiented before entering the normalized chart |
| Reduced OGF $\leftrightarrow$ rational mask | equivalence on the unit-periodic essential image | $F(0) = 1$, periodic rational $F$, reduced regular mask $R$ | exact series, functional equation, reduced rational mask, minimal period | equality of series and masks | undefined for nonunit series; unrestricted rational masks may have nonperiodic products |
| Mask $\rightarrow$ Cartier numerator representation | constructor | reduced $A/B$ over $\mathbb{F}_p$ | exact coefficient semantics, digit matrices, theorem degree bound | not generally reflective | introduces basis and denominator coordinates and may contain unreachable ambient states |
| Ambient Cartier compiler $\rightarrow$ minimal DFAO | reachable restriction | full finite numerator-state compiler | every reachable coefficient section and every future digit behavior | equality of the represented $p$-kernel states | removes only ambient states outside the orbit of the initial numerator |
| Unrestricted automatic $\dashrightarrow$ rational mask | partial bridge only | automatic sequences whose unit inverse mask is rational and whose product lies in the declared periodic class | coefficient semantics on the domain of definition | no unrestricted reflection theorem | no claim that every automatic sequence has a rational periodic mask |

### 9.3.1 The rational-to-digital construction

For a periodic word $w$ of length $T$, construct the finite pair automaton from Equation (6), then quotient by equality of the induced subsequences. This gives the canonical minimal DFAO directly. Conversely, a minimal DFAO in the selected chart is promised to produce a purely periodic sequence. Its minimal period can be recovered exactly by enumerating $N = 1, 2, \ldots$, constructing the finite-state transducer for addition by $N$, and testing equivalence between the original output and its $N$-shift. Equivalence of finite deterministic output automata is a finite product-graph calculation. The promise of pure periodicity guarantees termination. Once $T$ is known, Equation (1) gives the rational series, which is then reduced.

This inverse is effective but not claimed to be complexity optimal. The point is effectivity, not a sharp automata algorithm.

### 9.3.2 The rational-mask compiler lane

Let

$$R(z) = \frac{A(z)}{B(z)}, \qquad A(0) = B(0) = 1,$$

with

$$a = \deg A, \qquad b = \deg B, \qquad c = a + (p-2)b,$$

and define

$$D = \max\left\{b, \left\lceil \frac{c}{p-1} \right\rceil\right\}. \tag{13}$$

The rational-mask Cartier theorem gives an invariant numerator space of degree at most $D$ under

$$P \longmapsto \Lambda_d(PAB^{p-2}), \qquad 0 \le d < p.$$

The resulting linear state vector belongs to $\mathbb{F}_p^{D+1}$, so the raw output automaton has at most

$$p^{D+1} \tag{14}$$

states [8]. It computes the coefficient sequence exactly.

**Proposition 9.7** (Compiler reachability lands in the canonical digital chart)**.** *For a mask in* $\mathbf{Mask}_p^{\times,\mathrm{per}}$*, the reachable part of the fixed-denominator Cartier compiler is uniquely isomorphic to the canonical p-kernel automaton of proposition 9.3. In particular, the subsequent quotient by equality of future output behavior is trivial.*

*Proof.* The fixed-denominator intertwining map sends the numerator reached by a digit word $w$ to the Cartier section $\Lambda_w F$. It is injective, as proved in the more general theorems 10.4 and 10.7. Hence distinct reachable numerator states represent distinct section series and are distinguished by some future coefficient. The reachable compiler state set is therefore exactly the canonical $p$-kernel state set, with matching transitions and outputs. □

## 9.4 Triple-overlap and quadruple coherence

There are four nonempty triple overlaps:

$$(\mathbf{Rec}, \mathbf{Rat}, \mathrm{Aut}), \qquad (\mathbf{Rec}, \mathbf{Rat}, \mathbf{Mask}), \qquad (\mathbf{Rec}, \mathrm{Aut}, \mathbf{Mask}), \qquad (\mathbf{Rat}, \mathrm{Aut}, \mathbf{Mask}).$$

All four charts meet on the same unit periodic semantic objects.

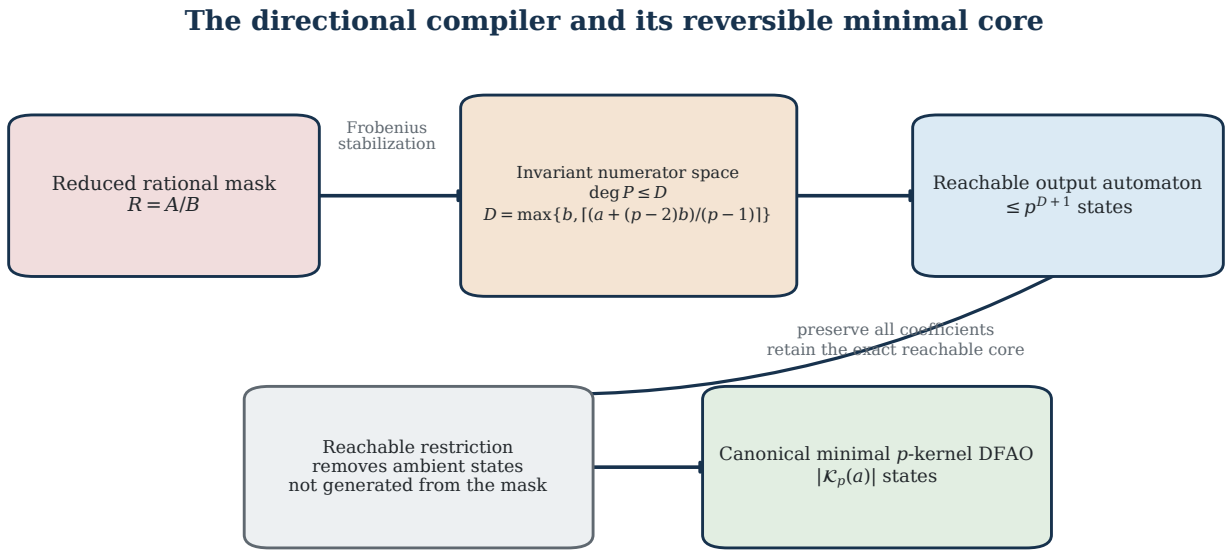



**Figure 12:** The raw mask compiler is a directional constructor. Reachability removes the ambient states outside the numerator orbit. Injectivity of the fixed-denominator realization then shows that the remaining states are already the unique minimal digital normal form.

**Lemma 9.8** (Rigidity of normalized fibers)**.** *Fix $a \in \mathbf{Per}_p^{\times,\mathrm{per}}$. In each of the four normalized charts, the groupoid of presentations of $a$ is contractible.*

*Proof.* The minimal recurrence with its initial data, the reduced rational function, and the reduced mask are unique, so their fibers are terminal groupoids. A normalized digital presentation is a reachable minimal automaton. Any automorphism fixes the start state and commutes with every transition. Reachability then forces it to fix every state. Hence its automorphism group is trivial, and any two minimal presentations are joined by the unique behavioral isomorphism. □

**Theorem 9.9** (Coherence of the periodic heterogeneous atlas)**.** *Choose every pairwise bridge by the explicit constructions above and choose every comparison* 2*-cell to be the unique normalized isomorphism over the common sequence. Then:*

(i) *every one of the four triple-overlap comparison diagrams commutes;*

(ii) *the two composites of comparison cells on the four-chart overlap agree;*

(iii) *the quadruple-overlap coherence defect $\Omega$ is the identity.*

*Proof.* Every comparison in question is an isomorphism between normalized presentations of one fixed semantic sequence. By lemma 9.8, there is exactly one such isomorphism. Any two composites with the same source and target must therefore agree. This proves all triple laws and the quadruple law simultaneously. □

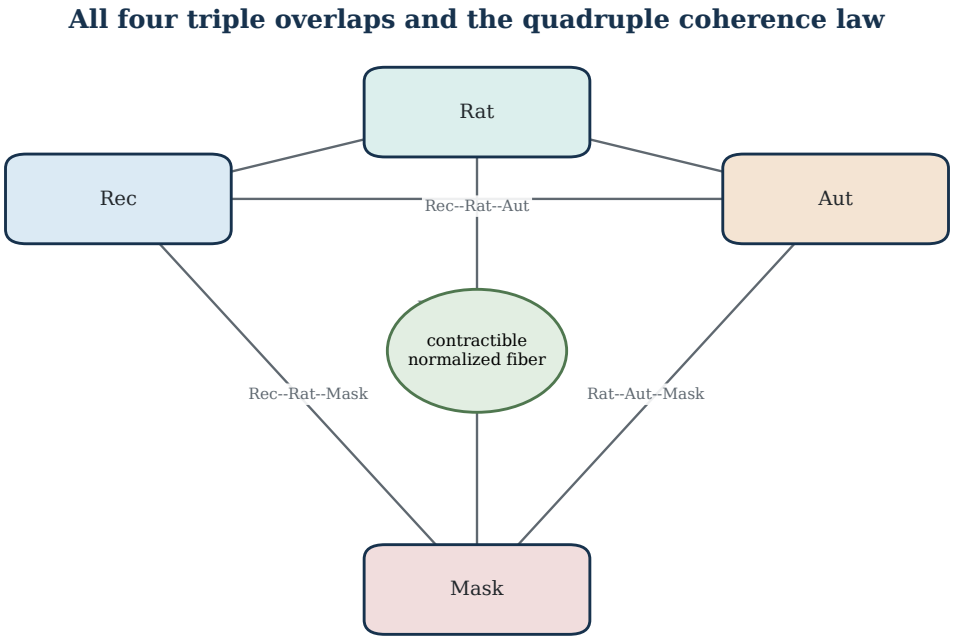



**Figure 13:** The coherence tetrahedron. Contractibility of every normalized semantic fiber makes each comparison cell unique, so all triple and quadruple coherence equations hold automatically after the bridge constructions have been typed.

## 9.5 Effective descent for objects and morphisms

Let $\mathfrak{R}_p^{\mathrm{per}}$ denote the four-chart pseudofunctor defined by the preceding passports and comparison cells.

**Theorem 9.10** (First heterogeneous effective-descent theorem)**.** *The semantic pseudonatural transformation induces an equivalence*

$$\mathrm{Desc}(\mathfrak{R}_p^{\mathrm{per}}) \simeq \mathbf{Per}_p^{\times,\mathrm{per}}. \tag{15}$$

*In particular, descent is effective for both objects and morphisms.*

*Proof.* Given $a \in \mathbf{Per}_p^{\times,\mathrm{per}}$, form its minimal recurrence, reduced rational OGF, canonical minimal $p$-kernel automaton, and reduced rational mask. The explicit bridges supply a descent object. This defines a functor

$$N : \mathbf{Per}_p^{\times,\mathrm{per}} \longrightarrow \mathrm{Desc}(\mathfrak{R}_p^{\mathrm{per}}).$$

Conversely, any descent object has local presentations whose semantic images agree on every overlap. Since the semantic target is discrete, they determine one sequence $a$. Normalization and lemma 9.8 identify the local presentations with those constructed by $N(a)$. Thus $N$ is essentially surjective and fully faithful.

For morphisms, a compatible local family lies over one equality of semantic sequences. Each normalized fiber has at most one morphism, so the local family glues uniquely. Identities, composition, equality, and invertibility are therefore detected componentwise and descend. □

**Corollary 9.11** (A verified instance of the assembly theorem)**.** *The atlas $\mathfrak{R}_p^{\mathrm{per}}$ satisfies realization, semantic adequacy, typed overlaps, higher coherence, effective descent, and preservation for the finite algebraic constructions*

*used in this section. Therefore theorem 6.3 applies without a remaining categorical hypothesis on this restricted domain.*

The conclusion is intentionally local to the selected atlas. It does not imply effective descent for arbitrary automatic sequences, unrestricted rational masks, general local analytic objects, or the full eight-stratum registry.

## 9.6 A compatible complete invariant family

For $a \in \mathbf{Per}_p^{\times,\mathrm{per}}$, define the periodic resolved invariant package

$$\mathcal{J}_p(a) = \big(T(a), w(a), m_a(x), P_a(z)/Q_a(z), \mathcal{K}_p(a), \mathcal{A}_p(a), R_a(z)\big), \tag{16}$$

where $\mathcal{A}_p(a)$ is the canonical minimal digital automaton. Its comparison identities include

$$\begin{aligned} \deg m_a &= \deg Q_a = \operatorname{rank} H(a) = \dim \mathbf{State}_{\min}(a), \\ T(a) &= \min\{N : m_a \mid x^N - 1\} = \min\{N : Q_a \mid 1 - z^N\}, \\ |\mathcal{A}_p(a)| &= |\mathcal{K}_p(a)| \le T(a)\big(\nu_p(T(a)) + \operatorname{ord}_M(p)\big), \\ R_a(z) &= \frac{F_a(z)}{F_a(z^p)}, \qquad T(a) = p^{\nu_p(T(a))}M, \quad \gcd(M,p) = 1. \end{aligned} \tag{17}$$

**Theorem 9.12** (Invariant descent and global completeness on the periodic atlas)**.** *The native invariants in the recurrence, rational, digital, and mask charts admit coherent comparison maps to $\mathcal{J}_p$. These maps descend to*

$$\mathcal{J}_p : \mathrm{Desc}(\mathfrak{R}_p^{\mathrm{per}}) \longrightarrow \mathbf{Inv}_p^{\mathrm{per}}.$$

*The descended invariant is complete on the declared semantic category.*

*Proof.* Every component of $\mathcal{J}_p(a)$ is reconstructed from the coefficient sequence by the explicit normalization procedures above. Hence every pairwise bridge preserves the package and the comparison cells are identities after semantic identification. Triple coherence follows from theorem 9.9. If $\mathcal{J}_p(a) = \mathcal{J}_p(b)$, then the primitive period words agree, so $a = b$. Under Equation (15), equality of semantic objects is exactly isomorphism in the descent category. □

The completeness claim has a narrow classification target: unit purely periodic sequences over $\mathbb{F}_p$. It is not a complete invariant for all C-finite, all automatic, or all rational functional-Mahler sequences.

## 9.7 Exact examples and a normalization boundary

**Table 12:** Named exact examples in the heterogeneous periodic atlas.

| Example | Field / word | Minimal recurrence | Reduced OGF denominator | Reduced mask numerator | Kernel states | Compiler bound |
|---|---|---|---|---|---|---|
| Even indicator | $\mathbb{F}_2$ / 10 | $1 + x^2$ | $1 + z^2$ | $1 + z^2$ | 3 | 8 |
| Alternating unit | $\mathbb{F}_3$ / 12 | $1 + x$ | $1 + z$ | $1 + 2z + z^2$ | 2 | 9 |
| Period-three word | $\mathbb{F}_2$ / 110 | $1 + x + x^2$ | $1 + z + z^2$ | $1 + z + z^2$ | 3 | 8 |

**Even indicator over $\mathbb{F}_2$.** For the word 10,

$$T = 2, \qquad m(x) = x^2 + 1 = (x+1)^2, \qquad F(z) = \frac{1}{1+z^2}, \qquad R(z) = 1 + z^2.$$

The repeated recurrence root is compatible with pure periodicity because the field has characteristic two. The canonical 2-kernel has three states: the original sequence, the constant-one sequence, and the constant-zero sequence. The rational-mask compiler gives the safe ambient bound $2^3 = 8$ before reachability restriction.

**Alternating unit over $\mathbb{F}_3$.** For the word 12,

$$T = 2, \qquad m(x) = x + 1, \qquad F(z) = \frac{1}{1+z}, \qquad R(z) = \frac{1+z^3}{1+z} = 1 + 2z + z^2.$$

The recurrence order is one although the minimal period is two. The 3-kernel consists of the sequence and its negative, giving two minimal digital states. The compiler bound is nine.

**Period-three unit word over $\mathbb{F}_2$.** For the word 110,

$$T = 3, \qquad m(x) = x^2 + x + 1, \qquad F(z) = \frac{1}{1+z+z^2}, \qquad R(z) = 1 + z + z^2.$$

The reachable pair model has six representatives, while equality of subsequence behavior collapses them to three kernel states. This is a concrete instance of the directional quotient in proposition 9.7.

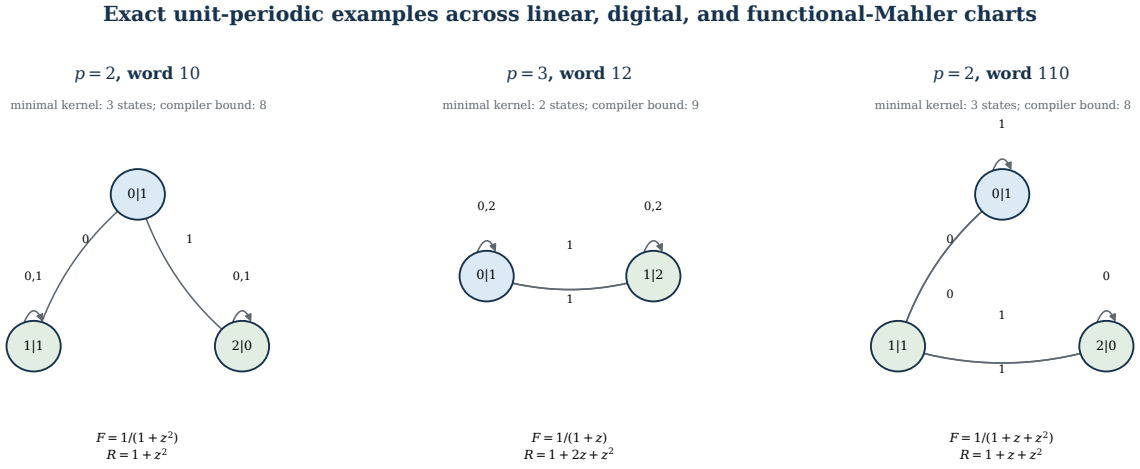



**Figure 14:** Three exact examples. A state label $s \mid o$ gives the state identifier and output. The compiler bounds are ambient theorem bounds before reachability restriction, not claims of minimal state count.

**Negative control: a nonunit periodic sequence.** Over $\mathbb{F}_2$, the word 01 gives

$$F(z) = \frac{z}{1+z^2}.$$

Then

$$\frac{F(z)}{F(z^2)} = \frac{1+z^2}{z},$$

which is Laurent rather than regular at the origin. The sequence remains purely periodic, C-finite, and automatic, but it is not an object of $\mathbf{Mask}_2^{\times,\mathrm{per}}$. This verifies that the unit overlap condition is structural rather than cosmetic.

### 9.8 Exact finite verification

**Table 13:** Exact finite validation of the Block 03 periodic heterogeneous atlas.

| Check | Recorded result |
|---|---|
| Enumerated normalized objects | $p = 2$ through period 8, $p = 3$ through period 6; 583 primitive unit-periodic words. |
| Exact identities and automaton checks | 39805 checks; 0 failures. |
| Arithmetic model | exact prime-field and polynomial arithmetic. |
| Overall status | PASS. |
| Boundary | Finite enumeration validates the declared ranges and implementation formulas. It does not replace the symbolic proofs or establish unrestricted automatic-to-Mahler equivalence. |

The supplied verifier enumerates every primitive unit-periodic word over $\mathbb{F}_2$ through period eight and over $\mathbb{F}_3$ through period six. For each object it checks, using exact prime-field and polynomial arithmetic:

1. Berlekamp-Massey recovery of the minimal recurrence;
2. divisibility by $x^T - 1$ and $1 - z^T$;
3. recovery of the least period from both normalized linear charts;
4. the reduced rational functional-Mahler identity;
5. the exact reachable pair model and its behavioral quotient;
6. the multiplier-orbit formula Equation (7);
7. coefficient output of the minimal digit automaton;
8. the Cartier compiler state bound Equation (14).

The finite computation supports the implementation and examples. The symbolic theorems above do not depend on the enumeration.

**Section result.** The manuscript now contains a fully declared finite atlas spanning three genuinely different strata: minimal finite-linear recurrences, minimal digital automata, and rational functional-Mahler masks. Every reversible bridge has a complete passport. The raw Cartier compiler is retained as a directional constructor with an exact loss statement. All four triple overlaps and the quadruple coherence equation are proved through rigidity of normalized fibers. Objects and morphisms descend effectively, and the compatible periodic invariant package is globally complete on the declared unit-periodic semantic category. This is the first theorem in the manuscript that satisfies the finite heterogeneous completion criterion rather than only the one-stratum cross-presentation criterion.

## 10 Rational-mask digital descent beyond pure periodicity

Periodic atlas verified a four-chart atlas on unit purely periodic sequences. That domain made the linear, rational, digital, and functional-Mahler charts meet simultaneously, but it left open the larger

overlap between rational functional-Mahler masks and automatic sequences. This section removes the periodicity hypothesis while keeping the normalization and bridge standards unchanged.

Fix a prime $p$. Let

$$\mathbf{RMah}_p^{\times} = \left\{ F(z) \in 1 + z\mathbb{F}_p[[z]] : \frac{F(z)}{F(z^p)} \in \mathbb{F}_p(z) \right\}$$

be the discrete category of unit formal series with rational canonical functional-Mahler mask. This category contains the periodic objects of Section 9, but for odd $p$ it also contains genuinely nonrational and non-C-finite automatic series.

### 10.1 Frobenius-radical characterization

For a unit formal series, define its canonical local mask by

$$R_F(z) = \frac{F(z)}{F(z^p)}. \tag{18}$$

The coefficientwise infinite product

$$\mathcal{M}_p[R](z) = \prod_{j \geq 0} R\left(z^{p^j}\right) \tag{19}$$

is well defined for every $R \in 1 + z\mathbb{F}_p[[z]]$, because only finitely many factors contribute to a fixed coefficient.

**Theorem 10.1** (Frobenius-radical characterization)**.** *Let $F \in 1 + z\mathbb{F}_p[[z]]$. Then*

$$R_F(z) = F(z)^{1-p}. \tag{20}$$

*Consequently, the following are equivalent.*

(i) *The canonical mask $R_F$ is rational.*

(ii) *The power $F^{p-1}$ belongs to $\mathbb{F}_p(z)$.*

(iii) *There are coprime polynomials $A, B \in \mathbb{F}_p[z]$ with*

$$A(0) = B(0) = 1$$

*and*

$$B(z)F(z) = A(z)F(z^p). \tag{21}$$

*For the reduced mask $R_F = A/B$, one has*

$$F(z)^{p-1} = \frac{B(z)}{A(z)}. \tag{22}$$

*The ratio and product constructions are strict inverses:*

$$F \longmapsto R_F, \qquad R \longmapsto \mathcal{M}_p[R].$$

*In particular, every object of $\mathbf{RMah}_p^{\times}$ is algebraic over $\mathbb{F}_p(z)$ of degree at most $p-1$.*

*Proof.* In characteristic $p$, Frobenius gives

$$F(z^p) = F(z)^p.$$

Substitution into Equation (18) gives Equation (20). Thus $R_F$ is rational exactly when $F^{p-1} = R_F^{-1}$ is rational. Writing the reduced rational mask as $A/B$ gives Equation (21) and Equation (22).

Conversely, a reduced rational mask $A/B$ with unit constant terms defines a unique formal solution of Equation (21): the product in Equation (19). Telescoping gives

$$\frac{\mathcal{M}_p[R](z)}{\mathcal{M}_p[R](z^p)} = R(z),$$

while uniqueness follows by comparing coefficients recursively. Hence the ratio and product constructions are strict inverses. Finally, Equation (22) is an algebraic equation of degree $p-1$. □

*Boundary* 10.2 (Functional Mahler versus Newton-Mahler). The word "Mahler" continues to name two distinct constructions. This section concerns the functional equation

$$F(z) = R(z)F(z^p).$$

It does not identify rational masks with Newton-Mahler expansions

$$f(x) = \sum_{r\geq 0} c_r \binom{x}{r}$$

or with $p$-adic analytic interpolation. Any bridge to that local analytic chart still requires its own passport and proof.

### 10.2 The rational-collapse obstruction

Let $R = A/B$ be reduced and normalized. For each monic irreducible polynomial $\pi \in \mathbb{F}_p[z]$, define

$$\omega_\pi(R) = \big(v_\pi(B) - v_\pi(A)\big) \bmod (p-1).$$

Include the valuation at infinity

$$\omega_\infty(R) = \big(\deg A - \deg B\big) \bmod (p-1).$$

The finite-support family

$$\omega_{p-1}(R) = \big(\omega_v(R)\big)_v \tag{23}$$

is the *rational-collapse obstruction*.

**Theorem 10.3** (Exact rational-collapse criterion)**.** *Let $F = \mathcal{M}_p[A/B]$. The following are equivalent.*

(i) $F \in \mathbb{F}_p(z)$.

(ii) $B/A$ *is a* $(p-1)$*-st power in* $\mathbb{F}_p(z)$.

(iii) $\omega_{p-1}(A/B) = 0$.

*When these conditions hold, there is a unique rational function $G \in \mathbb{F}_p(z)$ with $G(0) = 1$ and*

$$G^{p-1} = B/A,$$

*and $F = G$.*

*If $p = 2$, every rational mask collapses to a rational series. If $p > 2$ and $\omega_{p-1}(A/B) \neq 0$, then $F$ is nonrational, non-C-finite, and not eventually periodic.*

*Proof.* The equivalence of (i) and (ii) follows from Equation (22). If $B/A = G^{p-1}$, every valuation of $B/A$ is divisible by $p-1$, so (ii) implies (iii).

Conversely, suppose all valuation residues vanish. Since $A$ and $B$ are coprime, every irreducible exponent in each polynomial is divisible by $p-1$. Factoring into monic irreducibles therefore gives

$$A = C^{p-1}, \qquad B = D^{p-1}$$

for polynomials $C, D$ after a constant normalization. The unit conditions $A(0) = B(0) = 1$ remove the remaining scalar obstruction. Thus $B/A = (D/C)^{p-1}$. Multiplying $D/C$ by its inverse constant term does not change its $(p-1)$-st power, and gives the unique root with constant term one. The formal solution is unique, so $F = G$.

For $p = 2$, the exponent $p-1$ is one, hence the obstruction group is trivial and $F = B/A$. Over a finite field, a rational coefficient series is C-finite and eventually periodic, while an eventually periodic sequence has a rational generating function. Therefore a nonzero obstruction forces all three failures stated in the theorem. □

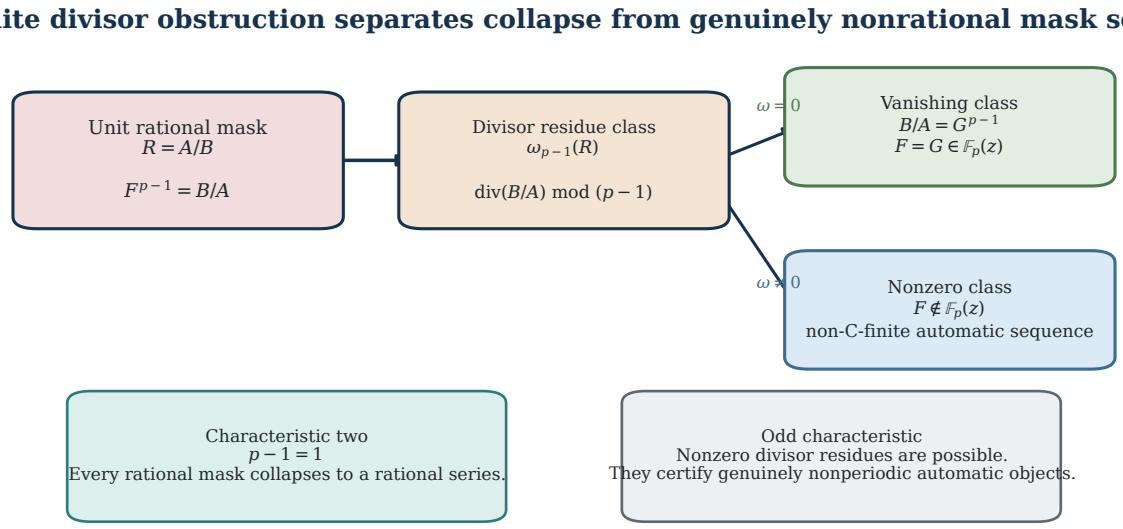



**Figure 15:** The rational-collapse obstruction. A rational mask always gives an automatic series, but it gives a rational or C-finite series exactly on the vanishing divisor-residue locus.

### 10.3 Denominator stabilization and the canonical Cartier module

Write

$$a = \deg A, \qquad b = \deg B, \qquad H(z) = A(z)B(z)^{p-2},$$

and define

$$D(A,B) = \max\left\{b, \left\lceil \frac{a+(p-2)b}{p-1} \right\rceil \right\}. \tag{24}$$

Let $\mathcal{P}_D = \mathbb{F}_p[z]_{\le D}$. For $0 \le d < p$, define

$$T_d(P) = \Lambda_d(PH), \tag{25}$$

where $\Lambda_d$ selects the coefficients in degrees congruent to $d$ modulo $p$.

**Theorem 10.4** (Fixed-denominator Cartier realization)**.** *Let $F = \mathcal{M}_p[A/B]$ and $D = D(A,B)$. Then:*

(i) *every $T_d$ preserves $\mathcal{P}_D$;*

(ii) *the linear map*

$$\Theta_{A,B} : \mathcal{P}_D \longrightarrow \mathbb{F}_p[[z]], \qquad \Theta_{A,B}(P) = \frac{P}{B}F, \tag{26}$$

*is injective;*

(iii) *the transitions intertwine exactly:*

$$\Lambda_d \Theta_{A,B}(P) = \Theta_{A,B}(T_d(P)); \tag{27}$$

(iv) *starting from $P_0 = B$, the coefficient of index*

$$n = d_0 + d_1 p + \cdots + d_{\ell-1}p^{\ell-1}$$

*is*

$$[z^n]F = \epsilon_0\big(\Theta_{A,B}\big(T_{d_{\ell-1}} \cdots T_{d_0} B\big)\big), \tag{28}$$

*where $\epsilon_0(G) = [z^0]G$.*

*Proof.* If $\deg P \le D$, then

$$\deg(PH) \le D + a + (p-2)b.$$

Cartier selection divides the retained degrees by $p$. The definition of $D$ gives

$$\deg T_d(P) \le \left\lfloor \frac{D + a + (p-2)b}{p} \right\rfloor \le D.$$

This proves (i).

The series $F/B$ is a unit in $\mathbb{F}_p[[z]]$. Multiplication by a unit is injective, so $\Theta_{A,B}$ is injective. The rational-mask Cartier identity imported from [8] is precisely Equation (27). Iterating it from $\Theta(B) = F$ and taking constant terms proves Equation (28). □

For a digit word $w = d_0 \cdots d_{\ell-1}$, read least significant digit first and write

$$\Lambda_w = \Lambda_{d_{\ell-1}} \cdots \Lambda_{d_0}.$$

Define the Cartier kernel and its linear span by

$$\mathcal{K}_p(F) = \{\Lambda_w F : w \in \{0,\dots,p-1\}^*\}, \qquad \mathcal{V}_p(F) = \operatorname{span}_{\mathbb{F}_p} \mathcal{K}_p(F). \tag{29}$$

**Definition 10.5** (Canonical Cartier module and Cartier rank)**.** The canonical Cartier module of $F$ is

$$\mathsf{C}_p(F) = \left(\mathcal{V}_p(F), (\Lambda_d|_{\mathcal{V}_p(F)})_{0\le d<p}, F, \epsilon_0\right). \tag{30}$$

Its dimension

$$r_p(F) = \dim_{\mathbb{F}_p} \mathcal{V}_p(F) \tag{31}$$

is the *Cartier rank*.

**Theorem 10.6** (Minimality of the canonical Cartier module)**.** *For every $F \in \mathbf{RMah}_p^{\times}$, the module $\mathsf{C}_p(F)$ is finite dimensional, reachable, and observable. It is therefore a minimal digit-linear realization of the coefficient function. Every other reachable-observable digit-linear realization of the same coefficient function is uniquely similar to $\mathsf{C}_p(F)$.*

*Proof.* By theorem 10.4, every section $\Lambda_w F$ lies in the $(D+1)$-dimensional image of $\Theta_{A,B}$. Hence $\mathcal{V}_p(F)$ is finite dimensional. Reachability is built into its definition as the span of the orbit of $F$.

For observability, let $G \in \mathcal{V}_p(F)$ satisfy

$$\epsilon_0(\Lambda_w G) = 0$$

for every digit word $w$. For any $n \ge 0$, choose the base-$p$ digits of $n$. The section identity gives

$$[z^n]G = \epsilon_0(\Lambda_w G) = 0.$$

Thus $G = 0$, so the observation family separates points.

For uniqueness, let $(V, (L_d), v, \lambda)$ be another reachable-observable realization of the same digit function. Send the reachable vector $L_w v$ to $\Lambda_w F$. If a linear combination of reachable vectors vanishes, applying every continuation and then $\lambda$ shows that the corresponding combination of Cartier sections has every coefficient zero. Observability makes the assignment well defined. Reachability makes it surjective, and the symmetric construction gives an inverse. The intertwining, initial-vector, and output identities are immediate. Any such similarity is determined on the reachable spanning set, so it is unique. □

## 10.4 The exact reachable compiler core

Let $\mathcal{R}(A,B) \subseteq \mathcal{P}_D$ be the finite set of numerator states reachable from $B$ under the transitions $T_d$, and let

$$W(A,B) = \operatorname{span}_{\mathbb{F}_p} \mathcal{R}(A,B).$$

**Theorem 10.7** (Reachable numerator core)**.** *The map $\Theta_{A,B}$ restricts to*

$$\mathcal{R}(A,B) \xrightarrow{\sim} \mathcal{K}_p(F) \tag{32}$$

*and to a linear isomorphism*

$$W(A,B) \xrightarrow{\sim} \mathcal{V}_p(F). \tag{33}$$

*The reachable deterministic output automaton of the fixed-denominator compiler is already minimal. No nontrivial output-equivalence quotient remains after reachability restriction.*

*Proof.* For every word $w$, repeated use of Equation (27) gives

$$\Theta_{A,B}(T_w B) = \Lambda_w F.$$

Thus $\Theta_{A,B}$ maps the reachable numerator set onto the Cartier kernel. Injectivity of $\Theta_{A,B}$ makes the map bijective, and taking linear spans gives Equation (33).

If two reachable numerators $P \neq Q$ had identical future output behavior, the two series $\Theta(P)$ and $\Theta(Q)$ would have identical coefficients and would therefore be equal. Injectivity would force $P = Q$, a contradiction. Hence all reachable states are behaviorally distinct. Reachability and distinguishability prove minimality. □

The preceding theorem sharpens the generic reduction language used in Periodic atlas. A behavioral quotient remains a safe general construction for arbitrary output automata, but it is trivial for the normalized fixed-denominator numerator compiler.

Let

$$\kappa_p(F) = |\mathcal{K}_p(F)|. \tag{34}$$

**Corollary 10.8** (Exact state-complexity hierarchy)**.** *For a reduced rational mask $A/B$,*

$$r_p(F) \le \kappa_p(F) \le p^{r_p(F)} \le p^{D(A,B)+1}. \tag{35}$$

*Moreover,*

$$r_p(F) = \dim W(A,B), \qquad \kappa_p(F) = |\mathcal{R}(A,B)|.$$

*Proof.* The Cartier kernel spans $\mathcal{V}_p(F)$, so its cardinality is at least the dimension. It is a subset of the $p^{r_p(F)}$ vectors in $\mathcal{V}_p(F)$. Finally, $\mathcal{V}_p(F)$ embeds into the $(D+1)$-dimensional compiler space by theorem 10.7. □

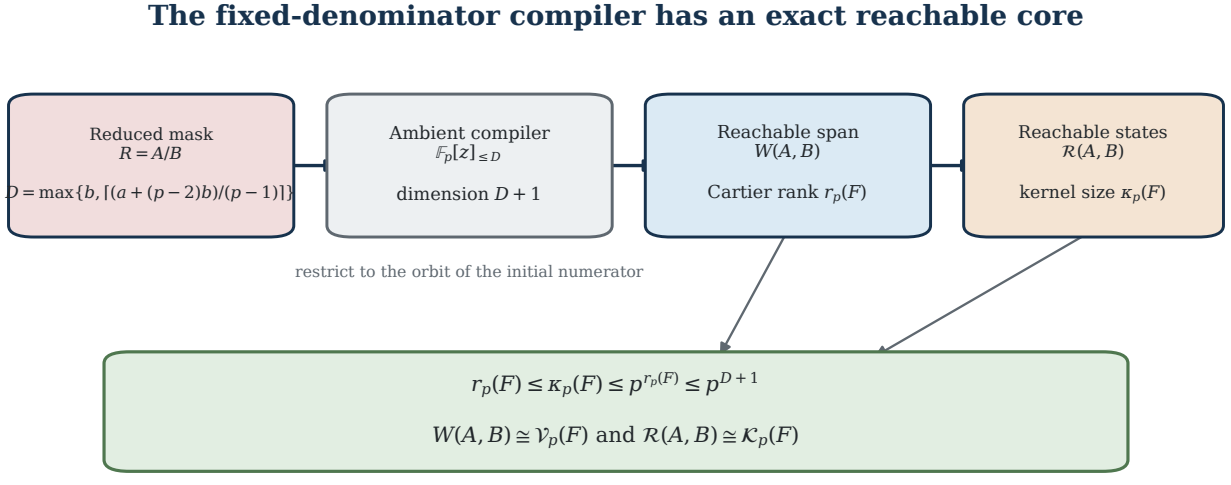



**Figure 16:** The exact reachable core of the fixed-denominator compiler. The linear rank and deterministic state count are different invariants, but both are bounded by the explicit mask degree profile.

## 10.5 Three normalized charts

The rational-mask domain has three normalized charts.

**Reduced mask chart.** An object of $\mathbf{Mask}_p^{\mathrm{rat}}$ is a reduced rational function

$$R(z) = \frac{A(z)}{B(z)}, \qquad A(0) = B(0) = 1.$$

Morphisms preserve the rational function. The semantics is $R \mapsto \mathcal{M}_p[R]$. The inverse chart map is the canonical ratio $F \mapsto F/F(z^p)$.

**Minimal Cartier-module chart.** An object of $\mathbf{Cart}_p^{\mathrm{min,rat}}$ is a finite-dimensional tuple

$$(V, (L_d)_{d=0}^{p-1}, v, \lambda)$$

that is reachable and observable, whose digit coefficient function belongs to $\mathbf{RMah}_p^{\times}$. Morphisms are similarities preserving every $L_d$, the initial vector, and the output functional. Its normalized representative is $\mathsf{C}_p(F)$.

**Minimal digital chart.** An object of $\mathbf{Aut}_p^{\mathrm{min,rat}}$ is a reachable minimal least-significant-digit-first $p$-DFAO whose coefficient series belongs to $\mathbf{RMah}_p^{\times}$. Its canonical representative has state set $\mathcal{K}_p(F)$, transition $G \mapsto \Lambda_d G$, start state $F$, and output $G \mapsto G(0)$.

**Table 14:** Bridge passports for the rational-mask digital atlas.

| Bridge | Class | Preserved data | Exact boundary |
|---|---|---|---|
| Mask $\leftrightarrow$ series | strict inverse pair | every coefficient and the canonical mask | the mask must be rational and unit normalized |
| Series $\leftrightarrow$ Cartier module | normalized equivalence | all Cartier sections, linear relations, initial vector, output | the module is restricted to reachable-observable realizations |
| Series $\leftrightarrow$ minimal DFAO | normalized equivalence | the complete $p$-kernel and coefficient function | the automaton uses the fixed radix and LSD-first convention |
| Mask $\rightarrow$ ambient compiler | directional constructor | exact coefficients and fixed-denominator transitions | adds unreachable ambient numerator states |
| Ambient compiler $\rightarrow$ normalized core | reachable restriction | all reachable series and all future outputs | discards only states outside the orbit of $B$ |

**Theorem 10.9** (Rational-mask three-chart equivalence)**.** *The semantic functors induce equivalences of groupoids*

$$\mathbf{Mask}_p^{\mathrm{rat}} \simeq \mathbf{Cart}_p^{\mathrm{min,rat}} \simeq \mathbf{Aut}_p^{\mathrm{min,rat}} \simeq \mathbf{RMah}_p^{\times}. \tag{36}$$

*The mask-series bridge is a strict inverse pair. The Cartier and digital bridges are normalized equivalences with unique comparison isomorphisms.*

*Proof.* The strict mask-series equivalence is theorem 10.1. The canonical Cartier construction gives an object of the second chart, and theorem 10.6 gives a unique similarity from every other minimal realization of the same series. The canonical $p$-kernel automaton is finite by theorem 10.4. It is reachable by construction. Distinct kernel series differ in some coefficient, and the digit word for that coefficient distinguishes their future outputs, so the automaton is minimal. The usual behavioral map gives the unique isomorphism from any other reachable minimal DFAO for the same series. □

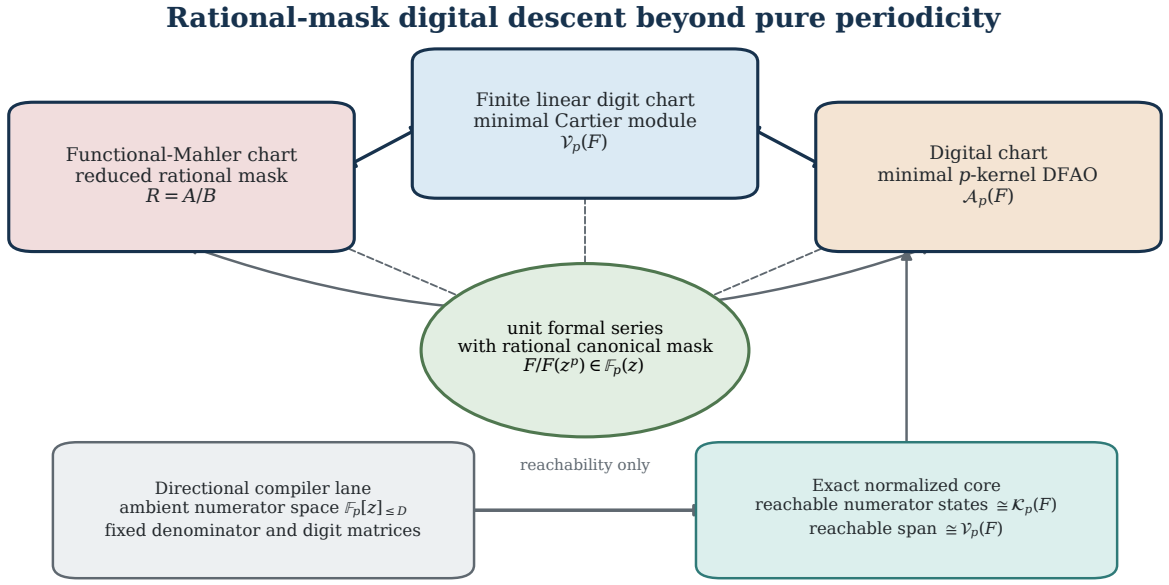



**Figure 17:** The Rational-mask atlas atlas. The normalized reversible core contains a rational mask, a minimal Cartier module, and a minimal digital automaton. The full polynomial compiler remains a larger directional presentation.

## 10.6 Coherence and effective descent

**Lemma 10.10** (Rigidity of rational-mask normalized fibers)**.** *Fix $F \in \mathbf{RMah}_p^{\times}$. The groupoid of normalized presentations of $F$ in each of the three charts is contractible.*

*Proof.* The reduced canonical mask is unique. Any automorphism of a reachable Cartier module that fixes the initial vector and commutes with all digit operators fixes a spanning set, hence is the identity. Any automorphism of a reachable deterministic automaton that fixes the start state and commutes with every digit transition fixes every state, hence is the identity. Existence and uniqueness of isomorphisms between two normalized realizations follow from theorems 10.6 and 10.9. □

Let $\mathfrak{R}_p^{\mathrm{rm}}$ denote the three-chart pseudofunctor defined by the passports above.

**Theorem 10.11** (Rational-mask coherence and effective descent)**.** *Choose every pairwise bridge by the canonical constructions and every comparison cell by the unique normalized isomorphism over the common series. Then the triple-overlap coherence law holds, and*

$$\mathrm{Desc}(\mathfrak{R}_p^{\mathrm{rm}}) \simeq \mathbf{RMah}_p^{\times}. \tag{37}$$

*Descent is effective for objects and morphisms.*

*Proof.* On the only nonempty triple overlap, both composites are isomorphisms between normalized presentations of the same series. By lemma 10.10, the isomorphism is unique, so the comparison diagram commutes.

Given $F \in \mathbf{RMah}_p^{\times}$, its reduced mask, canonical Cartier module, and minimal $p$-kernel automaton form descent data. Conversely, compatible local objects have one common semantic series. Fiber rigidity identifies them uniquely with its normalized presentations. The same argument applies to morphisms. Hence the normalization functor is fully faithful and essentially surjective. □

This theorem is strictly broader than theorem 9.10: no periodicity or C-finiteness hypothesis is imposed. It is also strictly narrower than an atlas of all automatic sequences, because an automatic series may have a nonrational canonical mask.

## 10.7 Compatible invariants and collapse stratification

For $F \in \mathbf{RMah}_p^{\times}$, define

$$\mathcal{J}_p^{\mathrm{rm}}(F) = \big(R_F, \omega_{p-1}(R_F), D(R_F), \mathcal{V}_p(F), r_p(F), \mathcal{K}_p(F), \kappa_p(F), \mathcal{A}_p(F)\big)\,. \tag{38}$$

**Theorem 10.12** (Invariant descent on the rational-mask atlas)**.** *The native mask, Cartier-module, and automaton invariants admit coherent comparison maps to $\mathcal{J}_p^{\mathrm{rm}}$. They descend to the category in Equation (37). The descended invariant is complete on $\mathbf{RMah}_p^{\times}$.*

*Proof.* The fixed-denominator intertwining theorem identifies the reachable numerator span with $\mathcal{V}_p(F)$ and the reachable numerator set with $\mathcal{K}_p(F)$. Hence all components of the package agree under the bridges. Coherence follows from theorem 10.11. If two packages agree, their reduced canonical masks agree. The coefficientwise mask product then reconstructs the same formal series, so the semantic objects are equal. □

The obstruction $\omega_{p-1}$ divides the semantic category into two exact loci:

$$\mathbf{RMah}_p^{\times} = \mathbf{RMah}_{p,\mathrm{col}}^{\times} \sqcup \mathbf{RMah}_{p,\mathrm{ncol}}^{\times}.$$

The collapse locus consists of rational, hence ultimately periodic, series. The noncollapse locus consists of non-C-finite automatic series. The unit-periodic atlas of Periodic atlas is the persistent, zero-transient subatlas inside $\mathbf{RMah}_{p,\mathrm{col}}^{\times}$.

## 10.8 Exact examples and strict boundaries

**Cantor-digit indicator.** Over $\mathbb{F}_3$, let

$$R(z) = 1 + z.$$

Then

$$F(z) = \prod_{j \geq 0} (1 + z^{3^j})$$

has coefficient one exactly when the ternary expansion of the index uses only the digits zero and one. The functional equation is

$$F(z) = (1+z)F(z^3), \qquad F(z)^2 = \frac{1}{1+z}.$$

**Table 15:** Named exact examples in the rational-mask digital atlas.

| Example | Field | Reduced mask $A/B$ | First coefficients | $r_p/\kappa_p$ | Collapse status / compiler bound |
|---|---|---|---|---|---|
| Cantor-digit indicator | $\mathbb{F}_3$ | $(1+z)/(1)$ | 110110000110110000 | 1/2 | non-collapse compiler bound 9 |
| Square-root denominator | $\mathbb{F}_3$ | $(1)/(1+z)$ | 121121000121121000 | 2/4 | non-collapse compiler bound 9 |
| Alternating collapse | $\mathbb{F}_3$ | $(1+2z+z^2)/(1)$ | 1212121212121212 | 1/2 | collapse compiler bound 9 |
| Finite transient | $\mathbb{F}_2$ | $(1)/(1+z+z^2)$ | 1110000000000000 | 3/4 | collapse compiler bound 8 |

The factor $1+z$ has odd divisor multiplicity, so the collapse obstruction is nonzero. Thus the sequence is automatic but not C-finite or eventually periodic. The canonical automaton has two states, while the Cartier rank is one.

**A genuine denominator example.** Over $\mathbb{F}_3$, take

$$R(z) = \frac{1}{1+z}.$$

Then

$$F(z)^2 = 1+z.$$

The reduced denominator remains fixed under every Cartier section. The ambient compiler has dimension two, its reachable numerator set is

$$\{0, 1, 2, 1+z\},$$

and its reachable span has dimension two. Hence

$$r_3(F) = 2, \qquad \kappa_3(F) = 4.$$

The nonzero collapse obstruction again proves that the automatic coefficient sequence is not eventually periodic.

**Collapse back to the periodic atlas.** For

$$R(z) = (1+z)^2 = 1+2z+z^2$$

over $\mathbb{F}_3$, one has

$$F(z)^2 = \frac{1}{(1+z)^2}, \qquad F(z) = \frac{1}{1+z}.$$

The coefficients alternate between one and two. This object lies in the rational-collapse locus and in the unit-periodic atlas of Periodic atlas.

**Characteristic-two transient.** Over $\mathbb{F}_2$, choose

$$R(z) = \frac{1}{1+z+z^2}.$$

Since $p-1=1$,

$$F(z) = 1+z+z^2.$$

Its coefficient sequence is $1,1,1,0,0,\ldots$. It is ultimately periodic but not purely periodic. This is the simplest exact witness that Rational-mask atlas extends the semantic domain even in characteristic two.

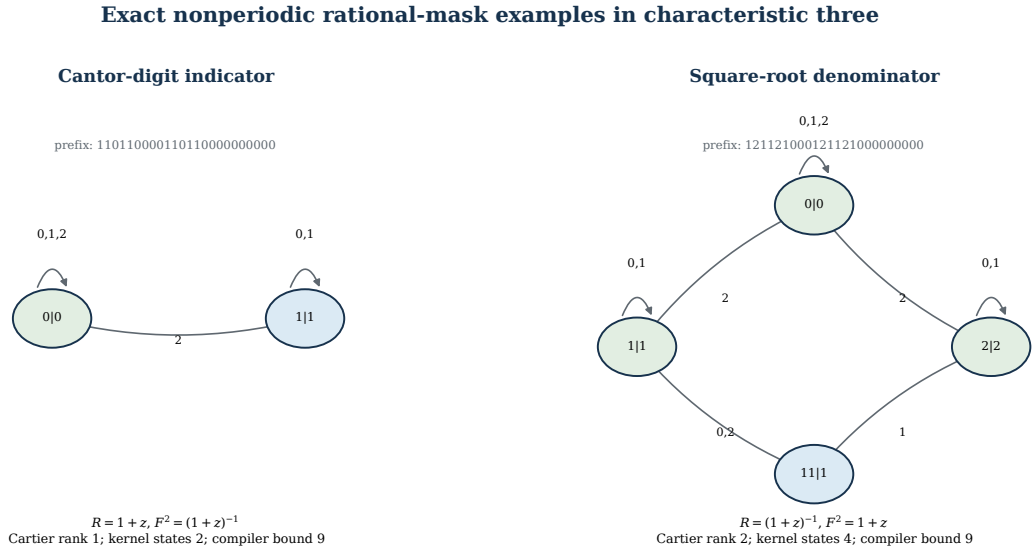



**Figure 18:** Two exact nonperiodic objects in the rational-mask atlas. State labels give the reachable numerator polynomial followed by its output.

**Negative control: automatic does not imply rational mask.** Let $t_n \in \mathbb{F}_2$ be the parity of the binary digit sum of $n$, and put

$$u_n = 1 + t_n.$$

The sequence $u$ is unit and 2-automatic. It is not eventually periodic. Indeed, eventual period $T$ would propagate backwards through the identities

$$t_{2^k+n} = 1 + t_n \qquad (0 \le n < 2^k)$$

and force a pure period $T$. Writing $T = 2^\nu q$ with $q$ odd, the binary digit count of $2^m - T$ has parity

$$m - \nu - s_2(q-1)$$

for all sufficiently large $m$. Choosing the parity of $m$ makes

$$t_{2^m - T} \neq t_{2^m},$$

contradicting pure periodicity.

Let $U(z) = \sum_{n\ge 0} u_n z^n$. If its canonical mask were rational, then theorem 10.3 with $p = 2$ would make $U$ rational, hence eventually periodic. Therefore $U/U(z^2)$ is not rational. The rational-mask atlas is a proper normalized subatlas of the unit automatic stratum.

**Table 16:** Exact finite validation of the Block 04 rational-mask digital atlas.

| Check | Recorded result |
|---|---|
| Enumerated reduced unit masks | $p = 2$ with $\deg A, \deg B \leq 3$, $p = 3$ with $\deg A, \deg B \leq 2$, $p = 5$ with $\deg A, \deg B \leq 1$; 125 masks in total. |
| Rational-collapse split | 51 collapse masks and 74 genuinely nonrational mask series. |
| Exact identities and state checks | 11391 checks; 0 failures. |
| Arithmetic model | exact polynomial, finite-field, Cartier-transition, and formal-series arithmetic. |
| Overall status | PASS. |
| Boundary | Finite enumeration checks the compiler, reachable Cartier module, state hierarchy, examples, and collapse classification on the declared ranges. It does not replace the unbounded proofs or classify all automatic sequences. |

### 10.9 Exact finite verification

The Rational-mask atlas verifier enumerates every reduced unit mask with

$$\deg A, \deg B \leq 3 \quad (p = 2), \qquad \deg A, \deg B \leq 2 \quad (p = 3), \qquad \deg A, \deg B \leq 1 \quad (p = 5).$$

For every mask it checks, using exact finite-field and polynomial arithmetic:

1. the invariant degree bound on the full ambient numerator space;
2. the functional-equation coefficient recursion against compiler output;
3. transition closure and fixed-denominator intertwining;
4. distinguishability of every pair of reachable numerator states;
5. the identities
$$W(A, B) \cong \mathcal{V}_p(F), \qquad \mathcal{R}(A, B) \cong \mathcal{K}_p(F);$$
6. the state hierarchy in Equation (35);
7. characteristic-two collapse and the named collapse or noncollapse examples.

The finite calculation validates the implementation on the recorded ranges. It is not used as a substitute for the unbounded proofs.

**Section result.** The verified heterogeneous atlas now extends beyond pure periodicity. Every unit rational functional-Mahler mask over $\mathbb{F}_p$ has a finite canonical Cartier module and a finite canonical $p$-kernel automaton. The three normalized charts satisfy coherence and effective descent. The fixed-denominator compiler has an exact reachable core: reachable numerator states are already the minimal digital states, and their span is the minimal Cartier module. The rational-collapse obstruction separates the ultimately periodic sublocus from genuinely non-C-finite automatic series. The resulting invariant package is globally complete on the declared rational-mask semantic category, but no claim is made for automatic sequences whose canonical mask is nonrational.

## 11 Fixed-radix regular normalization and the automatic finite-orbit boundary

Rational-mask atlas closes a substantial automatic slice, but its semantic domain is still defined by the existence of a rational functional-Mahler mask. The next digital question is more basic and more general:

what is the canonical normalized representation of a sequence whose complete fixed-radix section orbit spans a finite-dimensional vector space, even when that orbit itself is infinite?

This section answers that question over a field. It separates two invariants that coincide only in special cases:

linear section rank and cardinality of the section orbit.

The first controls regularity and minimal digit-linear dimension. The second controls automaticity and minimal deterministic-state cardinality. Their exact relationship is the automatic–regular boundary developed below.

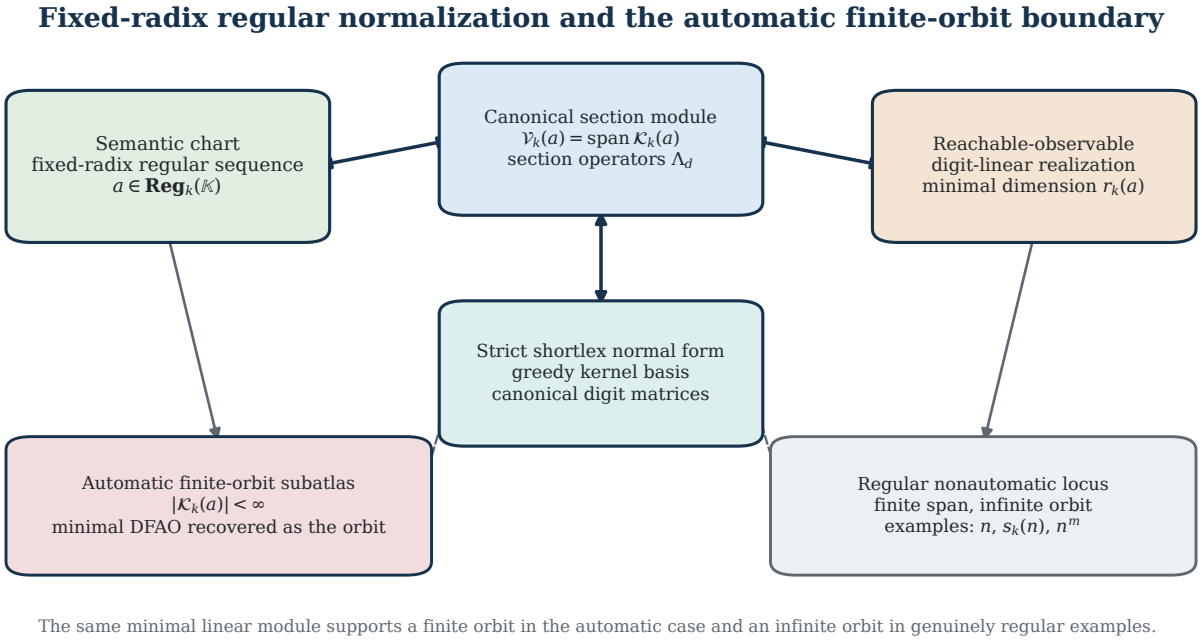



**Figure 19:** The fixed-radix regular atlas. The canonical section module and its strict shortlex matrix form exist throughout the regular locus. The minimal DFAO chart appears exactly on the finite-orbit sublocus.

## 11.1 Section operators and the canonical kernel module

Fix an integer radix $k \geq 2$ and a field $K$. Let

$$\Sigma_k = \{0, 1, \ldots, k-1\}.$$

Words are read from least significant digit to most significant digit. For

$$w = d_0 d_1 \cdots d_{\ell-1} \in \Sigma_k^*,$$

define

$$|w| = \ell, \qquad [w]_k = \sum_{j=0}^{\ell-1} d_j k^j.$$

The empty word $\varepsilon$ has length zero and value zero.

For a sequence $a = (a_n)_{n \geq 0} \in K^{\mathbb{N}}$, define the digit-section operators

$$(\Lambda_d a)(n) = a(kn + d), \qquad 0 \leq d < k.$$

For a word $w = d_0 \cdots d_{\ell-1}$, put

$$\Lambda_w = \Lambda_{d_{\ell-1}} \cdots \Lambda_{d_1} \Lambda_{d_0}.$$

Then

$$(\Lambda_w a)(n) = a\big(k^{|w|} n + [w]_k\big). \tag{39}$$

**Definition 11.1** (Fixed-radix kernel and section module)**.** The $k$-kernel and its linear span are

$$\mathcal{K}_k(a) = \{\Lambda_w a : w \in \Sigma_k^*\}, \qquad \mathcal{V}_k(a) = \operatorname{span}_K \mathcal{K}_k(a).$$

The sequence is *$k$-regular over $K$* when $\mathcal{V}_k(a)$ is finite dimensional. Its regular rank is

$$r_k(a) = \dim_K \mathcal{V}_k(a).$$

It is *$k$-automatic in the present reading convention* when $\mathcal{K}_k(a)$ is finite. In that case set

$$\kappa_k(a) = |\mathcal{K}_k(a)|.$$

The terminology records two different finiteness statements. Regularity asks for a finite-dimensional linear hull. Automaticity asks for a finite orbit under the section semigroup itself.

**Definition 11.2** (Digit-linear realization)**.** A digit-linear realization of $a$ is a tuple

$$\mathsf{L} = (W, A_0, \dots, A_{k-1}, v, \lambda),$$

where $W$ is a finite-dimensional $K$-vector space, $A_d \in \operatorname{End}_K(W)$, $v \in W$, and $\lambda \in W^*$, such that for every word $w = d_0 \cdots d_{\ell-1}$,

$$a_{[w]_k} = \lambda A_w v, \qquad A_w = A_{d_{\ell-1}} \cdots A_{d_0}. \tag{40}$$

Because different words can represent the same integer after terminal high zeros are appended, equation (40) includes the required leading-zero consistency.

**Theorem 11.3** (Section-module realization theorem)**.** *For a sequence $a \in K^{\mathbb{N}}$, the following are equivalent:*

1. *$a$ is $k$-regular over $K$;*
2. *$a$ admits a finite-dimensional digit-linear realization.*

*When these conditions hold, the tuple*

$$\mathsf{C}_k(a) = \big(\mathcal{V}_k(a), \Lambda_0, \dots, \Lambda_{k-1}, a, \epsilon_0\big), \qquad \epsilon_0(f) = f(0), \tag{41}$$

*is a canonical realization of dimension $r_k(a)$.*

*Proof.* Assume first that $\mathcal{V}_k(a)$ is finite dimensional. It is invariant under every $\Lambda_d$ by construction. Choose any basis, represent the section operators by matrices, take the initial vector to be $a$, and take output to be evaluation at zero. For every word $w$,

$$\epsilon_0(\Lambda_w a) = (\Lambda_w a)(0) = a_{[w]_k},$$

so the resulting realization satisfies (40).

Conversely, suppose $a$ has a realization $(W, A_d, v, \lambda)$. For $x \in W$, define its represented behavior by

$$\mathcal{B}(x)(n) = \lambda A_{\mathrm{dig}_k(n)} x,$$

where $A_{\mathrm{dig}_k(n)}$ is the product associated with the canonical least-significant-digit-first expansion of $n$. Equation (40) and concatenation of digit words give

$$\Lambda_w a = \mathcal{B}(A_w v).$$

Hence every kernel section belongs to $\mathcal{B}(W)$, so

$$\dim_K \mathcal{V}_k(a) \le \dim_K W.$$

Thus $a$ is regular. The realization in (41) has dimension exactly $r_k(a)$. □

**Proposition 11.4** (Reachability and observability)**.** *The canonical section realization $\mathsf{C}_k(a)$ is linearly reachable and observable:*

$$\mathrm{span}_K\{\Lambda_w a : w \in \Sigma_k^*\} = \mathcal{V}_k(a),$$

*and*

$$\bigcap_{w\in\Sigma_k^*} \ker(\epsilon_0 \Lambda_w) = \{0\}.$$

*Proof.* Reachability is the definition of $\mathcal{V}_k(a)$. If $f \in \mathcal{V}_k(a)$ satisfies $(\epsilon_0\Lambda_w)(f) = 0$ for every word $w$, then

$$f([w]_k) = 0$$

for every word. Every nonnegative integer has such an expansion, so $f = 0$. □

## 11.2 Word-Hankel rank and minimal digit-linear dimension

The canonical module can be read directly from a Hankel-type matrix indexed by digit words.

**Definition 11.5** (Word-Hankel matrix)**.** The fixed-radix word-Hankel matrix of $a$ is the infinite matrix

$$H_a(u, v) = a_{[u]_k + k^{|u|}[v]_k} = (\Lambda_u a)([v]_k), \qquad u, v \in \Sigma_k^*. \tag{42}$$

**Theorem 11.6** (Regular rank theorem)**.** *Let $a$ be $k$-regular over $K$. Then*

$$\boxed{r_k(a) = \mathrm{rank}_K H_a = \min\{\dim_K W : W \text{ supports a digit-linear realization of } a\}.} \tag{43}$$

*Moreover:*

1. *there exist finite word sets $U, V \subset \Sigma_k^*$, each of cardinality $r_k(a)$, for which the minor $H_a[U, V]$ is nonsingular;*
2. *every reachable-observable realization of dimension $r_k(a)$ is isomorphic to $\mathsf{C}_k(a)$;*
3. *any two minimal reachable-observable realizations are related by a unique similarity intertwining all digit operators, the initial vector, and the output functional.*

*Proof.* The row indexed by $u$ in $H_a$ is the behavior of the section $\Lambda_u a$ evaluated on all continuation words. By observability in proposition 11.4, evaluation on all words is injective on $\mathcal{V}_k(a)$. Therefore the row span of $H_a$ is naturally isomorphic to $\mathcal{V}_k(a)$, and

$$\mathrm{rank}_K H_a = r_k(a).$$

For an arbitrary realization $(W, A_d, v_{\mathrm{in}}, \lambda)$, concatenation gives the factorization

$$H_a(u, v) = \lambda A_v A_u v_{\mathrm{in}}.$$

Thus $H_a$ factors through $W$, so rank $H_a \leq \dim W$. The canonical realization has dimension $r_k(a)$, proving the minimality formula.

An infinite matrix of finite rank $r_k(a)$ has a nonsingular finite $r_k(a) \times r_k(a)$ minor, which gives the first assertion. For the remaining assertions, define the behavior map of any realization by

$$\mathcal{B}_W(x)(n) = \lambda A_{\mathrm{dig}_k(n)} x.$$

Observability makes this map injective. Reachability and equality of the represented sequence make its image equal to $\mathcal{V}_k(a)$. In minimal dimension it is therefore an isomorphism intertwining the digit operators, initial vector, and output. Composing the two behavior isomorphisms gives the unique similarity between any two minimal reachable-observable realizations. □

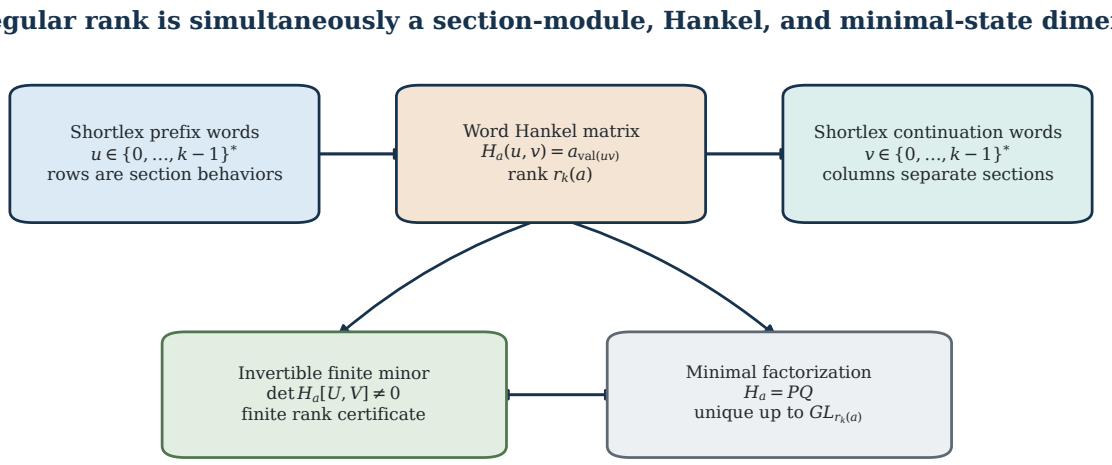



**Figure 20:** Three exact meanings of the regular rank. The finite nonsingular minor is a certificate rather than an approximation: it proves a lower bound that is attained by the canonical section module.

*Remark* 11.7 (Finite certification). The theorem is infinite in statement but finite in certificate. A proposed rank $r$ can be certified by:

1. an explicit $r$-dimensional section-stable span containing $a$, which proves $r_k(a) \leq r$;
2. an explicit nonsingular $r \times r$ word-Hankel minor, which proves $r_k(a) \geq r$.

When both are supplied, the regular rank is exact.

## 11.3 Strict shortlex normalization

Minimal realizations are unique up to similarity, but the stratified atlas needs a literal normalized chart rather than an unnamed similarity class. The actual section functions supply a canonical basis choice.

Order $\Sigma_k^*$ by shortlex order: shorter words precede longer words, and words of equal length are ordered lexicographically. Starting from the empty list, scan the words in this order and retain a word precisely when its section is not in the span of the previously retained sections.

**Definition 11.8** (Greedy shortlex kernel basis)**.** For a regular sequence $a$, let

$$U_a = (u_1, \dots, u_{r_k(a)})$$

be the unique ordered list produced by the greedy shortlex rule, and put

$$b_i = \Lambda_{u_i} a.$$

For the zero sequence, the list is empty.

Because membership in a linear span is intrinsic, the resulting ordered basis depends only on the represented sequence, the field, the radix, and the fixed word order.

**Construction 11.9** (Strict shortlex realization)**.** Write

$$\Lambda_d b_j = \sum_{i=1}^{r_k(a)} (M_d(a))_{ij} b_i, \qquad a = \sum_i v_i(a) b_i, \qquad \ell_i(a) = b_i(0).$$

The strict shortlex record is

$$\mathsf{SL}_{k,K}(a) = \big(U_a, M_0(a), \dots, M_{k-1}(a), v(a), \ell(a)\big). \tag{44}$$

**Theorem 11.10** (Strict fixed-radix normal form)**.** *The record $\mathsf{SL}_{k,K}(a)$ is uniquely determined by $a$ and reconstructs $a$ exactly through*

$$a_{[w]_k} = \ell(a) M_w(a) v(a).$$

*It has dimension $r_k(a)$. Two regular sequences have the same strict shortlex record if and only if they are equal.*

*Proof.* The greedy word list is uniquely determined by the actual section functions. Once the ordered basis is fixed, the coefficients of every digit section, the initial vector, and the output functional are unique. The reconstruction identity is the coordinate form of the canonical section realization. Equality of records therefore implies equality of every coefficient, while equality of sequences gives the same sections and hence the same greedy record. □

**Theorem 11.11** (Fixed-radix regular normalized atlas)**.** *Let $\mathbf{Reg}_k(K)$ be the discrete semantic category of $K$-valued $k$-regular sequences. Let $\mathbf{Sec}_k^{\mathrm{can}}(K)$ be the category of canonical section-module records (41), and let $\mathbf{Lin}_{k,K}^{\mathrm{sl}}$ be the category of strict shortlex records (44), with morphisms required to preserve the represented sequence. Then*

$$\boxed{\mathbf{Reg}_k(K) \simeq \mathbf{Sec}_k^{\mathrm{can}}(K) \simeq \mathbf{Lin}_{k,K}^{\mathrm{sl}}.} \tag{45}$$

*Every normalized fiber over a fixed sequence is contractible. Consequently the associated finite presentation atlas has effective object and morphism descent.*

*Proof.* A sequence determines its canonical section module and its strict shortlex record functorially. Conversely, either record reconstructs every coefficient. The two composites are identities because the section module is defined from the represented sequence and the shortlex basis is intrinsic. The uniqueness in theorem 11.10 leaves no nontrivial automorphism in a normalized fiber. Compatible local objects and morphisms therefore glue uniquely. □

**Definition 11.12** (Fixed-radix regular invariant)**.** The normalized fixed-radix invariant is

$$\mathcal{J}^{\mathrm{reg}}_{k,K}(a) = \big(r_k(a), \mathsf{C}_k(a), \mathsf{SL}_{k,K}(a), [H_a[U,V]]\big), \tag{46}$$

where $[H_a[U,V]]$ denotes any recorded nonsingular rank certificate together with its word addresses. The strict normal form makes this package complete on $\mathbf{Reg}_k(K)$.

The finite Hankel minor is not canonical unless an ordering rule is imposed on candidate column sets. It is therefore treated as a certificate attached to the canonical invariant, not as the invariant itself.

## 11.4 The automatic finite-orbit subatlas

The automatic locus is not a second unrelated theory. It is the locus on which the orbit of the distinguished initial vector inside the canonical regular module is finite.

**Theorem 11.13** (Kernel automaton theorem)**.** *Assume $\mathcal{K}_k(a)$ is finite. Define a deterministic automaton with output by*

$$\text{state set } \mathcal{K}_k(a), \qquad f \xrightarrow{d} \Lambda_d f, \qquad \text{initial state } a, \qquad \text{output } f(0).$$

*Then:*

1. *the automaton represents $a$ under least-significant-digit-first reading;*
2. *every state is reachable;*
3. *distinct states are behaviorally distinguishable;*
4. *it is the unique minimal DFAO up to state renaming.*

*Proof.* After reading a word $w$, the state is $\Lambda_w a$, whose output is $a_{[w]_k}$. Reachability is immediate from the definition of the kernel. If $f \neq g$, then there is an integer $n$ with $f(n) \neq g(n)$. Reading a digit word for $n$ from either state distinguishes them. Thus no two states can be merged, and the reachable automaton is minimal. The usual residual-behavior argument then gives uniqueness up to renaming. □

**Theorem 11.14** (Automatic–regular finite-orbit equivalence)**.** *For a $k$-regular sequence $a$, the following are equivalent:*

1. *$a$ is $k$-automatic;*
2. *the orbit $\{\Lambda_w a : w \in \Sigma_k^*\}$ of the initial vector in $\mathsf{C}_k(a)$ is finite;*
3. *the orbit of $v(a)$ under the strict shortlex digit matrices is finite.*

*On this locus, the minimal DFAO is recovered as the orbit itself. Hence*

$$\mathbf{Aut}_k(K) \simeq \mathbf{FinOrbSec}_k(K) \simeq \mathbf{FinOrbLin}^{\mathrm{sl}}_{k,K} \simeq \mathbf{DFAO}^{\min}_{k,K}. \tag{47}$$

*If $K = \mathbb{F}_q$ is finite, every $k$-regular $K$-valued sequence is automatic.*

*Proof.* The first three conditions are the same orbit statement written in semantic, intrinsic-module, and coordinate form. The kernel automaton in theorem 11.13 recovers the deterministic chart, while its state-to-section map recovers the finite orbit inside the canonical module. These constructions are inverse on normalized objects. If $K = \mathbb{F}_q$ and $r_k(a) < \infty$, the vector space $\mathcal{V}_k(a)$ has only $q^{r_k(a)}$ elements, so the section orbit is automatically finite. □

**Corollary 11.15** (State-rank hierarchy). *Let $a$ be automatic with values in $\mathbb{F}_q$. Then*

$$\boxed{r_k(a) \le \kappa_k(a) \le q^{r_k(a)}.} \tag{48}$$

*The first inequality can be strict: behavior-distinct kernel states may be linearly dependent.*

*Proof.* The kernel states span $\mathcal{V}_k(a)$, so their number is at least its dimension. They form a subset of the $q^{r_k(a)}$-element vector space $\mathcal{V}_k(a)$, proving the upper bound. □

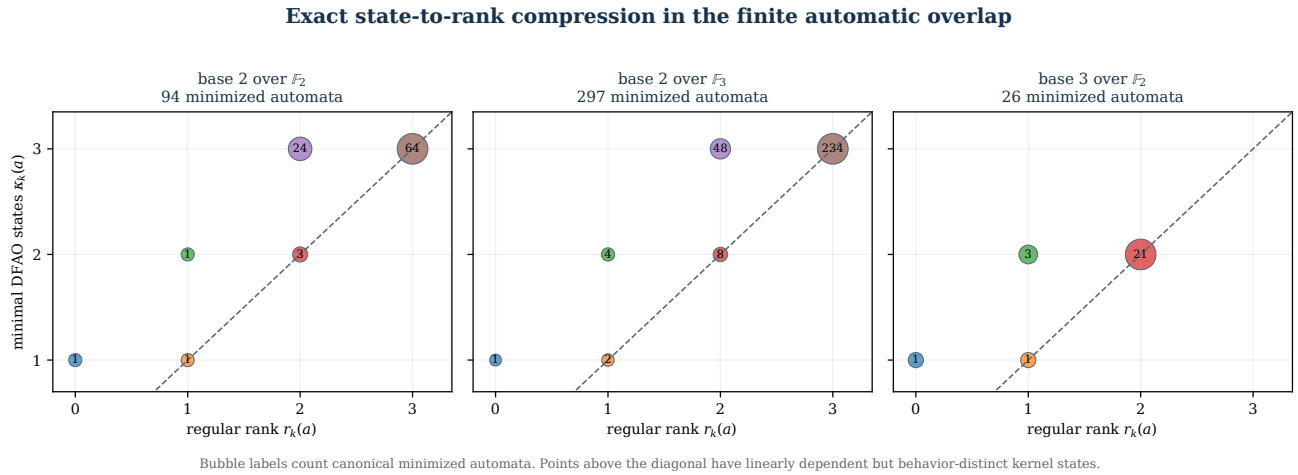



**Figure 21:** Exact bounded enumeration of the automatic overlap. Bubble labels count distinct minimized automata. Points above the diagonal are finite kernel orbits whose state behaviors are distinct but linearly dependent.

The corollary explains why deterministic state minimization and linear-state minimization must remain distinct coordinates. The minimal automaton records the finite orbit as a set with digit action. The regular rank records the dimension of its linear span. Neither number alone reconstructs the other.

## 11.5 Exact regular examples beyond automaticity

Over an infinite field, finite linear rank does not force a finite section orbit. The following families give exact, unbounded witnesses.

**Theorem 11.16** (Polynomial regular rank in characteristic zero). *Let $K$ have characteristic zero and let $P \in K[x]$ be nonzero of degree $m$. For the sequence $a_n = P(n)$,*

$$r_k(a) = m + 1.$$

*If $m \ge 1$, its $k$-kernel is infinite.*

*Proof.* Every section has the form

$$(\Lambda_w a)(n) = P(k^{|w|}n + [w]_k),$$

which is a polynomial in $n$ of degree at most $m$. Hence the section span has dimension at most $m + 1$. Choose $\ell$ with $k^\ell > m$ and consider the $m + 1$ sections

$$P(k^\ell n + r), \qquad 0 \le r \le m.$$

When expanded in the basis $1, n, \dots, n^m$, their coefficient functions as functions of $r$ have successive degrees $m, m-1, \dots, 0$, with nonzero leading coefficients. Evaluation at the distinct points $0, 1, \dots, m$ therefore gives an invertible generalized Vandermonde matrix. These sections are linearly independent, proving rank $m+1$.

For $m \geq 1$, the sections $P(k^\ell n + r)$ are distinct as $r$ varies through arbitrarily large complete residue ranges, so the kernel orbit is infinite. □

**Corollary 11.17.** *For $a_n = n$, one has $r_k(a) = 2$ and exactly $k^\ell$ distinct sections at depth $\ell$. For $a_n = n^2$, one has $r_k(a) = 3$ and again exactly $k^\ell$ distinct sections at depth $\ell$.*

**Theorem 11.18** (Digit-sum regularity)**.** *Let $s_k(n)$ be the sum of the base-k digits of n, regarded as a sequence over a characteristic-zero field. Then*

$$r_k(s_k) = 2,$$

*and*

$$\mathcal{K}_k(s_k) = \{s_k + c : c \in \mathbb{Z}_{\geq 0}\}. \tag{49}$$

*At exact depth $\ell$, the number of distinct sections is*

$$(k-1)\ell + 1.$$

*Thus $s_k$ is k-regular but not k-automatic over a characteristic-zero field.*

*Proof.* The digit identity

$$s_k(kn + d) = s_k(n) + d$$

gives

$$\Lambda_d s_k = s_k + d.$$

Iterating shows that every section is $s_k + c$, so the span is contained in $\operatorname{span}\{1, s_k\}$. The two sequences are independent, giving rank two. At depth $\ell$, the additive constant is the digit sum of an $\ell$-digit residue. Every integer from 0 through $(k-1)\ell$ occurs, giving exactly $(k-1)\ell + 1$ states. □

**Table 17:** Named examples at the automatic–regular boundary.

| Example | Base / field | Regular rank | Kernel or states | Classification |
|---|---|---|---|---|
| Ternary Cantor-digit indicator | 3 / $\mathbb{F}_3$ | 1 | 2 | automatic and regular |
| Thue-Morse parity | 2 / $\mathbb{F}_2$ | 2 | 2 | automatic and regular |
| Identity sequence $n$ | 2 / $\mathbb{Q}$ | 2 | infinite | regular, not automatic |
| Binary digit sum $s_2(n)$ | 2 / $\mathbb{Q}$ | 2 | infinite | regular, not automatic |
| Square sequence $n^2$ | 2 / $\mathbb{Q}$ | 3 | infinite | regular, not automatic |

## 11.6 Exact finite verification

The Fixed-radix regular atlas verifier performs two complementary exact audits.

First, it exhaustively enumerates bounded deterministic automata in three configurations:

$$(k, q, s_{\max}) = (2, 2, 3), \qquad (2, 3, 3), \qquad (3, 2, 2).$$

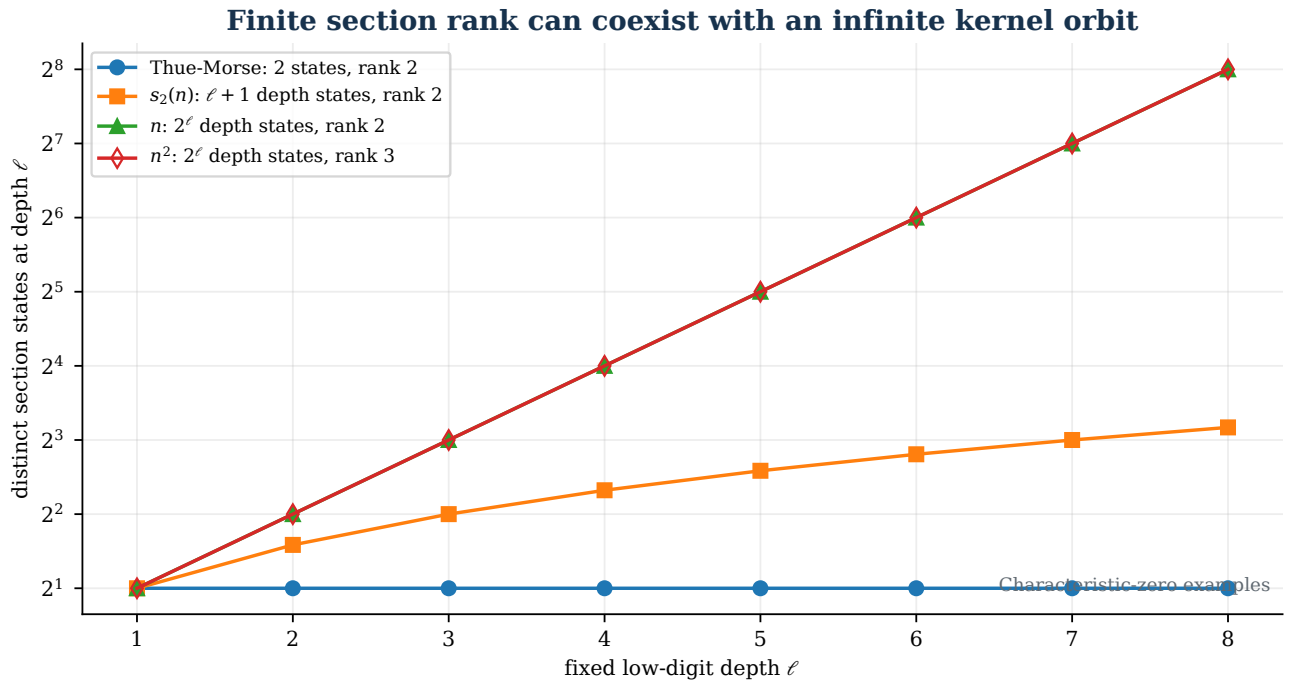



**Figure 22:** Fixed section rank does not bound orbit cardinality over an infinite field. The Thue–Morse orbit is finite, while $n$, $n^2$, and the digit sum have finite linear rank but unboundedly many distinct sections.

**Table 18:** Exact finite validation of the Fixed-radix regular atlas fixed-radix regular atlas.

| Check | Recorded result |
|---|---|
| Exhaustive finite-state enumeration | base 2 over $\mathbb{F}_2$ through 3 raw states: 5,898 raw candidates, 2,830 leading-zero-consistent candidates, 94 distinct minimized automata; base 2 over $\mathbb{F}_3$ through 3 raw states: 19,830 raw candidates, 6,990 leading-zero-consistent candidates, 297 distinct minimized automata; base 3 over $\mathbb{F}_2$ through 2 raw states: 258 raw candidates, 170 leading-zero-consistent candidates, 26 distinct minimized automata. |
| Automatic-to-linear checks | 86,207 exact checks; 83 minimized automata with strict state-to-rank compression. |
| Unbounded regular examples | Polynomial sequences $n^m$ for bases 2 and 3 through degree 6, plus digit sums in bases 2, 3, and 4; 2,438 exact checks. |
| Combined Fixed-radix regular atlas checks | 89,055 checks; 0 failures. |
| Overall status | PASS. |
| Boundary | The computation validates the bounded automata and named exact examples. It does not prove an all-radix, all-ring, semiring, or all-moduli minimality theorem. |

Every candidate is restricted to reachable states, minimized by behavioral equivalence, and filtered by the terminal-high-zero consistency required by integer semantics. For every resulting normalized automaton the verifier checks:

1. reachability and pairwise behavioral distinguishability;
2. construction of the canonical linear quotient from continuation-output rows;
3. transition and output equivariance of the state embedding;
4. the inequalities in Equation (48);
5. equality of word-Hankel rank and regular rank;
6. exact equality between the finite linear orbit and the minimized automaton state set;
7. coefficient agreement on a fixed exact test range.

Second, it checks unbounded symbolic families using exact integer and rational matrices. Polynomial sequences $n^m$ are checked for bases two and three through degree six, and digit sums are checked in bases two, three, and four, including their exact depth-orbit growth formulas.

The finite audit records 89,055 exact checks and no failures. It supports the implementation, examples, and bounded state-rank distribution. The unbounded theorems above are proved symbolically and do not depend on the enumeration.

**Exact boundary of Fixed-radix regular atlas.** The normalization theorem is fixed-radix and field-valued. It does not yet give one integral normal form valid simultaneously modulo every prime power, a semiring minimality theorem, or a canonical all-radix comparison invariant. Over a general commutative ring, the section module can have torsion, fail to be free, and admit inequivalent minimal generating systems. Saturation, Smith/Fitting data, prime-power reduction towers, and local completion therefore remain separate arithmetic obligations rather than being hidden inside the field theorem.

**Section result.** Every field-valued fixed-radix regular sequence has a canonical section module, a minimal reachable-observable digit-linear realization, an exact word-Hankel rank, and a strict shortlex normal form. These charts satisfy effective normalized descent and yield a complete invariant on the declared fixed-radix regular category. The automatic locus is exactly the finite-orbit locus inside the same module, where the minimal DFAO is recovered as the orbit of the distinguished initial vector. Over finite fields regularity and automaticity coincide, while over characteristic-zero fields polynomial and digit-sum examples have finite rank and infinite section orbit. This closes fixed-radix linear-state minimality over fields, not the all-moduli or integral regular-sequence problem.

## 12 Integral saturation, Smith–Fitting defects, and prime-power effectivity

Fixed-radix regular atlas proves a complete fixed-radix normalization theorem over a field. The next question is not obtained by replacing the coefficient field with $\mathbb{Z}$ symbol by symbol. Over $\mathbb{Z}$, two canonical lattices appear inside the same rational section space. Their finite-index difference is invisible over $\mathbb{Q}$, but it controls reduction modulo every integer, the appearance of ghost coordinates, and the distinction between an effective $p$-adic lift and an effective integral lift.

Throughout this section, $k \geq 2$ is fixed and

$$a : \mathbb{N} \longrightarrow \mathbb{Z}$$

is an integer-valued sequence whose rational section space

$$V_{\mathbb{Q}}(a) = \operatorname{span}_{\mathbb{Q}} \mathcal{K}_k(a) \subseteq \mathbb{Q}^{\mathbb{N}}$$

has finite dimension

$$\rho_k(a) = \dim_{\mathbb{Q}} V_{\mathbb{Q}}(a).$$

Thus $a$ is $k$-regular after extension of scalars to $\mathbb{Q}$.

## 12.1 The raw section lattice and its canonical saturation

**Definition 12.1** (Raw and saturated section lattices)**.** The *raw section lattice* and the *saturated section lattice* are

$$M_k(a) = \operatorname{span}_{\mathbb{Z}} \mathcal{K}_k(a), \qquad L_k(a) = V_{\mathbb{Q}}(a) \cap \mathbb{Z}^{\mathbb{N}}.$$

The intersection defining $L_k(a)$ is taken inside $\mathbb{Q}^{\mathbb{N}}$.

The raw lattice is generated by the actual radix sections. The saturated lattice contains every integer-valued sequence lying in their rational span. These lattices agree over $\mathbb{Q}$, but need not agree over $\mathbb{Z}$.

**Lemma 12.2** (Finite coordinate detection)**.** *Let $V \subseteq \mathbb{Q}^{\mathbb{N}}$ be a vector space of finite dimension $\rho$. There exist indices*

$$0 \leq n_1 < \cdots < n_\rho$$

*such that the evaluation map*

$$E_{\mathbf{n}} : V \longrightarrow \mathbb{Q}^{\rho}, \qquad f \longmapsto \big(f(n_1), \ldots, f(n_\rho)\big)$$

*is an isomorphism.*

*Proof.* The coordinate functionals on $\mathbb{Q}^{\mathbb{N}}$ separate points of $V$. Choose $n_1$ for which some element of $V$ has nonzero value. If $n_1, \ldots, n_j$ have been chosen and the joint evaluation map has rank $j < \rho$, its kernel contains a nonzero $f$. Choose $n_{j+1}$ with $f(n_{j+1}) \neq 0$. The rank increases. After $\rho$ steps, the evaluation map has full rank. □

**Theorem 12.3** (Canonical finite saturated section lattice)**.** *The groups $M_k(a)$ and $L_k(a)$ are free abelian of rank $\rho_k(a)$. They are stable under every digit section $\Lambda_d$, and*

$$M_k(a) \subseteq L_k(a)$$

*has finite index. Moreover, $L_k(a)$ is the unique maximal subgroup of $V_{\mathbb{Q}}(a)$ whose elements are integer-valued.*

*Proof.* Choose a coordinate-detection set $\mathbf{n}$ by lemma 12.2. Evaluation embeds $L_k(a)$ into $\mathbb{Z}^\rho$, so $L_k(a)$ is a finitely generated free abelian group of rank at most $\rho$. The raw lattice $M_k(a)$ is contained in $L_k(a)$, and its rational span is all of $V_{\mathbb{Q}}(a)$. Hence $M_k(a)$ has rank $\rho$, and therefore $L_k(a)$ also has rank $\rho$. A subgroup of a finitely generated free abelian group is finitely generated and free, so $M_k(a)$ is free of rank $\rho$. Equal-rank lattice inclusion has finite index.

Every $\Lambda_d$ preserves $V_{\mathbb{Q}}(a)$ and preserves integer-valued sequences. Hence it preserves $L_k(a)$. It also maps each radix section to another radix section, so it preserves $M_k(a)$. Finally, any integer-valued subgroup of $V_{\mathbb{Q}}(a)$ lies in $V_{\mathbb{Q}}(a) \cap \mathbb{Z}^{\mathbb{N}} = L_k(a)$. □

**Definition 12.4** (Integral saturation defect)**.** The finite abelian group

$$C_k(a) = L_k(a)/M_k(a)$$

is the *integral saturation defect*. Its order

$$\delta_k(a) = [L_k(a) : M_k(a)]$$

is the *saturation index*.

By the Smith normal form, there are uniquely determined integers

$$1 \le d_1(a) \mid d_2(a) \mid \cdots \mid d_\rho(a)$$

such that

$$C_k(a) \cong \bigoplus_{i=1}^{\rho} \mathbb{Z}/d_i(a)\mathbb{Z}.$$

Factors with $d_i = 1$ are harmless but are retained so that the list has length $\rho$.

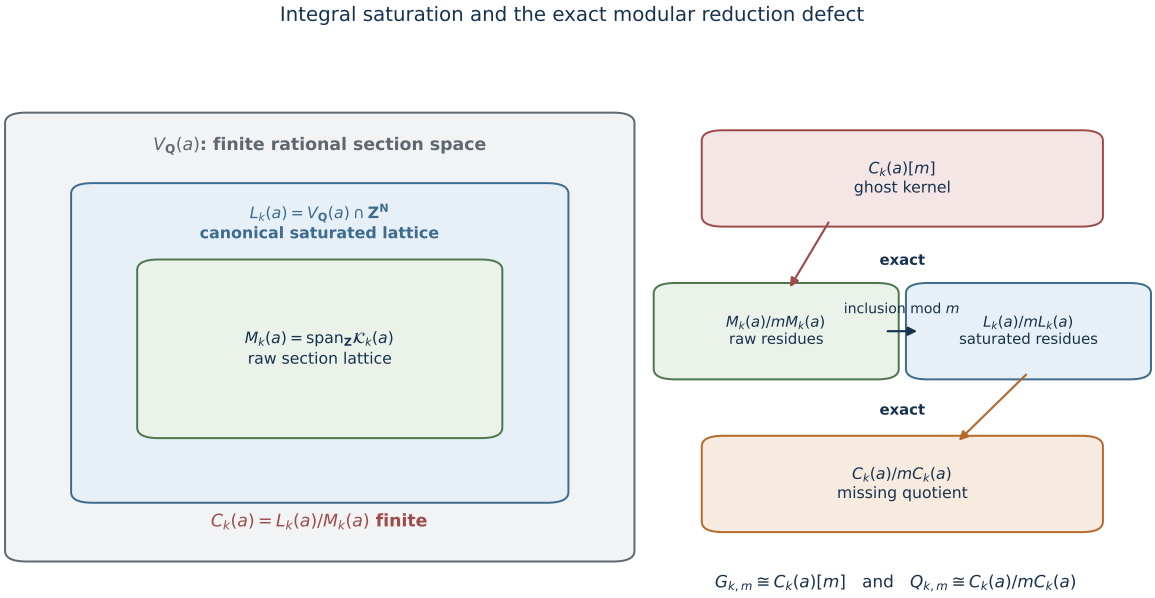



**Figure 23:** The rational section space contains the raw section lattice and its canonical integer-valued saturation. The finite quotient is invisible over $\mathbb{Q}$, but it controls every modular reduction.

**Example 12.5** (A rank-two nontrivial defect)**.** Let $s_k(n)$ be the base-$k$ digit-sum sequence and let $a = 2s_k$. Since

$$\Lambda_d s_k = s_k + d,$$

the rational section space is spanned by $s_k$ and the constant sequence 1. The actual sections of $2s_k$ generate

$$M_k(2s_k) = 2\mathbb{Z}\, s_k \oplus 2\mathbb{Z}\, 1,$$

whereas

$$L_k(2s_k) = \mathbb{Z}\, s_k \oplus \mathbb{Z}\, 1.$$

Thus

$$C_k(2s_k) \cong (\mathbb{Z}/2\mathbb{Z})^2.$$

The rational regular rank is two, but reduction modulo two loses the entire semantic lattice.

## 12.2 The exact reduction sequence

For an integer $m \geq 2$, the raw coefficient reduction is

$$M_k(a)/mM_k(a),$$

while the semantic reduction inside the saturated lattice is

$$\overline{M}_{k,m}(a) = \operatorname{im}\left(M_k(a)/mM_k(a) \longrightarrow L_k(a)/mL_k(a)\right).$$

These need not agree.

**Definition 12.6** (Ghost and missing reduction modules)**.** Define

$$G_{k,m}(a) = \ker\left(M_k(a)/mM_k(a) \longrightarrow L_k(a)/mL_k(a)\right)$$

and

$$Q_{k,m}(a) = \operatorname{coker}\left(M_k(a)/mM_k(a) \longrightarrow L_k(a)/mL_k(a)\right).$$

The first records raw residue coordinates that represent the zero semantic sequence. The second records saturated residue classes not reached by raw sections.

**Theorem 12.7** (Smith–Tor reduction sequence)**.** *For every $m \geq 2$, tensoring*

$$0 \longrightarrow M_k(a) \longrightarrow L_k(a) \longrightarrow C_k(a) \longrightarrow 0$$

*with $\mathbb{Z}/m\mathbb{Z}$ gives a canonical digit-equivariant exact sequence*

$$0 \longrightarrow C_k(a)[m] \longrightarrow M_k(a)/mM_k(a) \longrightarrow L_k(a)/mL_k(a) \longrightarrow C_k(a)/mC_k(a) \longrightarrow 0.$$

*Consequently,*

$$G_{k,m}(a) \cong C_k(a)[m], \qquad Q_{k,m}(a) \cong C_k(a)/mC_k(a).$$

*Proof.* Both $M_k(a)$ and $L_k(a)$ are free abelian. The long exact Tor sequence therefore begins

$$0 \longrightarrow \operatorname{Tor}_1^{\mathbb{Z}}(C_k(a), \mathbb{Z}/m\mathbb{Z}) \longrightarrow M_k(a) \otimes \mathbb{Z}/m\mathbb{Z} \longrightarrow L_k(a) \otimes \mathbb{Z}/m\mathbb{Z}.$$

For any abelian group $C$,

$$\operatorname{Tor}_1^{\mathbb{Z}}(C, \mathbb{Z}/m\mathbb{Z}) \cong C[m], \qquad C \otimes \mathbb{Z}/m\mathbb{Z} \cong C/mC.$$

The digit-section maps preserve the original short exact sequence, so naturality of Tor makes the five-term sequence digit-equivariant. □

**Corollary 12.8** (Exact Smith formulas)**.** *Let $g_i(m) = \gcd(m, d_i(a))$. Then*

$$G_{k,m}(a) \cong Q_{k,m}(a) \cong \bigoplus_{i=1}^{\rho} \mathbb{Z}/g_i(m)\mathbb{Z},$$

*and*

$$\left|\overline{M}_{k,m}(a)\right| = \prod_{i=1}^{\rho} \frac{m}{g_i(m)}.$$

*The reduction map is an isomorphism if and only if*

$$\gcd\big(m, d_\rho(a)\big) = 1.$$

*Equivalently, every prime dividing a reduction defect divides the saturation index.*

*Proof.* Choose Smith bases in which the inclusion $M_k(a) \hookrightarrow L_k(a)$ is the diagonal matrix

$$D = \operatorname{diag}(d_1, \dots, d_\rho).$$

Modulo $m$, the kernel and cokernel of multiplication by $d_i$ are both cyclic of order $\gcd(m, d_i)$, and the image has order $m/\gcd(m, d_i)$. The map is invertible in every coordinate exactly when every $d_i$ is a unit modulo $m$, which is equivalent to $\gcd(m, d_\rho) = 1$. □

**Proposition 12.9** (Fitting-ideal certificate)**.** *For* $0 \le j < \rho$,

$$\operatorname{Fitt}_j(C_k(a)) = \left(d_1(a)d_2(a)\cdots d_{\rho-j}(a)\right),$$

*and*

$$\operatorname{Fitt}_j(C_k(a)) = \mathbb{Z} \qquad (j \ge \rho).$$

*Thus the Smith profile and the Fitting filtration contain the same reduction-defect data at different resolutions.*

*Proof.* Use the diagonal presentation $D : \mathbb{Z}^\rho \to \mathbb{Z}^\rho$. The $j$-th Fitting ideal is generated by the minors of size $\rho - j$. Since $d_1 \mid \cdots \mid d_\rho$, the product of the first $\rho - j$ diagonal entries divides every other such minor and is itself one of the minors. □

*Boundary* 12.10 (What the defect classifies). The group $C_k(a)$ classifies the finite-index failure of the raw section lattice to be saturated. It does not classify the whole integral digit module, the sequence, or its section orbit. Two nonisomorphic digit modules can have the same Smith profile.

### 12.3 Digit equivariance and the prime-power tower

Choose Smith bases for $M_k(a)$ and $L_k(a)$, and let

$$D = \operatorname{diag}(d_1, \dots, d_\rho)$$

be the inclusion matrix. Let $A_d$ and $B_d$ be the integer matrices of $\Lambda_d$ on the raw and saturated lattices.

**Proposition 12.11** (Intertwining across saturation)**.** *For every digit* $d$,

$$B_d D = D A_d.$$

*Consequently, the raw modules, semantic images, ghost modules, and missing modules at every modulus form compatible digit modules.*

*Proof.* The inclusion $M_k(a) \hookrightarrow L_k(a)$ commutes with $\Lambda_d$. The displayed matrix identity is that commutative square in the chosen bases. Reduction modulo $m$, passage to kernel, image, and cokernel preserve the induced digit action. □

Fix a prime $p$ and write

$$\nu_i = \nu_{p,i}(a) = v_p(d_i(a)).$$

**Theorem 12.12** (Prime-power defect profile)**.** *For* $r \ge 1$,

$$G_{k,p^r}(a) \cong Q_{k,p^r}(a) \cong \bigoplus_{i=1}^{\rho} \mathbb{Z}/p^{\min(r,\nu_i)}\mathbb{Z},$$

*and*

$$\left|\overline{M}_{k,p^r}(a)\right| = p^{\sum_{i=1}^{\rho}(r-\min(r,\nu_i))}.$$

*The minimal number of generators of* $\overline{M}_{k,p^r}(a)$ *as a* $\mathbb{Z}/p^r\mathbb{Z}$*-module is*

$$\mu_{p^r}(a) = \#\{i : \nu_i < r\}.$$

*In particular,* $p$ *is a good reduction prime exactly when every* $\nu_i = 0$*.*

*Proof.* Apply corollary 12.8 to $m = p^r$. The $i$-th semantic image is the ideal

$$p^{\min(r,\nu_i)}\mathbb{Z}/p^r\mathbb{Z}.$$

It is nonzero and cyclic exactly when $\nu_i < r$. Over the local ring $\mathbb{Z}/p^r\mathbb{Z}$, the minimal number of generators of a direct sum of cyclic ideals is the number of nonzero summands. □

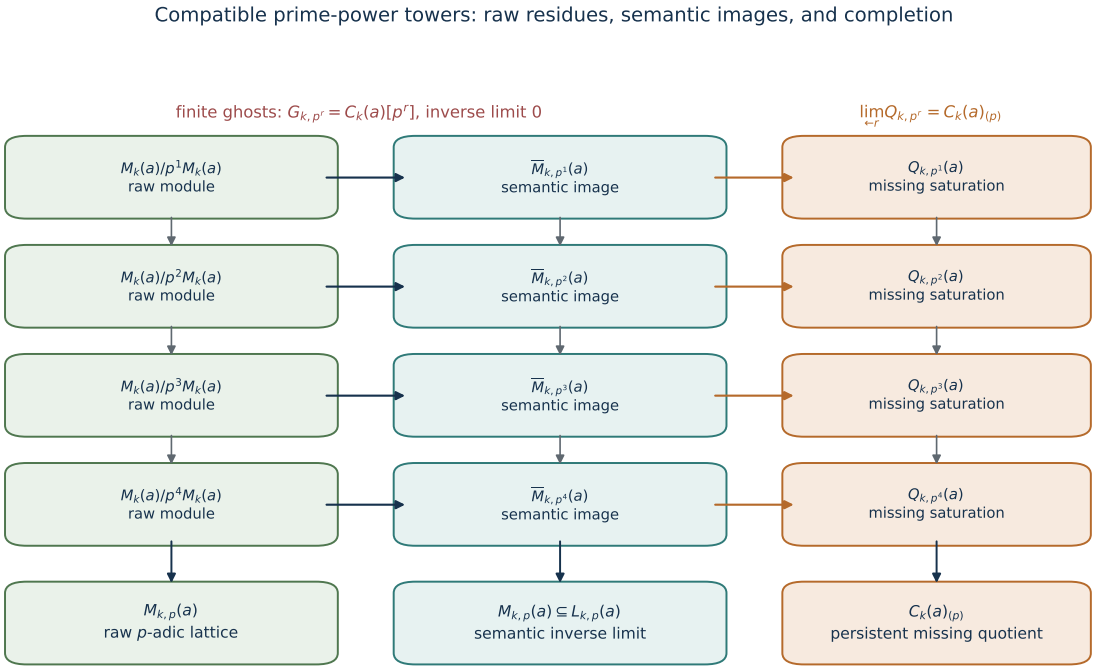



**Figure 24:** The raw residue tower maps onto the semantic prime-power tower. Ghost coordinates occur at finite depth when the raw lattice is not $p$-saturated. The compatible semantic tower converges to the embedded $p$-adic raw lattice.

**Definition 12.13** (Prime-power section automaton)**.** The semantic $p^r$-kernel is

$$\mathcal{K}^{\mathrm{sem}}_{k,p^r}(a) = \{\Lambda_w a \bmod p^r L_k(a) : w \in \Sigma_k^*\} \subseteq \overline{M}_{k,p^r}(a).$$

Its cardinality is denoted

$$\kappa^{\mathrm{sem}}_{k,p^r}(a).$$

**Theorem 12.14** (Finite prime-power automata)**.** *For every* $r \geq 1$*, the semantic* $p^r$*-kernel is finite and is the state set of the unique minimal least-significant-digit-first deterministic output automaton for the coefficient sequence* $a \bmod p^r$*. Moreover,*

$$\kappa^{\mathrm{sem}}_{k,p^r}(a) \leq \left|\overline{M}_{k,p^r}(a)\right| = p^{\sum_i(r-\min(r,\nu_i))}.$$

*Reduction induces surjective digit-equivariant maps*

$$\mathcal{K}^{\mathrm{sem}}_{k,p^{r+1}}(a) \twoheadrightarrow \mathcal{K}^{\mathrm{sem}}_{k,p^r}(a).$$

*Proof.* The semantic section module is finite, so its orbit under the digit maps is finite. As in the field-valued proof of theorem 11.13, every orbit state is reachable. Distinct section sequences have a continuation on which they differ, so they are behaviorally distinguishable. This gives the minimal deterministic automaton. The cardinality bound is the ambient module bound. The same section word at level $r+1$ reduces to the corresponding section word at level $r$, so the transition map on orbit states is surjective. □

**Corollary 12.15** (Good-prime transfer)**.** *If $p \nmid \delta_k(a)$, then for every $r \geq 1$,*

$$M_k(a)/p^r M_k(a) \xrightarrow{\sim} \overline{M}_{k,p^r}(a) = L_k(a)/p^r L_k(a).$$

*At a good prime, the raw and saturated prime-power towers agree exactly.*

**Table 19:** Canonical integral defect profiles for named fixed-radix families.

| Family | Smith profile | Bad primes | Interpretation |
|---|---|---|---|
| Digit sum $s_k$ | $(1,1)$ | none | Saturated rank-two lattice; no modular defect. |
| Doubled digit sum $2s_k$ | $(2,2)$ | 2 | Rank-two defect $(\mathbb{Z}/2)^2$; total semantic collapse modulo 2. |
| Constant sequence 2 | $(2)$ | 2 | One raw ghost coordinate modulo 2; one semantic state. |
| Constant sequence 6 | $(6)$ | 2, 3 | Bad primes 2 and 3; good reduction at every other prime. |

## 12.4 p-adic completion and the disappearance of finite ghosts

Define

$$M_{k,p}(a) = M_k(a) \otimes_{\mathbb{Z}} \mathbb{Z}_p, \qquad L_{k,p}(a) = L_k(a) \otimes_{\mathbb{Z}} \mathbb{Z}_p.$$

**Theorem 12.16** ($p$-adic saturation sequence)**.** *There is a digit-equivariant short exact sequence*

$$0 \longrightarrow M_{k,p}(a) \longrightarrow L_{k,p}(a) \longrightarrow C_k(a)_{(p)} \longrightarrow 0,$$

*where $C_k(a)_{(p)}$ is the $p$-primary subgroup of $C_k(a)$. In Smith coordinates,*

$$M_{k,p}(a) = \bigoplus_{i=1}^{\rho} p^{\nu_i}\mathbb{Z}_p e_i \subseteq \bigoplus_{i=1}^{\rho} \mathbb{Z}_p e_i = L_{k,p}(a).$$

*Proof.* The $\mathbb{Z}$-module $\mathbb{Z}_p$ is torsion free and hence flat. Tensor the integral short exact sequence with $\mathbb{Z}_p$. For a finite abelian group $C$,

$$C \otimes_{\mathbb{Z}} \mathbb{Z}_p \cong C_{(p)}.$$

The Smith-coordinate formula follows by tensoring the diagonal inclusion. □

**Theorem 12.17** (Raw and semantic inverse limits)**.** *There are canonical digit-equivariant identifications*

$$\varprojlim_r M_k(a)/p^r M_k(a) \cong M_{k,p}(a)$$

*and*

$$\varprojlim_r \overline{M}_{k,p^r}(a) \cong M_{k,p}(a) \subseteq L_{k,p}(a).$$

*Furthermore,*

$$\varprojlim_r G_{k,p^r}(a) = 0, \qquad \varprojlim_r Q_{k,p^r}(a) \cong C_k(a)_{(p)}.$$

*Proof.* The first identification is the definition of the $p$-adic completion of a finite free lattice. In Smith coordinate $i$, the semantic image at level $r$ is

$$p^{\min(r,\nu_i)}\mathbb{Z}/p^r\mathbb{Z}.$$

Its inverse limit is $p^{\nu_i}\mathbb{Z}_p$, giving the second identification.

A compatible ghost tower represents an element $x \in \mathbb{Z}_p$ satisfying $p^{\nu_i}x = 0$. Since $\mathbb{Z}_p$ is torsion free, $x = 0$. Hence the inverse limit of the ghost modules vanishes. The missing quotient stabilizes coordinatewise at $\mathbb{Z}/p^{\nu_i}\mathbb{Z}$, whose product is the $p$-primary Smith quotient. □

The finite ghosts are therefore real finite-level defects, but they do not survive as nonzero points of the completed raw lattice. By contrast, the missing saturated quotient survives exactly as the $p$-primary saturation defect.

## 12.5 Orbit closure and three levels of effectivity

Let

$$\mathcal{O}_k(a) = \{\Lambda_w a : w \in \Sigma_k^*\} \subseteq M_k(a)$$

be the actual section orbit, and let

$$\mathcal{O}^{\mathrm{raw}}_{k,p^r}(a)$$

be its image in $M_k(a)/p^r M_k(a)$.

**Theorem 12.18** (Raw orbit-closure descent)**.** *The reduction maps*

$$\mathcal{O}^{\mathrm{raw}}_{k,p^{r+1}}(a) \twoheadrightarrow \mathcal{O}^{\mathrm{raw}}_{k,p^r}(a)$$

*are surjective, and*

$$\overline{\mathcal{O}_k(a)}^{\,p} \xrightarrow{\sim} \varprojlim_r \mathcal{O}^{\mathrm{raw}}_{k,p^r}(a),$$

*where the closure is taken in $M_{k,p}(a)$.*

*Proof.* A section word at level $r$ is lifted by the same word at level $r+1$, proving surjectivity. Every $p$-adic limit of orbit points gives a compatible tower. Conversely, choose for each compatible residue state an orbit representative $x_r$. Compatibility gives

$$x_{r+1} - x_r \in p^r M_k(a),$$

so $(x_r)$ is Cauchy in $M_{k,p}(a)$. Its limit lies in the orbit closure and maps to the prescribed tower. □

**Definition 12.19** (Three effectivity obstructions)**.** Let $x \in M_{k,p}(a)$.

1. The *p-adic effectivity condition* is simply $x \in M_{k,p}(a)$; every compatible full semantic module tower satisfies it by theorem 12.17.
2. The *integral lattice obstruction* is
$$\epsilon_{\mathrm{int}}(x) = [x] \in M_{k,p}(a)/M_k(a).$$
It vanishes exactly when $x$ is represented by one integral lattice element.
3. The *section-orbit obstruction* is membership in
$$M_k(a) \setminus \mathcal{O}_k(a).$$
Even after integral effectivity holds, the lift need not be an actual radix section.

*Boundary* 12.20 (Semantic orbit towers). The inverse limit of the full semantic modules is always $M_{k,p}(a)$. For the smaller semantic orbit sets, surjectivity of reduction remains automatic, but lifting to an actual orbit closure can be obscured by finite ghost fibers. The unconditional orbit-closure theorem is therefore stated for the raw orbit tower. A semantic-orbit effectivity theorem requires a compatible choice of raw lifts or an equivalent fiberwise Mittag–Leffler condition.

**Example 12.21** (Digit sum separates all three levels)**.** For the base-$k$ digit sum $s_k$,
$$\mathcal{O}_k(s_k) = \{s_k + c : c \in \mathbb{Z}_{\geq 0}\},$$
and
$$M_k(s_k) = L_k(s_k) = \mathbb{Z}s_k \oplus \mathbb{Z}1.$$
Hence
$$\overline{\mathcal{O}_k(s_k)}^{\,p} = \{s_k + c : c \in \mathbb{Z}_p\}.$$
The partial sums
$$c_N = \sum_{j=0}^{N} p^{2j}$$
are nonnegative integers and therefore produce actual section states $s_k + c_N$. They converge in $\mathbb{Z}_p$ to
$$c_\infty = \frac{1}{1-p^2},$$
which is not an ordinary integer. Thus $s_k + c_\infty$ is $p$-adically effective and lies in the orbit closure, but its integral obstruction is nonzero.

By contrast, $s_k - 1$ is an integral lattice point and lies in the $p$-adic orbit closure because $-1 \in \mathbb{Z}_p$ is a limit of nonnegative integers. It is not an actual section, since every actual offset is nonnegative. Integral effectivity therefore does not imply section-orbit effectivity.

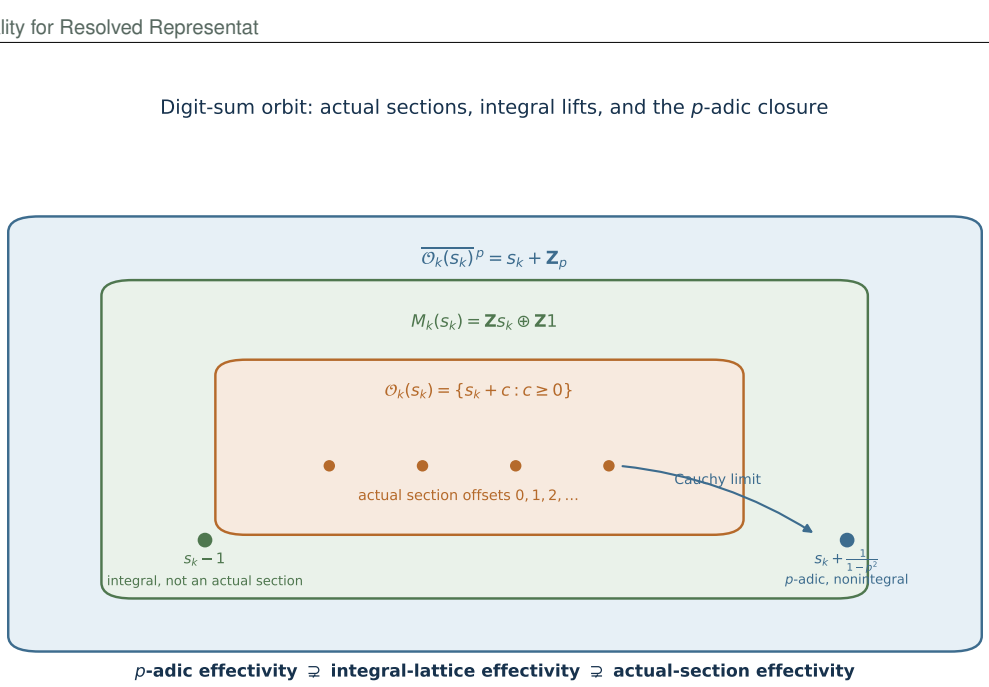



**Figure 25:** For the digit-sum sequence, actual section states form a nonnegative integral ray. Its $p$-adic closure contains all $p$-adic offsets, including nonintegral limits and integral points that are not actual sections.

## 12.6 All-moduli completion and the integral effectivity obstruction

Let

$$\widehat{M_k(a)} = \varprojlim_m M_k(a)/mM_k(a)$$

be the profinite completion over divisibility of moduli.

**Theorem 12.22** (Profinite saturation sequence)**.** *There are canonical digit-equivariant identifications*

$$\widehat{M_k(a)} \cong \prod_p M_{k,p}(a), \qquad \widehat{L_k(a)} \cong \prod_p L_{k,p}(a),$$

*and a short exact sequence*

$$0 \longrightarrow \widehat{M_k(a)} \longrightarrow \widehat{L_k(a)} \longrightarrow C_k(a) \longrightarrow 0.$$

*A compatible all-moduli raw tower has an ordinary integral lift exactly when its class in*

$$\widehat{M_k(a)}/M_k(a)$$

*vanishes.*

*Proof.* Finite free abelian groups have profinite completion equal to the product of their $p$-adic completions. In Smith coordinates, the inclusion is multiplication by $d_i$ in each profinite coordinate. Its cokernel is

$$\widehat{\mathbb{Z}}/d_i\widehat{\mathbb{Z}} \cong \mathbb{Z}/d_i\mathbb{Z}.$$

Taking the direct sum over $i$ gives $C_k(a)$. The final assertion is the definition of belonging to the diagonal image of the integral lattice inside its profinite completion. □

**Corollary 12.23** (Local-global separation)**.** *Every compatible prime-power tower is effective in a p-adic completion. A compatible family over all primes is effective in the profinite completion. Neither statement alone implies an ordinary integral lift. Integral effectivity is the separate diagonal condition*

$$\widehat{x} \in M_k(a) \subseteq \widehat{M_k(a)}.$$

This is the precise sense in which prime-power effectivity and integral effectivity differ. Completion solves the Cauchy problem in the declared topology. It does not force the resulting point to lie in the original discrete lattice.

## 12.7 Canonical integral record and directional reduction atlas

**Definition 12.24** (Canonical integral regular record)**.** The canonical integral record of $a$ is

$$\mathcal{I}_k(a) = (V_{\mathbb{Q}}(a), M_k(a), L_k(a), C_k(a), (\Lambda_d)_{0\le d<k}, a, \mathrm{ev}_0)\,.$$

Its Smith–Fitting profile is

$$\mathsf{SF}_k(a) = \big(d_1, \dots, d_\rho; \mathrm{Fitt}_0(C_k(a)), \dots, \mathrm{Fitt}_{\rho-1}(C_k(a))\big)\,.$$

The record is canonical but not a single field-valued normal form. It retains both the raw generative lattice and the maximal integer-valued lattice, together with the exact quotient between them.

**Theorem 12.25** (Integral normalization and directional local reduction)**.** *For fixed $k$, the assignment*

$$a \longmapsto \mathcal{I}_k(a)$$

*is functorial for digit-module morphisms preserving the distinguished sequence and evaluation. It is uniquely determined by the semantic sequence. For every prime $p$, reduction defines a directional bridge*

$$\mathcal{I}_k(a) \longmapsto \Big(\overline{M}_{k,p^r}(a), \mathcal{K}^{\mathrm{sem}}_{k,p^r}(a)\Big)_{r\ge 1}$$

*whose exact information-loss passport is:*

1. *finite-depth ghost kernel $C_k(a)[p^r]$;*
2. *finite-depth missing quotient $C_k(a)/p^r C_k(a)$;*
3. *completed essential image $M_{k,p}(a) \subseteq L_{k,p}(a)$;*
4. *integral effectivity obstruction $M_{k,p}(a)/M_k(a)$;*
5. *actual-section obstruction inside the integral lattice.*

*Proof.* Every component of $\mathcal{I}_k(a)$ is defined from the semantic sequence and its digit sections. A compatible morphism carries actual sections to actual sections and integer-valued rational combinations to integer-valued rational combinations, so it induces maps on $M_k(a)$, $L_k(a)$, and the quotient. The local reduction statements are theorems 12.7 and 12.17 and definition 12.19. □

**Section result.** For every integer-valued fixed-radix sequence that is regular over $\mathbb{Q}$, the actual sections generate a canonical finite free lattice $M_k(a)$, and the integer-valued part of the rational

section space is a canonical finite free saturation $L_k(a)$. Their Smith–Fitting quotient controls every modular reduction exactly. At each prime power, the coefficient sequence has a finite minimal semantic section automaton. The compatible tower reconstructs the $p$-adic raw lattice, while finite ghost coordinates vanish in the inverse limit and the missing saturated quotient survives as the $p$-primary defect. $p$-adic, profinite, integral-lattice, and actual-section effectivity are distinct and are separated by explicit obstruction quotients.

**Table 20:** Exact finite validation of the Integral prime-power atlas integral and prime-power layer.

| Check family | Recorded result |
|---|---|
| Smith and modular profiles | 1984 divisibility chains of ranks one through four; moduli 2 through 24; 45632 chain-modulus cases. |
| Fitting and prime-power profiles | 8840 Fitting cases and 39680 prime-power profile cases over $p = 2, 3, 5, 7$. |
| Digit-equivariant systems | 320 exact Smith-square systems with integral and modular intertwining checks. |
| Orbit and completion controls | Digit-sum state formulas over four primes and 1681 bounded ghost-contraction samples. |
| Total exact checks | 697958; 0 failures. |
| Overall status | PASS. |
| Boundary | Bounded exact verification supports the printed formulas and examples. It does not replace the symbolic proofs or establish unrestricted integral recognition. |

**Exact boundary of Integral prime-power atlas.** The results classify saturation and reduction defects for integer-valued sequences that are already known to have finite rational section rank. They do not prove finite-data recognition of that hypothesis, a minimal realization theorem over arbitrary rings or semirings, a base-independent integral normal form, or compatibility across different radices. The prime-power tower is a directional local reduction system, not an equivalence between integral and modular presentations.

## 13 Filtered Euler products, prime-power seeds, and the divisor–ghost bridge

The next native-invariant layer has two different index monoids. Ordinary generating functions use the additive monoid of coefficient addresses: Cauchy multiplication combines indices by addition. Arithmetic functions use the multiplicative monoid of positive integers: Dirichlet convolution combines divisor addresses by multiplication. These structures meet exactly in selected local and logarithmic-derivative coordinates, but they are not globally interchangeable. This section constructs the fixed-basis filtered-product normal form, the prime-power normal form for multiplicative arithmetic functions, and one rigorously typed cross-stratum bridge between them.

### 13.1 Filtered products and coefficient stabilization

**Definition 13.1** (Coefficientwise filtered product)**.** Let $R$ be a commutative ring. A filtered factor family is a sequence

$$F_m(z) \in 1 + z^{w(m)} R[[z]], \qquad w(m) \longrightarrow \infty.$$

Its coefficientwise product is

$$\prod_{m\geq 1} F_m(z),$$

where the coefficient of $z^N$ is computed from the finitely many factors satisfying $w(m) \leq N$.

**Proposition 13.2** (Filtered product completion)**.** *Every filtered factor family has a unique coefficientwise product in* $1 + zR[[z]]$*. For every* $N$*, the truncation modulo* $z^{N+1}$ *is equal to the product of the finitely many factors with* $w(m) \leq N$*.*

*Proof.* Fix $N$. Every factor with $w(m) > N$ is congruent to 1 modulo $z^{N+1}$, so only finitely many factors can affect the coefficient prefix through degree $N$. These finite products are compatible as $N$ increases. Their inverse limit in the $z$-adic filtration is the required series. Uniqueness follows because every coefficient is fixed at a finite stage. □

The proposition supplies existence and exact finite-prefix evaluation. It does not assert that an arbitrary factor family is structurally compressed. A finite grammar requires an effective rule for the factors and a proof of stabilization; otherwise the factor list can merely store the coefficient data in another form.

## 13.2 Canonical Euler coordinates

Let

$$\mathcal{U}_{\mathbb{Z}} = 1 + z\mathbb{Z}[[z]]$$

be the multiplicative group of integral unit series, and let

$$\mathcal{E}_{\mathbb{Z}} = \mathbb{Z}^{\mathbb{N}_{\geq 1}}$$

be the additive group of integer exponent sequences.

**Definition 13.3** (Euler-coordinate map)**.** For $b = (b_m)_{m\geq 1} \in \mathcal{E}_{\mathbb{Z}}$, define

$$\mathcal{E}(b)(z) = \prod_{m\geq 1} (1 - z^m)^{-b_m}.$$

The product is coefficientwise filtered because the $m$th factor is congruent to 1 modulo $z^m$.

**Theorem 13.4** (Integral Euler-coordinate classification)**.** *The map*

$$\mathcal{E} : (\mathcal{E}_{\mathbb{Z}}, +) \longrightarrow (\mathcal{U}_{\mathbb{Z}}, \cdot)$$

*is a group isomorphism. Consequently, every* $A(z) \in 1 + z\mathbb{Z}[[z]]$ *has a unique representation*

$$\boxed{A(z) = \prod_{m\geq 1} (1 - z^m)^{-b_m}, \qquad b_m \in \mathbb{Z}.}$$

*Proof.* Filtered multiplication gives

$$\mathcal{E}(b + b') = \mathcal{E}(b)\mathcal{E}(b').$$

To prove surjectivity and uniqueness, construct the exponents recursively. Suppose $b_1, \ldots, b_{n-1}$ have been chosen so that

$$A(z) \prod_{m<n} (1 - z^m)^{b_m} \equiv 1 + r_n z^n \pmod{z^{n+1}}.$$

Because

$$(1-z^n)^{-r_n} \equiv 1 + r_n z^n \pmod{z^{n+1}},$$

the unique choice $b_n = r_n$ cancels the degree-$n$ residual. Every $r_n$ is integral because all preceding operations occur in $\mathbb{Z}[[z]]$. Induction produces one exponent sequence with the required product. If two exponent sequences differed first at $n$, their quotient would have nonzero coefficient $(b_n - b'_n)z^n$ modulo $z^{n+1}$, contradicting equality. Hence the representation is unique. □

**Corollary 13.5** (Finite-prefix triangularity)**.** *For each $N$, the coefficient prefix*

$$(a_1, \dots, a_N) \quad \textit{of} \quad A(z) = 1 + \sum_{n \geq 1} a_n z^n$$

*and the exponent prefix $(b_1, \dots, b_N)$ determine one another by integral triangular recursions. No exponent $b_m$ with $m > N$ affects the coefficient prefix through degree $N$.*

## 13.3 Ghost coordinates and logarithmic-derivative recurrence

**Definition 13.6** (Euler ghost coordinates)**.** For $b \in \mathcal{E}_{\mathbb{Z}}$, define

$$c_n(b) = \sum_{d|n} d\, b_d, \qquad n \geq 1.$$

Let $\mathcal{G}_{\mathbb{Z}}$ be the set of integer sequences $c = (c_n)$ satisfying

$$\frac{1}{n} \sum_{d|n} \mu\Big(\frac{n}{d}\Big)\, c_d \in \mathbb{Z} \qquad (n \geq 1).$$

**Theorem 13.7** (Ghost-coordinate equivalence)**.** *The divisor ghost map*

$$\mathcal{W} : \mathcal{E}_{\mathbb{Z}} \longrightarrow \mathcal{G}_{\mathbb{Z}}, \qquad b \longmapsto c(b),$$

*is an additive group isomorphism. Its inverse is*

$$\boxed{b_n = \frac{1}{n} \sum_{d|n} \mu\Big(\frac{n}{d}\Big)\, c_d.}$$

*If $A(z) = \mathcal{E}(b)(z)$, then*

$$\boxed{\frac{zA'(z)}{A(z)} = \sum_{n \geq 1} c_n z^n.}$$

*Proof.* Formal logarithmic differentiation gives

$$\frac{zA'}{A} = \sum_{m \geq 1} b_m \frac{mz^m}{1 - z^m} = \sum_{m \geq 1} \sum_{r \geq 1} m b_m z^{mr}.$$

The coefficient at $z^n$ is $\sum_{m|n} m b_m = c_n$. Möbius inversion gives the displayed inverse formula. The definition of $\mathcal{G}_{\mathbb{Z}}$ is exactly the integrality condition for that inverse. □

**Theorem 13.8** (Exact coefficient recurrence)**.** *Let*

$$A(z) = 1 + \sum_{n \geq 1} a_n z^n$$

*and let $c_n$ be its Euler ghost coordinates. Then*

$$\boxed{n a_n = \sum_{j=1}^{n} c_j a_{n-j} \qquad (n \geq 1),}$$

*with $a_0 = 1$. Conversely, any $c \in \mathcal{G}_{\mathbb{Z}}$ and this recurrence reconstruct the integral unit series corresponding to its Euler exponents.*

*Proof.* The logarithmic-derivative identity is equivalent to

$$zA'(z) = \left( \sum_{j \geq 1} c_j z^j \right) A(z).$$

Comparing coefficients gives the recurrence. Conversely, the recurrence uniquely determines the coefficient sequence over $\mathbb{Q}$. Since $c \in \mathcal{G}_{\mathbb{Z}}$ reconstructs an integral exponent sequence, the resulting series is the Euler product from theorem 13.4 and therefore has integral coefficients. □

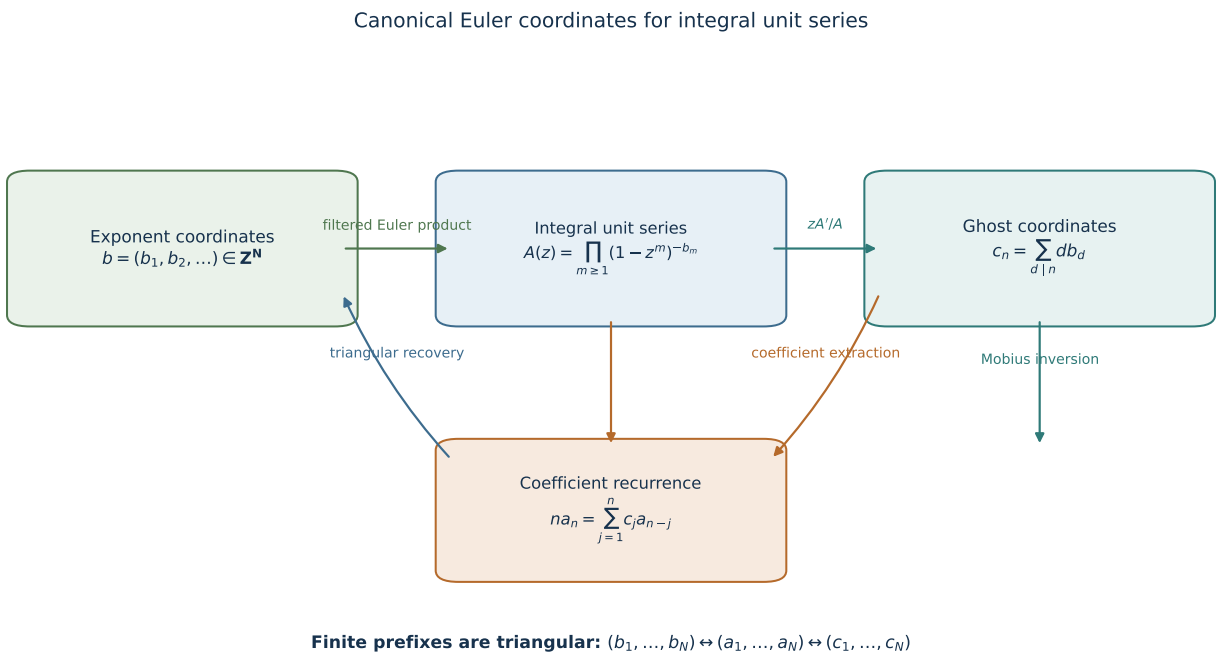



**Figure 26:** The fixed Euler basis gives three exact coordinate charts: integral exponents, coefficients, and divisor ghosts. Every finite prefix is triangular, while the ghost chart is restricted by its explicit Möbius divisibility conditions.

**Example 13.9** (Partition and power families)**.** The following fixed-basis exponent functions give familiar filtered products:

| $b_n$ | $A_b(z)$ | $c_n$ |
|---|---|---|
| $1$ | $\prod_{n\geq 1}(1-z^n)^{-1}$ | $\sigma_1(n)$ |
| $n$ | $\prod_{n\geq 1}(1-z^n)^{-n}$ | $\sigma_2(n)$ |
| $n^r$ | $\prod_{n\geq 1}(1-z^n)^{-n^r}$ | $\sigma_{r+1}(n)$. |

The first row is the ordinary partition series, and the second is the plane-partition series. More generally, the power family converts the exponent rule $n^r$ into the divisor-sum ghost $\sigma_{r+1}$.

**Example 13.10** (Distinct parts and normalization)**.** The product

$$\prod_{m\geq 1}(1+z^m)=\prod_{m\geq 1}\frac{1-z^{2m}}{1-z^m}$$

has normalized Euler exponent

$$b_n=\begin{cases}1, & n \text{ odd},\\ 0, & n \text{ even}.\end{cases}$$

Thus the distinct-part and odd-part products become the same object after normalization in the fixed Euler basis. This is an exact equality inside the declared product grammar, not a claim that arbitrary product grammars possess one preferred factorization.

*Boundary* 13.11 (Coordinate universality versus compact structural realization)*.* Theorem 13.4 gives a unique coordinate sequence for every integral unit series. It does not make every such series finitely describable. If the exponent sequence is merely an arbitrary list encoding all coefficients, the representation is storage universality. A compact seed grammar additionally requires an effective finite rule for the exponent sequence or factor family.

## 13.4 Multiplicative arithmetic functions as prime-power descent

For arithmetic functions $f, g : \mathbb{N}_{\geq 1} \to \mathbb{Z}$, write

$$(f *_D g)(n)=\sum_{d\mid n} f(d)g(n/d)$$

for Dirichlet convolution. Its identity is $\varepsilon(1)=1$ and $\varepsilon(n)=0$ for $n>1$.

**Definition 13.12** (Integral multiplicative category)**.** Let $\mathbf{Mult}_{\mathbb{Z}}$ be the discrete category whose objects are multiplicative arithmetic functions $f : \mathbb{N}_{\geq 1} \to \mathbb{Z}$ satisfying

$$f(1)=1, \qquad f(mn)=f(m)f(n) \quad \text{when } (m,n)=1.$$

The monoidal operation is Dirichlet convolution.

**Proposition 13.13** (Dirichlet inverse and multiplicative closure)**.** *If $f(1)=1$, then $f$ has a unique integral Dirichlet inverse. If $f$ and $g$ are multiplicative, then $f *_D g$ and $f^{-1_D}$ are multiplicative.*

*Proof.* The coefficient equation at $n$ is triangular:

$$g(1) = 1, \qquad g(n) = -\sum_{\substack{d \mid n \\ d<n}} f(n/d)g(d).$$

Hence the inverse exists integrally and uniquely. The standard coprime-divisor factorization of a divisor of $mn$ proves closure of multiplicative functions under convolution; uniqueness of the inverse then proves multiplicativity of $f^{-1_D}$. □

**Definition 13.14** (Prime-power seed series)**.** For a multiplicative function $f$ and a prime $p$, define

$$F_{f,p}(T) = \sum_{e \geq 0} f(p^e)T^e \in 1 + T\mathbb{Z}[[T]].$$

**Theorem 13.15** (Prime-power descent equivalence)**.** *The assignment*

$$f \longmapsto \big(F_{f,p}\big)_p$$

*is a group isomorphism*

$$\boxed{(\mathbf{Mult}_{\mathbb{Z}}, *_D) \simeq \prod_{p \text{ prime}} (1 + T\mathbb{Z}[[T]], \cdot).}$$

*The inverse reconstructs*

$$\boxed{f(n) = \prod_{p^e \| n} f(p^e).}$$

*Under this correspondence,*

$$F_{f *_D g,p}(T) = F_{f,p}(T)F_{g,p}(T).$$

*Proof.* Unique factorization writes every positive integer as a finite product of pairwise coprime prime powers, so multiplicativity gives the reconstruction formula. Conversely, an arbitrary family of local unit series defines a multiplicative function by the same finite product. For $n = p^e$, Dirichlet convolution becomes

$$(f *_D g)(p^e) = \sum_{r=0}^{e} f(p^r)g(p^{e-r}),$$

which is exactly the coefficient of $T^e$ in the local Cauchy product. □

## 13.5 Prime-Euler and local ghost coordinates

Apply the Euler-coordinate theorem independently at each prime:

$$F_{f,p}(T) = \prod_{m \geq 1} (1 - T^m)^{-\beta_{p,m}(f)}.$$

Define local ghosts

$$\gamma_{p,e}(f) = \sum_{d \mid e} d\, \beta_{p,d}(f).$$

**Theorem 13.16** (Complete prime-Euler coordinates)**.** *For integral multiplicative functions, the following normalized data are equivalent and complete:*

$$f, \qquad \big(F_{f,p}\big)_p, \qquad \big(\beta_{p,m}(f)\big)_{p,m}, \qquad \big(\gamma_{p,e}(f)\big)_{p,e}.$$

*Dirichlet convolution is linearized by the last two charts:*

$$\beta_{p,m}(f *_D g) = \beta_{p,m}(f) + \beta_{p,m}(g),$$

$$\gamma_{p,e}(f *_D g) = \gamma_{p,e}(f) + \gamma_{p,e}(g).$$

*The ghost chart consists exactly of the prime-indexed sequences satisfying the local Möbius divisibility conditions*

$$\frac{1}{e}\sum_{d|e} \mu\Big(\frac{e}{d}\Big)\, \gamma_{p,d} \in \mathbb{Z}.$$

*Proof.* Theorem 13.4 and Theorem 13.7 apply to each local unit series $F_{f,p}$. The prime-power descent theorem then reconstructs the global function. Local multiplication corresponds to Dirichlet convolution, while Euler exponents and ghosts add under multiplication. □

**Theorem 13.17** (Valuation logarithmic derivative)**.** *Fix a prime $p$. Let $\Gamma_{f,p}$ be the arithmetic function supported on powers of $p$ with*

$$\Gamma_{f,p}(1) = 0, \qquad \Gamma_{f,p}(p^e) = \gamma_{p,e}(f) \quad (e \geq 1).$$

*Then*

$$\boxed{(v_p \cdot f)(n) = (\Gamma_{f,p} *_D f)(n) \qquad (n \geq 1).}$$

*Equivalently,*

$$\frac{TF'_{f,p}(T)}{F_{f,p}(T)} = \sum_{e\geq 1} \gamma_{p,e}(f) T^e.$$

*Proof.* The local logarithmic-derivative recurrence gives

$$ef(p^e) = \sum_{j=1}^{e} \gamma_{p,j}(f) f(p^{e-j}).$$

Write $n = p^e u$ with $(u, p) = 1$ and multiply by $f(u)$. Since $\Gamma_{f,p}$ is supported on $p$-powers, the resulting sum is exactly the Dirichlet convolution at $n$. □

**Proposition 13.18** (Multiplicative residue-packet law)**.** *For $N \geq 1$, let $P_{N,r} f$ be the arithmetic function equal to $f(n)$ when $n \equiv r \pmod N$ and zero otherwise. Then*

$$\boxed{P_{N,k}(f *_D g) = \sum_{rs \equiv k\,(N)} (P_{N,r} f) *_D (P_{N,s} g).}$$

*Thus the packet address algebra for Dirichlet convolution is the finite multiplicative monoid $\mathbb{Z}/N\mathbb{Z}$, including its zero divisors.*

*Proof.* In each divisor pair $n = d(n/d)$, the residue of $n$ modulo $N$ is the product of the two divisor residues. Group the divisor sum by those two residues. □

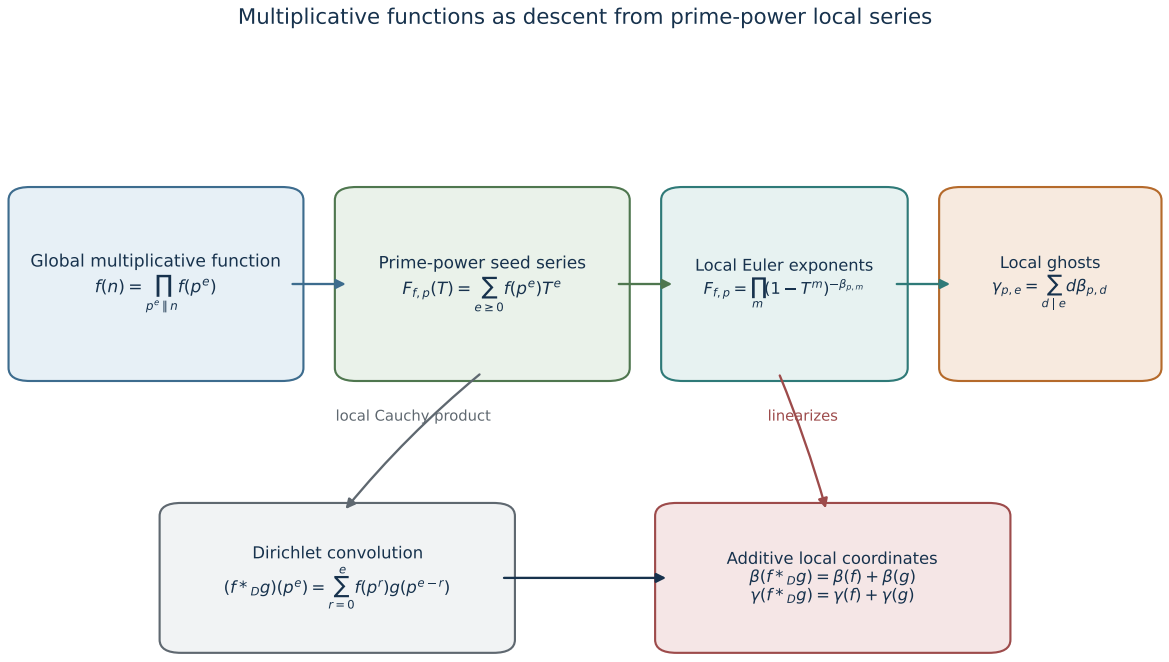



**Figure 27:** A multiplicative arithmetic function is effective descent data over its prime-power local series. Local Euler exponents and local ghosts turn Dirichlet convolution into addition.

**Table 21:** Named prime-power seed families in local Euler coordinates.

| Arithmetic function | Nonzero local Euler exponents | Prime-power seed | Local ghost |
|---|---|---|---|
| Constant-one function $\mathbf{1}$ | $\beta_1 = 1$ | $1, 1, 1, 1, 1, 1, \ldots$ | $1, 1, 1, 1, 1, 1, \ldots$ |
| Möbius $\mu$ | $\beta_1 = -1$ | $1, -1, 0, 0, 0, 0, \ldots$ | $-1, -1, -1, -1, -1, -1, \ldots$ |
| Liouville $\lambda$ | $\beta_1 = -1, \beta_2 = 1$ | $1, -1, 1, -1, 1, -1, \ldots$ | $-1, 1, -1, 1, -1, 1, \ldots$ |
| Squarefree indicator $\mu^2$ | $\beta_1 = 1, \beta_2 = -1$ | $1, 1, 0, 0, 0, 0, \ldots$ | $1, -1, 1, -1, 1, -1, \ldots$ |
| Three-fold divisor function $\tau_3$ | $\beta_1 = 3$ | $1, 3, 6, 10, 15, 21, \ldots$ | $3, 3, 3, 3, 3, 3, \ldots$ |

### 13.6 The divisor–ghost cross-stratum bridge

The Euler ghost transform can itself be written in the Dirichlet-convolution language. Let $\mathbf{1}(n) = 1$, let $\mathrm{id}(n) = n$, and let pointwise multiplication be denoted by a centered dot.

**Definition 13.19** (Divisor–ghost transform)**.** For an arithmetic exponent function $b : \mathbb{N}_{\geq 1} \to \mathbb{Z}$, define

$$\mathfrak{G}(b) = \mathbf{1} *_D (\mathrm{id} \cdot b),$$

so that

$$\mathfrak{G}(b)(n) = \sum_{d|n} d\, b(d).$$

**Theorem 13.20** (Exact divisor–ghost bridge)**.** *The map $b \mapsto c = \mathfrak{G}(b)$ is injective, with inverse*

$$\boxed{b(n) = \frac{1}{n}(\mu *_D c)(n).}$$

*Its integral image consists exactly of the arithmetic functions $c$ satisfying*

$$n \mid (\mu *_D c)(n) \qquad (n \geq 1).$$

*For the Euler product*

$$A_b(z) = \prod_{n \geq 1} (1 - z^n)^{-b(n)},$$

*one has*

$$\frac{z A_b'(z)}{A_b(z)} = \sum_{n \geq 1} c(n) z^n.$$

*Proof.* The first identity is the convolution form of the divisor sum. Since $\mu *_D \mathbf{1} = \varepsilon$,

$$\mu *_D c = \mathrm{id} \cdot b.$$

Division by $n$ gives the inverse and its exact integrality condition. The logarithmic-derivative identity is Theorem 13.7 with the exponent sequence regarded as an arithmetic function. □

**Theorem 13.21** (Multiplicativity is preserved and reflected)**.** *Assume $b(1) = 1$ and $c = \mathfrak{G}(b)$. Then*

$$\boxed{b \text{ is multiplicative} \iff c \text{ is multiplicative.}}$$

*On this locus, both $b$ and $c$ are reconstructed from prime-power seeds. For every prime $p$ and $e \geq 1$,*

$$\boxed{c(p^e) = \sum_{j=0}^{e} p^j b(p^j),}$$

$$\boxed{b(p^e) = \frac{c(p^e) - c(p^{e-1})}{p^e}.}$$

*Proof.* If $b$ is multiplicative, then $\mathrm{id} \cdot b$ is multiplicative, and Dirichlet convolution with $\mathbf{1}$ preserves multiplicativity. Conversely, if $c$ is multiplicative, then $\mu *_D c$ is multiplicative. Dividing pointwise by the completely multiplicative function id preserves multiplicativity over $\mathbb{Q}$; the integral image condition ensures that the resulting values are integers. The prime-power formulas follow by listing the divisors of $p^e$ and subtracting consecutive sums. □

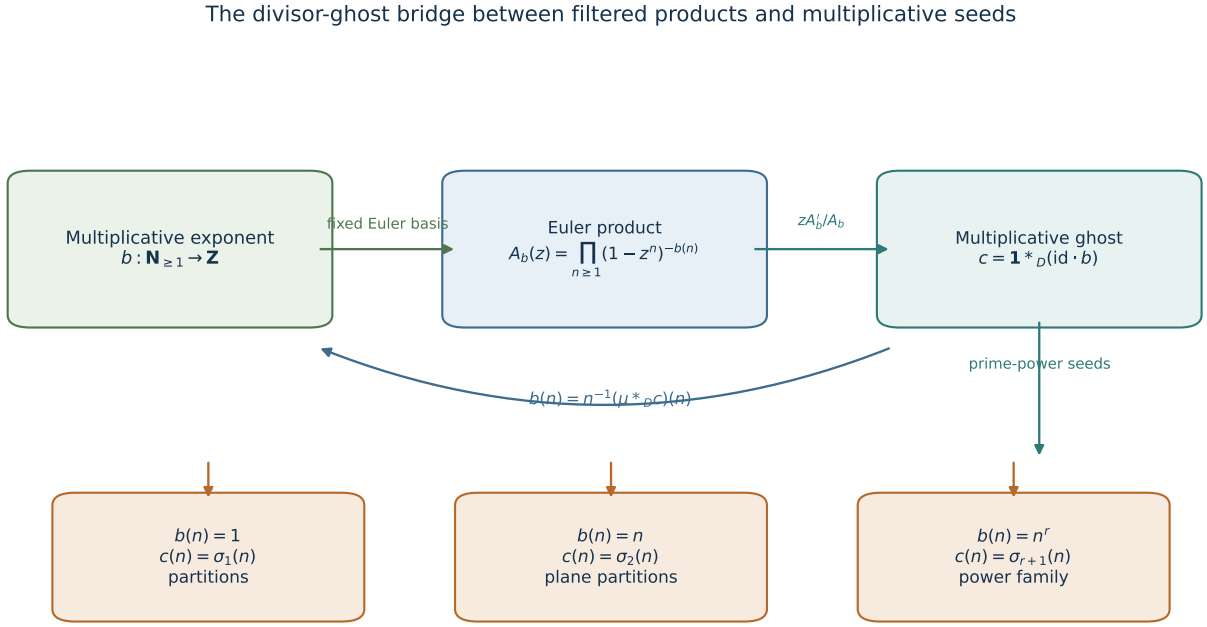



**Figure 28:** The divisor–ghost transform gives a reversible invariant bridge on the multiplicative exponent locus. It connects a fixed-basis ordinary Euler product to multiplicative prime-power data without identifying the two global convolution algebras.

## 13.7 A restricted product–multiplicative atlas

**Definition 13.22** (Multiplicative Euler-overlap category)**.** Let $\mathbf{EulMult}_{\mathbb{Z}}$ be the discrete category of multiplicative exponent functions

$$b : \mathbb{N}_{\geq 1} \to \mathbb{Z}, \qquad b(1) = 1.$$

Associate to $b$ the four normalized charts

$$\mathsf{B}(b) = b, \qquad \mathsf{A}(b) = A_b(z), \qquad \mathsf{C}(b) = \mathfrak{G}(b), \qquad \mathsf{P}(b) = \big(b(p^e), c(p^e)\big)_{p,e}.$$

**Theorem 13.23** (Effective descent on the divisor–ghost overlap)**.** *The exponent, fixed Euler-product, multiplicative ghost, and prime-power seed charts form a finite normalized atlas*

$$\mathfrak{R}_{\mathrm{DG}}.$$

*Every bridge is reversible on the declared overlap, every multiple-overlap comparison is the unique identity over the represented exponent function, and*

$$\boxed{\mathrm{Desc}(\mathfrak{R}_{\mathrm{DG}}) \simeq \mathbf{EulMult}_{\mathbb{Z}}.}$$

*Descent is effective for objects and morphisms.*

*Proof.* The Euler-product chart is uniquely inverted by Theorem 13.4. The ghost chart is uniquely inverted by Theorem 13.20. The prime-power chart is uniquely inverted by multiplicativity and unique

factorization. Hence every normalized fiber over $b$ is a singleton. All comparison cells and all multiple-overlap coherence laws are therefore forced to be identities. A compatible local family glues to its common exponent function, and morphism effectivity is automatic because the chart categories are discrete. □

**Theorem 13.24** (Complete descended prime-power invariant)**.** *The prime-power package*

$$\boxed{\mathcal{J}_{\mathrm{DG}}(b) = (b(p^e), c(p^e))_{p \text{ prime}, e\geq 0}}$$

*subject to*

$$p^e b(p^e) = c(p^e) - c(p^{e-1}) \quad (e \geq 1)$$

*is complete on* $\mathbf{EulMult}_{\mathbb{Z}}$*. It reconstructs $b$, $c$, the Euler product $A_b$, and the coefficient recurrence of $A_b$.*

*Proof.* Prime-power values reconstruct the multiplicative functions $b$ and $c$. Theorem 13.4 reconstructs $A_b$, and Theorem 13.8 reconstructs its coefficient sequence from $c$. Therefore equal invariant packages imply equality in every chart. □

**Example 13.25** (Power bridge)**.** For $b(n) = n^r$, which is completely multiplicative, the divisor ghost is

$$c(n) = \sum_{d|n} d^{r+1} = \sigma_{r+1}(n).$$

At a prime power,

$$\sigma_{r+1}(p^e) = 1 + p^{r+1} + \cdots + p^{e(r+1)}.$$

Thus one simple multiplicative exponent rule simultaneously produces a filtered ordinary product, a multiplicative divisor-sum ghost, and a one-dimensional geometric local rule at every prime.

## 13.8 Why the bridge is restricted

**Proposition 13.26** (The multiplicative exponent locus is not a product subgroup)**.** *The set of multiplicative Euler exponent functions is not closed under the addition of exponent coordinates. Consequently, multiplication of the corresponding ordinary Euler products does not define an internal group law on* $\mathbf{EulMult}_{\mathbb{Z}}$*.*

*Proof.* The constant function $b(n) = 1$ is multiplicative. But $b + b$ has value 2 at 1 and therefore is not multiplicative under the normalization $f(1) = 1$. Since ordinary Euler-product multiplication adds exponents, the multiplicative exponent locus is not closed under that operation. □

**Proposition 13.27** (Euler coefficients are not multiplicative semantics)**.** *The coefficient sequence of $A_b(z)$ need not be a multiplicative arithmetic function even when $b$ is multiplicative. For example, $b(n) = 1$ gives the partition numbers, and*

$$p(6) = 11 \neq p(2)p(3) = 6.$$

*Boundary* 13.28 (Prime-power data require multiplicativity). Two arbitrary arithmetic functions can agree on every prime power and differ on a composite supported at more than one prime. Prime-power seeds are complete only after the multiplicativity axiom has been declared. A compact local seed rule also does not remove the computational cost of factoring the input integer.

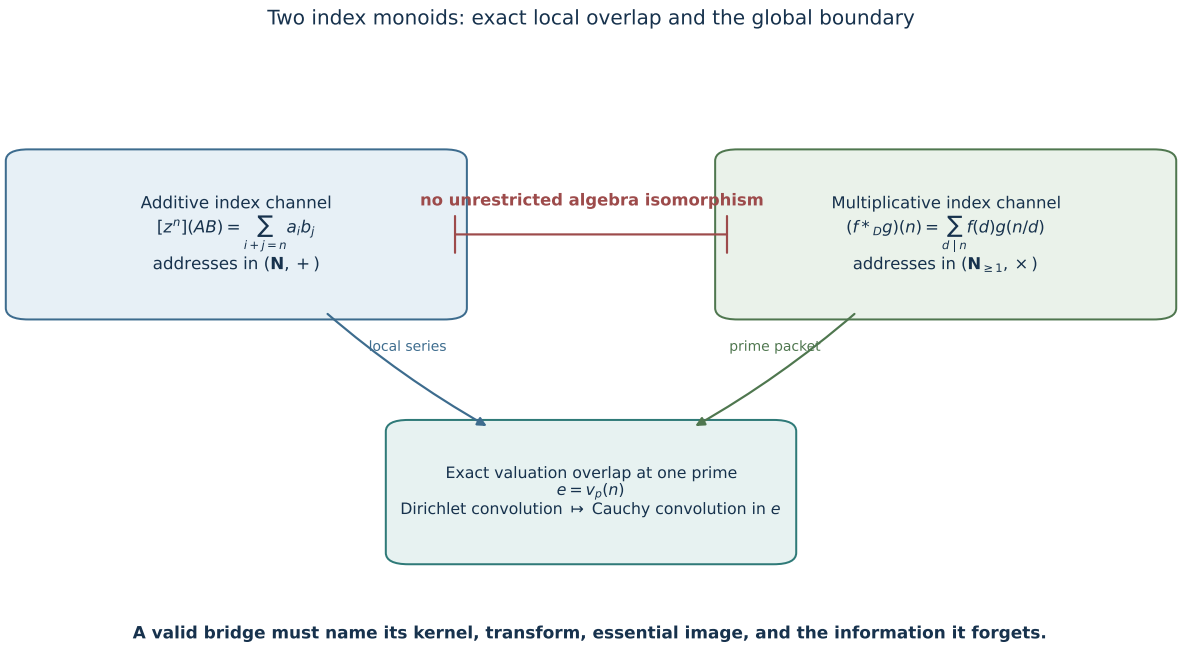



**Figure 29:** Cauchy and Dirichlet convolution use different global address monoids. They overlap exactly after localization at one valuation coordinate, but no unrestricted algebra equivalence follows.

*Boundary* 13.29 (No universal additive–multiplicative equivalence). The divisor–ghost transform is an exact invariant bridge on a named essential image. It is not an algebra isomorphism between ordinary Cauchy convolution and Dirichlet convolution, does not identify the coefficients of an Euler product with a multiplicative function, and does not produce a canonical factorization across arbitrary product grammars. Any larger bridge must name its transform, kernel, essential image, and information-loss profile.

## 13.9 Exact finite verification

**Table 22:** Exact finite validation of the Product-multiplicative atlas filtered-product and multiplicative layer.

| Check family | Recorded result |
|---|---|
| Euler-coordinate atlas | 15625 exponent prefixes and 3125 arbitrary integral unit-series prefixes. |
| Prime-power multiplicative atlas | 96 deterministic local systems and 48 Dirichlet-convolution pairs. |
| Divisor-ghost overlap | 128 multiplicative exponent systems and 6 power families. |
| Named local coordinates | 5 arithmetic families and 6 geometric necklace modes. |
| Total exact checks | 595964; 0 failures. |
| Overall status | PASS. |
| Boundary | Bounded exact verification supports the printed formulas and examples. It does not establish compactness or minimality for arbitrary product grammars, nor a global Cauchy–Dirichlet algebra isomorphism. |

The Product-multiplicative atlas verifier performs four exact audits. First, it exhaustively checks the coefficient, exponent, and ghost triangular maps for every exponent prefix in $\{-2,-1,0,1,2\}^6$ and every unit coefficient prefix in $\{-2,-1,0,1,2\}^5$. Second, it constructs deterministic prime-power systems, reconstructs global multiplicative functions, and verifies local Euler inversion, local logarithmic

derivatives, and Dirichlet convolution. Third, it checks the divisor–ghost bridge and the power family $b(n) = n^r$. Fourth, it verifies the named local Euler coordinates printed in Table 21. The recorded 595,964 exact checks have no failures.

**Exact boundary of Product-multiplicative atlas.** The fixed Euler basis gives a canonical coordinate system for integral unit series, and prime-power seed series give a canonical coordinate system for integral multiplicative functions. The divisor–ghost transform produces one complete cross-stratum overlap on multiplicative exponent functions. The block does not prove compactness for arbitrary exponent data, a minimal product compiler, closure of the multiplicative exponent slice under ordinary product multiplication, a global Cauchy–Dirichlet algebra isomorphism, or a canonical factorization across unrestricted product grammars.

**Section result.** Integral unit series admit unique fixed-basis Euler exponents and unique divisor ghosts, with exact logarithmic-derivative recurrence and finite-prefix triangularity. Integral multiplicative functions are effective descent from prime-power local series; local Euler exponents and local ghosts linearize Dirichlet convolution and form complete invariants. On the multiplicative exponent locus, the divisor–ghost transform gives a reversible four-chart atlas linking exponent functions, ordinary filtered Euler products, multiplicative ghosts, and prime-power seeds. This closes one explicit product–multiplicative invariant bridge while preserving the global distinction between additive and multiplicative index monoids.

# 14 Local Newton–Mahler coordinates, affine polyphase descent, and precision ladders

Local Mahler-polyphase atlas develops the local stratum promised by the work program. Its purpose is not to merge every use of the word "Mahler." It freezes one precise local semantic doctrine, constructs its normalized coefficient and polyphase charts, types the characteristic-zero, integral, and residue-level affine channels separately, and identifies the exact data needed to pass from finite modular dynamics to certified local analytic packets.

## 14.1 Two Mahler languages and the declared local doctrine

Two constructions in the Library use the same historical name but have different variables and different semantics.

1. A *functional-Mahler equation*
$$F(z) = R(z)F(z^p)$$
is an identity for a formal coefficient series in the variable $z$. Cartier operators act on the coefficient index. the periodic and rational-mask atlases use this channel over finite fields.

2. A *Newton–Mahler expansion*
$$f(x) = \sum_{r\geq 0} c_r \binom{x}{r}$$
is a coordinate expansion for a function of a $p$-adic input variable $x$. Affine substitutions $x = Mq + s$ produce polyphase branches of the input domain.

This section treats the second channel. Fix a prime $p$. Let

$$\mathcal{C}_p = C(\mathbb{Z}_p, \mathbb{Z}_p)$$

with the uniform norm, and let

$$c_0(\mathbb{Z}_p) = \{c = (c_r)_{r\geq 0} : c_r \in \mathbb{Z}_p,\ c_r \longrightarrow 0\}$$

with the coefficient sup norm.

**Theorem 14.1** (Mahler coordinate theorem)**.** *The synthesis map*

$$\mathcal{M}_p : c_0(\mathbb{Z}_p) \longrightarrow \mathcal{C}_p, \qquad c \longmapsto \left(x \longmapsto \sum_{r\geq 0} c_r \binom{x}{r}\right),$$

*is an isometric isomorphism of $\mathbb{Z}_p$-modules. Its inverse is*

$$\boxed{c_r = \Delta^r f(0).}$$

*In particular, the Newton–Mahler coefficient sequence is a canonical complete coordinate for a continuous $\mathbb{Z}_p$-valued function.*

*Proof.* This is the classical Mahler coordinate theorem [14]. Finite Newton interpolation gives the coefficient identity on nonnegative integers. Continuity implies that the forward-difference coefficients tend to zero, so the binomial series converges uniformly on $\mathbb{Z}_p$. Conversely, every coefficient sequence tending to zero gives a uniformly convergent continuous function. Uniqueness follows from the finite-difference formula. □

**Definition 14.2** (Exact valuation profile and certified class)**.** For $f = \mathcal{M}_p(c)$, define

$$\nu_f(r) = v_p(c_r) \in \mathbb{Z}_{\geq 0} \cup \{\infty\}.$$

If $w : \mathbb{N} \to \mathbb{Z}_{\geq 0}$ is nondecreasing and tends to infinity, put

$$\mathcal{M}_w = \{c \in c_0(\mathbb{Z}_p) : v_p(c_r) \geq w(r)\}, \qquad \mathcal{C}_w = \mathcal{M}_p(\mathcal{M}_w).$$

The function $w$ is a declared precision certificate. The class $\mathcal{C}_w$ is not asserted to be a characterization of every possible notion of local analyticity.

## 14.2 Complete clopen packets and effective local descent

For $a \geq 1$ and $0 \leq s < p^a$, define the branch

$$\mathcal{B}_{a,s} f(q) = f(p^a q + s), \qquad q \in \mathbb{Z}_p,$$

and the complete packet

$$\mathcal{B}_a f = (\mathcal{B}_{a,s} f)_{0\leq s<p^a}.$$

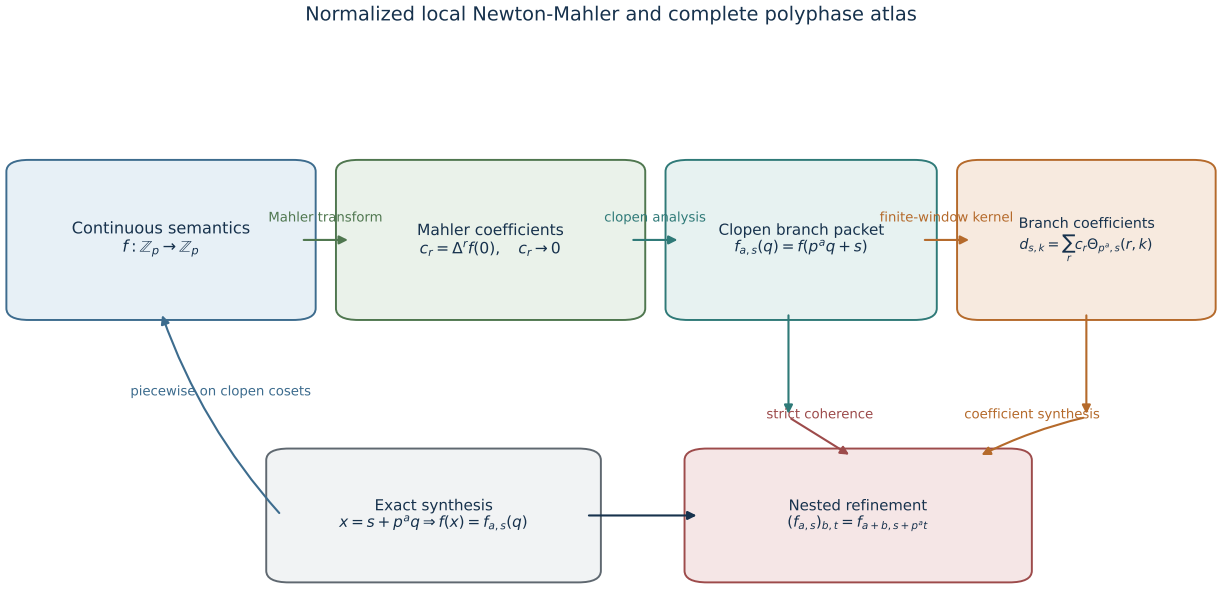



**Figure 30:** The normalized local atlas. Continuous semantics, canonical Mahler coefficients, complete clopen branch packets, and branchwise Mahler coefficients are equivalent charts. A single continuous branch remains directional.

**Theorem 14.3** (Complete clopen packet equivalence)**.** *The analysis map*

$$\mathcal{B}_a : \mathcal{C}_p \longrightarrow \prod_{s=0}^{p^a-1} \mathcal{C}_p$$

*is an isometric isomorphism. Its inverse is the piecewise synthesis*

$$\boxed{(\mathcal{S}_a g)(x) = g_s\left(\frac{x-s}{p^a}\right) \quad \text{for } x \in s + p^a\mathbb{Z}_p.}$$

*Thus the clopen residue cover of $\mathbb{Z}_p$ has effective descent for both objects and equality morphisms.*

*Proof.* The cosets $s + p^a\mathbb{Z}_p$ are pairwise disjoint, clopen, and cover $\mathbb{Z}_p$. Restriction followed by the displayed synthesis is the identity. Conversely, synthesis followed by restriction recovers every component. Continuity is checked separately on each clopen component, and the uniform norm is the maximum of the branch norms. □

**Theorem 14.4** (Strict nested-branch law)**.** *For $a, b \geq 1$, $0 \leq s < p^a$, and $0 \leq t < p^b$,*

$$\boxed{(f_{a,s})_{b,t} = f_{a+b,s+p^a t}.}$$

*All multiple-overlap comparison cells for the nested $p$-power branch atlas are identities. Hence its higher coherence is strict rather than merely up to a chosen natural isomorphism.*

*Proof.* Direct substitution gives

$$f_{a,s}(p^b q + t) = f(p^a(p^b q + t) + s) = f(p^{a+b} q + s + p^a t).$$

The address is uniquely determined in the interval $0 \le s + p^a t < p^{a+b}$. □

A single branch $\mathcal{B}_{a,s}$ is not injective on $\mathcal{C}_p$ when $a \ge 1$: any nonzero continuous function supported on another clopen coset lies in its kernel. The complete packet is therefore the reversible object. This observation will be contrasted below with the finite-degree characteristic-zero polynomial chart, where one affine branch is invertible.

## 14.3 The affine Mahler kernel and mixed-radix coherence

For $M \ge 1$, $s \ge 0$, and $r, k \ge 0$, define

$$\Phi_M(z) = (1+z)^M - 1$$

and

$$\boxed{\Theta_{M,s}(r,k) = [z^r](1+z)^s \Phi_M(z)^k.}$$

Equivalently,

$$\boxed{\Theta_{M,s}(r,k) = \sum_{j=0}^{k} (-1)^{k-j} \binom{k}{j} \binom{Mj+s}{r}.}$$

The support is finite:

$$\Theta_{M,s}(r,k) = 0 \quad \text{unless} \quad k \le r \le Mk + s.$$

**Theorem 14.5** (Affine Newton–Mahler transfer)**.** *Let*

$$f(x) = \sum_{r \ge 0} c_r \binom{x}{r}$$

*be a convergent Mahler expansion and put $g_s(q) = f(Mq + s)$. Then*

$$g_s(q) = \sum_{k \ge 0} d_{s,k} \binom{q}{k},$$

*where*

$$\boxed{d_{s,k} = \sum_{r=k}^{Mk+s} c_r \Theta_{M,s}(r,k).}$$

*Every output coefficient depends on a finite source window.*

*Proof.* Expand

$$(1+z)^{Mq+s} = (1+z)^s \big(1 + \Phi_M(z)\big)^q = \sum_{k \ge 0} \binom{q}{k} (1+z)^s \Phi_M(z)^k.$$

Taking $[z^r]$ gives the affine expansion of $\binom{Mq+s}{r}$. Substitution into the Mahler series gives the formula. The finite support of $\Theta_{M,s}$ makes each coefficient sum finite. □

Let $\mathcal{T}_{M,s}$ denote this coefficient operator. Conjugating the clopen packet theorem by $\mathcal{M}_p$ gives the following normalized coefficient atlas.

**Corollary 14.6** (Complete coefficient-packet equivalence). *For $M = p^a$, the map*

$$\mathcal{T}_a : c_0(\mathbb{Z}_p) \longrightarrow \prod_{s=0}^{p^a-1} c_0(\mathbb{Z}_p), \qquad c \longmapsto (\mathcal{T}_{p^a,s}c)_s,$$

*is a topological isomorphism. It is the coefficient conjugate of complete clopen analysis.*

**Theorem 14.7** (Mixed-radix kernel composition). *For $M, N \geq 1$,*

$$\boxed{\sum_{k\geq 0} \Theta_{M,s}(r,k)\Theta_{N,t}(k,\ell) = \Theta_{MN,Mt+s}(r,\ell).}$$

*Equivalently,*

$$\boxed{\mathcal{T}_{N,t}\mathcal{T}_{M,s} = \mathcal{T}_{MN,Mt+s}.}$$

*When $\gcd(M,N) = 1$, the two Chinese-remainder refinement paths to a common address agree exactly. Their holonomy is the identity.*

*Proof.* Apply the affine substitution $x = Mq + s$, then $q = Ny + t$. The composite is $x = MNy + Mt + s$. Uniqueness of Mahler coefficients yields the kernel identity. The Chinese-remainder diamond is the same equality written along two factorizations of one affine address. □

**Normalized local atlas.** For every fixed prime $p$ and depth $a$, the following normalized charts are equivalent:

$$\boxed{\mathbf{Loc}_p^{\mathrm{cts}} \simeq \mathbf{Mah}_p^{c_0} \simeq \mathbf{Branch}_{p,a}^{\mathrm{cts}} \simeq \mathbf{BranchMah}_{p,a}^{c_0}.}$$

The first chart contains continuous functions on $\mathbb{Z}_p$, the second their unique Mahler coefficients, the third the complete clopen branch packet, and the fourth the corresponding branchwise coefficient packet. Every normalized fiber is contractible. The descent category is therefore equivalent to the discrete semantic category $\mathbf{Loc}_p^{\mathrm{cts}}$.

## 14.4 Finite-degree bridge ladder and collective recovery

The same integer kernel matrix has different categorical status after changing the coefficient doctrine. Fix $d \geq 0$ and write

$$\mathcal{M}_d(R) = R^{d+1}$$

for the formal truncated Mahler coefficient module. Let

$$A_{M,s}^{(d)} = \big[\Theta_{M,s}(r,k)\big]_{0\leq k,r\leq d},$$

where the target degree $k$ is the row index.

**Theorem 14.8** (Typed affine-channel ladder). *For every $M \geq 1$, $s \geq 0$, and $d \geq 0$:*

1. *The matrix $A_{M,s}^{(d)}$ is upper triangular with diagonal*

$$1, M, M^2, \ldots, M^d.$$

*Hence*

$$\boxed{\det A_{M,s}^{(d)} = M^{d(d+1)/2}.}$$

*Every characteristic-zero polynomial chart is invertible.*

2. *On the integral lattice $\mathbb{Z}^{d+1}$, one channel is injective. If $M > 1$ and $d \geq 1$, its image has index $M^{d(d+1)/2}$, so the channel has no integer linear left inverse.*

3. *Let $p$ be prime and put $\beta_p = p^{v_p(M)}$. Reduction modulo $p$ has exact rank*

$$\boxed{\operatorname{rank}_{\mathbb{F}_p} \overline{A}^{(d)}_{M,s} = \left\lfloor \frac{d}{\beta_p} \right\rfloor + 1.}$$

   *A local channel loses residual rank exactly at primes dividing $M$.*

4. *A complete neighboring packet can recover the source integrally. The canonical prefix of $\min(M, d+1)$ standard shifts has an integer left inverse, valid after base change to every commutative ring.*

*Proof.* The diagonal follows from the leading term of $\binom{Mq+s}{r}$, or from the generating identity for $\Theta_{M,s}$. The determinant gives the integral index statement. Modulo $p$, the first nonzero source degree in target row $k$ is $\beta_p k$, which gives the rank formula. For the prefix packet, choose from channel $s$ and target row $k$ the equation indexed by $n = Mk + s$. The selected square coefficient matrix is unit lower triangular, so its inverse is integral and remains a left inverse after every base change. □

**Theorem 14.9** (Sharp standard packet size)**.** *Define*

$$B(M) = \max\left(\{1\} \cup \{p^{v_p(M)} : p \mid M\}\right).$$

*The least number of standard affine channels whose stacked map has an integer left inverse is*

$$\boxed{L_{\mathbb{Z}}(M,d) = \min(d+1, B(M)).}$$

*The prefix $\{0, 1, \ldots, L_{\mathbb{Z}}(M,d) - 1\}$ attains the minimum.*

*For a fixed modulus $N \geq 2$, set*

$$B_N(M) = \max\left(\{1\} \cup \{p^{v_p(M)} : p \mid \gcd(M,N)\}\right).$$

*The least packet size for a left inverse over $\mathbb{Z}/N\mathbb{Z}$ is*

$$\boxed{L_N(M,d) = \min(d+1, B_N(M)).}$$

*The exponents $v_p(N)$ do not change the minimum; the first residue layer already detects the obstruction.*

*Proof.* This is the primary-rank and Smith/Hermite criterion of Core-Transfer Addendum 04. At a prime $p \mid M$, selected shifts are visible only through their residues modulo $p^{v_p(M)}$. A prefix of the stated length has full rank at every obstructing prime, hence a unimodular-row left inverse. Any smaller packet fails at a prime attaining the largest relevant primary component. A nonzero first-layer kernel vector lifts to a kernel vector at every higher prime-power depth. □

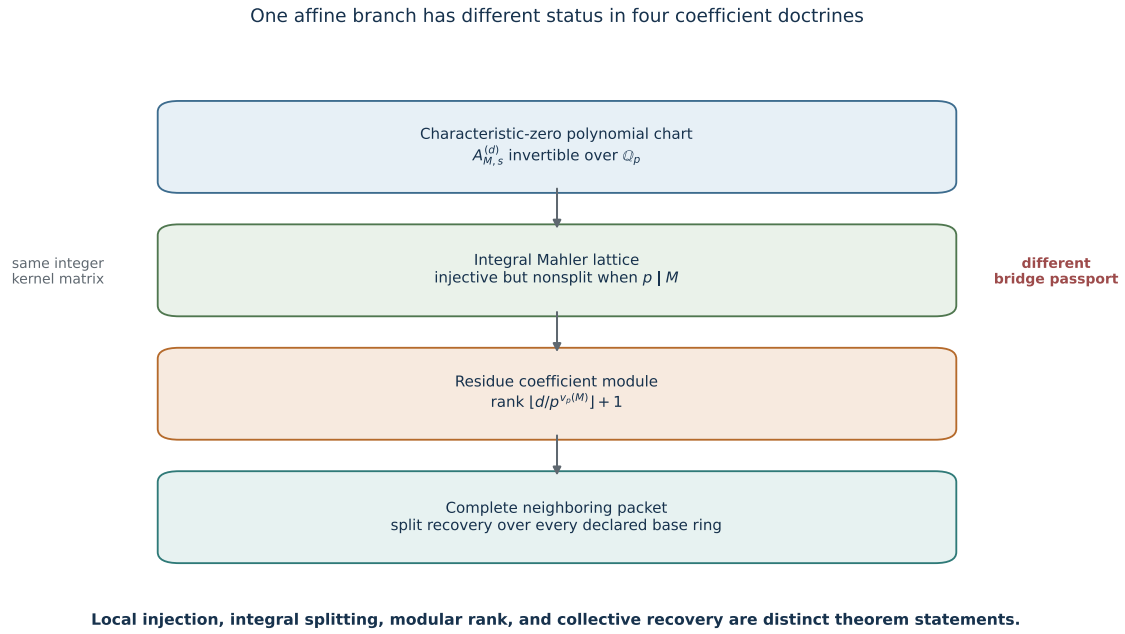



**Figure 31:** The same affine Mahler kernel has four distinct bridge passports. Characteristic-zero invertibility, integral injection, modular rank, and complete-packet splitting must not be conflated.

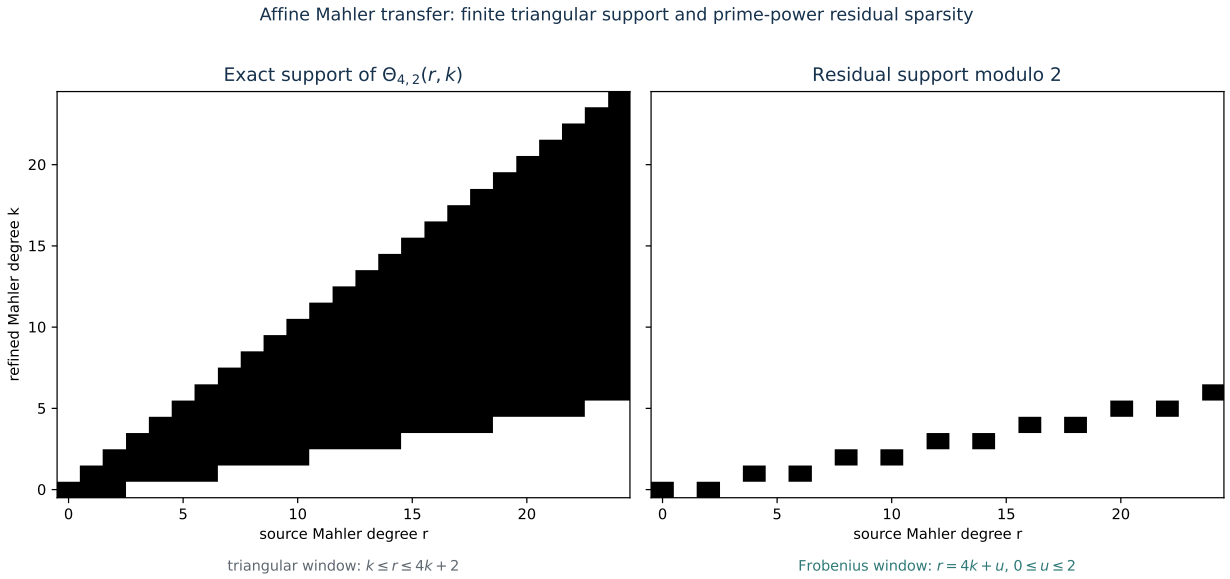



**Figure 32:** The finite triangular support of the affine kernel and its Frobenius-sparse residue pattern at a prime-power radix.

## 14.5 Valuation ledgers and Frobenius sparsity

The coefficient transform carries a precise lower-bound calculus.

**Theorem 14.10** (Exact branchwise valuation ledger)**.** *For every refined coefficient,*

$$\boxed{v_p(d_{s,k}) \geq \min_{k \leq r \leq Mk+s} \left( v_p(c_r) + v_p(\Theta_{M,s}(r,k)) \right).}$$

*If $v_p(c_r) \geq w(r)$ for a nondecreasing weight $w$, then*

$$\boxed{v_p(d_{s,k}) \geq w(k).}$$

*Thus every declared monotone Mahler precision ladder survives affine polyphase refinement.*

*Proof.* The transfer sum is finite. Apply the non-Archimedean triangle inequality. Since $r \geq k$, monotonicity gives $w(r) \geq w(k)$, and every kernel entry is integral. □

Define the min-plus certificate transform

$$\boxed{(\mathfrak{W}_{M,s} w)(k) = \min_{k \leq r \leq Mk+s} \left( w(r) + v_p(\Theta_{M,s}(r,k)) \right).}$$

This transform is a certified lower bound. It need not be the exact output valuation, because cancellation can increase the valuation beyond the termwise minimum.

**Theorem 14.11** (Prime-power Frobenius sparsification)**.** *For $M = p^a$,*

$$\boxed{\Theta_{p^a,s}(r,k) \equiv \binom{s}{r - p^a k} \pmod{p},}$$

*where the binomial coefficient is zero outside $0 \leq r - p^a k \leq s$. Therefore*

$$\boxed{d_{s,k} \equiv \sum_{u=0}^{s} \binom{s}{u} c_{p^a k + u} \pmod{p}.}$$

*In particular,*

$$\boxed{d_{0,k} \equiv c_{p^a k} \pmod{p}.}$$

*Proof.* In characteristic $p$,

$$(1+z)^{p^a} - 1 \equiv z^{p^a}.$$

Substitute this into the generating definition of $\Theta_{p^a,s}$ and compare coefficients. □

## 14.6 Carmichael–Mahler state constructors and precision amplification

Finite modular state dynamics provide a directional constructor into the local Mahler chart. Let

$$v_{n+1} = C v_n, \qquad a_n = w^{\mathsf{T}} C^n v_0,$$

with $C \in M_d(\mathbb{Z}_p)$ invertible modulo $p$.

**Theorem 14.12** (Matrix Carmichael–Mahler constructor)**.** *Assume*

$$C^H = I + p^L B, \qquad L \geq 1.$$

*For every address $j$,*

$$\boxed{a_{Hx+j} = \sum_{r\geq 0} p^{Lr} \binom{x}{r} w^{\mathsf{T}} C^j B^r v_0,}$$

*where the series converges for $x \in \mathbb{Z}_p$. Its Mahler coefficients satisfy*

$$\boxed{v_p(c_{j,r}) \geq Lr,}$$

*and*

$$\boxed{\Delta_H^r a_n \equiv 0 \pmod{p^{Lr}}.}$$

*Proof.* Use

$$C^{Hx+j} = C^j (I + p^L B)^x$$

and expand the principal-unit matrix power by the convergent binomial series. One forward difference in $x$ contributes the factor $p^L B$. □

**Theorem 14.13** (Principal-unit precision amplification)**.** *If $X = I + p^L B$, then for every $a \geq 0$ there exists $B_a \in M_d(\mathbb{Z}_p)$ such that*

$$\boxed{X^{p^a} = I + p^{L+a} B_a.}$$

*Consequently, for $H_a = Hp^a$, every branch $x \mapsto a_{H_a x+j}$ has Mahler coefficients satisfying*

$$\boxed{v_p(c_{a,j,r}) \geq (L+a)r.}$$

*Each additional $p$-power refinement contributes at least one further digit of precision per Mahler depth.*

*Proof.* Induct on $a$. If $X_a = I + p^{L+a} B_a$, the binomial expansion of $X_a^p$ has linear term divisible by $p^{L+a+1}$, and every higher term has at least the same valuation. Apply theorem 14.12 at the refined jump. □

**Example 14.14** (Refined dyadic Fibonacci packets)**.** For the Fibonacci companion matrix

$$C = \begin{pmatrix} 1 & 1 \\ 1 & 0 \end{pmatrix},$$

one has

$$C^{12} = I + 8 \begin{pmatrix} 29 & 18 \\ 18 & 11 \end{pmatrix}.$$

Hence

$$\boxed{\Delta_{12\cdot 2^a}^r F_n \equiv 0 \pmod{2^{(a+3)r}}.}$$

The state-to-local construction is directional. A local branch can forget unreachable state directions, nonminimal coordinates, or modes annihilated by the output functional. Recovering a state presentation requires a separate recognition or minimality theorem and is not part of the Carmichael–Mahler constructor itself.

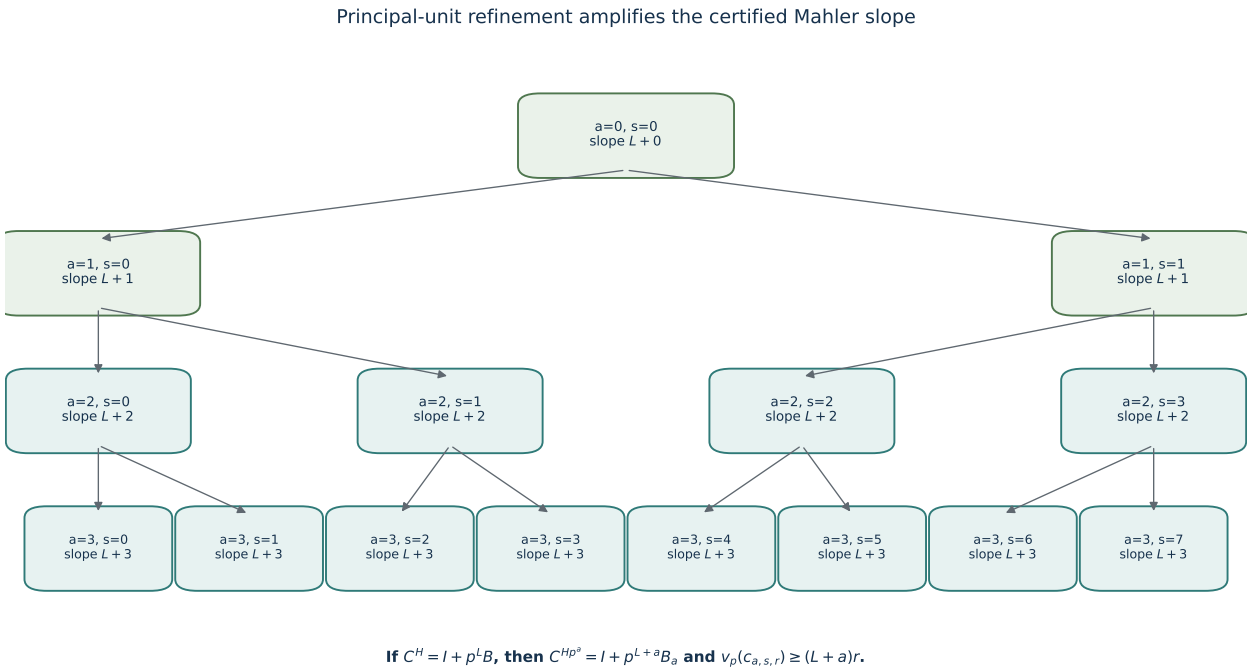



**Figure 33:** A principal-unit state packet acquires one additional guaranteed $p$-adic digit per Mahler depth at each $p$-power refinement.

## 14.7 The exact boundary with functional-Mahler masks

**Proposition 14.15** (No canonical unrestricted bridge between the two Mahler channels)**.** *Functional-Mahler mask data over $\mathbb{F}_p$ does not determine a unique Newton–Mahler chart over $\mathbb{Z}_p$, and a continuous Newton–Mahler function does not in general determine a rational functional-Mahler mask.*

*Proof.* A residue sequence $(\bar{a}_n)$ admits many integral lifts. If $(a_n)$ is one lift, then $(a_n + pn)$ is another with the same reduction modulo $p$. Their Newton–Mahler coefficients differ by the nonzero coefficient sequence of $pn$. Thus the residue-series or functional-mask presentation cannot select one local interpolation without a declared lifting rule.

Conversely, a continuous function $f : \mathbb{Z}_p \to \mathbb{Z}_p$ canonically determines its Newton–Mahler coefficients, but rationality of an ordinary generating series or of the mask $F(z)/F(z^p)$ is an additional property of a separate coefficient-series presentation. Continuity alone does not supply it. □

**Exact local boundary.** Local Mahler-polyphase atlas proves a complete normalized atlas for continuous $\mathbb{Z}_p$-valued functions and their complete $p^a$-branch packets. It proves exact affine coefficient transport, mixed-radix coherence, finite-degree characteristic-zero invertibility, integral split recovery, modular rank loss, valuation preservation, and principal-unit precision amplification under the printed hypotheses. It does not identify every continuous function as locally analytic, compute exact higher valuations of every $\Theta_{p^a,s}(r,k)$, choose an optimal mixed-radix refinement tree, or construct the combined spectral–local invariant requested by the broader program.

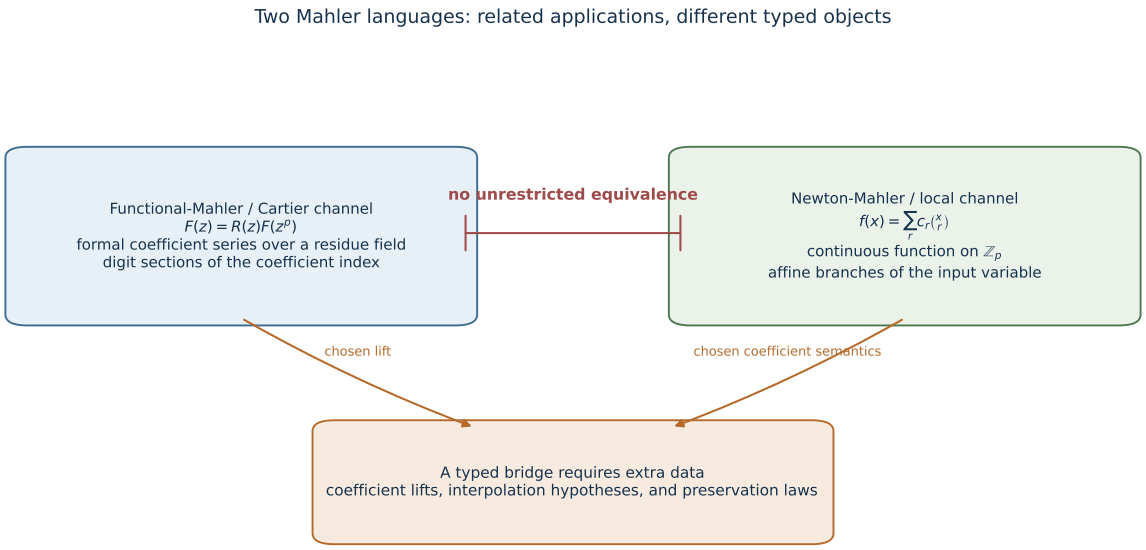



**Figure 34:** Functional-Mahler and Newton–Mahler constructions require different variables, coefficient doctrines, and normalization data. A bridge exists only after those extra choices are declared.

## 14.8 Exact examples and finite verification

For $f(x) = x^2$, the source Mahler vector is

$$(c_0, c_1, c_2) = (0, 1, 2).$$

The two dyadic branches are

$$f(2q) = 4\binom{q}{1} + 8\binom{q}{2},$$

and

$$f(2q+1) = 1 + 8\binom{q}{1} + 8\binom{q}{2}.$$

This example exhibits exact finite-window coefficient transport.

For a principal unit $u = 1 + p$,

$$u^x = \sum_{r \geq 0} p^r \binom{x}{r}.$$

The branch $x = pq$ has coefficients

$$\left(u^p - 1\right)^k,$$

whose valuation is at least $2k$. The branch therefore improves the original slope-one certificate.

At $p = 2$, $M = 2$, and $d = 3$, each single reduced channel has rank two, while the two-channel packet has rank four. This is the smallest visible instance of collective recovery.

The verifier checks the affine generating identity, finite polynomial transport, triangular determinants, mixed-radix composition, Chinese-remainder diamonds, nested branch addresses, prime-power Frobenius sparsity, exact local ranks, packet minimality, integer decoders, composite primary minima, valuation ledgers, scalar principal-unit amplification, and the refined Fibonacci matrix congruences. It also includes a negative control showing that equal residue data can have distinct Newton–Mahler lifts.

**Table 23:** Exact local Mahler and polyphase examples used in Local Mahler-polyphase atlas.

| Example | Source Mahler data | Refined data or rank |
|---|---|---|
| $x^2$, branch 2q+0 | $(0,1,2)$ | $(0,4,8)$ |
| $x^2$, branch 2q+1 | $(0,1,2)$ | $(1,8,8)$ |
| $(1+2)^x$, branch 2q | $c_r = 2^r,\ 0 \le r \le 4$ | $d_k = 8^k,\ 0 \le k \le 4$ |
| $(1+3)^x$, branch 3q | $c_r = 3^r,\ 0 \le r \le 4$ | $d_k = 63^k,\ 0 \le k \le 4$ |
| $(1+5)^x$, branch 5q | $c_r = 5^r,\ 0 \le r \le 4$ | $d_k = 7775^k,\ 0 \le k \le 4$ |
| mod-2 rank distribution, M=2,d=3 | $(2,2)$ | $(4,4)$ |

**Table 24:** Local Mahler-polyphase atlas exact verification summary.

| Validation class | Recorded result |
|---|---|
| Affine-kernel rows | 312 exact row cases |
| Finite coefficient transports | 936 source/chart cases |
| Mixed-radix compositions and CRT diamonds | 2,102 exact diagrams |
| Prime-power rank and sparsity cases | 95 degree/radix cases |
| Integral decoder and composite-minimum cases | 156 cases |
| Valuation-ledger cases | 5,100 coefficient ladders |
| Scalar and matrix precision cases | 923 cases |
| **Total exact checks** | **229,743** |
| Failures | 0 |

**Local Mahler–polyphase result.** The local continuous, Newton–Mahler coefficient, complete clopen branch, and branch-coefficient presentations form an effective normalized atlas. Affine polyphase kernels compose strictly and transport declared valuation ladders. The finite-degree restriction exposes a four-level bridge ladder: reversible characteristic-zero charts, nonsplit integral channels, rank-deficient residue channels, and split neighboring packets. Carmichael–Mahler transfer embeds finite principal-unit state dynamics into the local atlas with a certified precision slope that improves under $p$-power refinement. Functional-Mahler masks remain a distinct typed channel unless coefficient lifts and interpolation data are supplied.

## 15 Holonomic Ore charts, multisection modules, and a Fuchsian packet theorem

Holonomic atlas develops the next native stratum in the declared work program. The general holonomic problem has two logically separate parts. First, a D-finite series and its P-recursive coefficient sequence require normalized operator charts that remember the finite initial data lost by tail recurrences. Second, arithmetic multisection preserves holonomicity but can change minimal order through root-orbit aliasing, resonance, and address-dependent cancellation. The first part is closed here on the ordinary-point locus. The second is organized in general and solved exactly for a nontrivial regular-singular family.

Throughout this section, $K$ is a characteristic-zero field. When local monodromy is discussed, $K$ is embedded in $\mathbb{C}$ and all local exponents are taken over an algebraic closure.

### 15.1 Ore annihilators and normalized holonomic charts

Let

$$\mathcal{D}_K = K(z)\langle D\rangle, \qquad Dq = qD + q',$$

be the differential Ore algebra, and let

$$\mathcal{S}_K = K(n)\langle S\rangle, \qquad Sq(n) = q(n+1)S,$$

be the forward-shift Ore algebra. Both are Euclidean skew-polynomial rings in their operator variable, so their nonzero left ideals have unique monic generators [11].

**Definition 15.1** (Minimal differential annihilator)**.** For a nonzero D-finite series $F \in K[[z]]$, define

$$\mathrm{Ann}_{\mathcal{D}}(F) = \{L \in \mathcal{D}_K : LF = 0\}.$$

Its unique monic generator is denoted

$$\boxed{L_F.}$$

The differential order

$$r_D(F) = \mathrm{ord}_D\, L_F$$

is the minimal scalar differential order of $F$ over $K(z)$.

**Definition 15.2** (Minimal tail recurrence)**.** For a sequence $a = (a_n)_{n\ge 0}$, define its tail annihilator by

$$\mathrm{Ann}_{\mathrm{tail}}(a) = \{R \in \mathcal{S}_K : (Ra)_n = 0 \text{ for all sufficiently large } n\}.$$

For a non-eventually-zero P-recursive sequence, its unique monic generator is denoted

$$\boxed{R_a.}$$

If the sequence is eventually zero, the tail generator is 1 and has order zero.

Write

$$R_a = S^s + \sum_{j=0}^{s-1} r_j(n) S^j.$$

Let $\nu_a$ be the least index from which $R_a$ annihilates the sequence, and define $N_a$ to be the least integer $N \ge \nu_a$ larger than every nonnegative pole of the rational functions $r_j(n)$. Then

$$\mathfrak{R}(a) = \big(R_a, N_a, a_0, \dots, a_{N_a+s-1}\big)$$

is a canonical complete recurrence chart. The operator controls the tail, while the finite prefix crosses every singular index and fixes the exact sequence rather than only its eventual equivalence class.

**Proposition 15.3** (Derivative-module rank)**.** *For a nonzero D-finite series $F$,*

$$\boxed{r_D(F) = \dim_{K(z)} \mathrm{span}_{K(z)}\{F, DF, D^2F, \dots\}.}$$

*Proof.* A differential operator of order $r$ gives a linear dependence among $F, DF, \dots, D^rF$. Minimality of $L_F$ says that no dependence exists among the first $r$ derivative vectors. Therefore they form a basis of the derivative span. □

## 15.2 The exact coefficient bridge

The classical equivalence between P-recursive sequences and D-finite ordinary generating functions is effective in both directions [12]. The following formulas make the finite residual explicit.

Let

$$F(z) = \sum_{n \geq 0} a_n z^n$$

and

$$L = \sum_{j=0}^{r} q_j(z) D^j, \qquad q_j(z) = \sum_{m=0}^{d_j} q_{j,m} z^m.$$

**Theorem 15.4** (Differential-to-recurrence coefficient formula)**.** *For every $n \geq 0$,*

$$\boxed{[z^n]LF = \sum_{j=0}^{r} \sum_{m=0}^{\min(d_j,n)} q_{j,m}(n-m+j)^{\underline{j}} a_{n-m+j},}$$

*where*

$$x^{\underline{j}} = x(x-1)\cdots(x-j+1).$$

*Consequently, every polynomial-coefficient differential equation yields an explicit polynomial recurrence after a finite reindexing.*

*Proof.* The coefficient of $z^{n-m}$ in $D^j F$ is

$$(n-m+j)^{\underline{j}} a_{n-m+j}.$$

Multiplication by $q_{j,m} z^m$ shifts that contribution to degree $n$. Summing over $j$ and $m$ gives the formula. □

Conversely, suppose

$$\sum_{s=0}^{q} p_s(n) a_{n+s} = 0 \qquad (n \geq N),$$

where $p_s \in K[n]$, and put

$$\theta = zD.$$

**Theorem 15.5** (Recurrence residual as an Euler-operator polynomial)**.** *Define*

$$\boxed{Q = \sum_{s=0}^{q} z^{q-s} p_s(\theta - s).}$$

*Then*

$$\boxed{[z^{n+q}]QF = \sum_{s=0}^{q} p_s(n) a_{n+s}.}$$

*Hence $QF$ is a polynomial of degree less than $N+q$, and*

$$\boxed{D^{N+q} QF = 0.}$$

*Proof.* The operator $p_s(\theta - s)$ multiplies the coefficient of $z^k$ by $p_s(k-s)$. After multiplication by $z^{q-s}$, the coefficient at $z^{n+q}$ is $p_s(n)a_{n+s}$. The recurrence kills every coefficient from degree $N+q$ onward. Differentiating more times than the residual degree gives a homogeneous annihilator. □

The polynomial residual is not noise. It is the exact finite-prefix certificate that distinguishes a recurrence valid only in the tail from an identity in the full formal-series chart.

### 15.3 The ordinary-point holonomic atlas

**Definition 15.6** (Ordinary-point locus)**.** A nonzero D-finite series $F \in K[[z]]$ belongs to

$$\mathbf{Hol}_K^{\mathrm{ord}}$$

when its monic minimal operator can be written

$$L_F = D^r + \sum_{j=0}^{r-1} \ell_j(z) D^j$$

with every $\ell_j$ regular at $z = 0$.

The normalized jet is

$$J_0(F) = \big(F(0), F'(0), \dots, F^{(r-1)}(0)\big).$$

**Theorem 15.7** (Ordinary-point reconstruction)**.** *Let*

$$L = D^r + \sum_{j=0}^{r-1} \ell_j(z) D^j$$

*with all $\ell_j$ regular at zero. For every jet*

$$(y_0, \dots, y_{r-1}) \in K^r$$

*there is a unique formal series $F \in K[[z]]$ satisfying*

$$LF = 0, \qquad F^{(j)}(0) = y_j.$$

*Proof.* Write $F(z) = \sum c_n z^n$. At coefficient degree $n$, the monic term $D^r F$ contributes

$$\frac{(n+r)!}{n!} c_{n+r},$$

while every lower derivative involves only $c_0, \dots, c_{n+r-1}$. Characteristic zero makes the displayed coefficient invertible. The equation therefore determines $c_{n+r}$ recursively from the jet. □

**Theorem 15.8** (Normalized ordinary holonomic atlas)**.** *On the ordinary-point locus, the following normalized presentations determine one another exactly:*

$$\boxed{\begin{array}{l} F \in K[[z]], \\ (L_F, J_0(F)), \\ \operatorname{span}_{K(z)}\{D^j F : j \geq 0\} \text{ with cyclic vector } F, \\ (R_a, N_a, a_0, \dots, a_{N_a+s-1}), \qquad a_n = [z^n]F. \end{array}}$$

*With equality morphisms, these charts form equivalent normalized groupoids, and every fiber over a fixed semantic series is contractible.*

*Proof.* The series gives its unique minimal Ore operators and finite data. The derivative module recovers $L_F$ as the first monic dependence among consecutive derivatives. The operator and jet recover $F$ by theorem 15.7. The recurrence chart reconstructs every coefficient after its singular prefix. The two explicit coefficient formulas transport between the differential and recurrence channels. Minimal monic normalization removes coordinate automorphisms, so each normalized fiber has only the identity. □

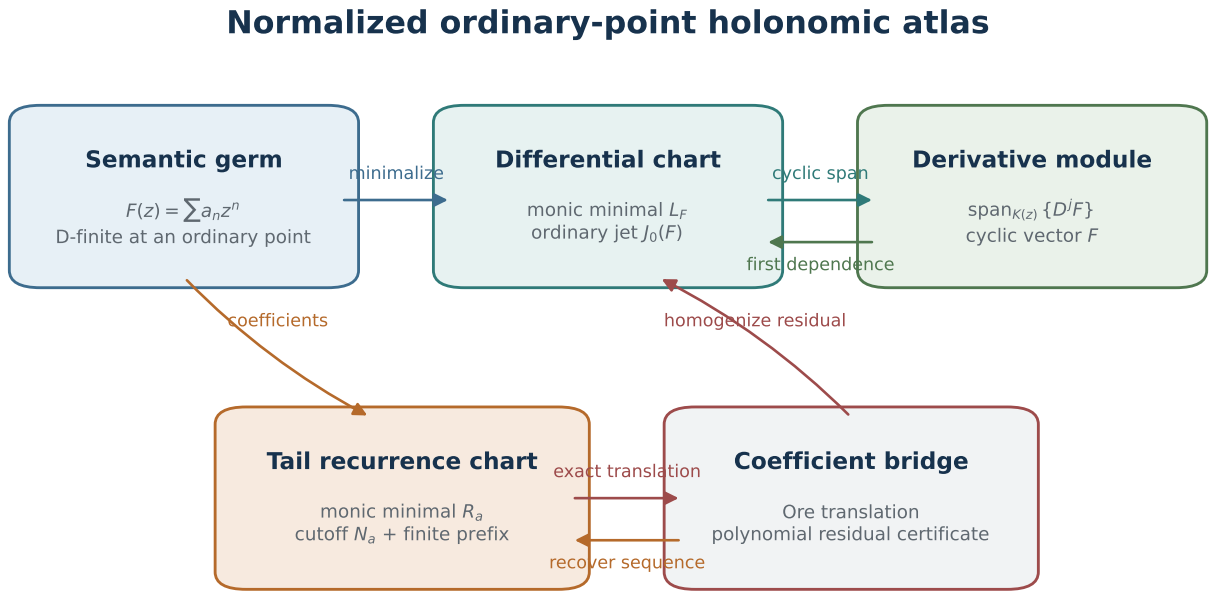



**Figure 35:** The ordinary holonomic atlas keeps the semantic series, minimal differential operator and jet, cyclic derivative module, and minimal tail recurrence with singular prefix as separate normalized charts.

## 15.4 General arithmetic multisection

For $N \geq 1$ and $0 \leq j < N$, define

$$\mathfrak{M}_{N,j}F(x) = \sum_{m \geq 0} a_{Nm+j} x^m.$$

If $\omega_N$ is a primitive $N$th root of unity and $x = t^N$, then

$$\boxed{t^j \mathfrak{M}_{N,j}F(t^N) = \frac{1}{N} \sum_{q=0}^{N-1} \omega_N^{-jq} F(\omega_N^q t).}$$

This is the character projector for the cyclic rotation action.

**Theorem 15.9** (Holonomic multisection closure)**.** *If $F$ is D-finite, then every $\mathfrak{M}_{N,j}F$ is D-finite. Equivalently, arithmetic sections of P-recursive sequences are P-recursive.*

*Proof.* The root-filter formula uses finitely many algebraic substitutions and a finite linear combination. D-finite series are closed under those operations. The resulting section has coefficients in the original base field, so the operator descends. □

Closure does not determine the smallest operator. A separate exact state construction gives a useful bound.

**Theorem 15.10** (Nonautonomous state jump)**.** *Suppose a P-recursive sequence is represented, beyond its singular prefix, by*

$$v_{n+1} = C(n)v_n, \qquad a_n = \lambda(n)v_n,$$

*where $v_n \in K^s$ and $C(n)$ is rational. Then the jth $N$-section has the jump system*

$$\boxed{w_{m+1} = J_{N,j}(m)w_m,}$$

*where*

$$\boxed{J_{N,j}(m) = C(Nm + j + N - 1) \cdots C(Nm + j).}$$

*After denominator clearing, every scalar output has a polynomial recurrence of order at most $s$.*

*Proof.* Compose the $N$ consecutive one-step transfers. The $s + 1$ consecutive scalar output rows are linearly dependent over $K(m)$, producing a recurrence of order at most $s$. □

The root filter also gives a construction-independent order ledger before the algebraic descent from $t$ to $x = t^N$. Work over a finite extension $E/K$ containing $\omega_N$. Put

$$F_q(t) = F(\omega_N^q t), \qquad G_{N,j}(t) = \frac{1}{N} \sum_{q=0}^{N-1} \omega_N^{-jq} F_q(t).$$

Let $L_q \in E(t)\langle D_t \rangle$ be the monic minimal annihilator of $F_q$. Rotation is an Ore-algebra automorphism, so every $L_q$ has order $r = \operatorname{ord} L_F$. Let

$$L_N^{\mathrm{orb}} = \mathrm{LCLM}(L_0, \ldots, L_{N-1}), \qquad r_N^{\mathrm{orb}} = \operatorname{ord} L_N^{\mathrm{orb}},$$

and, when $G_{N,j} \neq 0$, let $L_{N,j}^{\mathrm{char}}$ be its monic minimal annihilator with order $r_{N,j}^{\mathrm{char}}$. For a zero character packet put $r_{N,j}^{\mathrm{char}} = 0$.

**Definition 15.11** (Root-filter alias and address-cancellation defects)**.** Define

$$\mathfrak{a}_N(F) = Nr - r_N^{\mathrm{orb}}, \qquad \mathfrak{c}_{N,j}(F) = r_N^{\mathrm{orb}} - r_{N,j}^{\mathrm{char}}.$$

The first quantity measures dependence already present among the rotated holonomic modules. The second measures the additional loss caused by the $j$th character projector after the rotated orbit has been assembled.

**Theorem 15.12** (Exact two-stage root-filter defect identity)**.** *The defects in definition 15.11 are nonnegative and satisfy*

$$\boxed{Nr - r_{N,j}^{\mathrm{char}} = \mathfrak{a}_N(F) + \mathfrak{c}_{N,j}(F).}$$

*Thus orbit aliasing occurs before address selection, while address cancellation occurs after the Fourier character has been applied.*

*Proof.* The least common left multiple has order at most the sum of the orders of its inputs, hence $r_N^{\mathrm{orb}} \le Nr$. It annihilates every rotated series and therefore annihilates their character sum $G_{N,j}$. By minimality, $L_N^{\mathrm{orb}}$ belongs to the principal left annihilator ideal generated by $L_{N,j}^{\mathrm{char}}$ whenever the character sum is nonzero, so $r_{N,j}^{\mathrm{char}} \le r_N^{\mathrm{orb}}$. The zero case is immediate. The displayed identity is the telescoping decomposition

$$Nr - r_{N,j}^{\mathrm{char}} = (Nr - r_N^{\mathrm{orb}}) + (r_N^{\mathrm{orb}} - r_{N,j}^{\mathrm{char}}).$$

□

**Root-filter order versus packet order.** The preceding theorem is exact in the rotated $t$-coordinate over $E(t)$. The arithmetic packet is the series $\mathfrak{M}_{N,j}F(x)$ over the base field, related by

$$G_{N,j}(t) = t^j \mathfrak{M}_{N,j}F(t^N).$$

Algebraic pullback, base extension, gauge multiplication, and descent may change the minimal scalar operator visible in the $x$-chart. That comparison is a separately typed descent problem. The exact binomial–Fuchsian family below computes both sides and therefore resolves this additional step in a nontrivial model case.

Let $Q_{N,j}^{\mathrm{cl}}$ be an annihilator produced by a declared closure or elimination pipeline, and let $L_{N,j}$ be the monic minimal operator of the section. Since every annihilator belongs to the principal left ideal generated by $L_{N,j}$,

$$Q_{N,j}^{\mathrm{cl}} = A_{N,j} L_{N,j}$$

for some Ore operator $A_{N,j}$. The nonnegative quantity

$$\delta_{N,j}^{\mathrm{cl}} = \operatorname{ord} Q_{N,j}^{\mathrm{cl}} - \operatorname{ord} L_{N,j}$$

measures cancellation relative to that construction. It is not intrinsic until the construction has been fixed.

## 15.5 Operator singularities and local exponent packets

Multiply $L_F$ by a common denominator, divide the polynomial coefficients by their greatest common divisor, and normalize the leading coefficient to be monic. This gives a unique primitive polynomial representative

$$\widetilde{L}_F = \sum_{j=0}^{r} q_j(z) D^j.$$

Its operator singular support is

$$\Sigma_{\mathrm{op}}(F) = \{q_r(z) = 0\} \cup \{\infty\}.$$

Apparent singularities remain part of this operator coordinate until an explicit desingularization has been performed.

Let $\alpha$ be a finite point and put

$$v_j = v_\alpha(q_j), \qquad \mu = \min_j (v_j - j).$$

Write the first nonzero local coefficient of $q_j$ as $q_{j,v_j}$. The indicial polynomial is

$$\boxed{I_{\alpha,L}(\rho) = \sum_{v_j - j = \mu} q_{j,v_j} \rho^{\underline{j}}.}$$

At a regular singular point, its roots form the local exponent packet. Over $\mathbb{C}$, the corresponding local monodromy eigenvalues are

$$e^{2\pi i\rho}.$$

Integer differences between exponents signal resonance. Exponent eigenvalues alone do not determine logarithmic extension data or the full monodromy conjugacy class.

**Proposition 15.13** (Singularity orbit under multisection)**.** *Assume $F$ is an analytic germ at zero with analytic continuation away from a finite set $\Sigma$. Then every finite nonzero analytic singularity of $\mathfrak{M}_{N,j}F$ lies in*

$$\boxed{\Sigma^{[N]} = \{\alpha^N : \alpha \in \Sigma\}.}$$

*Distinct singularities in one fiber of $\alpha \mapsto \alpha^N$ are aliased by the multisection map. A character projection may remove some aliased local contributions.*

*Proof.* Away from $\Sigma^{[N]}$ and zero, choose a local analytic branch $t = x^{1/N}$. Every rotated argument $\omega_N^q t$ avoids $\Sigma$, so the root-filter expression is analytic. A singularity can therefore occur only when one rotated preimage meets $\Sigma$. □

At nonzero regular singular points, the map $t \mapsto t^N$ is unramified. It preserves local exponents before character projection. At zero and infinity it is ramified, so exponent scaling must be recorded separately.

## 15.6 An exact binomial–Fuchsian packet family

The general minimal multisection problem remains open. The family

$$\boxed{F_{\lambda,\alpha}(z) = (1 - \alpha z)^{-\lambda}}$$

provides a nontrivial exact model that contains irreducible Fuchsian packets, rational collapse, finite-support aliasing, and zero-address cancellation in one parameter space.

Its coefficients are

$$a_n = \frac{(\lambda)_n}{n!}\alpha^n.$$

For $0 \le j < N$, put

$$G_{N,j}^{\lambda,\alpha}(x) = \sum_{m\ge 0} \frac{(\lambda)_{Nm+j}}{(Nm+j)!}\alpha^{Nm+j}x^m.$$

Define the upper and lower parameter packets

$$A_{N,j}(\lambda) = \left\{\frac{\lambda + j + r}{N} : 0 \le r < N\right\},$$

$$B_{N,j} = \left\{\frac{j + 1 + r}{N} : 0 \le r < N\right\} \setminus \{1\}.$$

**Theorem 15.14** (Exact hypergeometric packet form)**.** *If $(\lambda)_j \neq 0$, then*

$$\boxed{G_{N,j}^{\lambda,\alpha}(x) = \frac{(\lambda)_j\alpha^j}{j!}\,{}_NF_{N-1}\left(\begin{matrix}A_{N,j}(\lambda)\\ B_{N,j}\end{matrix}; \alpha^N x\right).}$$

*Its coefficients satisfy the first-order polynomial recurrence*

$$\boxed{\prod_{r=0}^{N-1}(Nm+j+1+r)u_{m+1} = \alpha^N \prod_{r=0}^{N-1}(Nm+j+\lambda+r)u_m.}$$

*The series is annihilated by*

$$\boxed{\mathcal{H}_{N,j}^{\lambda,\alpha} = \theta \prod_{b\in B_{N,j}}(\theta+b-1) - \alpha^N x \prod_{a\in A_{N,j}(\lambda)}(\theta+a),}$$

*where* $\theta = xD_x$.

*Proof.* Split the rising factorials and ordinary factorials into their $N$ residue factors. The multiplication formula gives the displayed hypergeometric coefficients. Taking the ratio of consecutive packet coefficients gives the recurrence. Coefficient comparison with the standard ${}_NF_{N-1}$ operator gives the differential equation. □

**Theorem 15.15** (Minimal differential order phase diagram)**.** *Let*

$$r_D(N,j;\lambda) = r_D\big(G_{N,j}^{\lambda,\alpha}\big), \qquad \alpha \neq 0.$$

*Then:*

1. *If* $\lambda \notin \mathbb{Z}$, *then*
$$\boxed{r_D(N,j;\lambda) = N.}$$
2. *If* $\lambda = L \in \mathbb{Z}_{>0}$, *then every packet is a nonzero rational function with exact denominator*
$$(1-\alpha^N x)^L,$$
*and*
$$\boxed{r_D(N,j;L) = 1.}$$
3. *If* $\lambda = -M \in \mathbb{Z}_{\leq 0}$, *then* $G_{N,j}^{-M,\alpha}$ *is zero when* $j > M$. *Otherwise it is a nonzero polynomial of degree*
$$\left\lfloor \frac{M-j}{N} \right\rfloor$$
*and*
$$\boxed{r_D(N,j;-M) = \begin{cases} 1, & j \leq M, \\ 0, & j > M. \end{cases}}$$

*Proof.* For nonintegral $\lambda$, no difference between an upper parameter and a completed lower parameter is an integer. The classical irreducibility criterion for generalized hypergeometric operators therefore makes $\mathcal{H}_{N,j}^{\lambda,\alpha}$ irreducible of order $N$ [13]. Since the packet is nonzero, its minimal operator has order $N$.

For $L > 0$, the coefficient is a polynomial of degree $L-1$ in $m$ times $\alpha^{Nm+j}$. Its generating function is rational with denominator $(1-\alpha^N x)^L$, and the leading polynomial term prevents cancellation of the highest denominator power. Every nonconstant rational function has a first-order logarithmic-derivative annihilator.

For $\lambda = -M$, the source series is the polynomial $(1-\alpha z)^M$. Selecting one residue class leaves exactly the displayed finite support. A nonzero polynomial has differential order one, while the zero function has order zero. □

The tail recurrence order and differential order are different invariants. A nonzero finite-support coefficient sequence has tail recurrence order zero but its polynomial generating function has differential order one.

## 15.7 Orbit aliasing and address cancellation

Let $\omega_N$ be primitive and consider the rotated orbit

$$\mathcal{O}_N(F_{\lambda,\alpha}) = \left\{ (1-\alpha\omega_N^r t)^{-\lambda} : 0 \le r < N \right\}.$$

Let $r_{\mathrm{orb}}$ be its dimension over the constant field.

**Theorem 15.16** (Exact orbit rank)**.** *For the binomial family,*

$$\boxed{r_{\mathrm{orb}}(N;\lambda) = \begin{cases} N, & \lambda \notin \mathbb{Z}_{\le 0}, \\ \min(N, M+1), & \lambda = -M \in \mathbb{Z}_{\le 0}. \end{cases}}$$

*Proof.* If $\lambda$ is nonintegral, each rotated branch has a branch singularity at a different point. If $\lambda$ is a positive integer, each has a pole at a different point. A constant linear relation would therefore have zero coefficient at every branch.

If $\lambda = -M$, expand

$$(1-\alpha\omega_N^r t)^M = \sum_{n=0}^{M} \binom{M}{n} (-\alpha)^n \omega_N^{rn} t^n.$$

The rotation matrix is a truncated discrete Fourier matrix. Its rank is the number of available residue classes, namely $\min(N, M+1)$. □

Define the alias and cancellation deficits by

$$\boxed{A_N(\lambda) = N - r_{\mathrm{orb}}(N;\lambda),}$$

$$\boxed{C_{N,j}(\lambda) = r_{\mathrm{orb}}(N;\lambda) - r_D(N,j;\lambda).}$$

Then

$$\boxed{N - r_D(N,j;\lambda) = A_N(\lambda) + C_{N,j}(\lambda).}$$

**Corollary 15.17** (Exact defect formulas)**.** *The three parameter regimes have the following signatures.*

1. *If $\lambda \notin \mathbb{Z}$, then*
$$A_N(\lambda) = 0, \qquad C_{N,j}(\lambda) = 0.$$
2. *If $\lambda = L > 0$, then*
$$A_N(L) = 0, \qquad C_{N,j}(L) = N - 1.$$

3. *If* $\lambda = -M \le 0$, *then*

$$A_N(-M) = \max(0, N - M - 1),$$

*and*

$$C_{N,j}(-M) = \begin{cases} \min(N, M+1) - 1, & j \le M, \\ \min(N, M+1), & j > M. \end{cases}$$

This separates two mechanisms that are easily conflated. Orbit aliasing occurs before an address is selected. Address cancellation occurs after the Fourier projector has been applied.

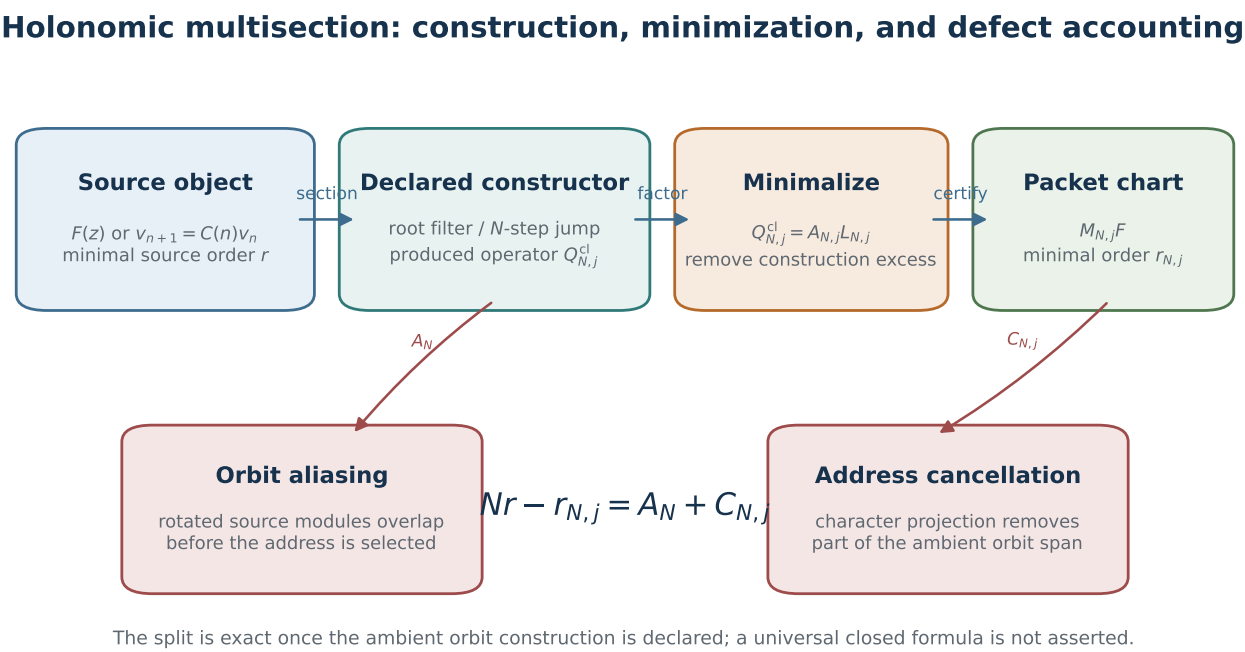



**Figure 36:** The declared holonomic multisection pipeline. General closure constructs an annihilator but does not prove minimality. The binomial–Fuchsian family admits an exact orbit-rank and address-cancellation decomposition.

## 15.8 Local exponent and monodromy packet

For $\lambda \notin \mathbb{Z}$, the hypergeometric operator in theorem 15.14 is Fuchsian with singularities

$$\boxed{0, \qquad \alpha^{-N}, \qquad \infty.}$$

Its exponent packets are

$$\boxed{E_0 = \{0\} \cup \{1 - b : b \in B_{N,j}\},}$$

$$\boxed{E_{\alpha^{-N}} = \{0, 1, \dots, N-2, -\lambda\},}$$

and

$$\boxed{E_\infty = A_{N,j}(\lambda).}$$

Modulo integers, $E_0$ is the complete $N$-torsion set

$$\left\{0, \frac{1}{N}, \dots, \frac{N-1}{N}\right\},$$

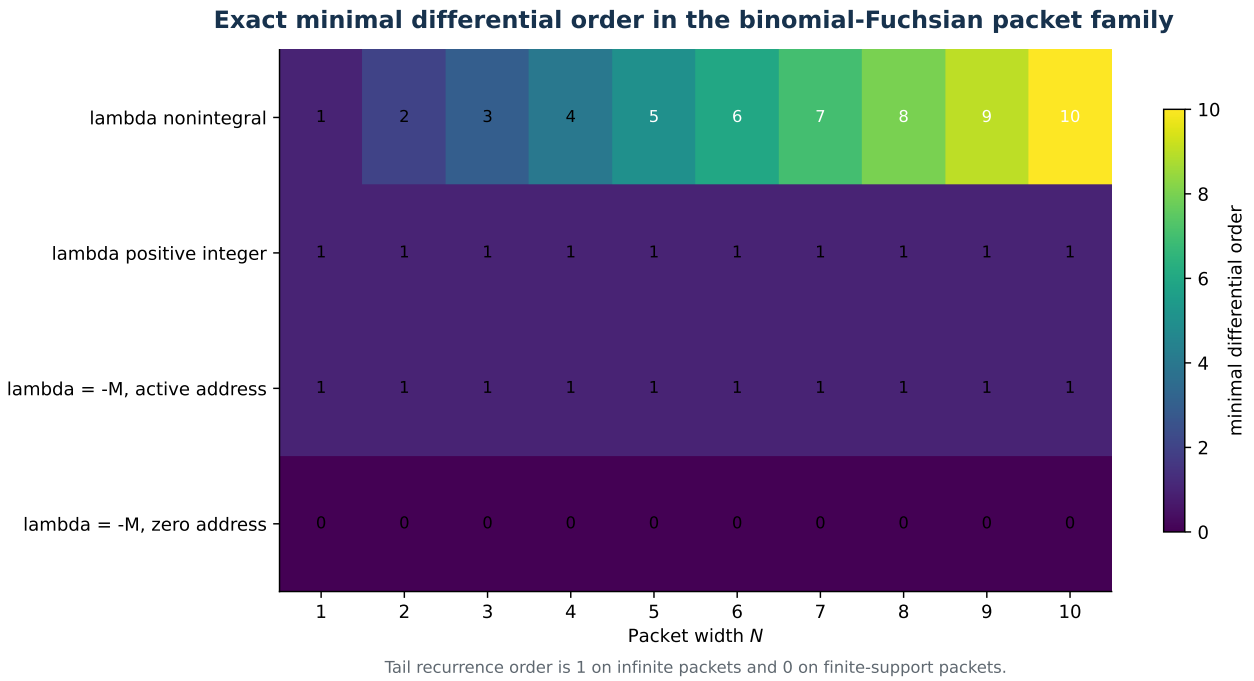



**Figure 37:** Minimal differential order in the binomial packet family. Nonintegral exponents retain order $N$, positive integers collapse to rational order one, and nonpositive integers terminate with explicit aliasing and zero-address packets.

and the pairwise differences in $E_\infty$ are also $N$-torsion.

**Proposition 15.18** (Local monodromy ledger)**.** *For nonintegral rational $\lambda$:*

1. *the monodromy eigenvalues at zero form the complete group of $N$th roots of unity;*
2. *the ratios of monodromy eigenvalues at infinity are $N$th roots of unity;*
3. *the distinguished nontrivial eigenvalue at $\alpha^{-N}$ is*

$$e^{-2\pi i\lambda}.$$

The local eigenvalues are finite-order when $\lambda \in \mathbb{Q}$. This does not imply that the global monodromy group is finite. Connection matrices and logarithmic extension data remain additional invariants.

## 15.9 Marked normalized packet atlas

The order theorem is most naturally a theorem about marked packets. Without the mark, distinct choices of source exponent, scale, width, and address can represent the same zero packet or the same rational function.

**Definition 15.19** (Marked binomial–Fuchsian packet)**.** A marked packet is a tuple

$$\mathfrak{b} = (\alpha, \lambda, N, j; G),$$

where $\alpha \neq 0$, $N \geq 1$, $0 \leq j < N$, and

$$G(x) = G_{N,j}^{\lambda,\alpha}(x).$$

The parameters $(\alpha, \lambda, N, j)$ are part of the semantic object rather than metadata to be forgotten.

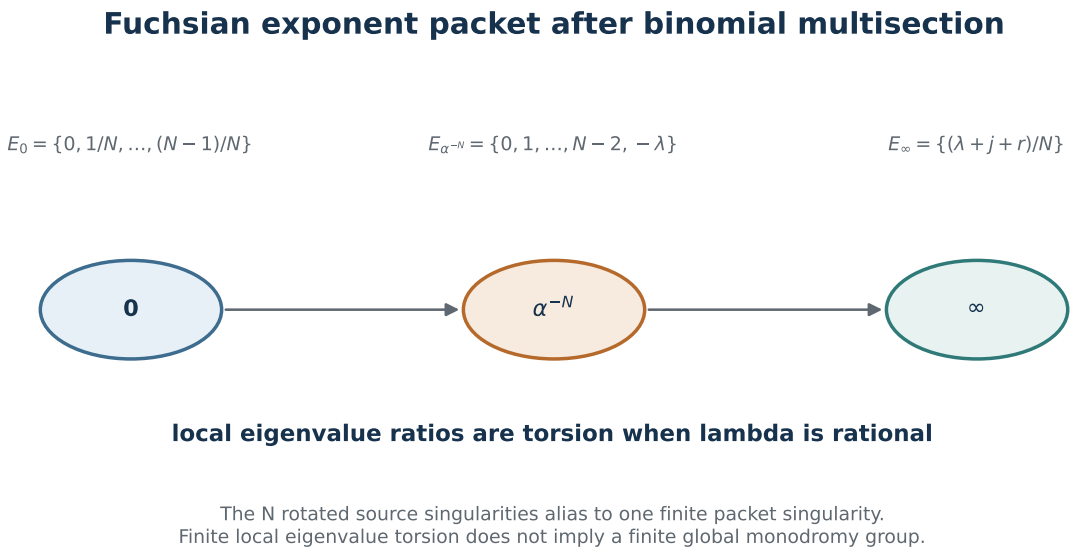



**Figure 38:** The exact Fuchsian exponent packet of a nonintegral binomial multisection. Root-orbit aliasing moves $N$ rotated source singularities into one finite singularity while the complete $N$-torsion exponent sets remain visible at zero and infinity.

For a nonzero marked packet, consider the following normalized charts:

(i) the marked coefficient series $G$;

(ii) the primitive first-order tail recurrence obtained from the exact coefficient ratio, together with its finite initial record;

(iii) the monic minimal differential operator from theorem 15.15, together with the distinguished power-series solution selected by the marked coefficient record;

(iv) the hypergeometric parameter packet $\left(A_{N,j}(\lambda), B_{N,j}; \alpha^N\right)$ and leading coefficient;

(v) the primitive minimal-operator singular and indicial record

$$\mathscr{E}(G) = \left(\Sigma_{\mathrm{op}}(G), \left(I_{\xi, L_G}\right)_{\xi \in \Sigma_{\mathrm{op}}(G)}\right),$$

together with the orbit-rank and defect data

$$\left(r_{\mathrm{orb}}, r_D, A_N, C_{N,j}\right).$$

In the nonintegral Fuchsian regime, $\mathscr{E}(G)$ is the explicit three-point packet

$$\left(E_0, E_{\alpha^{-N}}, E_\infty\right)$$

computed above. In the integral regimes it is computed from the corresponding minimal first-order operator. The zero packets in the terminated regime are retained as separately marked zero objects with the zero-operator convention.

**Theorem 15.20** (Effective marked binomial–Fuchsian atlas)**.** *The five normalized presentations above determine one another on the declared marked family. With equality morphisms they form equivalent discrete groupoids, every normalized fiber is contractible, and objects and morphisms descend effectively. The package*

$$\boxed{\mathcal{J}_{\mathrm{BF}} = \big(\alpha, \lambda, N, j, R_{N,j}, L_{N,j}, A_{N,j}(\lambda), B_{N,j}, \mathscr{E}(G), r_{\mathrm{orb}}, r_D, A_N, C_{N,j}\big)}$$

*is complete on this marked category.*

*Proof.* The mark constructs the coefficient packet directly. Consecutive coefficient ratios give the normalized recurrence chart, and the multiplication formula gives the hypergeometric chart. Theorem 15.15 identifies the monic minimal differential operator in every parameter regime. The primitive polynomial representative of that operator determines $\mathscr{E}(G)$ by the indicial construction in Section 15.5. In the nonintegral regime, proposition 15.18 gives its explicit Fuchsian eigenvalue ledger. Theorem 15.16 and corollary 15.17 compute the orbit and cancellation data in every regime. Conversely, the displayed invariant retains the complete mark and therefore reconstructs the source packet and every normalized chart. Uniqueness of monic Ore normalization and of the marked coefficient record leaves no nontrivial automorphism in a fiber. □

## 15.10 Examples and exact verification

The parity sections of

$$\frac{2}{1-z^2}$$

give the smallest singularity-alias example. The source singularities 1 and $-1$ both map to 1 under squaring. The even address is $2/(1-x)$, while the odd address vanishes.

For

$$2\cosh z,$$

the even packet is nonzero and the odd packet is zero. There is no finite singularity, so the cancellation occurs at the level of the character-projected solution rather than by finite singularity collision.

For the Catalan sequence, every arithmetic section remains hypergeometric in the packet index. Its recurrence order is one, while its ordinary generating function remains a second-order algebraic D-finite function. This again shows that recurrence order and scalar differential order are different coordinates.

For the Apéry numbers, the known two-dimensional nonautonomous state jumps to every arithmetic section. The jump theorem gives an exact order-two recurrence bound, but the present holonomic theorem does not claim a closed minimality formula for all Apéry addresses.

**Table 25:** Representative exact order profiles in the binomial–Fuchsian packet family.

| Source | Packet | $r_{\mathrm{tail}}$ | $r_D$ | $r_{\mathrm{orb}}$ | Alias | Cancel | Interpretation |
|---|---|---|---|---|---|---|---|
| $(1-z)^{-1/2}$ | $N=2,\ j=0$ | 1 | 2 | 2 | 0 | 0 | irreducible nonintegral packet |
| $(1-z)^{-1/3}$ | $N=3,\ j=2$ | 1 | 3 | 3 | 0 | 0 | finite local exponent torsion |
| $(1-z)^{-2}$ | $N=3,\ j=1$ | 1 | 1 | 3 | 0 | 2 | rational collapse |
| $(1-z)^{2}$ | $N=4,\ j=1$ | 0 | 1 | 3 | 1 | 2 | finite-support polynomial |
| $(1-z)^{2}$ | $N=4,\ j=3$ | 0 | 0 | 3 | 1 | 3 | zero address packet |

The Holonomic atlas verifier checks the binomial packet recurrence, the generalized hypergeometric differential coefficient identity, nonresonance of the irreducible parameter packets, zero and infinity

**Table 26:** Exact Holonomic atlas verification counts.

| Validation class | Exact checks |
|---|---|
| Nonintegral binomial packets | 110,880 |
| Positive-integral rational collapse | 27,720 |
| Nonpositive-integral aliasing | 11,492 |
| Root-filter and order ledger | 24,848 |
| Holonomic atlas total | 174,940 |
| Cumulative the preceding certified atlas program total | 1,838,856 |
| Failures | 0 |

exponent torsion classes, positive-integral rational collapse, nonpositive-integral orbit rank and address support, and root-filter orthogonality. It records 174,940 exact checks with no failures.

**Exact holonomic boundary.** The holonomic section proves normalized minimal Ore charts on the ordinary-point locus and an exact multisection minimality theorem for the binomial–Fuchsian packet family. It does not prove a universal formula for minimal multisection operators of arbitrary D-finite series. Irregular singularities, Stokes data, apparent-singularity removal, resonant logarithmic extensions, general differential-module cyclicity after character projection, and a finite all-address signature for unrestricted holonomic systems remain open.

**Section result.** P-recursive and D-finite presentations now form an explicit normalized atlas on the ordinary-point locus, with minimal Ore annihilators, finite prefix and jet certificates, and exact coefficient transport. General arithmetic multisection has a typed root-filter and state-jump construction, together with an explicit construction-relative minimality defect. The binomial–Fuchsian family supplies the first exact holonomic packet phase diagram: nonintegral exponents retain differential order $N$, positive integers collapse to rational order one, nonpositive integers terminate with a closed orbit-alias and address-cancellation formula, and the nonintegral local exponent packet exposes the complete finite torsion at zero and infinity.

## 16 Selected algebraic branches, packet Weil restriction, and collision invariants

Algebraic atlas develops the algebraic stratum after the fixed-radix, product, local, and holonomic milestones. The central issue is not algebraicity alone. A polynomial equation may have several formal branches, and a packet elimination can contain branch tuples that do not belong to the selected semantic germ. A normalized algebraic chart must therefore retain both a minimal polynomial and a finite branch selector. Arithmetic packets are then compiled as a finite polynomial system. The generic packet scheme is a Weil restriction of the source branch scheme, which gives a uniform degree bound. A separate collision ledger explains why the degree of one selected packet may be smaller than that bound.

Throughout this section, $K$ is a characteristic-zero field and $\overline{K}$ is an algebraic closure. Algebraic degree always means degree over the displayed rational-function field. All assertions about formal branches are made inside $\overline{K}[[z]]$ unless a different local field is named.

### 16.1 Minimal polynomials and finite branch selectors

Let $F \in K[[z]]$ be algebraic over $K(z)$. Its monic irreducible polynomial is

$$P_F(z, Y) \in K(z)[Y], \qquad P_F(z, F(z)) = 0.$$

Write

$$d(F) = \deg_Y P_F.$$

After multiplying by a common denominator and dividing by the greatest common divisor of the polynomial coefficients, one obtains a primitive representative in $K[z, Y]$, unique up to a nonzero scalar. We normalize that scalar by fixing the first nonzero coefficient in graded lexicographic order to be one.

A polynomial alone does not select a branch. Let

$$\mathrm{Br}_0(P_F) = \{G \in \overline{K}[[z]] : P_F(z, G(z)) = 0\}.$$

This set has cardinality at most $d(F)$.

**Definition 16.1** (Branch-separation index)**.** For $F \in \mathrm{Br}_0(P_F)$, define

$$\sigma(P_F, F) = \begin{cases} 0, & \mathrm{Br}_0(P_F) = \{F\}, \\ 1 + \max\limits_{G \in \mathrm{Br}_0(P_F),\, G \neq F} \mathrm{ord}_z(F - G), & \text{otherwise.} \end{cases}$$

The corresponding branch selector is the finite coefficient jet

$$\boxed{J_{\mathrm{alg}}(F) = (a_0, a_1, \ldots, a_{\sigma-1}), \qquad F(z) = \sum_{n \geq 0} a_n z^n.}$$

When $\sigma = 0$, the selector is empty.

**Theorem 16.2** (Finite branch separation)**.** *The pair*

$$\boxed{(P_F, J_{\mathrm{alg}}(F))}$$

*selects $F$ uniquely among the formal power-series branches of $P_F$ at the origin.*

*Proof.* There are at most $d(F)$ formal branches. The difference of two distinct formal series has finite $z$-adic order. By definition of $\sigma$, every other branch differs from $F$ in one of the coefficients recorded by $J_{\mathrm{alg}}(F)$. □

The simplest case is the ordinary implicit-function locus.

**Corollary 16.3** (Simple-branch normalization)**.** *If*

$$P_F(0, a_0) = 0, \qquad \partial_Y P_F(0, a_0) \neq 0,$$

*then $a_0$ alone selects a unique formal branch. Equivalently, $\sigma(P_F, F) \leq 1$.*

*Proof.* Coefficient comparison in $P_F(z, F(z)) = 0$ determines each next coefficient linearly, with diagonal coefficient $\partial_Y P_F(0, a_0)$. □

The finite selector is semantic data. It cannot be dropped merely because the polynomial is irreducible over $K(z)$. Irreducibility controls the generic function-field extension, while the jet chooses one local embedding of that extension into formal series.

## 16.2 The normalized selected-branch atlas

Let

$$A_F = K(z)[Y]/(P_F),$$

and let $\bar{Y}$ denote the residue class of $Y$. In the basis

$$1, \bar{Y}, \dots, \bar{Y}^{d-1},$$

multiplication by $\bar{Y}$ is represented by the companion matrix $M_F$. Its characteristic and minimal polynomials are both $P_F$.

**Theorem 16.4** (Normalized selected-branch algebraic atlas)**.** *The following normalized presentations determine one another exactly:*

$$\boxed{\begin{aligned}&F \in K[[z]],\\ &(P_F, J_{\mathrm{alg}}(F)),\\ &(A_F, \bar{Y}, J_{\mathrm{alg}}(F)),\\ &(M_F, J_{\mathrm{alg}}(F)).\end{aligned}}$$

*With equality morphisms, these presentations form equivalent normalized groupoids. Every fiber over a fixed semantic branch is contractible.*

*Proof.* The semantic branch gives its unique monic minimal polynomial and its finite branch selector. The polynomial gives the finite field algebra and its companion multiplication matrix. Conversely, the companion matrix recovers $P_F$ as its minimal polynomial. The branch selector then recovers the selected formal root by theorem 16.2. Every normalized presentation is determined literally, so a normalized automorphism fixing the semantic branch is the identity. □

## 16.3 The exact residue-packet polynomial compiler

Fix $N \geq 1$. For

$$F(z) = \sum_{n \geq 0} a_n z^n,$$

define the arithmetic packets

$$U_j(x) = \sum_{m \geq 0} a_{Nm+j} x^m, \qquad 0 \leq j < N.$$

They satisfy the exact synthesis identity

$$\boxed{F(z) = \sum_{j=0}^{N-1} z^j U_j(z^N).}$$

Let $P(z, Y) \in K[z, Y]$ be the normalized primitive representative of $P_F$. Introduce indeterminates

$$\mathbf{U} = (U_0, \dots, U_{N-1})$$

and substitute

$$Y = \sum_{j=0}^{N-1} z^j U_j.$$

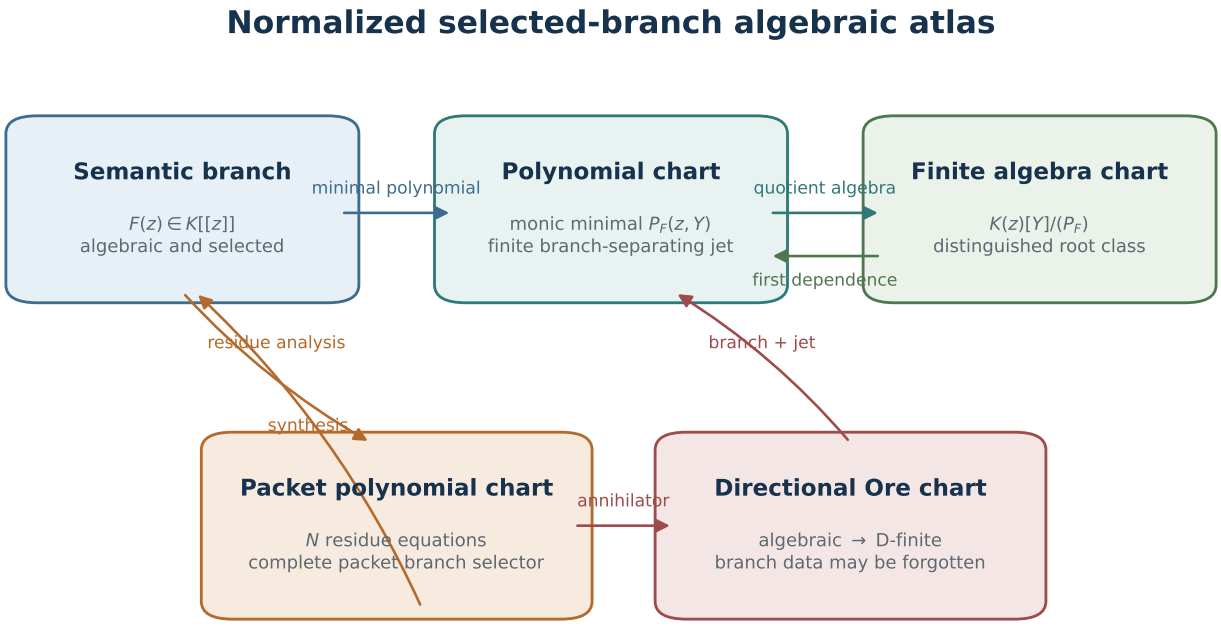



**Figure 39:** The selected algebraic branch, its minimal polynomial and finite selector, its finite quotient algebra, and its complete packet system are reversible normalized charts. The Ore chart is directional because an annihilator can forget branch data.

Every polynomial in $z$ has a unique decomposition modulo the relation $z^N = x$:

$$P\left(z, \sum_{j=0}^{N-1} z^j U_j\right) = \sum_{r=0}^{N-1} z^r \Phi_{N,r}(x, \mathbf{U}).$$

The polynomials

$$\boxed{\Phi_{N,r}(x, \mathbf{U}) \in K[x, \mathbf{U}]}$$

are the algebraic packet equations.

**Theorem 16.5** (Exact algebraic packet system)**.** *Let $d = \deg_Y P_F$. Then:*

1. *the semantic packet tuple $(U_0, \dots, U_{N-1})$ satisfies*
$$\Phi_{N,r}(x, \mathbf{U}) = 0 \qquad (0 \le r < N);$$
2. *every $\Phi_{N,r}$ has total degree at most $d$ in the packet variables;*
3. *a formal packet tuple satisfying all $N$ equations synthesizes a formal branch of $P_F$;*
4. *the packet tuple selected by the transported coefficient jet reconstructs $F$ uniquely.*

*Proof.* Substituting the semantic synthesis formula into $P_F(z, F(z)) = 0$ gives the first statement. Substitution does not increase degree in the $U_j$, so the second follows. If all residue polynomials vanish, then the synthesized series satisfies $P_F = 0$. The source branch selector is distributed among the packets by residue class. The resulting packet jet synthesizes the original jet, so theorem 16.2 identifies the selected branch. □

If the source selector records $a_0, \dots, a_{\sigma-1}$, the transported packet selector records precisely

$$[x^m]U_j = a_{Nm+j} \qquad \text{for } Nm + j < \sigma.$$

No information is added or lost. The coefficient prefix is merely rewritten in packet addresses.

### 16.4 Weil-restricted packet degree

Put

$$R = K(x), \qquad E_N = R[z]/(z^N - x).$$

Characteristic zero makes $z^N - x$ separable over $R$. Interpret the monic polynomial $P_F(z, Y)$ as a polynomial in $E_N[Y]$, and define

$$B_{N,F} = E_N[Y]/(P_F).$$

The packet polynomial system is the coordinate presentation of the finite Weil restriction

$$\mathrm{Res}_{E_N/R} \operatorname{Spec} B_{N,F}.$$

**Theorem 16.6** (Algebraic packet degree bound)**.** *Let $F$ have algebraic degree $d$ over $K(z)$. For every packet width $N$:*

1. *the generic geometric degree of the complete packet scheme is*

$$\boxed{d^N;}$$

2. *the joint field generated by a selected complete packet satisfies*

$$\boxed{[K(x)(U_0, \dots, U_{N-1}) : K(x)] \le d^N;}$$

3. *every individual packet satisfies*

$$\boxed{[K(x)(U_j) : K(x)] \le d^N.}$$

*Proof.* Over an algebraic closure of $K(x)$, the equation $z^N = x$ has $N$ distinct roots. The algebra $E_N$ therefore splits into a product of $N$ copies of the algebraic closure. At each address, the separable degree-$d$ polynomial $P_F$ has $d$ geometric roots. The Weil-restricted fiber is their Cartesian product and has $d^N$ points. A selected packet tuple is one point of this finite scheme, so its residue field and every coordinate subfield have degree at most the scheme degree. □

This bound is constructive. The quotient of

$$K(x)[U_0, \dots, U_{N-1}]$$

by the packet equations is a finite algebra of generic rank $d^N$. Multiplication by $U_j$ is therefore a matrix of size $d^N$. Its characteristic polynomial annihilates $U_j$ by Cayley–Hamilton.

**Corollary 16.7** (Constructive packet eliminant)**.** *For each $j$, one can compute an annihilating polynomial*

$$Q_{N,j}(x, T) \in K(x)[T]$$

*with*

$$\deg_T Q_{N,j} \le d^N$$

*by multiplication matrices, resultants, or a Gröbner elimination of the exact packet system.*

The bound is a universal degree ceiling for the minimal-polynomial grammar. It does not assert that every coordinate attains degree $d^N$ or that one elimination algorithm returns the minimal polynomial without factor selection.

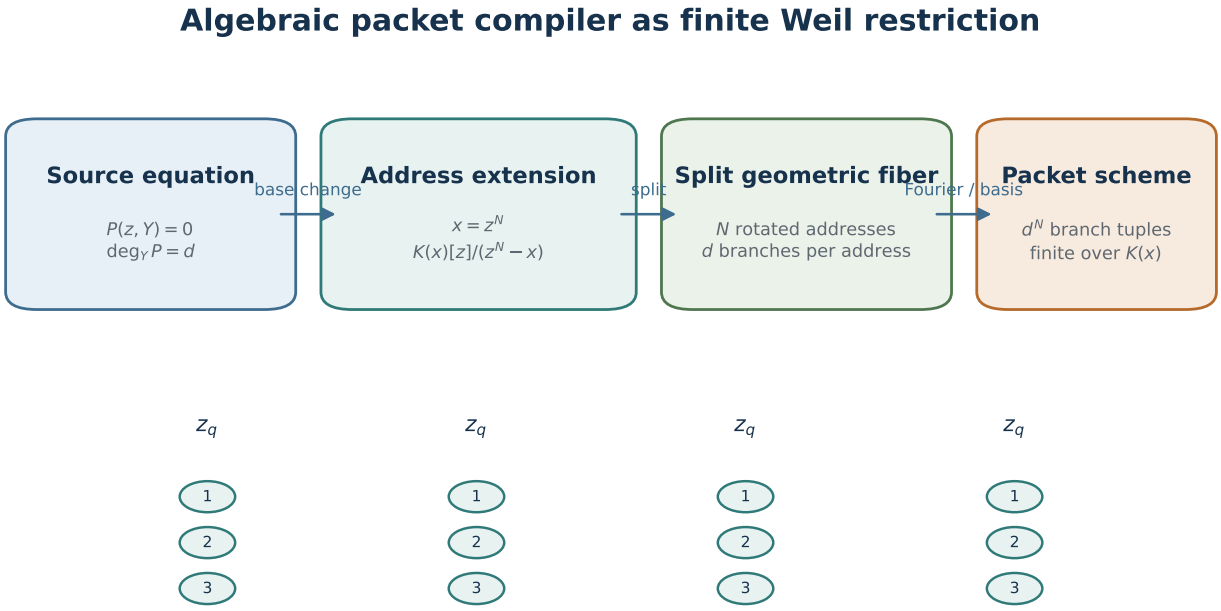



**Figure 40:** After the address extension $x = z^N$ splits, each of the $N$ addresses carries $d$ algebraic branches. The complete packet scheme is their Cartesian product and has generic degree $d^N$.

## 16.5 Tuple collision and selected-orbit loss

Let $\Omega$ be a normal splitting field of the generic packet scheme over $K(x)$, and let

$$\Gamma = \mathrm{Gal}(\Omega/K(x)).$$

After splitting $E_N$, the geometric packet branches form a set

$$\mathcal{B}_N$$

of cardinality $d^N$. Let

$$\pi_j : \mathcal{B}_N \to \Omega$$

be the $j$th packet coordinate, and set

$$\mathcal{C}_{N,j} = \pi_j(\mathcal{B}_N).$$

For the selected semantic packet $U_j$, separability gives

$$[K(x)(U_j) : K(x)] = |\Gamma \cdot U_j|.$$

**Definition 16.8** (Algebraic packet collision defects)**.** Define

$$\mathfrak{c}_{N,j}^{\mathrm{tuple}} = d^N - |\mathcal{C}_{N,j}|,$$

and

$$\mathfrak{s}_{N,j}^{\mathrm{Gal}} = |\mathcal{C}_{N,j}| - |\Gamma \cdot U_j|.$$

The first records collisions caused by projection from complete branch tuples to one packet coordinate. The second records the remaining loss caused by the Galois stabilizer of the selected coordinate.

**Theorem 16.9** (Exact algebraic degree-defect identity)**.** *The two defects are nonnegative and satisfy*

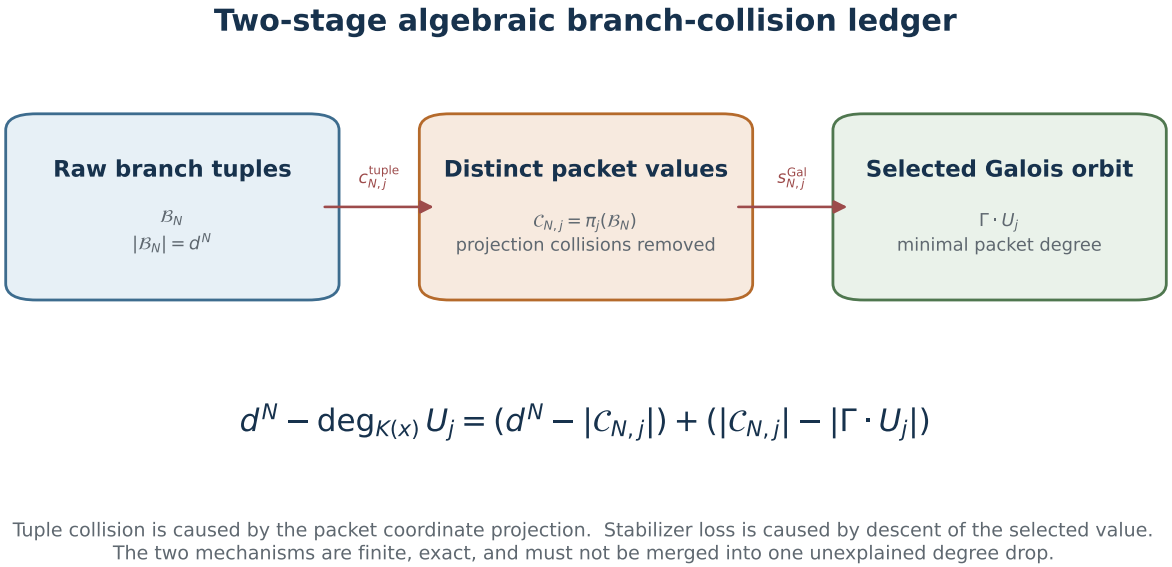
$$\boxed{d^N - [K(x)(U_j) : K(x)] = \mathfrak{c}_{N,j}^{\mathrm{tuple}} + \mathfrak{s}_{N,j}^{\mathrm{Gal}}.}$$

*Proof.* The coordinate image $\mathcal{C}_{N,j}$ has at most $d^N$ values. The Galois orbit of the selected value is contained in that image. The displayed identity is the telescoping decomposition

$$d^N - |\Gamma \cdot U_j| = (d^N - |\mathcal{C}_{N,j}|) + (|\mathcal{C}_{N,j}| - |\Gamma \cdot U_j|).$$

□

This signature separates two mechanisms that a raw resultant merges. Repeated projected values are a coordinate collision. A smaller selected orbit is a descent or stabilizer phenomenon. They are not the same obstruction.




Tuple collision is caused by the packet coordinate projection. Stabilizer loss is caused by descent of the selected value. The two mechanisms are finite, exact, and must not be merged into one unexplained degree drop.

**Figure 41:** The universal degree $d^N$ can drop first because several branch tuples have the same packet coordinate, then because the selected coordinate has a nontrivial Galois stabilizer.

## 16.6 A sharp Catalan parity theorem

Let

$$C(z) = 1 + zC(z)^2$$

be the Catalan branch with $C(0) = 1$, and write

$$C(z) = E(z^2) + zO(z^2).$$

Put $x = z^2$.

**Theorem 16.10** (Exact Catalan packet system)**.** *The parity packets satisfy*

$$\boxed{E = 1 + 2xEO, \qquad O = E^2 + xO^2.}$$

*Elimination gives*

$$\boxed{4xE^4 - E^2 + 1 = 0}$$

*and*

$$\boxed{4x^3O^4 - 8x^2O^3 + 5xO^2 - O + 1 = 0.}$$

*Both packets have algebraic degree four over $K(x)$. Hence the universal bound*

$$d^N = 2^2 = 4$$

*is sharp.*

*Proof.* Substitute $C = E + zO$ into $C = 1 + zC^2$ and separate even and odd powers. The two resultants give the displayed quartics.

For the even packet, put $T = E^2$. Then

$$4xT^2 - T + 1 = 0.$$

Its discriminant $1 - 16x$ is not a square in $K(x)$, so $[K(x)(T) : K(x)] = 2$. The norm of $T$ from this quadratic field is $1/(4x)$, which is not a square in $K(x)$. Therefore $T$ is not a square in its quadratic field and $E$ has degree four.

The first packet equation gives

$$O = \frac{E - 1}{2xE}, \qquad E = \frac{1}{1 - 2xO}.$$

Thus $K(x)(E) = K(x)(O)$, and the odd packet also has degree four. □

The Catalan parity packet has no tuple-collision or selected-orbit defect. Its one-coordinate degree already sees all four geometric branch tuples of the quadratic source over the two addresses.

## 16.7 A quadratic-radical collision phase diagram

Let

$$F_{\alpha,\beta}(z) = \sqrt{(1 - \alpha z)(1 - \beta z)}, \qquad F_{\alpha,\beta}(0) = 1,$$

and assume first that $\alpha \neq \beta$, so the normalized source degree is two. Write

$$F_{\alpha,\beta}(z) = E(x) + zO(x), \qquad x = z^2,$$

and put

$$s = \alpha + \beta, \qquad p = \alpha\beta.$$

**Theorem 16.11** (Quadratic-radical parity packets)**.** *The packets satisfy*

$$\boxed{E^2 + xO^2 = 1 + px, \qquad 2EO = -s.}$$

*Their eliminants are*

$$\boxed{E^4 - (1 + px)E^2 + \frac{s^2 x}{4} = 0}$$

*and*

$$\boxed{xO^4 - (1 + px)O^2 + \frac{s^2}{4} = 0.}$$

*If*

$$s \neq 0, \qquad \alpha^2 \neq \beta^2,$$

*then both selected packets have degree four over $K(x)$.*

*Proof.* The two equations follow by adding and subtracting the squares of

$$F(z) = E + zO, \qquad F(-z) = E - zO.$$

Elimination gives the quartics. Their quadratic discriminant is

$$\Delta(x) = (1 - \alpha^2 x)(1 - \beta^2 x),$$

which is not a square under the stated hypotheses. Hence $E^2$ generates a quadratic extension. Its norm is $s^2 x/4$, which is not a square in $K(x)$, so $E$ has degree four. Since $EO = -s/2$, the fields generated by $E$ and $O$ coincide. □

The symmetric case produces an exact collision.

**Corollary 16.12** (Antisymmetric branch collision)**.** *If $\beta = -\alpha \neq 0$, then*

$$\boxed{O = 0, \qquad E^2 = 1 - \alpha^2 x.}$$

*For the even coordinate,*

$$|\mathcal{B}_2| = 4, \qquad |\mathcal{C}_{2,0}| = 3, \qquad |\Gamma \cdot E| = 2.$$

*Thus*

$$\mathfrak{c}_{2,0}^{\mathrm{tuple}} = 1, \qquad \mathfrak{s}_{2,0}^{\mathrm{Gal}} = 1.$$

*For the selected odd coordinate,*

$$|\mathcal{C}_{2,1}| = 3, \qquad |\Gamma \cdot O| = 1,$$

*so*

$$\mathfrak{c}_{2,1}^{\mathrm{tuple}} = 1, \qquad \mathfrak{s}_{2,1}^{\mathrm{Gal}} = 2.$$

*Proof.* Now $F(z) = F(-z) = \sqrt{1 - \alpha^2 z^2}$ for the selected branch, so the odd packet vanishes. Over the split branch tuple set, the two signs are chosen independently. The even projection has values $E, 0, -E$, while the odd projection has values $0, E/z, -E/z$. The selected Galois orbits have sizes two and one, respectively. □

If $\alpha = \beta$, the quadratic equation

$$Y^2 - (1 - \alpha z)^2 = 0$$

is not the normalized source polynomial. The selected branch is rational:

$$F_{\alpha,\alpha}(z) = 1 - \alpha z,$$

so the correct source degree is one. This is a negative control against using a nonminimal defining equation in the degree ledger.

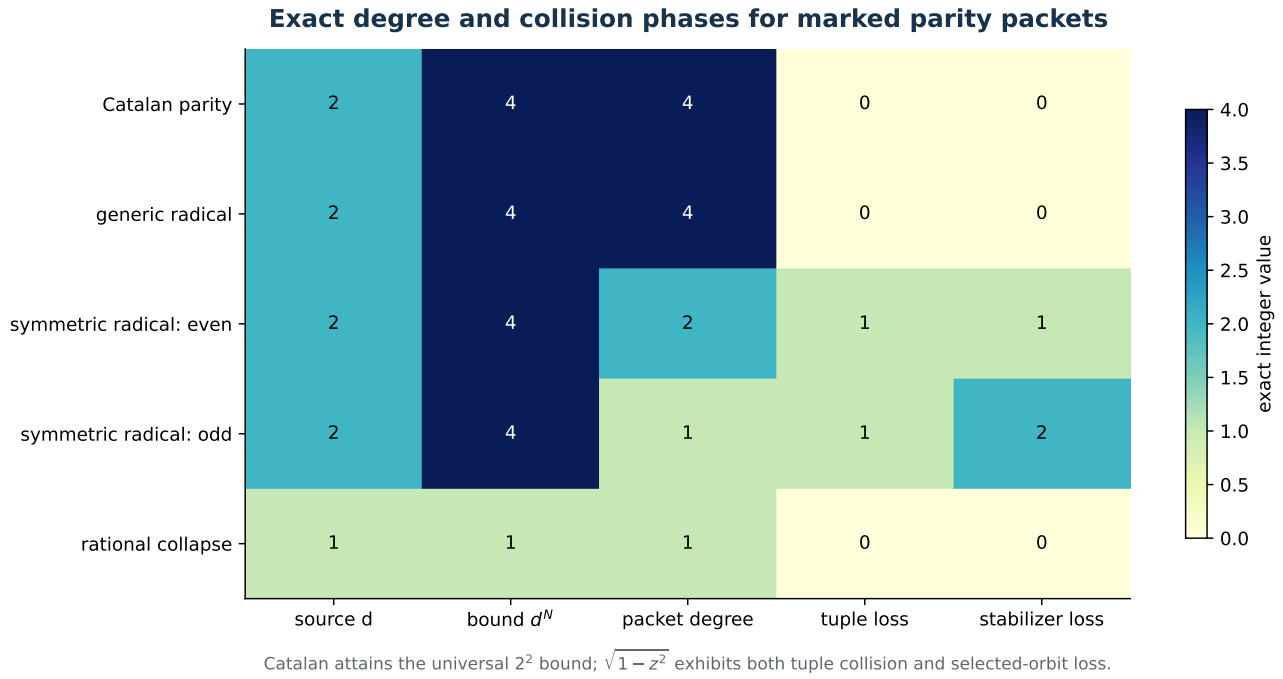



**Figure 42:** Catalan parity packets attain the universal quadratic bound. Generic radicals do the same, while the antisymmetric radical separates tuple collision from selected-orbit loss. A repeated linear factor must first be reduced to its minimal source polynomial.

## 16.8 The directional algebraic-to-holonomic bridge

Algebraic functions are D-finite, but this bridge is directional unless branch data is retained.

**Proposition 16.13** (Algebraic derivative closure)**.** *Let $F$ have separable minimal polynomial $P_F$ of degree $d$. Then*

$$F' = -\frac{\partial_z P_F(z,F)}{\partial_Y P_F(z,F)} \in K(z,F).$$

*Every higher derivative lies in the same degree-$d$ function field. Consequently, $F$ has a differential annihilator of order at most $d$.*

*Proof.* Differentiate $P_F(z, F(z)) = 0$. Separability makes $\partial_Y P_F(z,F)$ nonzero in the function field. The field is closed under the induced derivation. The $d+1$ elements $F, F', \ldots, F^{(d)}$ are linearly dependent over $K(z)$. □

The annihilator can forget both the polynomial relation and the selected branch. For example,

$$\sqrt{1+z} \quad \text{and} \quad -\sqrt{1+z}$$

satisfy the same first-order differential operator. Their initial values distinguish them. More generally, a D-finite equation may have transcendental solutions, so an Ore chart does not reconstruct an algebraic minimal polynomial without additional recognition data.

**Exact algebraic boundary.** Algebraic atlas proves finite selected-branch normalization, an exact packet polynomial compiler, the generic $d^N$ Weil-restriction degree, a constructive coordinate eliminant, and a two-stage collision invariant. It proves sharp packet degrees for Catalan parity and a complete collision phase for a marked quadratic-radical family. It does not prove that every elimination output is minimal without factor selection, one canonical minimal polynomial-system dimension across arbitrary multivariate grammars, an optimal packet-degree bound using all source symmetries, or unrestricted equivalence between algebraic and D-finite presentations.

## 16.9 Exact examples and finite verification

The verifier independently constructs packet equations by substitution and reduction modulo $z^N = x$. It checks Catalan, Motzkin, and marked radical branches at several packet widths. It verifies the sharp Catalan quartics, the quadratic-radical trace and norm systems, the generic and antisymmetric collision phases, the rejection of nonminimal quadratic equations, and finite branch-selector certificates.

**Section result.** A selected algebraic branch has a canonical minimal polynomial and a finite branch-separating jet. Complete arithmetic packets are the solutions of an explicit $N$-equation polynomial system obtained by residue reduction. The generic packet scheme is a finite Weil restriction of degree $d^N$, giving a constructive degree bound for every packet coordinate. Degree loss splits exactly into tuple projection collisions and Galois stabilizer loss. Catalan parity attains the universal quadratic bound, while the marked radical family exhibits generic sharpness, antisymmetric cancellation, and rational collapse. The algebraic-to-holonomic bridge remains directional unless the minimal polynomial and branch selector are retained.

**Table 27:** Representative exact degree and collision profiles in the Algebraic atlas algebraic packet atlas.

| Source | Packet | $d$ | $d^N$ | degree | tuple loss | stabilizer loss | Interpretation |
|---|---|---|---|---|---|---|---|
| $C = 1 + zC^2$ | parity $(E, O)$ | 2 | 4 | 4 | 0 | 0 | sharp Weil-restriction bound |
| $\sqrt{(1-z)(1-2z)}$ | parity even/odd | 2 | 4 | 4 | 0 | 0 | generic biquadratic packet |
| $\sqrt{1-z^2}$ | even packet | 2 | 4 | 2 | 1 | 1 | rotation alias plus descent stabilizer |
| $\sqrt{1-z^2}$ | odd packet | 2 | 4 | 1 | 1 | 2 | exact zero-address cancellation |
| $\sqrt{(1-z)^2} = 1-z$ | normalized source | 1 | 1 | 1 | 0 | 0 | nonminimal quadratic equation rejected |

**Table 28:** Exact finite validation of the Algebraic atlas algebraic packet layer.

| Validation class | Checks | Scope |
|---|---|---|
| General Packet Compiler | 3,690 | Catalan, Motzkin, and marked quadratic radicals at packet widths two through four |
| Catalan Sharp Parity | 7,426 | exact parity system, quartic eliminants, and irreducibility ledger |
| Quadratic Radical Collision Phase | 43,900 | generic degree four, antisymmetric cancellation, and rational collapse |
| Finite Branch Selectors | 16,632 | finite jets separating explicitly colliding formal branches |
| Collision Ledger Combinatorics | 1,440 | finite tuple-collision and selected-orbit defect identities |
| **Algebraic atlas total** | **73,088** | **0 failures** |
| Cumulative the preceding certified atlas program | 1,911,944 | frozen prior records plus recomputed Algebraic atlas |

# 17 Nonlinear polynomial fixed points, compressed packet composition, and finite tree signatures

Nonlinear tree atlas develops the nonlinear and rooted-tree stratum after the algebraic milestone. The existing nonlinear sources already prove exact packet jets, the packet Faà di Bruno law, colored operadic composition, refinement coherence, rooted-tree reconstruction, analytic majorant estimates, and local near-identity inversion [3, 2, 9]. The remaining problem is not whether nonlinear maps can be expanded. It is whether a declared nonlinear family admits a normalized finite presentation and a finite signature that controls a named packet complexity.

This section gives three restricted answers. First, a marked polynomial fixed-point system is organized into equivalent system, packet-hypergraph, operadic-tree, and exact packet-equation charts. Second, repeated-direction packet Faà di Bruno sums admit an exact orbit compression indexed by colored integer partitions rather than all labeled set partitions. Third, simply generated plane-tree equations possess a finite arity-gcd signature that determines every packet-support pattern and, under the classical smooth implicit schema, the complete dominant-singularity orbit after arithmetic packetization. A dependency condensation isolates the exact cyclic nonlinear core of a marked packet system. None of these results is promoted to a universal nonlinear normal form.

Throughout the analytic part, $X$ is a Banach space over $\mathbb{R}$ or $\mathbb{C}$. A finite packet system on $X$ is a family of bounded projections

$$P_i P_j = \delta_{ij} P_i, \qquad \sum_{i \in I} P_i = I_X.$$

All sums over packet addresses are finite. The formal-series part is valid over any characteristic-zero field unless positivity or singularity analysis is explicitly invoked.

## 17.1 Marked polynomial fixed-point systems

Let

$$A_m : X^m \longrightarrow X, \qquad 2 \le m \le D,$$

be bounded symmetric multilinear maps, and let $s \in X$. Consider the marked equation

$$\boxed{u = s + \Phi(u), \qquad \Phi(u) = \sum_{m=2}^{D} A_m[u, \dots, u].} \tag{11.1}$$

The word *marked* means that the source term, every multilinear operation, the packet system, and the selected convergence or filtration certificate are retained as part of the presentation. The fixed point $u$ alone is not assumed to reconstruct those data.

Put

$$a = \|s\|, \qquad b_m = \|A_m\|, \qquad \varphi(t) = \sum_{m=2}^{D} b_m t^m.$$

For a radius $R > 0$, define

$$\kappa_R = \varphi'(R) = \sum_{m=2}^{D} m b_m R^{m-1}.$$

**Theorem 17.1** (Selected polynomial fixed point and tree expansion)**.** *Assume*

$$a + \varphi(R) \le R, \qquad \kappa_R < 1.$$

*Then equation* (11.1) *has a unique solution in the closed ball $\overline{B}_R$. Moreover, that solution is the absolutely convergent sum*

$$\boxed{u = \sum_{T \in \mathcal{T}_{\mathcal{A}}} \mathrm{ev}(T),} \tag{11.2}$$

*where $\mathcal{A} = \{m : A_m \neq 0\}$, the leaves of $T$ evaluate to $s$, and an internal vertex of arity $m$ evaluates by $A_m$ applied to the ordered values of its children.*

*Proof.* The map

$$\Psi(x) = s + \Phi(x)$$

preserves $\overline{B}_R$ because

$$\|\Psi(x)\| \le a + \sum_{m=2}^{D} b_m R^m \le R.$$

For $x, y \in \overline{B}_R$, multilinearity gives

$$A_m[x^m] - A_m[y^m] = \sum_{r=1}^{m} A_m[y^{r-1}, x - y, x^{m-r}],$$

so

$$\|\Psi(x) - \Psi(y)\| \le \kappa_R \|x - y\|.$$

The contraction theorem gives the unique fixed point.

Let $u^{(0)} = 0$ and $u^{(h+1)} = \Psi(u^{(h)})$. Expanding recursively shows that $u^{(h)}$ is the sum of the evaluations of all allowed plane rooted trees of height at most $h - 1$. If $r_0 = 0$ and

$$r_{h+1} = a + \varphi(r_h),$$

then the sum of the norms of those tree evaluations is at most $r_h$. The scalar iterates increase and remain bounded by $R$, hence converge. Monotone convergence of the nonnegative norm majorant proves absolute convergence of the full tree sum. Regrouping trees by the arity of the root gives equation (11.1). □

*Remark* 17.2 (Formal filtered version). If $X$ is replaced by a complete filtered module, $s$ begins in positive filtration, and every $A_m$ raises total filtration, then the same tree expansion is coefficientwise finite at each filtration depth. It therefore defines the unique formal solution without a Banach norm. The analytic and formal doctrines are related but are not silently identified.

*Boundary* 17.3 (The selected object is a marked system). Two different polynomial systems can have the same fixed point. Conversely, a single polynomial system can have several fixed points outside the contraction ball. The normalized object in this section is therefore

$$(s, A_2, \dots, A_D; \mathcal{P}; \text{certificate}),$$

not an unmarked semantic vector $u$.

## 17.2 Packet jets, hypergraphs, and the marked nonlinear atlas

For $i, j_1, \dots, j_m \in I$, define the resolved multilinear block

$$A_{m;i|j_1,\dots,j_m} = P_i A_m(P_{j_1}\cdot, \dots, P_{j_m}\cdot).$$

Completeness of the packet family gives the exact reconstruction

$$\boxed{A_m = \sum_{i,j_1,\dots,j_m} A_{m;i|j_1,\dots,j_m}.} \tag{11.3}$$

Write

$$u_i = P_i u, \qquad s_i = P_i s.$$

Then equation (11.1) is equivalent to the complete packet system

$$\boxed{u_i = s_i + \sum_{m=2}^{D} \sum_{j_1,\dots,j_m} A_{m;i|j_1,\dots,j_m}[u_{j_1}, \dots, u_{j_m}].} \tag{11.4}$$

The active nonlinear transfer hypergraph has packet addresses as colors and one typed hyperedge

$$(j_1, \dots, j_m) \longrightarrow i$$

for every nonzero block $A_{m;i|j_1,\dots,j_m}$. Rooted substitution of these hyperedges is precisely the colored symmetric operad already present in the nonlinear core sources [2, 9].

**Theorem 17.4** (Normalized atlas of a marked polynomial system)**.** *Fix a finite packet system and a certificate satisfying the hypotheses of theorem 17.1, or a declared complete filtration satisfying the formal version. The following presentations determine one another exactly:*

| |
|---|
| *the marked polynomial system* $(s, A_2, \dots, A_D)$, |
| *the complete family of packet blocks* $A_{m;i\|j_1,\dots,j_m}$, |
| *the colored operadic tree grammar with its actual vertex operations,* |
| *the exact packet fixed-point system* (11.4). |

*Each chart reconstructs the same selected fixed point. With literal normalized data and equality morphisms, every semantic fiber is contractible.*

*Proof.* Equation (11.3) reconstructs each multilinear operation from its complete block family. The active hypergraph together with the actual block maps is simply another indexing of the same data. Rooted operadic substitution generates exactly the tree evaluations of theorem 17.1. Applying the output projections to the fixed-point equation gives (11.4), and synthesis recovers the original equation. Once the packet system, block maps, source term, and certificate are normalized literally, an automorphism fixing the semantic object and all marked data is the identity. □

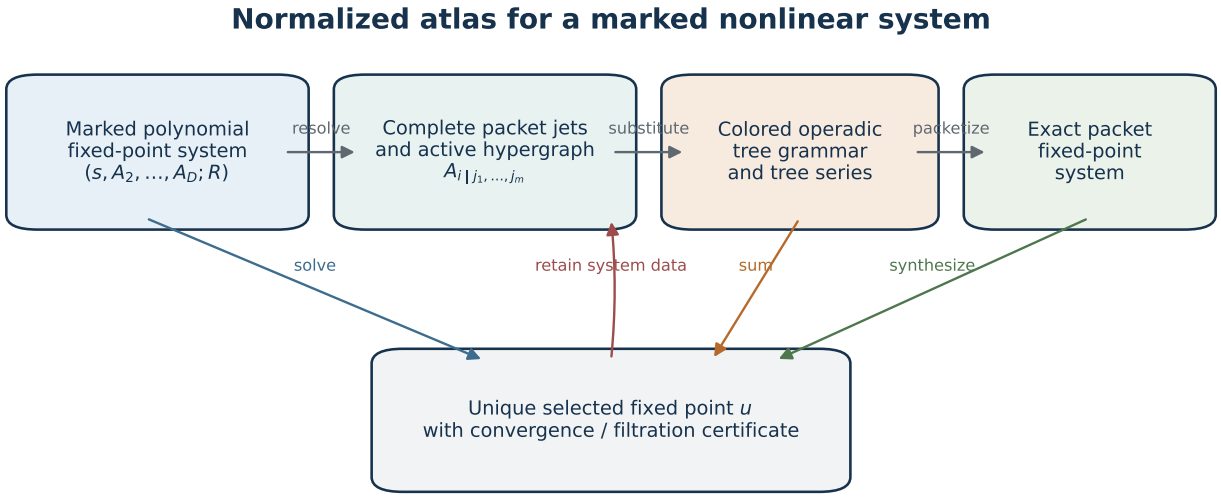



**Figure 43:** The marked system, its complete packet jets, its operation-labeled tree grammar, and its exact packet equations are reversible charts. The fixed point by itself is directional because it forgets the generating system.

## 17.3 Exact diagonal packet Faà di Bruno compression

The packet Faà di Bruno theorem from the nonlinear source expands an $n$th derivative over all set partitions and all intermediate packet labels [3, 2, 9]. When all directions are equal, the symmetric derivative tensors make many labeled terms identical. They can be grouped exactly by block-size and packet-color multiplicities.

Let $F : Y \to Z$ and $G : X \to Y$ be $n$ times differentiable. Fix an input packet $\beta$, an output packet $\delta$, a point $x$, and a direction $h \in P_\beta X$. For every intermediate packet $\gamma$ and every $r \geq 1$, put

$$g_{r,\gamma} = Q_\gamma D^r G(x)[h, \ldots, h].$$

A colored partition profile is a finite family

$$\mu = (\mu_{r,\gamma})_{r\geq 1,\, \gamma \in \Gamma}$$

of nonnegative integers satisfying

$$\sum_{r,\gamma} r\mu_{r,\gamma} = n.$$

Let

$$k(\mu) = \sum_{r,\gamma} \mu_{r,\gamma}.$$

**Theorem 17.5** (Compressed diagonal packet Faà di Bruno formula)**.** *With the notation above,*

$$\boxed{\begin{aligned}&P_\delta D^n(F\circ G)(x)[h,\dots,h]\\&=\sum_{\mu}\frac{n!}{\prod_{r,\gamma}(r!)^{\mu_{r,\gamma}}\mu_{r,\gamma}!}\,P_\delta D^{k(\mu)}F(Gx)\left[(g_{r,\gamma})^{\mu_{r,\gamma}}\right]_{r,\gamma}.\end{aligned}} \tag{11.5}$$

*Here the last line means that $g_{r,\gamma}$ is inserted $\mu_{r,\gamma}$ times; symmetry makes the insertion order irrelevant.*

*Proof.* Start with the packet Faà di Bruno sum over a set partition $\pi$ of $\{1,\dots,n\}$ and a packet color attached to every block. Because every input direction is $h$, the value of one term depends only on the number $\mu_{r,\gamma}$ of blocks of size $r$ carrying color $\gamma$. The symmetric group acts transitively on all colored set partitions with one fixed profile. The stabilizer permutes the $r$ entries inside each block and permutes the indistinguishable blocks of a fixed type $(r,\gamma)$. Its order is

$$\prod_{r,\gamma}(r!)^{\mu_{r,\gamma}}\mu_{r,\gamma}!,$$

so the orbit has the coefficient printed in (11.5). Summing one representative per orbit gives the result. □

**Corollary 17.6** (Colored integer-partition term count)**.** *If $Y$ has $M$ intermediate packets, the number of compressed diagonal profiles at order $n$ is*

$$\boxed{C_{n,M}=[x^n]\prod_{r\ge1}(1-x^r)^{-M}.} \tag{11.6}$$

*Before compression, the number of packet-labeled set-partition terms is*

$$N_{n,M}=\sum_{k=1}^{n}S(n,k)M^k.$$

*Proof.* For each block size $r$, the multiplicities among $M$ colors contribute

$$(1-x^r)^{-M}.$$

Multiplying over all $r$ and taking the coefficient of $x^n$ counts exactly the profiles satisfying the weighted-size constraint. The raw count is the existing packet term-count formula, grouped by the number of blocks. □

*Boundary* 17.7 (Scope of the compression theorem). Equation (11.5) closes the repeated-direction, single-input-packet case. For fully mixed directions, blocks carry the types of their actual input subsets; the relevant orbit type is finer and can approach the full set-partition expansion. No universal mixed-direction compression ratio is asserted.

## 17.4 The cyclic nonlinear core of a packet system

For the packet system (11.4), define the directed dependency graph $G_\Phi$ on $I$ by placing an edge

$$j\longrightarrow i$$

**Table 29:** Raw and compressed diagonal Faà di Bruno term counts for three intermediate packets.

| Order $n$ | Raw packet terms | Colored profiles | Compression factor |
|---|---|---|---|
| 1 | 3 | 3 | 1.0 |
| 2 | 12 | 9 | 1.3 |
| 3 | 57 | 22 | 2.6 |
| 4 | 309 | 51 | 6.1 |
| 5 | 1,866 | 108 | 17.3 |
| 6 | 12,351 | 221 | 55.9 |
| 7 | 88,563 | 429 | 206.4 |
| 8 | 681,870 | 810 | 841.8 |
| 9 | 5,597,643 | 1,479 | 3784.7 |
| 10 | 48,718,569 | 2,640 | 18454.0 |

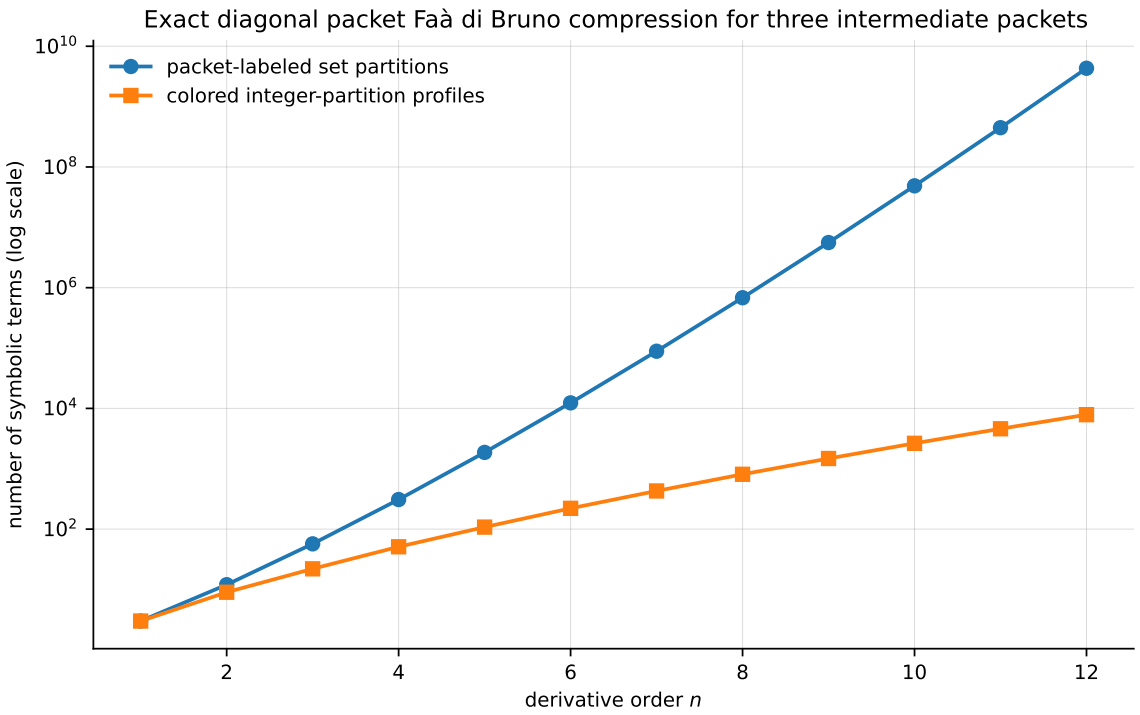



**Figure 44:** For repeated directions, packet-labeled set partitions collapse to colored integer-partition profiles. The compression is exact, not asymptotic.

when some active block contributing to the equation for $u_i$ contains $u_j$ as an input. Let

$$\mathrm{SCC}(G_\Phi)$$

be its strongly connected components. A component is called cyclic when it contains more than one address or is a singleton carrying a self-loop.

**Definition 17.8** (Address-preserving cyclic dimension)**.** The cyclic packet dimension of the marked system is

$$\boxed{\mathrm{cdim}_{\mathcal{P}}(\Phi) = \sum_{C \text{ cyclic SCC}} |C|.} \tag{11.7}$$

It measures the number of packet variables that remain in coupled nonlinear components after exact elimination of the acyclic singleton components.

**Theorem 17.9** (Exact SCC reduction)**.** *Order the SCC condensation graph topologically. Every acyclic singleton component can be substituted exactly once its predecessors have been determined. Repeating this elimination gives a solution-preserving bijection between:*

1. *solutions of the full packet system, and*
2. *solutions of the subsystem supported on the cyclic SCCs, followed by deterministic reconstruction along the condensation graph.*

*Consequently, the coupled nonlinear core has exactly* $\mathrm{cdim}_{\mathcal{P}}(\Phi)$ *packet variables.*

*Proof.* A singleton SCC without a self-loop has an equation in which its own variable does not occur. Once all predecessor components are known, that equation computes the variable directly. Substituting this expression into every successor equation is an algebraic identity and gives a bijection of solution sets. The condensation graph is acyclic, so repeated topological elimination terminates. Components containing a directed cycle cannot be removed by this one-pass address-preserving substitution because each contains a variable depending, directly or transitively, on itself. □

*Boundary* 17.10 (Not a universal nonlinear state minimum). The quantity $\mathrm{cdim}_{\mathcal{P}}$ is invariant under relabeling of the declared packet system and exact elimination within its dependency grammar. A nonlinear change of variables, hidden-variable introduction, algebraic elimination, or another packet family can change it. It is therefore a certified address-preserving system dimension, not a universal minimum over all nonlinear presentations.

## 17.5 A finite residue signature for simply generated trees

Consider the scalar marked equation

$$\boxed{u(z) = z + \Phi(u(z)), \qquad \Phi(y) = \sum_{m \in \mathcal{A}} w_m y^m,} \tag{11.8}$$

where $\mathcal{A} \subseteq \{2, 3, \dots\}$ is finite and every $w_m$ is a positive integer. Its unique formal solution belongs to $z\mathbb{Z}[[z]]$ and counts plane rooted trees whose internal arities lie in $\mathcal{A}$, weighted by the $w_m$.

Define the arity period

$$\boxed{d_{\mathcal{A}} = \gcd\{m - 1 : m \in \mathcal{A}\}.} \tag{11.9}$$

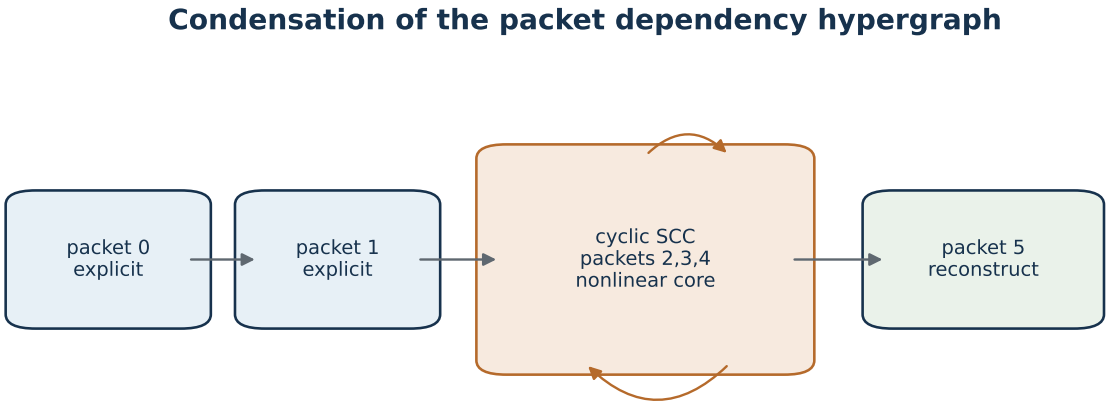



**Figure 45:** Condensation separates exact one-pass reconstruction from the cyclic nonlinear core. The resulting dimension is relative to the declared packet coordinates.

Every tree with internal vertices $v$ has leaf count

$$\ell(T) = 1 + \sum_{v} (\deg(v) - 1).$$

**Theorem 17.11** (Finite tree-address signature)**.** *Fix a packet width $N$ and put*

$$g_N = \gcd(N, d_{\mathcal{A}}).$$

*For the arithmetic packets*

$$U_j(x) = \sum_{r \geq 0} [z^{Nr+j}] u(z)\, x^r,$$

*the following are equivalent:*

1. $U_j \neq 0$;
2. $j - 1$ *belongs to the subgroup of* $\mathbb{Z}/N\mathbb{Z}$ *generated by* $\{m - 1 : m \in \mathcal{A}\}$;
3. $$\boxed{j \equiv 1 \pmod{g_N}.}$$

*Hence the exact number of active packet addresses is*

$$\boxed{\#\mathrm{Supp}_N(u) = \frac{N}{g_N}.} \tag{11.10}$$

*Proof.* Replacing one leaf by an $m$-ary vertex increases the leaf count by $m - 1$. Starting from the one-leaf tree, every nonnegative sum of allowed increments is realized by a sequence of leaf replacements. Positivity of the weights prevents cancellation, so the coefficient support is exactly

$$1 + \langle m - 1 : m \in \mathcal{A} \rangle_{\mathbb{N}}.$$

Modulo $N$, the monoid generated by the increments equals the subgroup they generate because every element of a finite cyclic subgroup has a nonnegative representative. That subgroup is $g_N\mathbb{Z}/N\mathbb{Z}$, which proves the congruence and the count. □

**Corollary 17.12** (Finite bottom-up residue automaton)**.** *Label every leaf by* $1 \in \mathbb{Z}/N\mathbb{Z}$ *and every* $m$*-ary vertex by the sum of its child labels. The reachable state set is exactly*

$$\{j : j \equiv 1 \pmod{g_N}\}.$$

*Thus the finite pair*

$$\boxed{\mathfrak{T}_N(\mathcal{A}) = (d_{\mathcal{A}}, g_N, N/g_N)} \tag{11.11}$$

*classifies packet support for the marked simply generated family.*

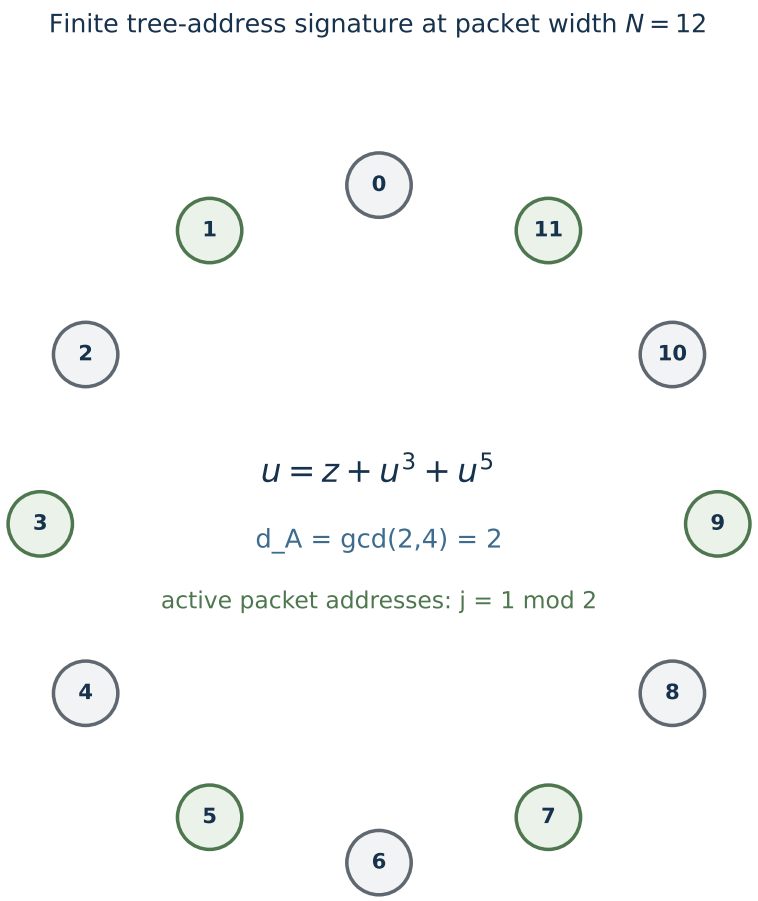



**Figure 46:** For arities three and five, the increment gcd is two. At width twelve, exactly the six addresses congruent to one modulo two are active.

## 17.6 Dominant singularity orbits

Assume now that the coefficients $w_m$ are positive real numbers. The classical smooth implicit-function schema for simply generated trees applies when there is a positive solution $\tau$ of

$$\Phi'(\tau) = 1$$

and

$$\rho = \tau - \Phi(\tau) > 0.$$

Under its standard nondegeneracy hypotheses, the reduced aperiodic series has a square-root singularity at its positive radius [15]. The arity period restores the complete source orbit.

**Theorem 17.13** (Complete dominant-orbit signature)**.** *Under the smooth implicit schema, the dominant singularities of $u(z)$ form*

$$\boxed{\rho\,\mu_{d_{\mathcal{A}}},} \tag{11.12}$$

*where $\mu_d$ is the group of dth roots of unity. After packetization with $x = z^N$, the union of dominant singularities of the complete packet tuple is*

$$\boxed{\rho^N\,\mu_{h_N}, \qquad h_N = \frac{d_{\mathcal{A}}}{\gcd(N, d_{\mathcal{A}})}.} \tag{11.13}$$

*Therefore the same finite arity signature determines both the number of active packet addresses and the size of the complete dominant-singularity orbit.*

*Proof.* By theorem 17.11, the coefficient support is contained in $1 + d_{\mathcal{A}}\mathbb{N}$ and the reduced exponent set is aperiodic by maximality of the gcd. Hence

$$u(z) = zV(z^{d_{\mathcal{A}}})$$

with $V$ aperiodic. The smooth implicit schema gives one positive dominant singularity for $V$, and pulling back through $z^{d_{\mathcal{A}}}$ gives (11.12). The map $z \mapsto z^N$ sends $\mu_{d_{\mathcal{A}}}$ onto a root group of cardinality

$$d_{\mathcal{A}} / \gcd(N, d_{\mathcal{A}}).$$

No packet can introduce a new dominant image outside this set. Conversely, if every packet were analytic at one image, the exact synthesis

$$u(z) = \sum_{j=0}^{N-1} z^j U_j(z^N)$$

would make $u$ analytic at every source point above that image, contradicting (11.12). Thus the union of packet singularities is exactly (11.13). □

*Boundary* 17.14 (Individual-packet cancellation). The theorem identifies the union of dominant singularities of the complete packet tuple. One individual packet can lose some orbit points through address cancellation. The finite signature does not, by itself, determine every individual local amplitude or cancellation coefficient.

## 17.7 The sharp full $q$-ary family

Take

$$\boxed{u = z + u^q, \qquad q \geq 2.} \tag{11.14}$$

Lagrange inversion gives the exact coefficient formula

$$\boxed{[z^n]u = \begin{cases} \dfrac{1}{(q-1)m+1}\dbinom{qm}{m}, & n = 1 + (q-1)m, \\ 0, & n \not\equiv 1 \pmod{q-1}. \end{cases}} \tag{11.15}$$

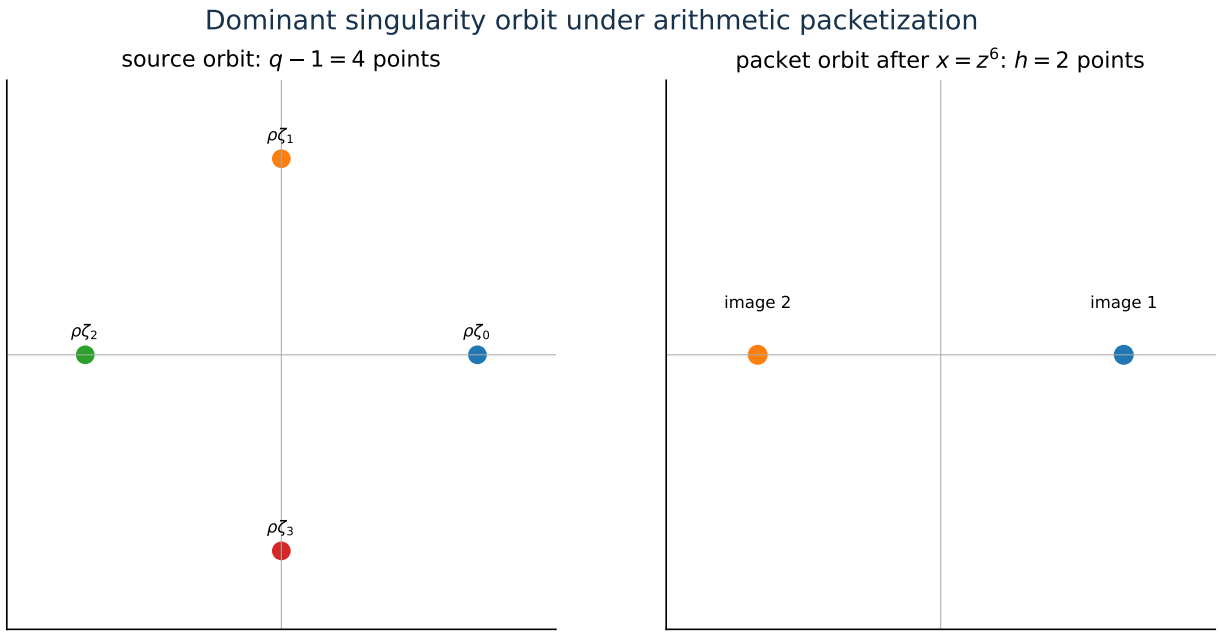



**Figure 47:** Arithmetic packetization maps the source root-of-unity singularity orbit through $z \mapsto z^N$. Distinct source singularities can alias to one packet-variable singularity.

The nonzero coefficients are the Fuss–Catalan numbers of full plane $q$-ary trees.

Write

$$u(z) = \sum_{j=0}^{N-1} z^j U_j(z^N), \qquad x = z^N.$$

**Theorem 17.15** (Exact $q$-ary packet phase theorem)**.** *Put*

$$g = \gcd(N, q-1), \qquad h = \frac{q-1}{g}.$$

*Then:*

1. *the active packet addresses are exactly*

$$\boxed{j \equiv 1 \pmod{g};}$$

2. *the complete packet system is*

$$\boxed{U_j(x) = \delta_{j,1} + \sum_{\substack{0 \le r_1,\dots,r_q < N \\ r_1+\cdots+r_q \equiv j \pmod N}} x^{(r_1+\cdots+r_q-j)/N} \prod_{a=1}^{q} U_{r_a}(x);} \tag{11.16}$$

3. *the smooth critical values are*

$$\tau = q^{-1/(q-1)}, \qquad \rho = (q-1)q^{-q/(q-1)};$$

4. *the source dominant orbit has $q-1$ points, while the complete packet orbit has exactly $h$ points.*

*The phase is therefore determined by the finite tuple*

$$\boxed{(q, N, g, N/g, h).} \tag{11.17}$$

*Proof.* Formula (11.15) follows from Lagrange inversion applied to

$$z = u(1 - u^{q-1}).$$

The support and active-address statements are theorem 17.11 with $d_{\mathcal{A}} = q - 1$. Expanding $u^q$ in complete packets and collecting the exponent carry

$$r_1 + \cdots + r_q = j + Nc$$

gives (11.16). The critical equations

$$q\tau^{q-1} = 1, \qquad \rho = \tau - \tau^q$$

give the printed values, and theorem 17.13 gives the orbit count. □

**Table 30:** Exact packet signatures for the marked full $q$-ary tree family $u = z + u^q$.

| $q$ | $N$ | $g = \gcd(N, q-1)$ | Active packets | Packet orbit | Active addresses |
|---|---|---|---|---|---|
| 2 | 5 | 1 | 5 | 1 | $\{0,1,2,3,4\}$ |
| 3 | 4 | 2 | 2 | 1 | $\{1,3\}$ |
| 3 | 5 | 1 | 5 | 2 | $\{0,1,2,3,4\}$ |
| 4 | 4 | 1 | 4 | 3 | $\{0,1,2,3\}$ |
| 4 | 6 | 3 | 2 | 1 | $\{1,4\}$ |
| 5 | 6 | 2 | 3 | 2 | $\{1,3,5\}$ |
| 5 | 7 | 1 | 7 | 4 | $\{0,1,2,3,4,5,6\}$ |
| 6 | 10 | 5 | 2 | 1 | $\{1,6\}$ |

## 17.8 Verification, status, and exact boundary

The Nonlinear tree atlas verifier performs four independent exact audits. It enumerates colored integer-partition profiles and compares their orbit-weighted Faà di Bruno values with the full set-partition expansion. It constructs exact fixed-point prefixes for marked polynomial tree families and checks the finite arity-gcd support theorem over many packet widths. It verifies Fuss–Catalan formulas and the complete carry-form packet equations for the full $q$-ary family. Finally, it checks dependency-graph reductions against exhaustive bounded graph instances.

**Section result.** Marked polynomial fixed-point systems admit exact packet, hypergraph, operadic-tree, and packet-equation charts. The repeated-direction packet Faà di Bruno expansion compresses exactly from colored set partitions to colored integer-partition profiles. The packet dependency graph has an exact SCC reduction whose cyclic vertices form the address-preserving nonlinear core. For positive simply generated tree systems, the arity gcd is a finite signature determining every arithmetic packet-support pattern and the complete dominant-singularity orbit. The full $q$-ary family supplies a closed Fuss–Catalan phase theorem and exact packet equations.

**Exact boundary of Nonlinear tree atlas.** The atlas classifies marked polynomial systems, not semantic fixed points independently of their generators. The compression theorem treats repeated directions; arbitrary mixed-direction jets can require a finer orbit type. The SCC dimension is relative to the declared packet coordinates. The tree signature classifies support and the complete dominant-

**Table 31:** Exact finite verification for Nonlinear tree atlas.

| Validation class | Exact checks |
|---|---|
| Colored profile counts | 100 |
| Orbit-size identity | 48 |
| Exact compressed Faà di Bruno values | 126 |
| Polynomial fixed-point prefixes | 300 |
| Finite tree-address signatures | 70,458 |
| Fuss-Catalan formulas | 2,892 |
| Exact q-ary packet systems | 37,567 |
| Dominant-orbit combinatorics | 176 |
| Dependency-core reductions | 4,054 |
| **Nonlinear tree atlas total** | **115,721** |
| Cumulative the preceding certified atlas program total | 2,027,665 |
| Failures | 0 |

singularity orbit for the marked simply generated family. It does not classify algebraic degree, universal minimal system dimension, every individual packet amplitude, arbitrary sign-canceling weights, noncontractive global dynamics, or all nonlinear operadic systems.

## 18 Finite Galois, profinite, and Tannakian resolved symmetry

Galois-Tannakian atlas develops the final declared stratum in the present eight-stratum program: finite semisimple Galois charts, cohomological descent, profinite refinement, and the tensor-fiber boundary at which a symmetry group can be reconstructed. The strongest Galois source already contains Reynolds projectors, the subgroup–fixed-field correspondence, normality and quotient compression, conjugate projector atlases, Mackey double-coset packets, ramification details, Haar projectors, Hilbert 90, the Brauer obstruction, finite étale permutation resolutions, and neutral Tannakian reconstruction [6]. The purpose here is to place those results into the same passport, bridge, obstruction, and effective-descent language used by the preceding sections.

The scope is deliberately semisimple or tensor-exact. For finite group averaging, the coefficient field has characteristic zero or characteristic prime to the relevant group order. Linear semilinear descent is taken over a finite Galois extension. Projective descent is typed separately from vector descent. Tannakian reconstruction is asserted only after a faithful exact tensor fiber functor has been supplied. Modular fixed points, wild integral descent, nonneutral fiber functors, and derived or flat replacements for failed averaging remain outside this block.

### 18.1 Finite subgroup, fixed-field, and Reynolds-projector charts

Let $L/K$ be a finite Galois extension with group

$$G = \mathrm{Gal}(L/K).$$

Let $V$ be a finite-dimensional representation of $G$ over a characteristic-zero field, or a unitary complex realization obtained after scalar extension. For every subgroup $H \leq G$, define

$$\boxed{P_H = \frac{1}{|H|} \sum_{h \in H} U_h.} \tag{12.1}$$

**Theorem 18.1** (Reynolds fixed packet and reverse order)**.** *The operator $P_H$ is the projector onto the fixed packet*

$$V^H = \{v : U_h v = v \text{ for all } h \in H\}.$$

*If $H \leq J$, then*

$$\boxed{P_H P_J = P_J P_H = P_J.} \tag{12.2}$$

*Consequently, subgroup inclusion reverses the fixed-projector order.*

*Proof.* The average is invariant under left and right multiplication by elements of $H$. Therefore $P_H^2 = P_H$, and its range is exactly the fixed subspace. If $H \leq J$, then $V^J \subseteq V^H$. The two projections are nested and multiply to the projector with smaller range. □

In the faithful regular realization, or in the field realization supplied by a normal basis, the projector determines the subgroup. Indeed, the support of the group-algebra idempotent

$$e_H = \frac{1}{|H|} \sum_{h \in H} h$$

is exactly $H$.

**Theorem 18.2** (Normalized finite Galois chart)**.** *Fix the finite Galois extension $L/K$. The following data determine one another exactly:*

$$\boxed{H \quad \longleftrightarrow \quad L^H \quad \longleftrightarrow \quad P_H} \tag{12.3}$$

*where the projector is taken in a faithful field or regular realization. The correspondence is order reversing:*

$$H \leq J \quad \Longleftrightarrow \quad L^H \supseteq L^J \quad \Longleftrightarrow \quad P_H \geq P_J.$$

*Thus the subgroup poset, the intermediate-field poset, and the faithful fixed-projector poset form three normalized charts of one finite semisimple Galois object.*

*Proof.* The finite Galois correspondence gives $H = \mathrm{Gal}(L/L^H)$ and $E = L^{\mathrm{Gal}(L/E)}$. The range of $P_H$ is $L^H$ after faithful scalar extension, and the support of $e_H$ recovers $H$. All three assignments are therefore mutually inverse on the declared charts. □

## 18.2 Compatibility, normality, and conjugate atlases

For two subgroups $H, J \leq G$, the common fixed packet is always

$$V^H \cap V^J = V^{\langle H, J \rangle}.$$

The two averaging projectors need not commute.

**Theorem 18.3** (Permutable subgroups and exact common refinement)**.** *In a faithful regular realization, the following are equivalent:*

1. *$HJ = JH$;*
2. *$HJ$ is a subgroup of $G$;*
3. *$P_H P_J = P_J P_H$.*

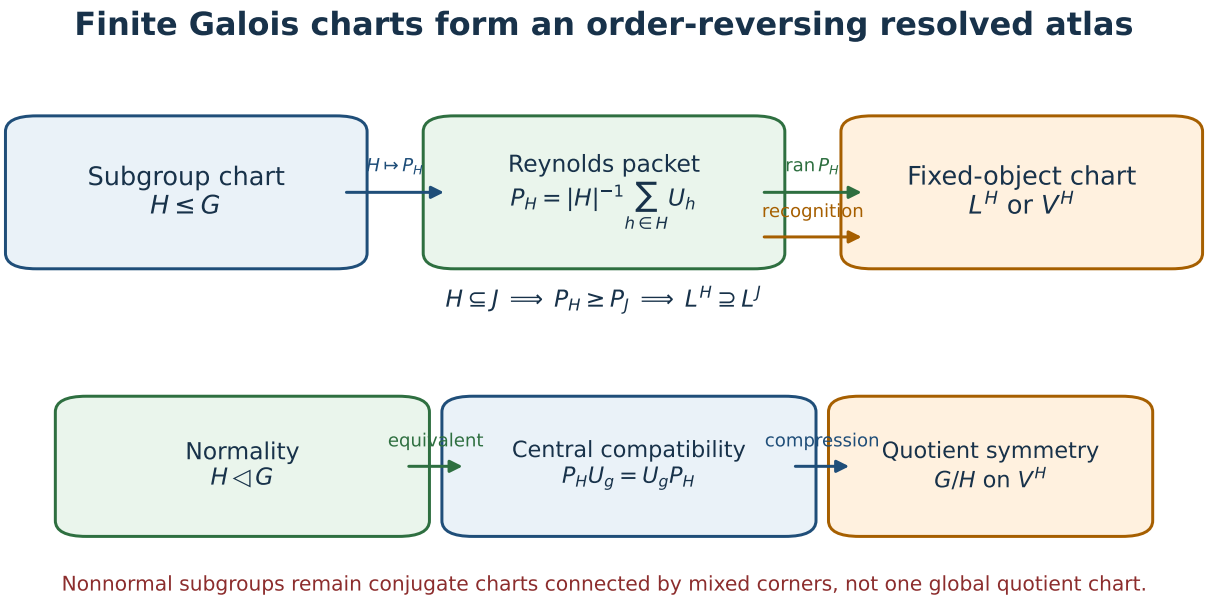



**Figure 48:** The finite subgroup, Reynolds-projector, and fixed-field charts are reversible in a faithful semisimple realization. Normality is the additional condition required for quotient compression.

*When these conditions hold,*

$$\boxed{P_H P_J = P_{HJ}.} \tag{12.4}$$

*If they fail, $P_H P_J$ and $P_J P_H$ are mixed atlas corners rather than projectors.*

*Proof.* If $HJ = JH$, every element of $HJ$ has $|H \cap J|$ representations as $hj$. Multiplying the two group averages therefore gives the average over $HJ$. Conversely, the support of $e_H e_J$ is $HJ$, while the support of $e_J e_H$ is $JH$. Equality in the regular group algebra forces equality of the product sets. □

**Theorem 18.4** (Normality and quotient compression)**.** *For a subgroup $H \leq G$, the following conditions are equivalent:*

1. *$H \lhd G$;*
2. *$e_H$ is central in the group algebra;*
3. *$P_H U_g = U_g P_H$ for every $g \in G$;*
4. *the fixed packet $V^H$ is $G$-invariant;*
5. *the fixed field $L^H$ is Galois over $K$.*

*When they hold, the compressed action on $V^H$ factors through $G/H$, and*

$$\boxed{\mathrm{Gal}(L^H/K) \cong G/H.} \tag{12.5}$$

*Proof.* Conjugation sends $e_H$ to $e_{gHg^{-1}}$. Centrality is therefore equivalent to normality. The represented identity

$$U_g P_H U_g^{-1} = P_{gHg^{-1}}$$

gives the operator conditions. The field and quotient statements are the normal-subgroup part of the finite Galois correspondence. □

If $H$ is not normal, its conjugates form a genuine atlas rather than one quotient chart. Put

$$\mathrm{Core}_G(H) = \bigcap_{g\in G} gHg^{-1}, \qquad \mathrm{Ncl}_G(H) = \left\langle gHg^{-1} : g \in G \right\rangle.$$

**Theorem 18.5** (Canonical envelopes of a nonnormal Galois atlas)**.** *Let $M = L^H$. Then*

$$\boxed{L^{\mathrm{Core}_G(H)} = \prod_{g\in G} g(M)} \tag{12.6}$$

*is the smallest Galois extension inside $L$ containing every conjugate chart, while*

$$\boxed{L^{\mathrm{Ncl}_G(H)} = \bigcap_{g\in G} g(M)} \tag{12.7}$$

*is the largest Galois subfield contained in every chart. The core and normal-closure projectors are the two canonical global envelopes of the conjugate atlas.*

*Proof.* Composita of intermediate fields correspond to intersections of subgroups, while intersections of fields correspond to generated subgroups. The core is the largest normal subgroup inside $H$, and the normal closure is the smallest normal subgroup containing $H$. □

**Example 18.6** (The $S_3$ nonnormal atlas)**.** Let $G = S_3$ and let $H$ be generated by one transposition. There are three conjugate order-two subgroups and hence three conjugate cubic fixed-field charts. Their subgroup core is trivial, while their normal closure is all of $S_3$. By contrast, the order-three subgroup $A_3$ is normal and its fixed chart carries the quotient symmetry $S_3/A_3 \cong C_2$.

## 18.3 Double cosets as exact transition packets

Restriction and induction connect subgroup charts that need not commute. Their exact address set is the double-coset space

$$K\backslash G/H.$$

**Theorem 18.7** (Mackey transition-packet decomposition)**.** *Let $H, K \le G$, let $W$ be a finite-dimensional representation of $H$, and choose representatives $x$ for $K\backslash G/H$. Then*

$$\boxed{\mathrm{Res}^G_K \mathrm{Ind}^G_H W \cong \bigoplus_{x\in K\backslash G/H} \mathrm{Ind}^K_{K\cap xHx^{-1}} \left({}^x\mathrm{Res}^H_{H\cap x^{-1}Kx} W\right).} \tag{12.8}$$

*Each double coset is one exact transfer packet between the $H$- and $K$-charts.*

*Proof.* The induced representation is a function space on $G$ with $H$-covariance. Functions supported on different double cosets are invariant direct summands under $K$. Identifying the summand on $KxH$ with an induced representation from $K \cap xHx^{-1}$ gives the decomposition. □

The dimension identity for the trivial $H$-representation is

$$\boxed{[G:H] = \sum_{x\in K\backslash G/H} [K : K\cap xHx^{-1}].} \tag{12.9}$$

This is the finite packet-count law audited by the Galois-Tannakian atlas verifier.

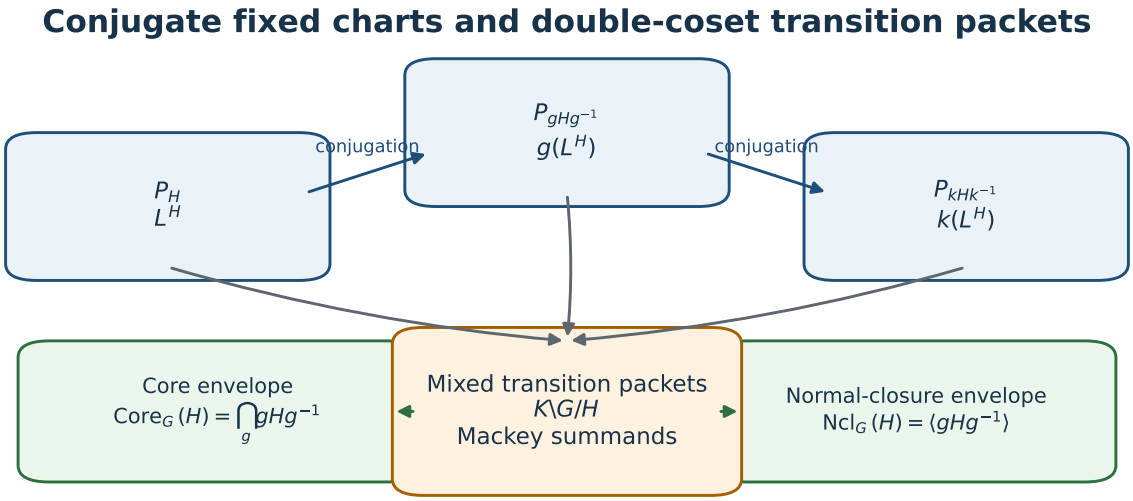



**Figure 49:** A nonnormal fixed object is an atlas of conjugate charts. Core and normal closure give two global envelopes, while double cosets give exact mixed transition packets.

**Table 32:** Finite group models used in the Galois-Tannakian atlas subgroup-projector audit.

| Group | Order | Subgroups | Normal | Permutable ordered pairs | Noncommuting ordered pairs | Double-coset packets audited |
|---|---|---|---|---|---|---|
| C2 | 2 | 2 | 2 | 4 | 0 | 5 |
| C3 | 3 | 2 | 2 | 4 | 0 | 6 |
| C4 | 4 | 3 | 3 | 9 | 0 | 15 |
| C5 | 5 | 2 | 2 | 4 | 0 | 8 |
| C6 | 6 | 4 | 4 | 16 | 0 | 30 |
| C8 | 8 | 4 | 4 | 16 | 0 | 37 |
| V4 | 4 | 5 | 5 | 25 | 0 | 37 |
| S3 | 6 | 6 | 3 | 30 | 6 | 65 |
| D4 | 8 | 10 | 6 | 92 | 8 | 195 |
| A4 | 12 | 10 | 3 | 64 | 36 | 250 |

### 18.4 Ramification as a nested resolution

Let $L/K$ be a finite Galois extension of local fields. Write

$$G_0 \supseteq G_1 \supseteq G_2 \supseteq \cdots$$

for the lower ramification filtration after inertia, and let $V$ be a finite-dimensional complex representation of $G$. Define

$$P_i = \frac{1}{|G_i|} \sum_{g \in G_i} U_g.$$

The ramification groups are nested and normal, so

$$P_0 \leq P_1 \leq P_2 \leq \cdots \leq I.$$

Put

$$D_i = P_{i+1} - P_i.$$

**Theorem 18.8** (Orthogonal ramification details)**.** *The operators $D_i$ are mutually orthogonal projectors, and*

$$\boxed{V = V^{G_0} \oplus \bigoplus_i D_i V.} \tag{12.10}$$

*Every detail packet is stable under the quotient action permitted by the corresponding normal subgroup.*

*Proof.* Nested orthogonal projectors commute, and the difference of two nested projectors is a projector onto the orthogonal difference of their ranges. The decomposition follows by telescoping. □

**Theorem 18.9** (Artin conductor as weighted unresolved rank)**.** *The Artin and Swan conductors satisfy*

$$\boxed{a(V) = \sum_{i \geq 0} \frac{|G_i|}{|G_0|} \operatorname{Tr}(I - P_i),} \tag{12.11}$$

$$\boxed{\operatorname{Sw}(V) = \sum_{i \geq 1} \frac{|G_i|}{|G_0|} \operatorname{Tr}(I - P_i).} \tag{12.12}$$

*If $d_j = \operatorname{rank} D_j$, then*

$$\boxed{a(V) = \sum_j d_j \sum_{i=0}^{j} \frac{|G_i|}{|G_0|}.} \tag{12.13}$$

*Thus the conductor is the weighted total rank that remains unresolved at each ramification scale.*

*Proof.* The classical conductor formula uses $\operatorname{codim} V^{G_i}$. Since $P_i$ projects onto $V^{G_i}$, this codimension is $\operatorname{Tr}(I - P_i)$. Also

$$\operatorname{codim} V^{G_i} = \sum_{j \geq i} d_j.$$

Reversing the finite sums gives the detail formula. □

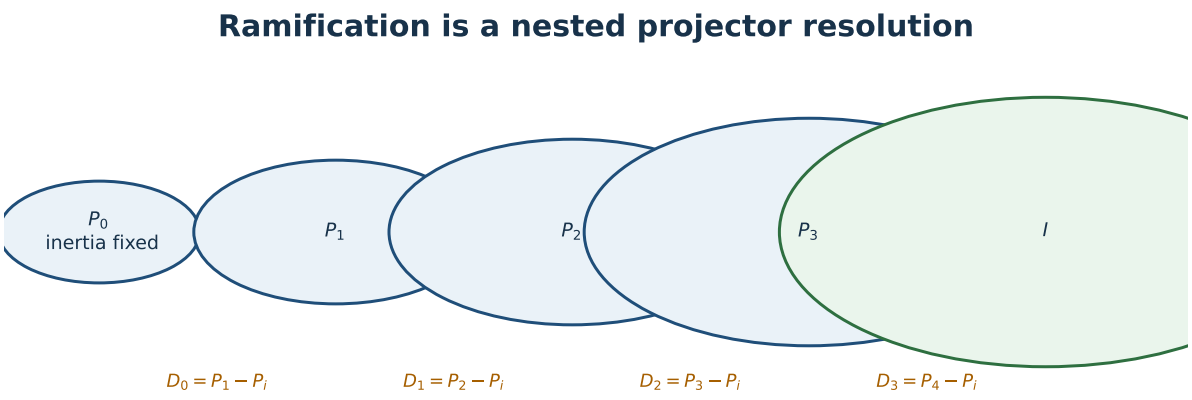



**Figure 50:** Ramification subgroups give nested fixed projectors. Their orthogonal differences are the resolved tame and wild detail packets, and the conductor is their weighted unresolved rank.

## 18.5 Profinite completion and finite quotient effectivity

Let $G$ be a compact group and let $U : G \to \mathcal{U}(\mathcal{H})$ be strongly continuous. For a closed subgroup $H$, normalized Haar measure defines

$$\boxed{P_H = \int_H U_h \, d\mu_H(h).} \tag{12.14}$$

The same averaging proof as in the finite case shows that $P_H$ is the orthogonal projector onto $\mathcal{H}^H$.

**Theorem 18.10** (Shrinking-subgroup reconstruction)**.** *Let $G$ be profinite and let*

$$U_1 \supseteq U_2 \supseteq \cdots$$

*be a neighborhood basis of the identity consisting of open normal subgroups. Then*

$$\boxed{P_{U_n} \longrightarrow I} \tag{12.15}$$

*strongly in every strongly continuous unitary representation. More generally, if $N \triangleleft G$ is closed and $U_n/N$ shrinks to the identity in $G/N$, then $P_{U_n} \to P_N$ strongly.*

*Proof.* For each $v \in \mathcal{H}$, strong continuity gives

$$\sup_{u \in U_n} \|U_u v - v\| \longrightarrow 0.$$

Averaging this estimate over $U_n$ proves the first statement. Apply it to the quotient action on the $N$-fixed packet for the second. □

**Corollary 18.11** (Finite-dimensional representations occur at finite level)**.** *Every continuous finite-dimensional complex representation of a profinite group has finite image and factors through a finite quotient.*

*Proof.* The image is a compact totally disconnected subgroup of $\mathrm{GL}_n(\mathbb{C})$. After conjugation it lies in a compact Lie group. A compact totally disconnected Lie group is finite. □

This finite-level factorization is a strong effectivity statement for finite-dimensional complex representations. It is not a statement that every integral, modular, or derived representation becomes semisimple at finite level.

### 18.6 Semilinear vector descent and Hilbert 90

Let $L/K$ be finite Galois with group $G$. A semilinear $G$-object is an $L$-vector space $V$ with maps

$$\rho_\sigma : V \to V, \qquad \rho_\sigma(\lambda v) = \sigma(\lambda)\rho_\sigma(v),$$

satisfying the group law. Scalar extension and fixed vectors define functors

$$L \otimes_K - : \mathrm{Vect}_K \longrightarrow \mathrm{Semilin}_G(L),$$

$$(-)^G : \mathrm{Semilin}_G(L) \longrightarrow \mathrm{Vect}_K .$$

**Theorem 18.12** (Effective finite Galois vector descent)**.** *The two functors above are quasi-inverse equivalences:*

$$\boxed{\mathrm{Vect}_K \simeq \mathrm{Semilin}_G(L).} \tag{12.16}$$

*For every semilinear object $V$, the fixed packet $W = V^G$ satisfies*

$$\boxed{W \otimes_K L \cong V.} \tag{12.17}$$

*The equivalence is effective on both objects and morphisms.*

*Proof.* This is finite Galois descent. After an $L$-basis is chosen, the semilinear action is represented by a cocycle

$$a_{\sigma\tau} = a_\sigma \sigma(a_\tau), \qquad a_\sigma \in \mathrm{GL}_n(L).$$

Nonabelian Hilbert 90 gives $B \in \mathrm{GL}_n(L)$ with

$$a_\sigma = B^{-1}\sigma(B).$$

The columns of $B^{-1}$ applied to a $K$-basis are fixed by the twisted action. They form an $n$-dimensional fixed packet, and scalar extension reconstructs $V$. An equivariant $L$-linear map restricts to a $K$-linear map on fixed packets, and scalar extension recovers it. □

A useful constructive form is obtained by choosing any matrix $C \in M_n(L)$ and setting

$$T(C) = \sum_{\sigma \in G} a_\sigma \sigma(C).$$

Then

$$a_\tau \tau(T(C)) = T(C).$$

Whenever $T(C)$ is invertible,

$$B = T(C)^{-1}$$

is a Hilbert 90 trivialization. Standard descent guarantees that such a $C$ exists.

**Definition 18.13** (Framed semilinear descent chart)**.** A framed descent chart retains an ordered $K$-basis of the fixed packet $W$. Its scalar extension gives a distinguished $L$-basis of $V$, and hence a literal cocycle matrix family.

**Proposition 18.14** (Gauge and intrinsic automorphisms remain distinct)**.** *For fixed rank $n$, nonabelian Hilbert 90 implies that every $\mathrm{GL}_n(L)$-cocycle is gauge equivalent to the trivial cocycle. The unframed descent groupoid is not contractible: its automorphism group is $\mathrm{GL}_n(K)$. After a global $K$-frame is retained, the normalized fiber becomes contractible.*

*Proof.* Hilbert 90 gives one isomorphism class. Automorphisms of the descended $K$-space are exactly $\mathrm{GL}_n(K)$. A chosen ordered basis kills those automorphisms. □

## 18.7 Projective descent and the Brauer obstruction

A projective cocycle takes values in $\mathrm{PGL}_n(L)$. Choose lifts

$$A_\sigma \in \mathrm{GL}_n(L).$$

Their cocycle failure is scalar:

$$\boxed{c(\sigma,\tau) = A_\sigma \sigma(A_\tau) A_{\sigma\tau}^{-1} \in L^\times.} \tag{12.18}$$

Changing the lifts alters $c$ by a scalar coboundary.

**Theorem 18.15** (Exact projective descent obstruction)**.** *The scalar class*

$$\boxed{[c] = \delta([\alpha]) \in H^2(G, L^\times) = \mathrm{Br}(L/K)} \tag{12.19}$$

*is independent of the chosen lifts. It vanishes exactly when the projective cocycle lifts to a linear semilinear cocycle. In that case theorem 18.12 produces a descended vector space. If it does not vanish, the descended object is a module over a central simple $K$-algebra split by $L$, not an ordinary global vector packet.*

*Proof.* Apply the connecting map in nonabelian cohomology to

$$1 \longrightarrow L^\times \longrightarrow \mathrm{GL}_n(L) \longrightarrow \mathrm{PGL}_n(L) \longrightarrow 1.$$

Vanishing is equivalent to rescaling the lifts so that the scalar defect is removed. The lifted cocycle then descends by Hilbert 90. The nonzero classes are the relative Brauer classes of central simple algebras split by $L$. □

**Example 18.16** (The quaternionic obstruction over $\mathbb{C}/\mathbb{R}$)**.** Let $G = \{1, \sigma\}$, where $\sigma$ is complex conjugation, and put

$$A_\sigma = \begin{pmatrix} 0 & 1 \\ -1 & 0 \end{pmatrix}.$$

Then

$$A_\sigma \sigma(A_\sigma) = -I.$$

The projective cocycle condition holds because $-I$ is scalar. Its boundary is represented by $-1$ in

$$\mathbb{R}^\times / N_{\mathbb{C}/\mathbb{R}}(\mathbb{C}^\times).$$

Every complex norm is positive, so $-1$ is nontrivial. The descended central simple algebra is the Hamilton quaternion algebra. Replacing $A_\sigma$ by

$$\begin{pmatrix} 0 & 1 \\ 1 & 0 \end{pmatrix}$$

gives scalar defect $+1$ and hence split vector descent.

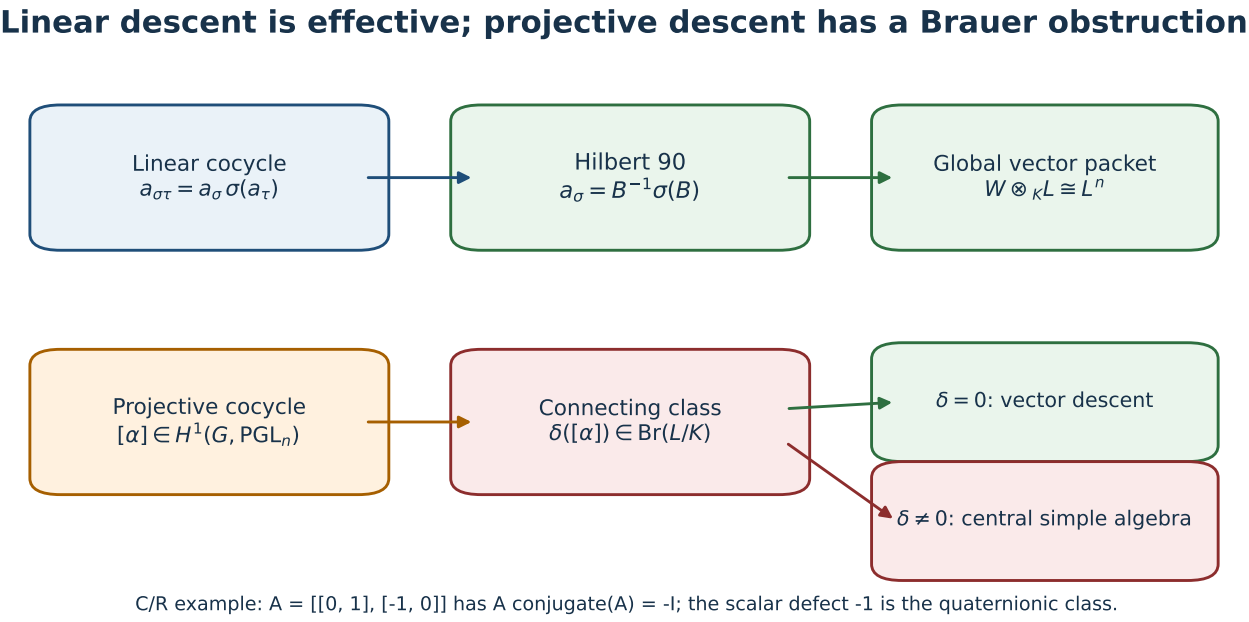



**Figure 51:** Linear cocycles are removed by Hilbert 90. Projective cocycles can satisfy every visible PGL overlap law while retaining a nonzero degree-two Brauer obstruction.

## 18.8 Finite étale and neutral Tannakian symmetry

For a connected scheme $X$ with geometric point $\bar{x}$, the fiber functor on finite étale covers identifies that category with finite continuous $\pi_1^{\text{ét}}(X, \bar{x})$-sets. Every finite fiber $S$ produces a permutation resolution on $\ell^2(S)$: coordinate projectors are indexed by points, orbit projectors by transitive components, and covering morphisms give equivariant packet transfers. The profinite fundamental group is the automorphism group of this fiber functor.

The tensor-linear version requires more structure.

**Theorem 18.17** (Neutral Tannakian reconstruction)**.** *Let $\mathcal{C}$ be a neutral Tannakian category over $k$, and let*

$$\omega : \mathcal{C} \longrightarrow \mathrm{Vect}_k$$

*be a faithful exact tensor fiber functor. Then*

$$\boxed{\mathcal{G} = \mathrm{Aut}^{\otimes}(\omega)} \tag{12.20}$$

*is an affine group scheme, and*

$$\boxed{\mathcal{C} \simeq \mathrm{Rep}_k(\mathcal{G})} \tag{12.21}$$

*as tensor categories. Declared packet idempotents and refinement maps preserved by $\omega$ become tensor-compatible concrete projector resolutions in every fiber.*

*Proof.* The group scheme and tensor equivalence are the neutral Tannakian reconstruction theorem. Additivity and exact tensor preservation transport the declared idempotent and refinement equations to the fibers. □

*Boundary* 18.18 (Faithful corner realization is not a fiber functor). A faithful additive or Hilbert-space realization can preserve packet idempotents, transfer blocks, and operator equations without preserving tensor products, duals, exact sequences, or the tensor unit. Such a realization does not by itself determine $\mathrm{Aut}^{\otimes}(\omega)$. Tannakian symmetry begins only after the faithful exact tensor gate has been verified.

**Proposition 18.19** (Finite group model of the tensor boundary)**.** *Let $G$ be finite and let $\omega : \mathrm{Rep}_k(G) \to \mathrm{Vect}_k$ be the forgetful functor. The regular representation is faithful, the action on tensor products is diagonal, the unit is fixed, and the dual action is inverse transpose. These data distinguish every $g \in G$ and realize the finite constant-group case of theorem 18.17.*

*Proof.* Left translation on the regular representation is faithful. Functoriality of the tensor product, unit, and dual actions is immediate from the representation axioms. Since different group elements act differently on the regular basis, the induced tensor automorphisms are distinct. □

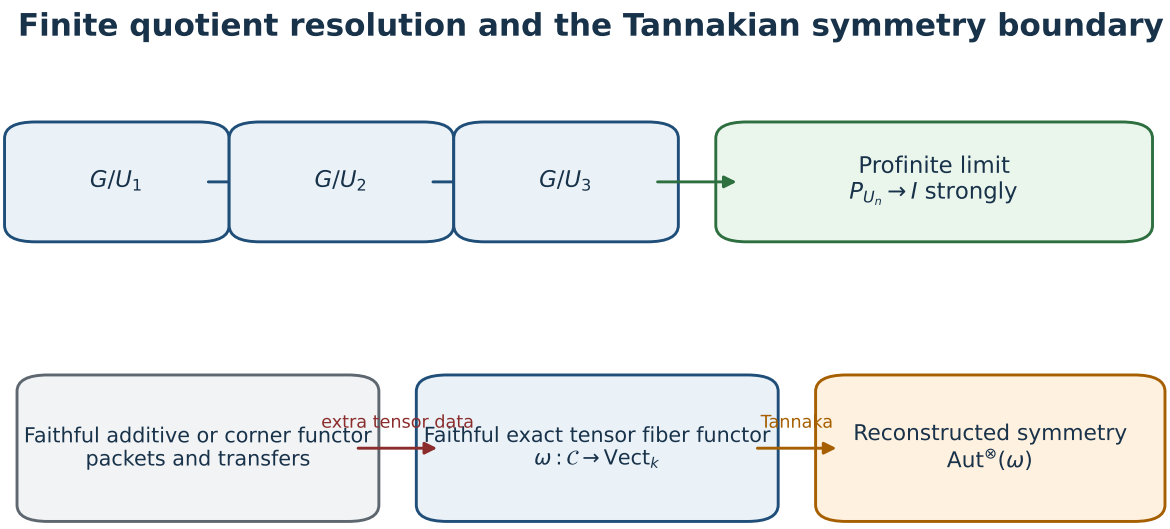



**Figure 52:** Finite quotient projectors converge strongly in profinite realizations. The lower row isolates the additional exact tensor structure required before a symmetry group scheme can be reconstructed.

## 18.9 The assembled finite Galois resolved atlas

The preceding results can be collected into one typed finite atlas. The reversible charts are:

1. subgroups $H \leq G$, fixed fields $L^H$, and faithful Reynolds projectors $P_H$;

2. finite-dimensional $K$-vector spaces and semilinear $L$-spaces with effective descent data;
3. finite étale fibers and their continuous permutation actions;
4. neutral Tannakian categories equipped with a specified faithful exact tensor fiber functor.

Directional or obstructed bridges include:

1. restriction and induction between subgroup charts, decomposed by Mackey packets;
2. passage from a nonnormal chart to its core or normal-closure envelope;
3. projectivization from linear to projective cocycles;
4. forgetting tensor structure from a Tannakian fiber functor to an additive or corner realization;
5. passage from finite quotients to a profinite inverse system.

**Theorem 18.20** (Finite semisimple Galois and Tannakian assembly)**.** *Under the hypotheses printed in this section:*

1. *the subgroup, fixed-field, and faithful fixed-projector charts form an order-reversing normalized atlas;*
2. *normal charts admit quotient compression, while nonnormal charts form conjugate projector atlases with canonical core and normal-closure envelopes;*
3. *double cosets give exact transition packets for induction and restriction;*
4. *ramification filtrations give nested fixed projectors whose weighted unresolved ranks are the Artin and Swan conductors;*
5. *continuous finite-dimensional profinite representations are detected at a finite quotient level;*
6. *linear semilinear descent is effective on objects and morphisms;*
7. *projective descent is effective exactly when its relative Brauer class vanishes;*
8. *neutral Tannakian symmetry is reconstructed exactly when a faithful exact tensor fiber functor is supplied.*

*These statements form a complete assembly theorem for the declared finite semisimple and neutral tensor strata. They do not imply effective descent for modular, wild, nonneutral, or arbitrary heterogeneous atlases.*

*Proof.* Items 1–5 are theorems 18.2, 18.4, 18.5, 18.7 and 18.9 and corollary 18.11. Item 6 is theorem 18.12. Item 7 is theorem 18.15. Item 8 is theorem 18.17. The final boundary follows because the hypotheses used by Reynolds averaging, Hilbert 90, and neutral Tannakian reconstruction are not automatic in the excluded settings. □

A complete chart record on the finite subgroup locus is

$$\mathcal{J}_{L/K}(H) = \left(H, L^H, P_H, \mathrm{Core}_G(H), \mathrm{Ncl}_G(H), \{K\backslash G/H\}_{K\leq G}\right).$$

The first three entries already classify the normalized object, while the remaining entries record its atlas position and transition structure. For a framed semilinear vector object, the descended $K$-space with its frame is complete. For a projective object, the Brauer class is an obstruction coordinate, not a complete invariant of all central simple algebras without the remaining algebra data.

## 18.10 Exact finite verification

The Galois-Tannakian atlas verifier uses exact rational group-algebra arithmetic, exact finite permutation combinatorics, and exact Gaussian-rational matrix algebra. It audits cyclic groups, $V_4$, $S_3$, $D_4$, and $A_4$; every subgroup Reynolds idempotent; subgroup inclusion and projector order; normality and centrality; core and normal closure; commuting and noncommuting subgroup pairs; double-coset partitions and the Mackey dimension law; cyclic ramification-style filtrations; explicit Hilbert 90 coboundaries over $\mathbb{C}/\mathbb{R}$; the split and quaternionic projective examples; and faithful regular tensor actions.

**Table 33:** Exact verification of the Galois-Tannakian atlas finite Galois and Tannakian models.

| Validation class | Checks |
|---|---|
| Finite subgroup and Reynolds-projector identities | 1,020 |
| Normality, core, and normal-closure identities | 192 |
| Double-coset and Mackey packet identities | 1,590 |
| Nested ramification-style projector filtrations | 39 |
| Exact Hilbert 90 cocycles over Gaussian rationals | 884 |
| Projective and Brauer obstruction examples | 44 |
| Finite faithful tensor-model checks | 7,426 |
| **Galois-Tannakian atlas exact checks** | **11,195** |
| **Failures** | **0** |

The verifier records 11,195 exact checks and no failures. Together with the preceding certified atlas program, the cumulative exact record is

$$\boxed{2{,}038{,}860}$$

checks with no recorded failures.

**Exact boundary of Galois-Tannakian atlas.** The finite subgroup/projector identities, semilinear vector descent, relative Brauer obstruction, profinite finite-level resolution, and neutral Tannakian tensor gate are established under their printed hypotheses. The block does not prove exactness of fixed points when the group order is not invertible, derived replacement of failed Reynolds projectors, integral wild descent, classification of all central simple algebras from the Brauer class alone, existence of a neutral fiber functor, or effective descent for the entire heterogeneous Komorebi atlas.

**Section result.** Finite semisimple Galois theory now appears as a fully typed resolved stratum. Subgroups, fixed fields, and faithful fixed projectors are reversible charts. Nonnormality produces conjugate atlases and mixed Mackey transition packets. Ramification is a nested detail resolution. Hilbert 90 makes linear semilinear descent effective, while the relative Brauer class is the exact obstruction to projective vector descent. Profinite quotient charts reconstruct continuous finite-dimensional symmetry, and a faithful exact tensor fiber functor crosses the separate Tannakian boundary to reconstruct an affine group scheme. This closes the declared finite Galois and neutral tensor stratum, not modular, wild, nonneutral, or unrestricted global descent.

# Part III

# Certified global synthesis and scope

## 19 Global invariant descent on the certified finite atlas

Global synthesis atlas performs the assembly step requested after the native stratum invariants. The preceding sections do not justify one unrestricted equivalence among all eight broad strata. They do, however, supply several finite connected systems of normalized charts for which the semantic object, overlap categories, bridge directions, information loss, coherence, and local completeness are explicit. This section freezes those systems into one authoritative certified atlas, constructs the invariant comparison maps, verifies their higher coherence, and proves the strongest global completeness theorem supported by the assembled results.

The global object in this section is deliberately a finite disjoint union of connected semantic components. Each component contains nontrivial reversible bridges across different kinds of presentation. The component tag is retained as part of the invariant. No bridge is invented between two components merely because their formulas use similar words or symbols. In particular, the functional-Mahler coefficient component and the continuous Newton–Mahler interpolation component remain distinct even though both belong to the broad local stratum.

### 19.1 The authoritative bridge matrix

Write

$$\mathsf{E}, \quad \mathsf{FF}, \quad \mathsf{D}, \quad \mathsf{P}, \quad \varnothing$$

for an equivalence on a named normalized overlap, a fully faithful inclusion, an information-losing directional functor, a partial or hypothesis-dependent bridge, and the absence of a certified broad bridge, respectively. The matrix below records only relations already established in the preceding sections or in the audited source concordance. A symbol carrying a subscript refers to the named overlap rather than to the whole broad stratum.

**Table 34:** Authoritative broad-stratum bridge matrix for the certified global synthesis atlas. Every decorated equivalence is restricted to the named normalized overlap; the undecorated broad categories are not thereby identified.

| Source \ target | LIN | HOL | DIG | ALG | TREE | PROD | LOC | GAL |
|---|---|---|---|---|---|---|---|---|
| LIN | E | FF | $E_{per}$ | – | – | – | $E_{per}$ | – |
| HOL | P | E | – | $E_{Fuss}$ / P | $E_{Fuss}$ / P | – | – | – |
| DIG | $E_{per}$ | P | E | P | – | – | $E_{rm}$ | – |
| ALG | – | $E_{Fuss}$ / D | P | E | $E_{Fuss}$ / P | – | – | – |
| TREE | – | $E_{Fuss}$ / D | – | $E_{Fuss}$ / D | E | – | – | – |
| PROD | D | – | – | – | – | E | P | – |
| LOC | $E_{per}$ | – | $E_{rm}$ | – | – | P | E | – |
| GAL | – | – | – | – | – | – | – | E |

**Legend.** E: equivalence; FF: fully faithful inclusion; D: information-losing directional functor; P: partial, constructor-dependent, or certificate-dependent bridge; –: no certified bridge. The subscripts per, rm, and Fuss denote the unit-periodic, rational functional-Mahler, and marked weighted Fuss overlaps. A cell of the form $E_{Fuss}$ / D means equivalence on the marked Fuss slice and directional loss on the ambient bridge. Functional-Mahler coefficient equations and Newton–Mahler interpolation remain distinct despite sharing the LOC row.

The matrix has three immediate consequences.

1. The reversible core is strictly smaller than the directed transformation category.
2. A bridge may become an equivalence after restricting to a normalized overlap without becoming invertible on the ambient stratum.
3. Empty cells are mathematical data. They prevent later arguments from silently transporting an invariant through an uncertified route.

The entries $E_{\mathrm{per}}$, $E_{\mathrm{rm}}$, and $E_{\mathrm{mark}}$ refer, respectively, to the unit-periodic overlap, the rational functional-Mahler overlap, and the marked polynomial fixed-point overlap. In particular, the functional-Mahler and Newton–Mahler languages remain separate outside their explicitly declared interfaces, and faithful corner realization remains separate from neutral Tannakian reconstruction.

The full object-level bridge ledger, including every normalized source, target, overlap, invariant comparison, and loss or gate, is retained as a machine-generated source artifact. The printed matrix and the component table below contain the proof-relevant summary; a relation absent from the ledger is not used in the descent nerve.

## 19.2 Certified connected components

**Definition 19.1** (Certified Global synthesis atlas atlas)**.** Fix a prime $p$, a characteristic-zero field $K$, and a finite Galois extension $L/K$ for the Galois component. The certified atlas $\mathfrak{A}_{13}$ is the finite coproduct of the following five connected profiled atlases.

(C1) $\mathfrak{A}_{\mathrm{DRLM},p}$, the fixed-prime digital–regular component with rational functional-Mahler and periodic linear subcharts;

(C2) $\mathfrak{A}_{\mathrm{Loc},p}$, the continuous Newton–Mahler and complete clopen-branch component;

(C3) $\mathfrak{A}_{\mathrm{Fuss}}$, the marked Fuss–Catalan nonlinear–algebraic–holonomic component;

(C4) $\mathfrak{A}_{\mathrm{EM}}$, the fixed-Euler-basis and prime-uniform multiplicative component;

(C5) $\mathfrak{A}_{\mathrm{Gal},L/K}$, the finite semisimple Galois component for the fixed extension $L/K$.

The reversible arrows are exactly the normalized equivalences printed below. Directional constructions, reductions, forgetful maps, and obstructed lifts are attached as satellites but do not enter the maximal subgroupoid used for invariant descent.

**Table 35:** Certified connected components of the Global synthesis atlas atlas.

| Component | Semantic domain and normalized charts | Complete coordinate and reversible overlap | Directional satellites or exact boundary |
|---|---|---|---|
| DRLM | fixed-prime regular sequences; canonical section module, strict shortlex record, and minimal DFAO; rational-mask/Cartier and periodic linear subcharts | strict shortlex pointed digit-linear record, refined on the rational-mask and unit-periodic full replete subcategories | integral reductions and Newton–Mahler interpolation are directional; many automatic sequences have no rational mask |
| LOC | continuous $\mathbb{Z}_p$-valued functions; Newton–Mahler coefficients, complete clopen branch packets, and affine branch coordinates | canonical Mahler coefficient sequence; complete branch analysis and synthesis at each declared depth | functional-Mahler equations require a separately declared coefficient lift and interpolation constructor |
| Fuss | marked $U = z + \alpha U^q$ tree system, selected algebraic branch, and compressed P-recursive coefficient chart | parameter pair $(q, \alpha)$ with its support and singularity-orbit package | forgetting the branch mark or generator grammar is information-losing |
| EM | fixed-basis Euler exponents, divisor ghosts, integral unit series, and prime-uniform multiplicative local factors | Euler exponent sequence on the fixed-basis, prime-uniform essential image | arbitrary product grammars and nonuniform prime-local fields remain outside the reversible overlap |
| Gal | subgroup, fixed field, and faithful Reynolds projector for one fixed finite Galois extension | actual subgroup $H \leq G$ with functorial core, normal-closure, and double-coset data | projective Brauer obstruction, modular or wild failure, and the tensor-fiber gate remain separately typed |

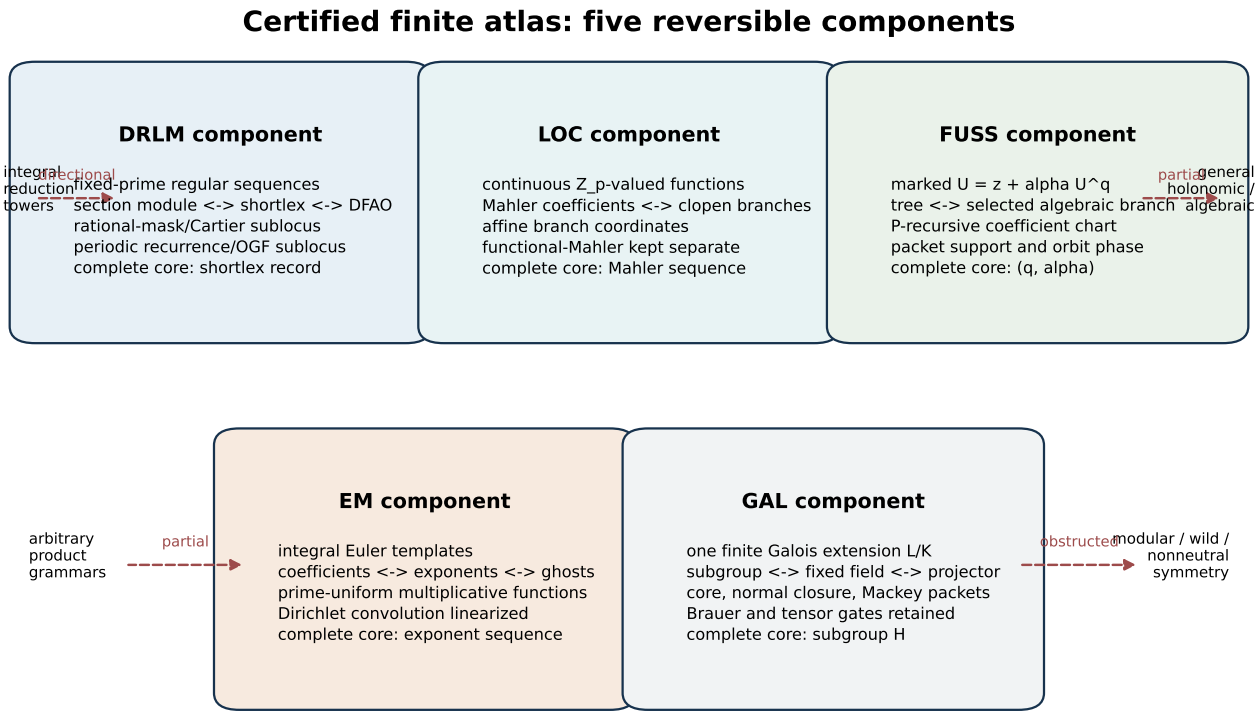



**Figure 53:** The certified finite atlas. Each box is a nontrivial connected system of normalized charts. Dashed external arrows are directional, partial, or obstructed satellites and are not promoted to equivalences.

The semantic category of the total atlas is

$$\mathcal{O}_{13} = \mathcal{O}_{\mathrm{DRLM}} \sqcup \mathcal{O}_{\mathrm{Loc}} \sqcup \mathcal{O}_{\mathrm{Fuss}} \sqcup \mathcal{O}_{\mathrm{EM}} \sqcup \mathcal{O}_{\mathrm{Gal}}.$$

The coproduct symbol is literal. It does not assert that a finite-field regular sequence, a continuous $p$-adic function, a characteristic-zero marked tree branch, an integral Euler template, and a finite Galois subgroup are objects of one untyped category. The tag records which semantic doctrine is in force.

## 19.3 Normalizer-induced higher coherence

Every connected component in definition 19.1 has a canonical semantic normalizer. For a chart $\mathcal{C}_{\lambda,a}$ in component $\lambda$, write

$$N_{\lambda,a} : \mathcal{C}_{\lambda,a} \longrightarrow \mathcal{O}_{\lambda}$$

for the semantic normalization functor and choose its canonical inverse chart

$$Q_{\lambda,a} : \mathcal{O}_{\lambda} \longrightarrow \mathcal{C}_{\lambda,a}.$$

The certified bridge from chart $a$ to chart $b$ is

$$\Phi_{ab} = Q_{\lambda,b} N_{\lambda,a}.$$

**Theorem 19.2** (Normalizer-induced coherence)**.** *Assume that every normalized fiber of $N_{\lambda,a}$ is contractible. Then the comparison isomorphism*

$$\eta_{abc} : \Phi_{bc}\Phi_{ab} \Longrightarrow \Phi_{ac}$$

*is unique. Every triple-overlap diagram commutes, every quadruple-overlap coherence equation holds, and the composite around every finite bridge cycle is the identity transformation of the normalized chart.*

*Proof.* Both $\Phi_{bc}\Phi_{ab}(X)$ and $\Phi_{ac}(X)$ are normalized presentations of the same semantic object $N_{\lambda,a}(X)$. Contractibility of the normalized fiber gives a unique isomorphism between them. Any two composites occurring in a coherence diagram are isomorphisms between the same two normalized presentations, so uniqueness makes them equal. The cycle statement follows by applying the same argument to the starting chart and itself. □

This theorem is not a substitute for constructing the normalizer. It applies here because the preceding sections have already supplied unique reduced masks, reachable-observable Cartier modules, minimal automata, canonical section modules, marked fixed-point systems, selected algebraic branches, fixed Euler exponents, prime-power local factors, fixed subgroups, fixed fields, and faithful Reynolds projectors on the declared domains.

## 19.4 Invariant descent theorem

For every chart $\mathcal{C}_{\lambda,a}$, let

$$I_{\lambda,a} : \mathcal{C}_{\lambda,a} \longrightarrow \mathcal{V}_{\lambda,a}$$

be its native normalized invariant. A bridge comparison is a natural isomorphism

$$\kappa_{ab} : J_{ab} I_{\lambda,a} \Longrightarrow I_{\lambda,b} \Phi_{ab},$$

where $J_{ab}$ transports invariant coordinates between their chart-specific target categories.

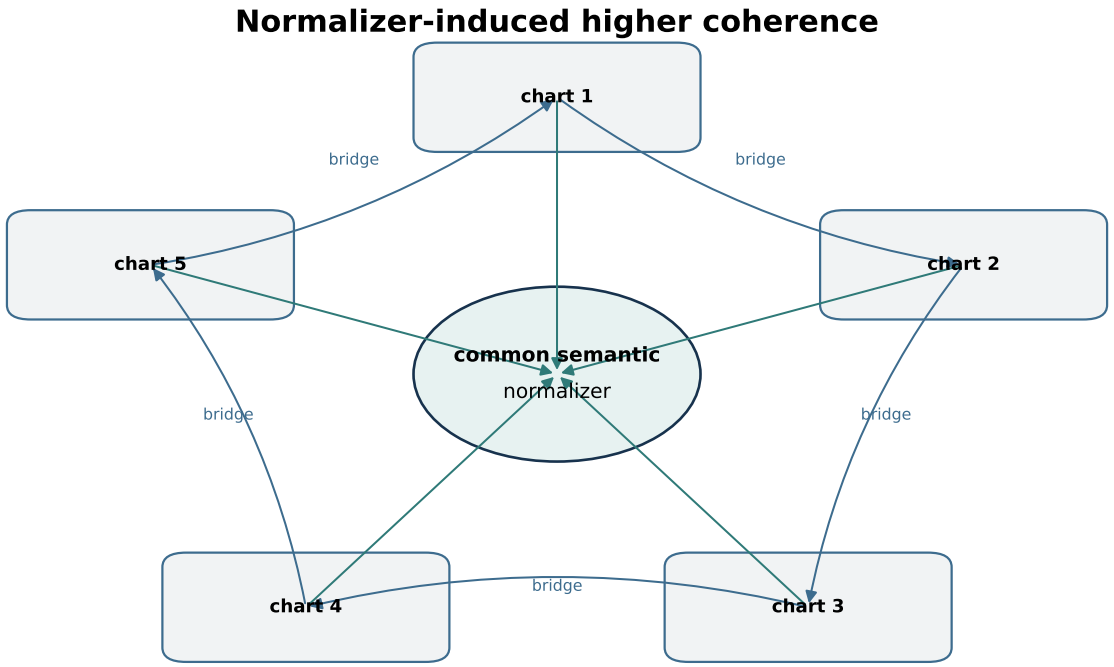



**Figure 54:** Every reversible chart in one certified component normalizes to the same semantic object. The unique normalized comparison forces all finite bridge cycles to commute.

**Definition 19.3** (Coherent invariant family)**.** The family $(I_{\lambda,a}, \kappa_{ab})$ is coherent when the two induced comparison maps from $a$ to $c$ agree on every triple overlap and the corresponding quadruple-overlap equation holds.

**Theorem 19.4** (Certified finite invariant descent)**.** *Let $\mathfrak{A}_{13}$ be the atlas of definition 19.1. Suppose that, in every connected component:*

1. *the local invariant is complete on every normalized chart;*
2. *the bridge comparisons are coherent;*
3. *invariant-compatible local isomorphisms satisfy effective descent.*

*Then the local invariants induce a functor*

$$\mathcal{I}_{13} : \mathrm{Desc}(\mathfrak{A}_{13}) \longrightarrow \mathrm{Desc}(\mathfrak{V}_{13})$$

*that reflects isomorphisms. If each semantic component is discrete, equality of descended invariants is equivalent to equality of the represented semantic objects.*

*Proof.* The local comparison maps form a pseudonatural invariant family, so theorem 6.3 gives the descended functor. Equality or isomorphism of the descended invariant gives compatible local invariant matches. Local completeness supplies local object isomorphisms. Effective isomorphism descent glues those local isomorphisms to an isomorphism in the descent category. On a discrete semantic component, every isomorphism is equality. □

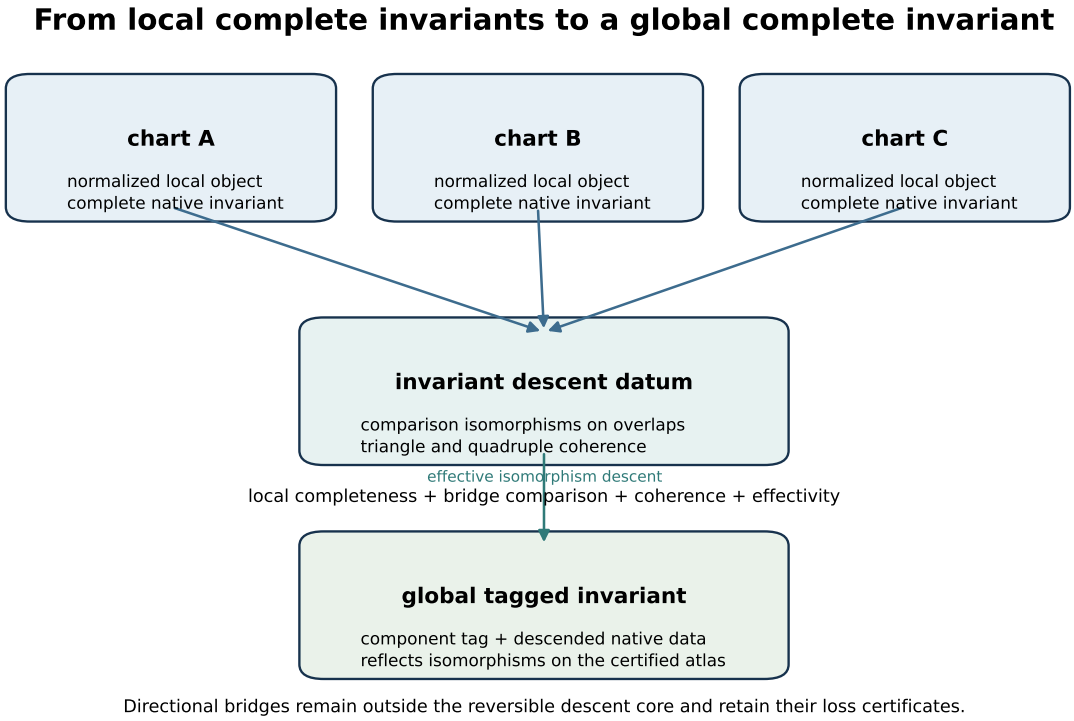



**Figure 55:** The global invariant theorem has four separate requirements. Local completeness alone is insufficient without comparison maps, higher coherence, and effective descent of the resulting isomorphisms.

## 19.5 Digital–regular–linear–functional-Mahler component

Fix the prime $p$ and let

$$\mathcal{O}_{\mathrm{DRLM}} = \mathbf{Reg}_p(\mathbb{F}_p)$$

be the discrete semantic category of $p$-regular sequences over $\mathbb{F}_p$. By the finite-field fixed-radix theorem, every object is also $p$-automatic. Its globally defined normalized charts are the canonical section module, the strict shortlex pointed digit-linear record, and the minimal least-significant-digit-first $p$-DFAO.

Two full replete subcategories carry additional charts.

1. On the rational-mask locus $\mathbf{RMah}_p^{\times}$, the reduced functional-Mahler mask and the minimal reachable-observable Cartier module are equivalent to the digital charts.
2. On the unit purely periodic locus, the minimal recurrence, reduced rational OGF, minimal finite linear state, primitive period word, and rational-mask chart are all equivalent.

For $a \in \mathcal{O}_{\mathrm{DRLM}}$, define

$$\mathcal{J}_{\mathrm{DRLM},p}(a) = \left(\mathsf{SL}_{p,\mathbb{F}_p}(a), \mathcal{P}_{\mathrm{rm}}(a), \mathcal{P}_{\mathrm{per}}(a)\right),$$

where $\mathsf{SL}_{p,\mathbb{F}_p}(a)$ is the strict shortlex record, $\mathcal{P}_{\mathrm{rm}}(a)$ is empty off the rational-mask locus and otherwise contains the reduced mask, Cartier module, collapse obstruction, and minimal automaton coordinates, and $\mathcal{P}_{\mathrm{per}}(a)$ is empty off the purely periodic locus and otherwise contains the primitive period word, exact period, minimal recurrence, reduced OGF, and periodic packet profile.

**Theorem 19.5** (Digital–regular–linear–Mahler comparison theorem)**.** *The invariant $\mathcal{J}_{\mathrm{DRLM},p}$ is preserved by every reversible bridge in $\mathfrak{A}_{\mathrm{DRLM},p}$. Its comparison cells satisfy all higher coherence equations. The strict shortlex*

*coordinate reconstructs the represented regular sequence, so the descended invariant is complete on* $\mathbf{Reg}_p(\mathbb{F}_p)$. *The mask and periodic packages are compatible exact refinements on their respective subloci.*

*Proof.* The canonical section module, strict shortlex record, and minimal orbit automaton normalize to the same coefficient sequence by the Fixed-radix regular atlas effective-descent theorem. On the rational-mask locus, fixed-denominator Cartier intertwining identifies the reachable numerator span with the canonical section module and the reachable numerator set with the minimal automaton states. On the periodic locus, the recurrence, rational, state, automaton, and mask charts normalize to the same primitive coefficient word. Every comparison therefore factors through the same semantic normalizer, and theorem 19.2 applies. Completeness follows from the strict shortlex reconstruction formula. □

**Table 36:** Representative cross-stratum invariant comparisons.

| Example | Period | Recurrence order | Regular rank | DFAO states | Mask compiler degree |
|---|---|---|---|---|---|
| $\mathbb{F}_2$/ word 10 | 2 | 2 | 2 | 3 | 2 |
| $\mathbb{F}_2$/ word 110 | 3 | 2 | 2 | 3 | 2 |
| $\mathbb{F}_3$/ word 12 | 2 | 1 | 1 | 2 | 1 |

The table gives representative objects for which recurrence order, regular rank, automaton size, and mask-compiler dimension are different coordinates of the same normalized semantic sequence. Equality of one displayed scalar alone is not a complete invariant; the complete records are the chart objects described above.

The inclusions of the rational-mask and periodic loci are not essentially surjective. Over a finite field every regular sequence is automatic, but many automatic sequences have no rational canonical mask, and many rational-mask sequences are not periodic. The optional fields in $\mathcal{J}_{\mathrm{DRLM},p}$ record these exact domain boundaries rather than forcing one chart to exist everywhere.

## 19.6 Continuous Newton–Mahler component

Let

$$\mathcal{O}_{\mathrm{Loc}} = C(\mathbb{Z}_p, \mathbb{Z}_p)$$

with equality morphisms. Its canonical coordinate is the Mahler sequence

$$\mathcal{M}_p(f) = (c_r(f))_{r\geq 0}, \qquad c_r(f) = \Delta^r f(0), \qquad c_r(f) \longrightarrow 0.$$

At every declared depth $p^a$, the complete clopen branch packet

$$\big(f(p^a q + s)\big)_{0\leq s<p^a}$$

and the corresponding branchwise Mahler coefficients are reversible by explicit piecewise synthesis. Affine branch kernels and mixed-radix refinements are comparison charts of the same semantic function.

**Theorem 19.6** (Continuous local invariant comparison)**.** *The Mahler coefficient sequence*

$$\mathcal{J}_{\mathrm{Loc},p}(f) = (c_r(f))_{r\geq 0}$$

*is a complete invariant of* $\mathfrak{A}_{\mathrm{Loc},p}$. *Complete branch packets, branchwise Mahler coordinates, affine coefficient kernels, and nested refinements admit coherent comparison maps to* $\mathcal{J}_{\mathrm{Loc},p}$.

*Proof.* Mahler analysis and synthesis are mutually inverse on $C(\mathbb{Z}_p, \mathbb{Z}_p)$. Complete clopen analysis and piecewise synthesis are mutually inverse at each depth, and the nested branch law is strict. Conjugating those maps by Mahler analysis gives the affine coefficient comparisons, whose mixed-radix composition was proved in Local Mahler-polyphase atlas. All normalized charts therefore return the same function and the same Mahler sequence, so theorem 19.2 gives higher coherence. □

Functional-Mahler equations for coefficient series are not included in this component. A finite-state or functional-Mahler object enters the Newton–Mahler component only through a separately declared lift and interpolation constructor carrying its own precision and information-loss certificate.

## 19.7 A genuine nonlinear–algebraic–holonomic overlap

Let $K$ be a characteristic-zero field. For an integer $q \geq 2$ and $\alpha \in K^\times$, let

$$U_{q,\alpha}(z) \in zK[[z]]$$

be the unique selected branch satisfying

$$U = z + \alpha U^q. \tag{50}$$

The derivative of

$$P_{q,\alpha}(z, Y) = Y - z - \alpha Y^q$$

with respect to $Y$ is one at $(0, 0)$, so the branch is simple and selected by $U(0) = 0$.

Put

$$x = z^{q-1}, \qquad U_{q,\alpha}(z) = zC_{q,\alpha}(x).$$

Then

$$C = 1 + \alpha x C^q. \tag{51}$$

Lagrange inversion gives

$$[x^n]C_{q,\alpha}(x) = c_n(q, \alpha) = \frac{\alpha^n}{(q-1)n+1}\binom{qn}{n}. \tag{52}$$

Define

$$A_q(n) = (n+1)\prod_{r=2}^{q}((q-1)n + r),$$

$$B_q(n) = \prod_{r=1}^{q}(qn + r).$$

Then the coefficient sequence satisfies the first-order polynomial recurrence

$$\boxed{A_q(n)c_{n+1} = \alpha B_q(n)c_n.} \tag{53}$$

After dividing the polynomial gcd of $A_q$ and $B_q$, this is the normalized first-order tail recurrence with initial value $c_0 = 1$.

**Theorem 19.7** (Fuss–Catalan three-stratum equivalence)**.** *The following normalized marked presentations determine one another exactly:*

1. *the polynomial tree system $U = z + \alpha U^q$;*

2. *the selected algebraic branch* $(P_{q,\alpha}, U(0) = 0)$;
3. *the compressed P-recursive coefficient chart* $(\text{Equation (53)}, c_0 = 1)$ *together with the support embedding* $U(z) = zC(z^{q-1})$.

*Every normalized fiber is contractible. All triangle comparisons return the same parameter pair* $(q, \alpha)$.

*Proof.* The marked tree equation is the selected algebraic equation. Simplicity at the origin gives its unique formal branch. Substitution $U = zC(z^{q-1})$ gives Equation (51). Lagrange inversion gives Equation (52), and taking the ratio of consecutive coefficients gives Equation (53). Conversely, the recurrence and initial value reconstruct $C$, the support embedding reconstructs $U$, and the reconstructed series satisfies the selected algebraic equation. A normalized automorphism fixes $q$, $\alpha$, and the unique branch, hence is the identity. □

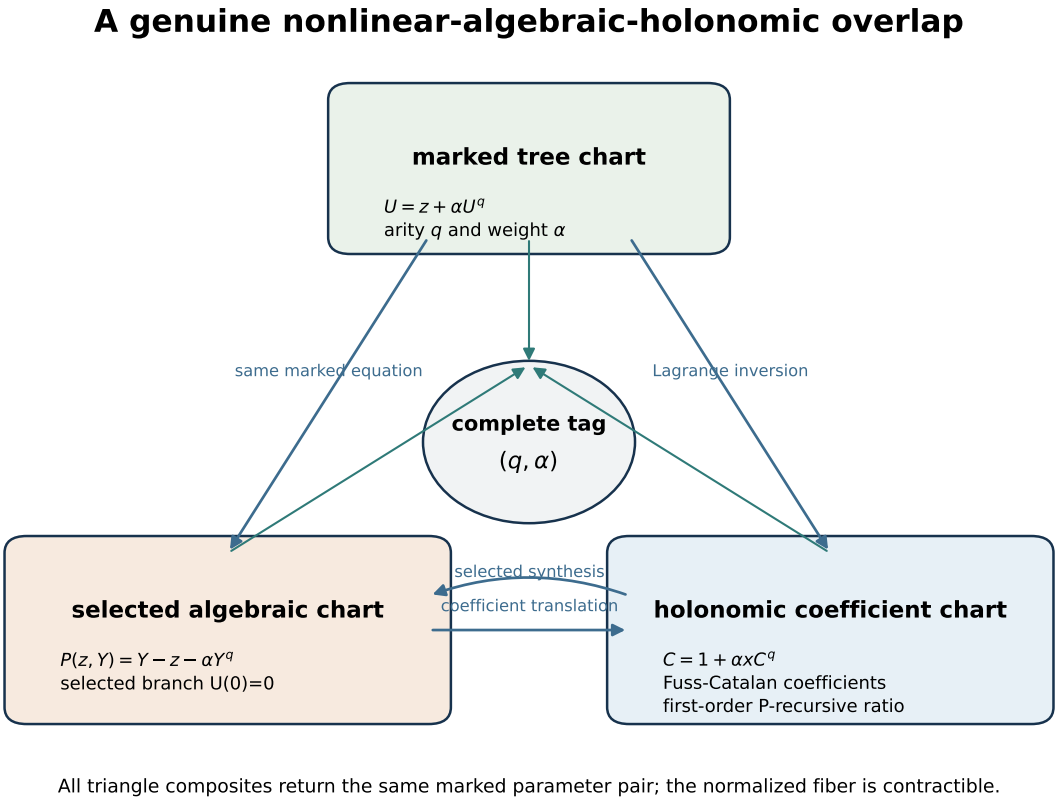



**Figure 56:** The marked Fuss–Catalan family gives a genuine overlap among the nonlinear tree, selected algebraic, and holonomic recurrence strata. Every path returns the same marked pair $(q, \alpha)$.

The tree arity period is $q - 1$. For packet modulus $N$, set

$$g_N = \gcd(N, q - 1).$$

The nonzero coefficient addresses of $U_{q,\alpha}$ are exactly

$$j \equiv 1 \pmod{g_N},$$

and the complete dominant singularity orbit has size

$$\frac{q-1}{g_N}$$

under the positive analytic hypotheses of theorem 17.15. These packet signatures agree in the tree and algebraic charts because both are computed from the same selected branch.

Define

$$\mathcal{J}_{\mathrm{Fuss}}(q,\alpha) = \left( q, \alpha, P_{q,\alpha}, \{c_n(q,\alpha)\}_{n\geq 0}, \{g_N\}_{N\geq 1}, \left\{ \frac{q-1}{g_N} \right\}_{N\geq 1} \right).$$

**Corollary 19.8** (Complete cross-stratum invariant on the marked Fuss family)**.** *The nonlinear, algebraic, holonomic, packet-support, and dominant-orbit invariants admit coherent comparison maps to $\mathcal{J}_{\mathrm{Fuss}}$. The package is complete on the declared marked family.*

*Proof.* Coherence follows from theorems 19.2 and 19.7. The first two entries reconstruct the marked fixed-point equation and therefore its unique selected branch. □

**Table 37:** Named weighted q-ary examples in the cross-stratum atlas.

| $q$ | $\lambda$ | Support period | First supported coefficients | Active addresses at $N=6$ | Packet-orbit size |
|---|---|---|---|---|---|
| 2 | 1 | 1 | $(1,1,2,5,\dots)$ | $\{0,1,2,3,4,5\}$ | 1 |
| 3 | 2 | 2 | $(1,2,12,96,\dots)$ | $\{1,3,5\}$ | 1 |
| 4 | $-1$ | 3 | $(1,-1,4,-22,\dots)$ | $\{1,4\}$ | 1 |
| 5 | $1/2$ | 4 | $(1,1/2,5/4,35/8,\dots)$ | $\{1,3,5\}$ | 2 |

The examples show that the finite invariant retains the weight parameter as well as the arity. Support period alone recovers only $q-1$; the coefficient $[z^q]U = \alpha$ supplies the second coordinate.

This is not a classification of arbitrary algebraic branches, arbitrary P-recursive sequences, or unmarked nonlinear fixed points. It is the first explicit complete invariant on a connected overlap of those three strata.

## 19.8 Euler–multiplicative component

Let

$$A_b(z) = \prod_{m\geq 1} (1-z^m)^{-b_m}$$

be an integral unit series in the fixed Euler basis, and let

$$c_n = \sum_{d\mid n} d\, b_d$$

be its divisor-ghost sequence. Define the prime-uniform multiplicative function

$$f_b(n) = \prod_{p^e \| n} [z^e] A_b(z).$$

Every prime has the same local factor $A_b(T)$. By theorems 13.4 and 13.23, the coefficient, exponent, ghost, and prime-uniform multiplicative charts are reversible on this declared locus.

**Theorem 19.9** (Euler–multiplicative invariant comparison)**.** *The exponent sequence*

$$\mathcal{J}_{\mathrm{EM}}(A_b) = b$$

*is a complete invariant of the certified Euler–multiplicative component. In every chart it is recovered by the same Möbius formula*

$$b_n = \frac{1}{n}\sum_{d\mid n}\mu(n/d)c_d,$$

*and Dirichlet convolution corresponds to exponent addition.*

*Proof.* Unique Euler factorization reconstructs $A_b$ from $b$. Prime-power reconstruction then reconstructs $f_b$. The logarithmic-derivative identity gives $c$, and Möbius inversion recovers $b$. Every bridge therefore factors through the same exponent normalizer, so higher coherence follows from theorem 19.2. □

The theorem remains confined to the fixed Euler basis and the prime-uniform multiplicative essential image. It does not identify arbitrary Cauchy-product grammars with arbitrary Dirichlet-convolution systems.

## 19.9 Finite Galois component

Fix a finite Galois extension $L/K$ in the semisimple setting. For each subgroup $H \le G$, define

$$\mathcal{J}_{\mathrm{Gal}}(H) = \left(H, L^H, P_H, \mathrm{Core}_G(H), \mathrm{Ncl}_G(H), \{J\backslash G/H\}_{J\le G}\right).$$

**Theorem 19.10** (Finite Galois invariant comparison)**.** *The subgroup, fixed-field, and faithful Reynolds-projector charts have coherent comparison maps to $\mathcal{J}_{\mathrm{Gal}}$. The invariant is complete on the normalized subgroup atlas for the fixed extension $L/K$.*

*Proof.* The first three entries determine one another by theorem 18.2. Core, normal closure, and double-coset packets are functorial constructions from the subgroup. The subgroup coordinate itself is complete, and the strict subgroup normalizer forces coherence. □

The Brauer class and Tannakian group scheme are not added to this complete subgroup invariant as if they were automatic coordinates. They belong to separately typed projective and tensor extensions whose hypotheses and obstructions were stated in Galois-Tannakian atlas.

## 19.10 The global tagged invariant

Let

$$\Lambda_{13} = \{\mathrm{DRLM}, \mathrm{Loc}, \mathrm{Fuss}, \mathrm{EM}, \mathrm{Gal}\}$$

be the component-tag set. Define

$$\mathcal{J}_{13}(X) = \big(\lambda(X), \mathcal{J}_{\lambda(X)}(X)\big).$$

**Theorem 19.11** (Certified global completeness theorem)**.** *The invariant $\mathcal{J}_{13}$ descends across every reversible bridge in $\mathfrak{A}_{13}$ and is complete on*

$$\mathcal{O}_{13} = \mathcal{O}_{\mathrm{DRLM}} \sqcup \mathcal{O}_{\mathrm{Loc}} \sqcup \mathcal{O}_{\mathrm{Fuss}} \sqcup \mathcal{O}_{\mathrm{EM}} \sqcup \mathcal{O}_{\mathrm{Gal}}.$$

*More precisely,*

$$\boxed{\mathcal{J}_{13}(X) = \mathcal{J}_{13}(Y) \quad \Longleftrightarrow \quad X = Y}$$

*inside the declared discrete semantic category. The associated invariant functor reflects isomorphisms on the descent category.*

*Proof.* Within each component, completeness is theorems 19.5, 19.6, 19.9 and 19.10 and corollary 19.8. Their comparison maps are coherent by theorem 19.2. The component tag prevents an object in one semantic doctrine from being identified with an object in another. Apply theorem 19.4 componentwise and then take the finite coproduct. □

*Remark* 19.12 (What is genuinely global). The theorem is not the tautology that every object is classified by itself. Each component invariant is computed in one native chart and transported through several nonidentical presentation categories. The global assertion is that these transported coordinates agree coherently and classify the descent object. The coproduct tag is nevertheless essential: the current Library does not provide reversible bridges joining all five components.

## 19.11 Directional satellites and exact loss records

The certified reversible core is surrounded by directional bridges that remain useful for theorem transport and computation. Their failure to enter $\mathcal{J}_{13}$ is controlled by explicit loss data.

**Table 38:** Directional satellites of the certified global invariant atlas.

| Directional bridge | Retained structure | Exact loss or obstruction |
|---|---|---|
| Integral regular lattice → residue section module | digit transitions and residue semantics | Smith–Tor ghost kernel and missing quotient |
| General regular sequence ⇢ rational mask | coefficient semantics on the essential image | rational-mask existence and collapse obstruction |
| Algebraic branch → holonomic annihilator | D-finite coefficient semantics | selected branch and minimal polynomial may be forgotten |
| Marked nonlinear system → semantic fixed point | the represented fixed point | generator labels, arities, and tree grammar may be forgotten |
| Finite-state dynamics → Newton–Mahler chart | congruence branch values and precision ladder | depends on a chosen lift and principal-unit hypothesis |
| Projective Galois cocycle ⇢ linear descent | projective action | relative Brauer class |
| Faithful corner realization ⇢ Tannakian symmetry | additive packet and operator equations | exact tensor, dual, unit, and fiber-functor data are absent |

**Proposition 19.13** (No completeness transport through an unreflected directional bridge)**.** *Let $T : \mathcal{C} \to \mathcal{D}$ be a directional bridge. A complete invariant on $\mathcal{D}$ pulls back to a complete invariant on $\mathcal{C}$ only if $T$ reflects isomorphisms on the declared source subcategory. In particular, any nontrivial object-collapse relation or obstruction fiber prevents automatic completeness transport.*

*Proof.* If $T$ does not reflect isomorphisms, there exist nonisomorphic $X, Y$ with $T(X) \cong T(Y)$. Every invariant depending only on the target object then takes the same value on $X$ and $Y$, so its pullback cannot be complete. □

## 19.12 Exact finite verification

Two complementary exact suites audit Global synthesis atlas. The first authenticates the frozen preceding verification records and checks the broad bridge matrix, periodic and product–multiplicative overlap replays, directional-loss controls, finite Čech holonomy models, and the five completeness gates. The second checks the weighted $q$-ary tree–algebraic–holonomic overlap, its coefficient and packet equations, parameter recovery, detailed bridge ledger, and tagged component separation.

**Table 39:** Exact verification of the Global synthesis atlas invariant-descent and weighted q-ary cross-stratum models.

| Validation class | Checks |
|---|---|
| Bridge-matrix structural checks | 172 |
| Weighted q-ary coefficient identities | 1,856 |
| Exact support-period identities | 8,192 |
| Formal fixed-point identities | 8,192 |
| Minimal-polynomial relation checks | 8,192 |
| Finite parameter recovery | 128 |
| Tree/algebraic/holonomic comparison paths | 64 |
| Supported first-order recurrence checks | 1,792 |
| Packet support and orbit-phase checks | 2,112 |
| Exact packet synthesis checks | 44,352 |
| Address-carry packet equations | 44,352 |
| Tagged component-separation checks | 49 |
| **Global synthesis exact checks** | **119,453** |
| **Failures** | **0** |

**Table 40:** Exact verification of the Global synthesis atlas global-invariant and cross-stratum synthesis layer.

| Validation suite | Exact assertions |
|---|---|
| Bridge matrix, overlap replay, directional-loss, and finite Čech suite | 154,209 |
| Weighted $q$-ary tree–algebraic–holonomic and tagged-invariant suite | 119,453 |
| Regression/authentication assertions already represented in the certified native-stratum program | 39,846 |
| **New Global synthesis atlas comparison and coherence assertions** | **233,816** |
| All assertions executed by the two Global synthesis atlas suites | 273,662 |
| Failures | 0 |

The two suites execute 273, 662 exact assertions with no failures. Of these, 39, 846 authenticate or replay assertions already represented in the preceding cumulative record. The global synthesis therefore contributes 233, 816 nonduplicative comparison, coherence, packet, and loss-control assertions. The blockwise cumulative record is

$$\boxed{2,272,676}$$

exact assertions with no recorded failures. Counting every regression assertion executed during the Global synthesis atlas replay gives 2, 312, 522 total executed assertions. Neither number is a count of independent theorems.

The bridge-synthesis suite replays primitive unit-periodic words over finite prime fields, compares their recurrence, OGF, automaton, section-module, and functional-Mahler coordinates, verifies the prime-

uniform Euler–multiplicative overlap, and tests finite nontrivial Čech cycle models. The weighted $q$-ary suite checks the fixed-point identity, Lagrange coefficients, first-order P-recursive recurrence, support phases, exact packet synthesis, address-carry equations, and all triangle normalizers over a declared finite parameter grid. Both machine-readable records are included in the source package.

**Exact boundary of Global synthesis atlas.** The global invariant theorem is proved for the five-component certified finite atlas in definition 19.1. It does not assert a complete invariant for every object in the eight broad strata, a reversible bridge between the five semantic components, effective descent for every directional satellite, cross-radix or all-ring normalization, modular or wild Galois effectivity, nonneutral Tannakian reconstruction, or classification of unmarked general holonomic, algebraic, and nonlinear systems.

**Section result.** The manuscript now contains an authoritative broad-stratum bridge matrix, a finite certified atlas with five nontrivial connected components, explicit invariant comparison maps, a normalizer-induced higher-coherence theorem, and a complete tagged global invariant on the declared semantic union. The new Fuss–Catalan triangle gives a genuine nonlinear–algebraic–holonomic overlap. The digital–regular–functional-Mahler, continuous Newton–Mahler, Euler–multiplicative, and finite Galois components consolidate the exact cross-presentation results of the preceding stratum sections without conflating the two Mahler theories. Directional bridges remain outside the reversible core and retain their precise loss or obstruction records. This closes the finite global-invariant milestone on a substantial atlas, not the unrestricted eight-stratum stack.

# 20 Universal lane transport at finite profile

The preceding parts of the manuscript establish packet coordinates in an additive idempotent-complete setting and verify them separately in several native strata. This section isolates the common finite theorem. The word “lane” will mean a packet together with its address, its chosen splitting, and its position in a declared refinement system. Thus a lane is more than a subsequence or a suggestive decomposition. It carries the exact data needed for analysis, synthesis, transfer, refinement, and reconstruction.

The theorem is universal only in a profiled sense. Its algebraic core applies to every additive realization that preserves the finite sums, compositions, split idempotents, and refinement identities used in the proof. Kernel, quotient, tensor, topological, metric, and nonlinear conclusions require the additional hypotheses stated where they occur.

## 20.1 Finite profiled lane systems

**Definition 20.1** (Finite resolution shape)**.** A finite resolution shape is a finite partially ordered set R. We write $s \succeq r$ when $s$ is finer than $r$. The shape contains no address sets: object-specific addresses and their refinement maps are declared in the lane system below.

**Definition 20.2** (Finite profiled lane system)**.** Let $\mathcal{C}$ be an additive idempotent-complete category, let $X \in \mathcal{C}$, and let R be a finite resolution shape. A finite profiled lane system $\mathcal{L}_X$ consists, for every $r \in \mathsf{R}$, of a finite address set $I_{X,r}$ and a family

$$\mathcal{P}_X^r = (p_{X,i}^r)_{i \in I_{X,r}} \subseteq \mathrm{End}_{\mathcal{C}}(X)$$

with

$$(p_{X,i}^r)^2 = p_{X,i}^r, \qquad p_{X,i}^r p_{X,j}^r = 0 \quad (i \neq j), \qquad \sum_{i \in I_{X,r}} p_{X,i}^r = 1_X,$$

together with chosen splittings

$$X_i^r \xrightarrow{\iota_{X,i}^r} X \xrightarrow{\pi_{X,i}^r} X_i^r, \qquad \iota_{X,i}^r \pi_{X,i}^r = p_{X,i}^r, \qquad \pi_{X,i}^r \iota_{X,i}^r = 1_{X_i^r}.$$

For $s \succeq r$, the system also contains a surjection

$$\rho_{sr}^X : I_{X,s} \twoheadrightarrow I_{X,r}$$

such that

$$p_{X,i}^r = \sum_{\rho_{sr}^X(j)=i} p_{X,j}^s, \qquad \rho_{tr}^X = \rho_{sr}^X \rho_{ts}^X.$$

Here $\rho_{rr}^X = 1_{I_{X,r}}$. The address sets and refinement maps are declared data; they are not inferred from their cardinalities. Its verified profile contains finite biproducts, addition of morphisms, composition, the displayed splittings, and these projector-sum refinement identities. Any further constructor is included only after its preservation has been verified.

At resolution $r$, write

$$\mathcal{A}_X^r := (\pi_{X,i}^r)_i : X \longrightarrow \bigoplus_i X_i^r, \qquad \mathcal{S}_X^r := (\iota_{X,i}^r)_i : \bigoplus_i X_i^r \longrightarrow X.$$

For profiled lane systems on $X$ and $Y$, define the coordinate block of $f : X \to Y$ at resolutions $r, u$ by

$$[f]_{ai}^{u,r} := \pi_{Y,a}^u f \iota_{X,i}^r : X_i^r \longrightarrow Y_a^u.$$

Its ambient corner is

$$p_{Y,a}^u f p_{X,i}^r = \iota_{Y,a}^u [f]_{ai}^{u,r} \pi_{X,i}^r.$$

## 20.2 The universal finite transport theorem

**Theorem 20.3** (Universal Lane Transport Theorem, finite profiled form)**.** *Let $\mathcal{C}$ be an additive idempotent-complete category. Give each of the objects $X_0, \dots, X_m$ a finite profiled lane system. Then all of the following statements hold.*

(L1) ***Exact analysis and synthesis.*** *At every declared resolution,*

$$\mathcal{S}_X^r \mathcal{A}_X^r = 1_X, \qquad \mathcal{A}_X^r \mathcal{S}_X^r = 1_{\oplus_i X_i^r}.$$

*Hence $X \cong \bigoplus_i X_i^r$.*

(L2) ***Unique lane matrix.*** *Every morphism $f : X \to Y$ is recovered uniquely from its lane blocks:*

$$f = \sum_{a,i} p_{Y,a}^u f p_{X,i}^r = \sum_{a,i} \iota_{Y,a}^u [f]_{ai}^{u,r} \pi_{X,i}^r.$$

*Equivalently, the assignment*

$$f \longmapsto \left([f]_{ai}^{u,r}\right)_{a,i}$$

*is a bijection from $\mathrm{Hom}_{\mathcal{C}}(X,Y)$ to the group of rectangular matrices with entries in $\mathrm{Hom}_{\mathcal{C}}(X_i^r, Y_a^u)$.*

(L3) ***Composition and path law.*** *If $f : X \to Y$ and $g : Y \to Z$, with the same resolution $u$ used on the intermediate object, then*

$$[gf]_{ci}^{v,r} = \sum_{a \in I_{Y,u}} [g]_{ca}^{v,u} [f]_{ai}^{u,r}.$$

*More generally, a block of a composable string is the finite sum of the products along all compatible intermediate address paths.*

(L4) ***Projector-sum refinement.*** *If $s \succeq r$ on $X$ and $v \succeq u$ on $Y$, then*

$$p_{Y,a}^u f p_{X,i}^r = \sum_{\rho_{vu}^Y(b)=a} \sum_{\rho_{sr}^X(j)=i} p_{Y,b}^v f p_{X,j}^s.$$

*Coarsening a fine composite gives the same ambient morphism as composing at the coarse level.*

(L5) ***Selectors and named residuals.*** *For $E \subseteq I_{Y,u} \times I_{X,r}$, put*

$$C_E^{u,r}(f) := \sum_{(a,i) \in E} p_{Y,a}^u f p_{X,i}^r, \qquad R_E^{u,r}(f) := f - C_E^{u,r}(f).$$

*As additive endomorphisms of $\mathrm{Hom}_{\mathcal{C}}(X,Y)$,*

$$C_E^2 = C_E, \qquad C_E C_F = C_{E \cap F}, \qquad R_E = 1 - C_E, \qquad f = C_E(f) + R_E(f).$$

*Thus deletion of a lane block is never silent. Its complement is an exact, named residual.*

(L6) ***Support transport.*** *If $f = C_E(f)$ and $g = C_F(g)$, then*

$$gf = C_{F \circ E}(gf),$$

*where $F \circ E$ is relational composition through the intermediate addresses. For arbitrary $f, g$, writing $f_E = C_E(f)$, $r_f = R_E(f)$, $g_F = C_F(g)$, and $r_g = R_F(g)$, one has the exact identity*

$$gf - g_F f_E = r_g f_E + g_F r_f + r_g r_f.$$

(L7) ***Additive realization.*** *Let $F : \mathcal{C} \to \mathcal{D}$ be an additive functor to another additive idempotent-complete category. If the verified profile of $F$ contains the chosen splittings and refinement identities, then*

$$F([f]^{u,r}_{ai}) = [F(f)]^{u,r}_{ai}$$

*after the declared splitting comparisons. The functor carries analysis, synthesis, matrix multiplication, projector-sum refinement, selectors, and named residuals to their corresponding constructions in $\mathcal{D}$.*

(L8) ***Exact fold loss.*** *Let $E$ be a finite set of retained lane positions and set*

$$B_e := \mathrm{Hom}_{\mathcal{C}}(X^r_i, Y^u_a) \quad \text{for } e = (a, i) \in E.$$

*Let $T$ be a finite set, let $\kappa : E \to T$, let $C_t$ be abelian groups, and let $\tau_e : B_e \to C_{\kappa(e)}$ be homomorphisms. With $C = \bigoplus_{t\in T} C_t$ and coordinate inclusions $j_t : C_t \to C$, the fold*

$$\Phi_{\kappa,\tau} : \bigoplus_{e\in E} B_e \longrightarrow C, \qquad (b_e)_e \longmapsto \sum_{e\in E} j_{\kappa(e)}\tau_e(b_e)$$

*has exact information-loss group $\ker \Phi_{\kappa,\tau}$. In particular, two retained lane matrices have the same folded record exactly when their difference belongs to this kernel.*

*Suppose, more strongly, that every $\tau_e$ is injective and that there are globally typed selectors $Q_e \in \mathrm{End}(C)$ satisfying, for every $e, e' \in E$ and every $b_{e'} \in B_{e'}$,*

$$Q_e j_{\kappa(e')}\tau_{e'}(b_{e'}) = \delta_{e,e'} j_{\kappa(e')}\tau_{e'}(b_{e'}).$$

*Then $\Phi_{\kappa,\tau}$ is injective. If there are also homomorphisms*

$$r_e : C \longrightarrow B_e, \qquad r_e j_{\kappa(e)}\tau_e = 1_{B_e},$$

*then*

$$L := \big(r_e Q_e\big)_{e\in E} : C \longrightarrow \bigoplus_{e\in E} B_e$$

*is a left inverse of $\Phi_{\kappa,\tau}$, so the fold is split lossless.*

*Proof.* For (L1), the first composite is

$$\sum_i \iota^r_{X,i}\pi^r_{X,i} = \sum_i p^r_{X,i} = 1_X.$$

The $(i, j)$-entry of the other composite is $\pi^r_{X,i}\iota^r_{X,j}$. It is the identity when $i = j$, and it is zero otherwise because the corresponding idempotents annihilate one another.

For (L2), insert the two reconstruction identities on the two sides of $f$. Applying $\pi^u_{Y,a}$ on the left and $\iota^r_{X,i}$ on the right proves uniqueness of every entry. For (L3), insert $1_Y = \sum_a \iota^u_{Y,a}\pi^u_{Y,a}$ between $g$ and $f$. Iteration gives the path formula.

For (L4), substitute the two projector-sum refinement identities into the coarse ambient corner and distribute the finite sums. The assertion about composition follows from the same substitution at the intermediate object.

For (L5), each selector either fixes an ambient block or kills it. Applying two selectors therefore retains precisely the intersection. The residual identities follow by subtraction. For (L6), expand each block of $gf$ through the intermediate resolution. A surviving summand supplies an intermediate address in the relational product. The residual formula is the finite expansion of $(g_F + r_g)(f_E + r_f) - g_F f_E$.

For (L7), additivity preserves zero maps and finite sums, functoriality preserves identities and composition, and the splitting comparisons identify the image of every source lane object with the declared target lane object. The profile hypothesis is needed precisely for those identifications and for the refinement equations.

For (L8), equality of two fold values is equivalent to the difference of the two input families lying in the kernel. Under the selector hypothesis, if $\Phi_{\kappa,\tau}((b_e)_e) = 0$, applying $Q_e$ gives $j_{\kappa(e)}\tau_e(b_e) = 0$. Both $j_{\kappa(e)}$ and $\tau_e$ are injective, hence $b_e = 0$ for every $e$. The chosen retractions compose with the $Q_e$ to give the displayed left inverse: its $e$-coordinate on the fold is $r_e Q_e j_{\kappa(e)}\tau_e = 1_{B_e}$, while strict separation kills every other coordinate. □

*Remark* 20.4 (Why the fold selectors live in one group). The endomorphisms $Q_e$ in (L8) all act on the single group $C = \bigoplus_t C_t$. Writing separate selectors on unrelated codomains would make the Kronecker relation ill-typed and would not prove injectivity of the combined fold.

**Proposition 20.5** (Exact visible-support loss ledger)**.** *Use the finite fold data of (L8) and fix an input family $b = (b_e)_{e\in E}$. Define*

$$S_0 := \{e \in E : b_e \neq 0\}, \qquad A_0 := \{e \in S_0 : \tau_e(b_e) = 0\}, \qquad S_1 := S_0 \setminus A_0,$$

*and let*

$$\Gamma := \kappa(S_1) \subseteq T.$$

*For $t \in T$, write the folded coordinate as*

$$\overline{b}_t := \sum_{\substack{e\in S_1\\ \kappa(e)=t}} \tau_e(b_e) \in C_t,$$

*and put*

$$\operatorname{supp}(\overline{b}) := \{t \in T : \overline{b}_t \neq 0\}, \qquad K_0 := \{t \in \Gamma : \overline{b}_t = 0\}.$$

*Then*

$$\boxed{|S_0| - |\operatorname{supp}(\overline{b})| = |A_0| + \big(|S_1| - |\Gamma|\big) + |K_0|.}$$

*The three terms record, respectively, annihilation by the local maps $\tau_e$, collision of surviving lane addresses under $\kappa$, and cancellation among folded values at a common address. If every $\tau_e$ is injective, then $A_0 = \varnothing$. If globally typed selectors satisfy the strict separation law of (L8), then $K_0 = \varnothing$.*

*Proof.* The first partition gives $|S_0| = |A_0| + |S_1|$. The definition of $K_0$ gives the disjoint partition

$$\Gamma = \operatorname{supp}(\overline{b}) \sqcup K_0,$$

so $|\Gamma| = |\operatorname{supp}(\overline{b})| + |K_0|$. Subtracting the second equality from the first proves the formula.

Injectivity of $\tau_e$ makes $\tau_e(b_e) \neq 0$ for every $e \in S_0$, so there is no annihilation. For strict selectors, suppose $t \in K_0$ and choose $e \in S_1$ with $\kappa(e) = t$. Applying $Q_e$ to

$$j_t\overline{b}_t = \sum_{\kappa(e')=t} j_t\tau_{e'}(b_{e'}) = 0$$

leaves $j_t\tau_e(b_e) = 0$, contrary to $e \in S_1$. Hence $K_0 = \varnothing$. □

## 20.3 Certified change of resolution and exact loss sequences

For resolutions $s \succeq r$ on $X$ and $v \succeq u$ on $Y$, let

$$\mathsf{B}^{v,s}(X,Y) := \bigoplus_{b \in I_{Y,v}} \bigoplus_{j \in I_{X,s}} \mathrm{Hom}_{\mathcal{C}}(X_j^s, Y_b^v),$$

and define $\mathsf{B}^{u,r}(X,Y)$ similarly. Analysis of a morphism gives an isomorphism

$$\mathfrak{a}_{X,Y}^{v,s} : \mathrm{Hom}_{\mathcal{C}}(X,Y) \xrightarrow{\sim} \mathsf{B}^{v,s}(X,Y),$$

whose inverse is lane synthesis.

**Proposition 20.6** (Certified coarsening is an exact coordinate change)**.** *The change from fine to coarse block coordinates, canonical relative to the chosen splittings, is*

$$\Gamma_{(v,s)}^{(u,r)} := \mathfrak{a}_{X,Y}^{u,r} \big(\mathfrak{a}_{X,Y}^{v,s}\big)^{-1}.$$

*For a fine matrix $h = (h_{bj})$, its $(a,i)$-entry is*

$$\big(\Gamma_{(v,s)}^{(u,r)} h\big)_{ai} = \sum_{b,j} \big(\pi_{Y,a}^{u} \iota_{Y,b}^{v}\big) h_{bj} \big(\pi_{X,j}^{s} \iota_{X,i}^{r}\big).$$

*Only descendants of $a$ and $i$ can contribute. The inverse is the corresponding fine analysis after coarse synthesis. Consequently, changing a complete lane resolution loses no information. Loss occurs only after a subsequent selector, quotient, summary, or fold is applied.*

*Proof.* The displayed definition is a composite of two isomorphisms from theorem 20.3. Expanding coarse analysis after fine synthesis gives the entry formula. If $b$ is not a descendant of $a$, then $p_{Y,a}^{u} p_{Y,b}^{v} = 0$, hence $\pi_{Y,a}^{u} \iota_{Y,b}^{v} = 0$. The source factor vanishes by the same argument when $j$ is not a descendant of $i$. Reversing analysis and synthesis produces the inverse. □

**Corollary 20.7** (Functorial coarsening)**.** *For $t \succeq s \succeq r$ and compatible target resolutions, the certified coordinate changes compose strictly. They also intertwine matrix multiplication. Thus a finite refinement diagram gives a genuine diagram of equivalent matrix-coordinate categories, not merely a family of numerically similar arrays.*

**Theorem 20.8** (Abelian fold-loss exact sequence)**.** *Let $\mathcal{A}$ be an abelian category. Suppose a finite family of lane objects $(B_e)_{e \in E}$, target objects $(C_t)_{t \in T}$, and morphisms $\tau_e : B_e \to C_{\kappa(e)}$ is given. Let $q_e : \bigoplus_{e' \in E} B_{e'} \to B_e$ be the coordinate projection and define*

$$\Phi := \sum_{e \in E} j_{\kappa(e)} \tau_e q_e : \bigoplus_{e \in E} B_e \longrightarrow \bigoplus_{t \in T} C_t.$$

*Then there are canonical short exact sequences*

$$0 \longrightarrow \ker \Phi \longrightarrow \bigoplus_{e} B_e \longrightarrow \mathrm{im}\, \Phi \longrightarrow 0$$

*and*

$$0 \longrightarrow \mathrm{im}\, \Phi \longrightarrow \bigoplus_{t} C_t \longrightarrow \mathrm{coker}\, \Phi \longrightarrow 0.$$

*The first sequence is the exact fold-loss certificate. Suppose every $\tau_e$ is monic and there are endomorphisms $Q_e \in \mathrm{End}(\bigoplus_t C_t)$ satisfying*

$$Q_e j_{\kappa(e')} \tau_{e'} = \delta_{e,e'} j_{\kappa(e')} \tau_{e'} \quad \text{as morphisms } B_{e'} \longrightarrow \bigoplus_{t} C_t.$$

*Then $\Phi$ is monic. If, in addition, there are morphisms*

$$r_e : \bigoplus_t C_t \longrightarrow B_e, \qquad r_e j_{\kappa(e)} \tau_e = 1_{B_e},$$

*then $L = (r_e Q_e)_e$ is a left inverse of $\Phi$. Thus the first exact sequence splits, $\ker \Phi = 0$, and the image inclusion in the second exact sequence also splits.*

*Proof.* The two sequences are the kernel–image and image–cokernel factorizations in an abelian category. The selector argument in (L8), interpreted internally in $\mathcal{A}$, makes $\Phi$ monic. The displayed morphism $L$ is a left inverse by strict separation. Hence the first sequence splits; moreover, $\Phi L$ is an idempotent with image $\operatorname{im} \Phi$, so the image inclusion in the second sequence splits as well. □

*Boundary* 20.9 (Coordinate coarsening versus statistic coarsening). The complete fine and coarse block matrices are isomorphic coordinate records. Replacing each coarse block by a dimension, norm, valuation, degree, support bit, or color is a different map. Its kernel or fiber must be computed in the native doctrine. The lane theorem does not make such a statistic complete.

## 20.4 The matrix category carried by a lane system

**Definition 20.10** (Lane matrix category at a fixed resolution)**.** Let $\mathcal{L}_{\mathsf{R}}$ be the category whose objects are objects of $\mathcal{C}$ equipped with full finite profiled lane systems over $\mathsf{R}$, with all underlying $\mathcal{C}$-morphisms allowed. For $r \in \mathsf{R}$, define $\mathrm{Mat}_r(\mathcal{L}_{\mathsf{R}})$ to have the tagged finite families $[X; (X_i^r)_{i \in I_{X,r}}]$ as objects and rectangular matrices

$$(h_{ai}), \qquad h_{ai} : X_i^r \to Y_a^r,$$

as morphisms. Composition is matrix contraction and identities are diagonal identity matrices.

For $s \succeq r$, define

$$\Gamma_{sr} : \mathrm{Mat}_s(\mathcal{L}_{\mathsf{R}}) \longrightarrow \mathrm{Mat}_r(\mathcal{L}_{\mathsf{R}})$$

by replacing each object tag with its $r$-tag and sending a fine matrix to the certified source-and-target coordinate change of proposition 20.6.

**Theorem 20.11** (Fixed-resolution matrix-category equivalence)**.** *The functor*

$$\mathfrak{M}_r : \mathcal{L}_{\mathsf{R}} \longrightarrow \mathrm{Mat}_r(\mathcal{L}_{\mathsf{R}}), \qquad X \longmapsto [X; (X_i^r)_i], \qquad f \longmapsto ([f]_{ai}^{r,r}),$$

*is an equivalence. A quasi-inverse returns the lane-decorated object named by the tag and sends a matrix to*

$$\sum_{a,i} \iota_{Y,a}^r h_{ai} \pi_{X,i}^r.$$

*For every $s \succeq r$, the coordinate changes are functors and satisfy*

$$\Gamma_{sr} \mathfrak{M}_s = \mathfrak{M}_r.$$

*For $t \succeq s \succeq r$, they also satisfy*

$$\Gamma_{tr} = \Gamma_{sr} \Gamma_{ts}.$$

*Thus the equivalences are compatible with every certified change of resolution.*

*Proof.* The unique lane matrix and composition clauses of theorem 20.3 show that $\mathfrak{M}_r$ is fully faithful. Every object of the displayed matrix category is, by definition, the lane family of an object of $\mathcal{L}_{\mathsf{R}}$, so it is essentially surjective. Analysis and synthesis furnish the unit and counit isomorphisms. Each $\Gamma_{sr}$ is conjugation by exact analysis and synthesis, so it preserves identities and matrix composition. The two displayed identities follow from cancellation of adjacent analysis–synthesis pairs, equivalently from functorial coarsening in corollary 20.7. □

*Remark* 20.12 (No dimension claim). The number $|I_{X,r}|$ counts declared addresses. A lane object can have arbitrary dimension, rank, length, measure, or entropy, including zero where the ambient doctrine permits it. Matrix equivalence therefore does not identify address count with any of those invariants.

## 20.5 Multilinear and specified-polynomial transport

The additive theorem does not automatically govern arbitrary nonlinear maps. There is, however, an exact extension in the category of modules when the multilinear pieces are supplied as data.

**Theorem 20.13** (Module multilinear lane expansion)**.** *Let $\Bbbk$ be a commutative ring. Let*

$$X^{(1)}, \dots, X^{(d)}, Y$$

*be $\Bbbk$-modules with finite split lane systems, and let*

$$T : X^{(1)} \times \cdots \times X^{(d)} \longrightarrow Y$$

*be a specified $\Bbbk$-multilinear map. Define*

$$T_{a;i_1,\dots,i_d} := \pi_{Y,a} T(\iota_{1,i_1} -, \dots, \iota_{d,i_d} -).$$

*Then*

$$T(x_1, \dots, x_d) = \sum_{a,i_1,\dots,i_d} \iota_{Y,a} T_{a;i_1,\dots,i_d}(\pi_{1,i_1} x_1, \dots, \pi_{d,i_d} x_d).$$

*Substitution of multilinear maps is governed by finite contraction over every intermediate lane address.*

*Separately, let $X, Y$ be $\Bbbk$-modules with finite split lane systems and suppose a polynomial map is presented with specified data*

$$P(x) = T_0 + T_1(x) + T_2(x,x) + \cdots + T_D(x, \dots, x),$$

*where*

$$T_0 \in Y, \qquad T_n : X^n \longrightarrow Y \quad (1 \le n \le D)$$

*and every $T_n$ is a supplied multilinear map. Then*

$$T_0 = \sum_a \iota_{Y,a} \pi_{Y,a}(T_0),$$

*and adding this degree-zero decomposition to the displayed multilinear expansions gives an exact lane expansion of $P$.*

*Proof.* Insert $x_\ell = \sum_{i_\ell} p_{\ell,i_\ell} x_\ell$ in every input, use multilinearity to distribute the finite sums, and insert $1_Y = \sum_a p_{Y,a}$ in the output. The coordinate formula follows from the chosen splittings. Repeating the calculation after substitution gives the contraction law. The degree-zero identity is output synthesis applied to $T_0$; the polynomial statement is then a finite sum of the specified homogeneous pieces. □

*Boundary* 20.14 (The nonlinear doctrine must be specified). Over a general commutative ring, a polynomial function need not determine a unique symmetric multilinear polarization. Infinite analytic expansions also require a declared topology and convergence theorem. Therefore theorem 20.13 is stated for supplied multilinear maps and supplied finite polynomial data. It does not assert a canonical lane calculus for every nonlinear category.

## 20.6 Factorial lanes and residue packets

The factorial construction is an exact arithmetic realization of the abstract lane mechanism. It is useful because the addresses, refinement maps, Fourier projectors, and hypergeometric coordinates can all be written explicitly.

For integers $N \geq 1$ and $n \geq 0$, define the step factorial

$$(a)_{n;N} := \prod_{k=0}^{n-1} (a + Nk), \qquad (a)_{0;N} := 1.$$

For a commutative ring $A$ and a formal series $F(z) = \sum_{m \geq 0} a_m z^m \in A[[z]]$, define its residue lane

$$\mathcal{P}_{N,j} F(z) := \sum_{\substack{m \geq 0 \\ m \equiv j \pmod N}} a_m z^m, \qquad 0 \leq j < N.$$

**Theorem 20.15** (Exact factorial–residue realization). *Let $N, c, n \in \mathbb{Z}$ with $N \geq 1$, $c \geq 0$, and $n \geq 0$. Then*

$$\boxed{\frac{(Nn + c)!}{c!} = \prod_{r=c+1}^{c+N} (r)_{n;N}.}$$

*Each integer factor from $c + 1$ through $c + Nn$ occurs in exactly one lane. For every commutative ring $A$, on the $A$-module $A[[z]]$ the operators $(\mathcal{P}_{N,j})_{0 \leq j < N}$ satisfy*

$$\mathcal{P}_{N,j}^2 = \mathcal{P}_{N,j}, \qquad \mathcal{P}_{N,j} \mathcal{P}_{N,k} = 0 \ (j \neq k), \qquad \sum_{j=0}^{N-1} \mathcal{P}_{N,j} = 1.$$

*If $M \in \mathbb{Z}$ and $M \geq 1$, their exact refinement law is*

$$\mathcal{P}_{N,j} = \sum_{\ell=0}^{M-1} \mathcal{P}_{NM,j+\ell N}.$$

*Suppose further that $K$ is a field, that $N$ is invertible in $K$, and that $K$ contains a primitive $N$-th root of unity $\omega$. Then for every $F \in K[[z]]$,*

$$\mathcal{P}_{N,j} F(z) = \frac{1}{N} \sum_{\ell=0}^{N-1} \omega^{-j\ell} F(\omega^\ell z).$$

*If, in addition, $K$ has characteristic zero, the exponential and hypergeometric series below are defined in $K[[z]]$. Put*

$$E_{N,j}(z) := \mathcal{P}_{N,j} e^z = \sum_{n \geq 0} \frac{z^{Nn+j}}{(Nn + j)!}.$$

*If*

$$\mathbf{b}_{N,j} := \left\{ \frac{j + r}{N} : 1 \leq r \leq N,\ r \neq N - j \right\},$$

*then*

$$E_{N,j}(z) = \frac{z^j}{j!}{}_0F_{N-1}\left(\begin{matrix}-\\ \mathbf{b}_{N,j}\end{matrix}; \frac{z^N}{N^N}\right).$$

*Thus coefficient-residue, root-of-unity, and hypergeometric descriptions are exact additive coordinate realizations of one residue-address decomposition. The step-factorial identity is an exact multiplicative companion with the same address arithmetic; it is not asserted to be an additive idempotent decomposition of the factorial.*

*Proof.* Every integer $m$ with $c < m \le c + Nn$ has a unique representation $m = r + Nk$ with $c + 1 \le r \le c + N$ and $0 \le k < n$. Multiplying these disjoint factors proves the factorial identity.

The projector laws follow coefficient by coefficient. The residue classes modulo $NM$ lying over $j \pmod N$ are precisely $j, j + N, \dots, j + (M-1)N$, which proves refinement. Character orthogonality gives the Fourier formula. Finally,

$$(Nn + j)! = j!\, N^{Nn} \prod_{r=1}^{N} \left(\frac{j+r}{N}\right)_n.$$

Exactly one factor in the product is $(1)_n = n!$. Removing it leaves the parameter set $\mathbf{b}_{N,j}$ and gives the hypergeometric series. □

**Corollary 20.16** (Factorial-lane genealogy)**.** *The step-factorial split supplies an exact multiplicative partition of the factor set, while the residue projectors supply an exact additive partition of the coefficient series. The residue projectors instantiate theorem 20.3 directly. The step-factorial product is realized by the supplied finite multilinear pointwise multiplication map on the module of lane sequences, as in theorem 20.13. Their common address refinement is divisibility of the modulus. Hence the additive transport law and the multiplicative companion share exact address-refinement combinatorics, without identifying a product factorization with an additive idempotent splitting.*

## 20.7 Typed native specializations

The next statements identify concrete realizations and record the hypotheses that make each use of the theorem legal. They do not identify the surrounding strata with one another.

### 20.7.1 Fourier and polyphase lanes

**Proposition 20.17** (Typed polyphase realization)**.** *Let $K$ be a field, let $N \in \mathbb{Z}$ with $N \ge 1$ be invertible in $K$, and suppose $K$ contains a primitive $N$-th root of unity. For $F(z) = \sum_{n\ge 0} a_n z^n \in K[[z]]$, set*

$$F_j(w) := \sum_{n\ge 0} a_{Nn+j} w^n.$$

*Then*

$$F(z) = \sum_{j=0}^{N-1} z^j F_j(z^N)$$

*is exact analysis and synthesis. The Fourier residue projectors and the polyphase components satisfy the explicit coordinate relation*

$$\mathcal{P}_{N,j} F(z) = z^j F_j(z^N).$$

*For every integer $M \ge 1$, refinement from $N$ to $NM$ is the projector-sum law of theorem 20.15.*

*Proof.* Every exponent has a unique quotient and remainder on division by $N$. The Fourier formula in theorem 20.15 identifies the same coefficient sections with character projectors. □

### 20.7.2 Cartier and fixed-radix lanes

**Proposition 20.18** (Typed Cartier realization)**.** *Let $K$ be a field and let $k \geq 2$. Work with $K$-valued formal series and fix the least-significant-digit-first convention. Define*

$$\Lambda_d\left(\sum_{n\geq 0} a_n z^n\right) := \sum_{n\geq 0} a_{kn+d} z^n, \qquad S_d(G) := z^d G(z^k), \quad 0 \leq d < k.$$

*Then*

$$\Lambda_d S_e = \delta_{de} 1, \qquad \sum_{d=0}^{k-1} S_d \Lambda_d = 1.$$

*For a digit word $w = d_0 d_1 \cdots d_{a-1}$, the iterated Cartier lane is*

$$\Lambda_{d_{a-1}} \cdots \Lambda_{d_1} \Lambda_{d_0} F.$$

*It selects coefficients with index*

$$k^a n + [w]_k, \qquad [w]_k = d_0 + k d_1 + \cdots + k^{a-1} d_{a-1}.$$

*Concatenation gives strict radix refinement and the lane path law.*

*Proof.* The first identities follow by coefficient extraction and unique quotient and remainder. Iterating in the stated reading convention gives the displayed address, and concatenation composes the affine index maps. □

### 20.7.3 Holonomic lanes

**Proposition 20.19** (Typed holonomic realization)**.** *Let $K$ be a characteristic-zero field and let the $K$-valued sequence $(u_n)$ satisfy a linear recurrence with polynomial coefficients. Beyond a finite singular prefix, write the recurrence as a finite-dimensional rational nonautonomous state model*

$$v_{n+1} = A(n) v_n, \qquad A(n) \in \mathrm{Mat}_d(K(n)).$$

*For a fixed integer $N \geq 1$ and residue $0 \leq j < N$, the lane state $w_m = v_{Nm+j}$ evolves by the exact $N$-step rational transfer*

$$w_{m+1} = A(Nm + j + N - 1) \cdots A(Nm + j) w_m$$

*whenever the displayed factors are defined. Equivalently, residue multisection of a D-finite generating series gives D-finite lanes. The finite singular prefix and any exceptional denominators remain explicit data.*

*Proof.* Iterate the state equation $N$ times. Closure of D-finite series under scaling the variable, finite sums, and root-of-unity multisection gives the equivalent generating-series statement after a field extension containing the needed roots. No autonomous finite-state claim is used. □

### 20.7.4 Local Newton–Mahler lanes

**Proposition 20.20** (Typed local clopen realization)**.** *Fix a prime $p$ and an integer $a \geq 0$. For $f \in C(\mathbb{Z}_p, \mathbb{Z}_p)$, with $q \in \mathbb{Z}_p$ the branch coordinate, define*

$$\mathcal{A}_{p^a}(f) := \big(q \mapsto f(p^a q + s)\big)_{0 \leq s < p^a}.$$

*Piecewise synthesis on the disjoint clopen cosets $s + p^a\mathbb{Z}_p$ is its inverse. Refining from $p^a$ to $p^{a+b}$, for every integer $b \geq 0$, gives the exact child-address and mixed-radix composition law. Let*

$$\mathcal{M} := \mathcal{M}_p^{-1} : C(\mathbb{Z}_p, \mathbb{Z}_p) \xrightarrow{\sim} c_0(\mathbb{Z}_p)$$

*be Mahler analysis from theorem 14.1, and write $R_{p^a,s} f(q) := f(p^a q + s)$. Conjugation gives the exact coefficient operator*

$$\mathcal{T}_{p^a,s} := \mathcal{M} R_{p^a,s} \mathcal{M}^{-1} : c_0(\mathbb{Z}_p) \longrightarrow c_0(\mathbb{Z}_p),$$

*whose affine kernel is computed in theorem 14.5. Its mixed-radix composition is theorem 14.7.*

*The assertion of complete clopen analysis is restricted to these prime-power packets. More general affine coefficient kernels may still compose according to their declared mixed-radix law, but an arbitrary integer modulus does not automatically partition $\mathbb{Z}_p$ into that many disjoint clopen branches.*

*Proof.* The $p^a$ cosets are disjoint, clopen, and cover $\mathbb{Z}_p$. Restricting after piecewise synthesis and synthesizing after restriction are identities. Writing a child address as $s + p^a t$ proves refinement. The cited Mahler isomorphism makes the displayed conjugation exact, and the two cited kernel theorems give its coefficient formula and composition law. □

### 20.7.5 Nonlinear tree lanes

**Proposition 20.21** (Typed Fuss–Catalan realization)**.** *Let $K$ be a characteristic-zero field, let $q \in \mathbb{Z}$ with $q \geq 2$, and let $\alpha \in K^\times$. The uniquely marked formal solution of*

$$U = z + \alpha U^q, \qquad U(0) = 0,$$

*has support*

$$[z^{1+(q-1)n}]U = \frac{1}{(q-1)n+1}\binom{qn}{n}\alpha^n \neq 0 \qquad (n \geq 0),$$

*and every other coefficient is zero. Thus its support is exactly the set of degrees congruent to $1 \pmod{q-1}$. For an integer packet width $N \geq 1$, set $g = \gcd(N, q-1)$. Exactly $N/g$ residue addresses are active, namely the congruence class $1 \pmod{g}$. Packetizing the specified multilinear map $(U_1, \ldots, U_q) \mapsto U_1 \cdots U_q$ gives the exact finite carry-convolution system supplied by theorem 20.13. On a cyclic orbit of order $q-1$, the power map used for packet synthesis has*

$$\frac{q-1}{\gcd(N, q-1)}$$

*distinct images. If a fixed embedding $K \hookrightarrow \mathbb{C}$ sends $\alpha$ to a positive real number and the marked branch is interpreted in the smooth implicit analytic schema, its critical points and values satisfy*

$$q\alpha\tau^{q-1} = 1, \qquad \rho = \tau - \alpha\tau^q = \frac{q-1}{q}\tau.$$

*The resulting orbit $\rho\mu_{q-1}$ is precisely the dominant singularity orbit, and packetization leaves $(q-1)/g$ distinct images.*

*Proof.* Lagrange inversion gives the displayed coefficient formula and zero at every other degree. Characteristic zero and $\alpha \neq 0$ make every displayed coefficient nonzero. Their residues modulo $N$ form the coset of the subgroup generated by $q-1$, whose size is $N/g$. Multilinear lane expansion of the

product gives the packet equation, including the power of the packet variable produced by the quotient in residue addition. On the cyclic group of order $q-1$, the kernel of multiplication by $N$ has order $g$, so the image has order $(q-1)/g$. The critical equations give the displayed values, while theorem 17.13 identifies their full orbit as the dominant one under the stated analytic hypotheses. □

### 20.7.6 Algebraic branch lanes

**Proposition 20.22** (Typed cyclic-radical realization)**.** *Let $K$ be a characteristic-zero field containing $\mu_d$ and a primitive $N$-th root of unity $\omega$, let $d, m, N \in \mathbb{Z}_{\geq 1}$, and choose the formal branch*

$$F(z) = (1 - \alpha z^m)^{-1/d}, \qquad \alpha \in K^\times.$$

*With $g = \gcd(N, m)$, its nonzero coefficients occupy exactly the subgroup of $\mathbb{Z}/N\mathbb{Z}$ generated by $m$, which has $N/g$ addresses. The rotated radicands*

$$1 - \alpha\omega^{jm} z^m, \qquad 0 \leq j < N,$$

*also have exactly $N/g$ distinct values.*

*If, in addition, their distinct Kummer classes generate a subgroup isomorphic to $(\mathbb{Z}/d\mathbb{Z})^{N/g}$ in the Kummer quotient*

$$K(z)^\times / K(z)^{\times d},$$

*then the compositum of the corresponding radical branch fields has degree*

$$d^{N/g}$$

*over $K(z)$. Without that independence hypothesis, the lane orbit count remains exact but the degree formula is only an upper bound.*

*Proof.* The binomial series is supported at exponents $mn$. The cyclic subgroup calculation gives both address and rotation counts. The degree statement is the standard Kummer independence calculation for the explicitly listed classes. A relation among the classes produces a field collision not detected by address count alone. □

### 20.7.7 Finite Galois lanes

**Proposition 20.23** (Typed semisimple Galois realization)**.** *Let $G$ be finite and let $K$ be a characteristic-zero splitting field for $G$. The primitive central idempotents*

$$e_\chi = \frac{\chi(1)}{|G|} \sum_{g \in G} \chi(g^{-1}) g \in K[G]$$

*for $\chi \in \mathrm{Irr}_K(G)$ form a complete pairwise-annihilating lane system on every finite-dimensional semisimple $K[G]$-module $V$:*

$$V = \bigoplus_{\chi \in \mathrm{Irr}_K(G)} e_\chi V.$$

*Every $G$-equivariant map is block diagonal in these isotypic lanes, while an arbitrary $K$-linear map has the full lane matrix of theorem 20.3.*

*For a subgroup $H \leq G$, the Reynolds operator*

$$e_H = \frac{1}{|H|} \sum_{h \in H} h$$

*is an idempotent projector onto $V^H$; equivalently, $(e_H, 1 - e_H)$ is a two-lane system on the underlying K-vector space. It is not in general a Boolean selector formed from the isotypic projectors above. Projectors belonging to unrelated subgroups need not annihilate one another, so they do not automatically form one lane system. Transport through induction, restriction, or subgroup refinement requires the corresponding Mackey or double-coset data.*

*Proof.* Maschke semisimplicity and the character idempotent relations give the first decomposition. An equivariant map commutes with the center of $K[G]$, hence with every $e_\chi$. Averaging proves that $e_H$ is idempotent with image $V^H$. Two subgroup averages generally fail the pairwise-annihilation axiom, which proves the stated boundary. □

## 20.8 Descent of lane systems through a finite atlas

The local theorem becomes global only when the addresses and splittings glue without address holonomy. The following statement makes those additional hypotheses explicit.

**Theorem 20.24** (Finite atlas descent for lane transport)**.** *Let $\mathfrak{R}$ be a finite profiled atlas whose participating chart categories are additive and idempotent-complete, with additive transition functors $F_{UV} : \mathfrak{R}(U) \to \mathfrak{R}(V)$ on its declared overlaps. Let*

$$X = (X_U, \theta^X_{UV}), \qquad Y = (Y_U, \theta^Y_{UV}), \qquad Z = (Z_U, \theta^Z_{UV})$$

*be three compatible descent objects. Thus the transition isomorphisms satisfy the identity and cocycle equations. Let*

$$f = (f_U) : X \longrightarrow Y, \qquad g = (g_U) : Y \longrightarrow Z$$

*be compatible descended morphisms.*

*Fix one finite resolution shape* R*. Suppose every local object $A_U$, for $A \in \{X, Y, Z\}$, carries a finite profiled lane system over* R*. For every overlap, every $r \in$ R*, and every such $A$, suppose there is an address bijection*

$$\lambda^{A,r}_{UV} : I_{A_U,r} \xrightarrow{\sim} I_{A_V,r}$$

*such that*

$$\lambda^{A,r}_{UU} = 1, \qquad \lambda^{A,r}_{UT} = \lambda^{A,r}_{VT} \lambda^{A,r}_{UV},$$

*on every triple overlap $(U, V, T)$, and, for $s \succeq r$,*

$$\rho^{A_V}_{sr} \lambda^{A,s}_{UV} = \lambda^{A,r}_{UV} \rho^{A_U}_{sr}.$$

*Require trivial address holonomy: for every $A$ and $r$, there is a global finite address set $I_{A,r}$, a global refinement map $\rho^A_{sr} : I_{A,s} \twoheadrightarrow I_{A,r}$, and bijections*

$$\mu^{A,r}_U : I_{A_U,r} \xrightarrow{\sim} I_{A,r}$$

*such that*

$$\mu^{A,r}_V \lambda^{A,r}_{UV} = \mu^{A,r}_U, \qquad \mu^{A,r}_U \rho^{A_U}_{sr} = \rho^A_{sr} \mu^{A,s}_U.$$

*Assume also that the transition isomorphisms intertwine the local projectors:*

$$\theta^A_{UV} F_{UV}(p^r_{A_U,i}) = p^r_{A_V, \lambda^{A,r}_{UV}(i)} \theta^A_{UV},$$

*and that the verified transition profiles preserve the chosen splittings, finite sums, composition, and refinement equations, with coherent splitting comparisons on triple overlaps.*

*Then:*

(D1) *after relabeling by the $\mu_U^{A,r}$, each local lane and its chosen splitting define a lane summand in* $\mathrm{Desc}(\mathfrak{R})$*, and the global addresses carry the declared projector-sum refinement;*

(D2) *the local matrices $([f_U]_{ai})$, $([g_U]_{ca})$, and $([g_U f_U]_{ci})$ glue after the prescribed address relabelings and splitting comparisons;*

(D3) *the descended matrices satisfy*

$$[gf]_{ci} = \sum_a [g]_{ca}[f]_{ai};$$

(D4) *every compatible family of support selectors and named residuals descends, and every compatible refinement square remains a projector-sum refinement square in the descent category;*

(D5) *every fold whose source objects, target objects, and structure maps are compatible descent data defines a fold in* $\mathrm{Desc}(\mathfrak{R})$*. Compatible selectors and left inverses descend, so a split-losslessness certificate descends directly from its left-inverse identity. Moreover, suppose the relevant local kernels $K_U = \ker(\Phi_U)$ exist, every transition functor preserves them, and there are coherent comparison isomorphisms*

$$\eta_{UV} : F_{UV}(K_U) \xrightarrow{\sim} K_V$$

*compatible with the kernel inclusions and satisfying the triple-overlap cocycle. Then the global kernel exists and is computed chartwise:*

$$\big(\ker_{\mathrm{Desc}(\mathfrak{R})} \Phi\big)_U \cong \ker_{\mathfrak{R}(U)}(\Phi_U).$$

*Proof.* For a global address $i \in I_{A,r}$, use the local projector indexed by $(\mu_U^{A,r})^{-1}(i)$. The trivialization identity makes these projectors correspond under the transition isomorphisms on every overlap; its refinement identity makes their local projector-sum laws agree. The coherent splitting comparisons make the corresponding inclusions and projections descent morphisms. Finite biproducts in the descent category are computed chartwise, so local analysis and synthesis glue and remain mutually inverse.

Compatibility of $f$ and $g$, followed by the splitting comparisons, shows that their local coordinate blocks agree on overlaps after applying the specified address relabelings. Hence the matrices descend. Matrix multiplication is a finite sum of compositions, both computed chartwise, so the local path law glues to the displayed global law. The same argument applies to projector sums, selectors, and residual differences.

Finally, a compatible fold is a morphism in the relevant descent category. Compatible selectors and left inverses glue, and their identities can be checked chartwise. Under the additional kernel hypotheses, the objects $(K_U, \eta_{UV})$ form a descent object; compatibility with the local kernel inclusions gives a global morphism into the fold source. Its universal property is checked in each chart, which proves the displayed chartwise kernel identity. The split case needs no kernel-preservation hypothesis: the compatible local left inverses glue directly. □

**Corollary 20.25** (Certified atlas lane transport)**.** *Let $\mathfrak{A}_{\mathrm{cert}}$ be the certified finite atlas of this manuscript. On every subatlas whose passports include additive split-lane systems, compatible refinement maps, coherent address relabelings with trivial address holonomy, and the required preservation profile, the Universal Lane Transport Theorem holds in the descent category. Kernel claims additionally require the kernel-preservation and coherence data in theorem 20.24. In particular, any of the typed specializations above may be transported across a certified reversible overlap after its native hypotheses, address trivializations, and splitting cocycles have been checked.*

*Proof.* Apply theorem 20.24 to the verified subatlas. The conclusion is deliberately restricted to the overlaps whose passports contain all of the listed data. □

*Boundary* 20.26 (Descent is conditional on address coherence). An equivalence of underlying semantic objects does not by itself identify two lane systems. Without the bijections $\lambda_{UV}^{A,r}$, their cocycle law, compatible global trivializations $\mu_U^{A,r}$, refinement compatibility, and coherent splitting comparisons, the local matrices need not glue as ordinary globally addressed lanes. Nontrivial address holonomy can permute lanes around a loop; then only invariant orbit sums, or lanes in a separately defined local-system-valued category, may descend. The theorem above verifies ordinary descent under trivial holonomy. It does not manufacture missing lane passports for an arbitrary heterogeneous atlas.

## 20.9 Sharp boundaries and a finite counterexample

**Proposition 20.27** (Endpoint selection does not implement refinement)**.** *Let $K$ be a field and let $X = K^2$. At the coarse resolution use the single projector $p = 1_X$. At the fine resolution use*

$$p_1 = \begin{pmatrix} 1 & 0 \\ 0 & 0 \end{pmatrix}, \qquad p_2 = \begin{pmatrix} 0 & 0 \\ 0 & 1 \end{pmatrix}, \qquad p = p_1 + p_2.$$

*For*

$$f = p_2,$$

*the unique coarse block is $pfp = f \neq 0$, whereas selecting the single fine endpoint $(p_1, p_1)$ gives $p_1 f p_1 = 0$. Therefore a coarse block is the sum over all compatible descendant source-target pairs. It cannot in general be represented by choosing one fine endpoint.*

*Proof.* The displayed matrix multiplication gives the two values immediately. The full refinement identity recovers $f = \sum_{a,i\in\{1,2\}} p_a f p_i$, whose only nonzero term here is $p_2 f p_2$. □

*Boundary* 20.28 (Finite profiled meaning of "universal"). The theorem proves a common calculus for finite split lanes in additive categories and for the explicitly stated profile extensions. It does not assert any of the following:

1. that every mathematical object has a canonical or minimal lane system;
2. that countably infinite lane sums converge without a topology and a convergence theorem;
3. that arbitrary nonlinear, probabilistic, operator-algebraic, or homotopical constructions preserve additive lane identities;
4. that address count equals vector-space dimension, module rank, information, entropy, algebraic degree, or computational complexity;
5. that a support pattern, heatmap, norm profile, valuation profile, or orbit count is a complete invariant;
6. that native invariants in different strata are equal merely because their formulas contain the same gcd or residue operation;
7. that the theorem supplies historical novelty evidence or external validation.

Each stronger conclusion requires a native theorem and a preservation certificate.

*Remark* 20.29 (Classical core and present synthesis). Finite biproduct coordinates, Peirce decompositions, block-matrix multiplication, residue filters, and polyphase identities have classical antecedents. The theorem packages that core with explicit address refinement, profile-controlled realization, named residuals, exact fold kernels, and typed descent. This manuscript treats the resulting assembly as an internal mathematical contribution. It does not infer a priority claim without a separate literature study.

## 20.10 Exact finite validation and interpretation

The accompanying verifier is an exact finite regression suite for selected implementation clauses. It checks integer and rational block reconstruction, matrix composition, refinement aggregation, support and residual identities, fold collision kernels, factorial-lane partitions, residue-projector refinement, and explicit negative controls. The proofs above do not depend on finite sampling. Conversely, the symbolic proofs do not certify that a particular program implements the formulas correctly. The two records serve different purposes.

**Table 41:** Exact finite regression for selected implementation clauses of the Universal Lane Transport theorem. This table is not an exhaustive proof or an external validation.

| Validation family | Exact assertions |
|---|---|
| Integer/unimodular lane matrices | 28,490 |
| Dense rational three-level refinement | 16,674 |
| Abstract additive folds and strict selectors | 1,000 |
| Actual-support loss decomposition | 300 |
| Factorial and residue-lane realization | 150,630 |
| Deliberately invalid negative controls | 5 |
| **Total selected implementation assertions** | **197,099** |
| Recorded failures | 0 |

**Universal Lane Transport result.** Finite split lane systems admit exact analysis and synthesis, unique transfer matrices, path composition, strict projector-sum refinement, Boolean support selectors, named residuals, and exact fold-loss kernels. Complete changes of resolution are coordinate equivalences. In abelian targets, fold loss sits in a canonical short exact sequence. In module targets, specified multilinear and finite polynomial operations expand lane by lane. Residue/Fourier, polyphase, Cartier, holonomic, local Newton–Mahler, Fuss–Catalan, cyclic radical, and semisimple Galois systems realize these clauses under their printed hypotheses. The step-factorial product is an exact multiplicative companion transported through a specified multilinear multiplication map, not an additive idempotent splitting. Compatible address trivializations, refinement, and splitting data make the calculus descend through a finite certified atlas when address holonomy is trivial. No claim is made beyond that finite profiled domain.

# 21 Holonomy-twisted lane transport and orbit descent

The finite atlas theorem in theorem 20.24 imposed trivial address holonomy in order to obtain one globally fixed set of lane labels. That hypothesis is sufficient for ordinary globally addressed lanes, but it is stronger than the hypothesis needed for transport itself. When addresses are permuted around atlas loops, the local lane matrices still glue. They glue as sections of a finite matrix local system rather than as one matrix with a fixed global row and column labeling.

This section isolates that distinction. The local analysis, synthesis, composition, refinement, selector, and residual laws survive arbitrary finite address holonomy. The holonomy orbits then give the finest ordinary global coarsening obtainable by summing the original lane projectors. Thus nontrivial holonomy is an obstruction to untwisted labels, not an obstruction to the finite transport calculus.

## 21.1 Holonomy-profiled lane data

Let $\mathscr{G}$ be a finite connected groupoid of charts. For an arrow $\gamma : U \to V$, let

$$F_\gamma : \mathcal{C}_U \longrightarrow \mathcal{C}_V$$

be an additive equivalence between additive idempotent-complete categories. The transition functors carry specified identity and composition comparisons. To keep the formulas readable, those comparison isomorphisms are suppressed; every displayed cocycle equation is understood after inserting the declared comparisons.

A descent object

$$A = (A_U, \theta^A_\gamma)$$

consists of objects $A_U \in \mathcal{C}_U$ and isomorphisms

$$\theta^A_\gamma : F_\gamma(A_U) \xrightarrow{\sim} A_V$$

satisfying the identity and cocycle equations. A descended morphism $f : X \to Y$ is a compatible family $(f_U)_U$ satisfying

$$\theta^Y_\gamma F_\gamma(f_U) = f_V \theta^X_\gamma.$$

**Definition 21.1** (Holonomy-profiled finite lane datum)**.** Fix a finite resolution shape $\mathsf{R}$. A holonomy-profiled finite lane datum on a descent object $A$ consists of the following information.

For every chart $U$ and resolution $r \in \mathsf{R}$, the object $A_U$ has a finite profiled lane system

$$\left(I_{A,U,r}, p^r_{A,U,i}, A^r_{U,i}, \iota^r_{A,U,i}, \pi^r_{A,U,i}\right)_{i \in I_{A,U,r}}$$

in the sense of definition 20.2. For every arrow $\gamma : U \to V$, there is an address bijection

$$\lambda^A_{\gamma,r} : I_{A,U,r} \xrightarrow{\sim} I_{A,V,r}$$

and, for every address $i$, a splitting comparison

$$\beta^A_{\gamma,r,i} : F_\gamma(A^r_{U,i}) \xrightarrow{\sim} A^r_{V,\lambda^A_{\gamma,r}(i)}.$$

They satisfy the address and splitting cocycle laws and the two compatibility identities

$$\theta^A_\gamma F_\gamma(\iota^r_{A,U,i}) = \iota^r_{A,V,\lambda^A_{\gamma,r}(i)} \beta^A_{\gamma,r,i},$$

$$\beta^{A}_{\gamma,r,i} F_\gamma(\pi^{r}_{A,U,i}) = \pi^{r}_{A,V,\lambda^{A}_{\gamma,r}(i)} \theta^{A}_{\gamma}.$$

For $s \succeq r$, the refinement maps are equivariant:

$$\rho^{A,V}_{sr} \lambda^{A}_{\gamma,s} = \lambda^{A}_{\gamma,r} \rho^{A,U}_{sr}.$$

No global address set and no global trivialization of the address bijections is assumed.

**Definition 21.2** (Matrix local system)**.** Let $X, Y$ carry holonomy-profiled lane data. At source resolution $r$ and target resolution $u$, define the matrix group over a chart $U$ by

$$\mathscr{M}^{u,r}_{Y,X}(U) := \bigoplus_{a \in I_{Y,U,u}} \bigoplus_{i \in I_{X,U,r}} \mathrm{Hom}_{\mathcal{C}_U}(X^{r}_{U,i}, Y^{u}_{U,a}).$$

For $h = (h_{ai}) \in \mathscr{M}^{u,r}_{Y,X}(U)$, define transport along $\gamma : U \to V$ by

$$(\gamma_* h)_{\lambda^{Y}_{\gamma,u}(a), \lambda^{X}_{\gamma,r}(i)} := \beta^{Y}_{\gamma,u,a} F_\gamma(h_{ai}) \left(\beta^{X}_{\gamma,r,i}\right)^{-1}.$$

The group of compatible sections is

$$\Gamma\left(\mathscr{G}, \mathscr{M}^{u,r}_{Y,X}\right) := \left\{ (h_U)_U : \gamma_* h_U = h_V \text{ for every } \gamma : U \to V \right\}.$$

## 21.2 The holonomy-twisted transport theorem

**Theorem 21.3** (Holonomy-Twisted Universal Lane Transport Theorem)**.** *Let $X, Y, Z$ be descent objects over $\mathscr{G}$, each equipped with a holonomy-profiled finite lane datum over the same finite resolution shape. Then the following statements hold.*

(H1) ***Matrix local system.*** *The maps $\gamma_*$ of definition 21.2 are additive isomorphisms and satisfy the identity and cocycle laws. Hence $\mathscr{M}^{u,r}_{Y,X}$ is a local system of abelian groups with finitely many matrix positions in every chart.*

(H2) ***Exact twisted analysis and synthesis.*** *Lane analysis induces an isomorphism*

$$\mathfrak{A}^{u,r}_{Y,X} : \mathrm{Hom}_{\mathrm{Desc}(\mathscr{G})}(X, Y) \xrightarrow{\sim} \Gamma\left(\mathscr{G}, \mathscr{M}^{u,r}_{Y,X}\right), \qquad f \longmapsto \left( \left( [f_U]^{u,r}_{ai} \right)_{a,i} \right)_U.$$

*Its inverse is chartwise lane synthesis:*

$$(h_U)_U \longmapsto \left( \sum_{a,i} \iota^{u}_{Y,U,a} h_{U,ai} \pi^{r}_{X,U,i} \right)_U.$$

*Thus nontrivial address holonomy does not destroy the complete matrix record. It changes the global type of that record from a constantly labeled matrix to a compatible section of a matrix local system.*

(H3) ***Twisted matrix composition.*** *For*

$$h \in \Gamma(\mathscr{G}, \mathscr{M}^{u,r}_{Y,X}), \qquad k \in \Gamma(\mathscr{G}, \mathscr{M}^{v,u}_{Z,Y}),$$

*define chartwise contraction by*

$$(k \star h)_{U,ci} := \sum_{a \in I_{Y,U,u}} k_{U,ca} h_{U,ai}.$$

*Then $k \star h$ is a compatible section of $\mathscr{M}^{v,r}_{Z,X}$, and*

$$\mathfrak{A}^{v,r}_{Z,X}(gf) = \mathfrak{A}^{v,u}_{Z,Y}(g) \star \mathfrak{A}^{u,r}_{Y,X}(f).$$

*The diagonal identity matrices are compatible sections. More precisely, fix one declared resolution $r_A$ for each lane-decorated descent object $A$. The category with the same objects, morphism groups*

$$\Gamma\left(\mathscr{G}, \mathscr{M}^{r_B,r_A}_{B,A}\right),$$

*and composition $\star$ is isomorphic, by analysis and synthesis, to the corresponding category of lane-decorated descent objects and their underlying descended morphisms.*

(H4) ***Equivariant refinement.*** *Every certified fine-to-coarse coordinate change from proposition 20.6 commutes with the transition maps $\gamma_*$. It therefore defines an isomorphism of matrix local systems. These isomorphisms compose strictly over chains of declared resolutions and intertwine twisted matrix contraction.*

(H5) ***Holonomy-compatible selectors and residuals.*** *Let*

$$E_U \subseteq I_{Y,U,u} \times I_{X,U,r}$$

*be a family satisfying*

$$E_V = (\lambda^Y_{\gamma,u} \times \lambda^X_{\gamma,r})(E_U)$$

*for every arrow $\gamma : U \to V$. Then the local selectors*

$$C_{E_U}(h_U)_{ai} = \begin{cases} h_{U,ai}, & (a,i) \in E_U, \\ 0, & (a,i) \notin E_U \end{cases}$$

*assemble to an idempotent endomorphism $C_E$ of the section group. For two compatible support families $E, F$,*

$$C_E C_F = C_{E \cap F}, \qquad R_E := 1 - C_E, \qquad h = C_E h + R_E h.$$

*Hence named residuals remain exact under arbitrary finite address holonomy, provided the retained support itself is holonomy compatible.*

*Proof.* For (H1), additivity and invertibility follow from the corresponding properties of $F_\gamma$ and the splitting comparisons $\beta$. The address and splitting cocycle laws give $(\delta\gamma)_* = \delta_* \gamma_*$ after the declared transition comparisons.

For (H2), let $f = (f_U)_U$ be descended. For a transition $\gamma : U \to V$, the transported $(a,i)$-block is

$$\begin{aligned} &\beta^Y_{\gamma,u,a} F_\gamma\left(\pi^u_{Y,U,a} f_U \iota^r_{X,U,i}\right) \left(\beta^X_{\gamma,r,i}\right)^{-1} \\ &\quad = \pi^u_{Y,V,\lambda^Y(a)} \theta^Y_\gamma F_\gamma(f_U) (\theta^X_\gamma)^{-1} \iota^r_{X,V,\lambda^X(i)} \\ &\quad = \pi^u_{Y,V,\lambda^Y(a)} f_V \iota^r_{X,V,\lambda^X(i)}, \end{aligned}$$

which is the corresponding block of $f_V$. Thus analysis produces a compatible section.

Conversely, let $h = (h_U)_U$ be a compatible section and synthesize

$$f_U := \sum_{a,i} \iota^u_{Y,U,a} h_{U,ai} \pi^r_{X,U,i}.$$

Transporting this sum, applying the splitting comparison identities, and reindexing through the address bijections gives $f_V$. Thus $(f_U)_U$ is a descended morphism. Chartwise analysis and synthesis are mutually inverse by theorem 20.3; therefore their restrictions to compatible families are mutually inverse.

For (H3), the local path law gives the displayed contraction formula in every chart. Applying $\gamma_*$ to a contracted block distributes over the finite sum and carries each product to the product of the transported blocks. Since $\lambda^Y_{\gamma,u}$ is a bijection, reindexing the intermediate address shows

$$\gamma_*(k_U \star h_U) = (\gamma_* k_U) \star (\gamma_* h_U) = k_V \star h_V.$$

The identity section is compatible by the splitting cocycle. The equivalence then follows from (H2).

For (H4), the local fine-to-coarse coordinate map is analysis after synthesis. Both operations commute with transition by (H2), so their composite does as well. The strict composition and contraction identities are the corresponding chartwise identities from corollary 20.7 and theorem 20.11.

For (H5), support compatibility implies $\gamma_* C_{E_U} = C_{E_V} \gamma_*$, so the selectors preserve compatible sections. Every Boolean and residual identity is then checked chartwise. □

**Corollary 21.4** (Base-fiber invariant normal form)**.** *Fix a base chart $U_0$. Evaluation at $U_0$ induces an isomorphism*

$$\Gamma\left(\mathscr{G}, \mathscr{M}^{u,r}_{Y,X}\right) \xrightarrow{\sim} \mathscr{M}^{u,r}_{Y,X}(U_0)^{\mathrm{Aut}_{\mathscr{G}}(U_0)},$$

*where the right-hand side is the subgroup fixed by every loop-transport map. Consequently,*

$$\mathrm{Hom}_{\mathrm{Desc}(\mathscr{G})}(X, Y) \cong \mathscr{M}^{u,r}_{Y,X}(U_0)^{\mathrm{Aut}_{\mathscr{G}}(U_0)}.$$

*After choosing one arrow $\tau_U : U_0 \to U$ for each chart, the inverse sends a fixed base matrix $h_0$ to the section $h_U = (\tau_U)_* h_0$. The result is independent of the chosen arrows because two choices differ by loop transport at $U_0$.*

*Proof.* A compatible section evaluates to a loop-fixed element at $U_0$. Conversely, for an arrow $\gamma : U \to V$, the two arrows $\gamma\tau_U$ and $\tau_V$ differ by a loop at $U_0$; loop invariance therefore gives $\gamma_* h_U = h_V$. Evaluation and this reconstruction are mutually inverse. Compose with the analysis isomorphism in (H2). □

*Remark* 21.5 (What has and has not been removed). The theorem removes only the global address trivializations $\mu^{A,r}_U$ from theorem 20.24. It does not remove the address cocycle, refinement naturality, projector compatibility, splitting comparisons, or additive preservation hypotheses. Without those data, even the matrix transition maps are undefined or fail their cocycle law.

## 21.3 Monodromy orbits and the finest untwisted coarsening

Fix a base chart $U_0$. Every loop $\gamma \in \mathrm{Aut}_{\mathscr{G}}(U_0)$ acts on an address set by $i \mapsto \lambda^A_{\gamma,r}(i)$. Write

$$H^r_A := \mathrm{im}(\mathrm{Aut}_{\mathscr{G}}(U_0) \longrightarrow \mathrm{Sym}(I_{A,U_0,r}))$$

for the resulting finite monodromy group. For a source-target pair, the same loop acts diagonally by

$$(a, i) \longmapsto \left(\lambda^Y_{\gamma,u}(a), \lambda^X_{\gamma,r}(i)\right).$$

Its image in the symmetric group of $I_{Y,U_0,u} \times I_{X,U_0,r}$ is denoted $H^{u,r}_{Y,X}$. This is the simultaneous monodromy image; it need not be the direct product of the two separate monodromy groups.

**Theorem 21.6** (Orbit descent and the finest globally labeled coarsening)**.** *Under the hypotheses of theorem 21.3, the following statements hold.*

(O1) *For every orbit $\mathcal{O} \subseteq I_{A,U_0,r}$ of $H^r_A$, path transport defines a path-independent orbit subset $\mathcal{O}_U \subseteq I_{A,U,r}$ in every chart. The local projector sums*

$$P^r_{A,U,\mathcal{O}} := \sum_{i \in \mathcal{O}_U} p^r_{A,U,i}$$

*descend to a split idempotent on $A$. As $\mathcal{O}$ ranges over the monodromy orbits, these projectors are pairwise annihilating and sum to $1_A$.*

(O2) *The orbit projectors form the finest ordinary globally labeled coarsening whose local projectors are sums of the original lane projectors. More precisely, any globally labeled projector of the form*

$$Q_U = \sum_{i \in S_U} p^r_{A,U,i}$$

*with $S_V = \lambda^A_{\gamma,r}(S_U)$ and with the same global label preserved around every loop has $S_{U_0}$ equal to a union of $H^r_A$-orbits.*

(O3) *A particular local lane descends as an individually labeled global lane exactly when its address is fixed by $H^r_A$. All original lane labels descend simultaneously exactly when the monodromy action on the address set is trivial.*

(O4) *Holonomy-compatible support families in (H5) are in bijection with unions of $H^{u,r}_{Y,X}$-orbits in the base pair-address set. The minimal nonempty compatible supports are therefore the single pair orbits. Their associated selectors need not act nontrivially on the section group: a single-orbit selector is nonzero exactly when that orbit supports a nonzero compatible section.*

(O5) *If $s \succeq r$, equivariance of the refinement map sends every fine monodromy orbit onto a coarse monodromy orbit. For a coarse orbit $\mathcal{O}$,*

$$P^r_{A,\mathcal{O}} = \sum_{\substack{\mathcal{Q} \text{ a fine orbit} \\ \mathcal{Q} \subseteq (\rho^A_{sr})^{-1}(\mathcal{O})}} P^s_{A,\mathcal{Q}}.$$

*Thus orbit descent and projector-sum refinement commute exactly.*

*Proof.* Choose a path from $U_0$ to $U$ and transport $\mathcal{O}$ along its address bijection. Two path choices differ by a loop at $U_0$, which preserves $\mathcal{O}$ setwise. Hence $\mathcal{O}_U$ is path independent. Projector compatibility gives

$$\theta^A_\gamma F_\gamma(P^r_{A,U,\mathcal{O}}) = P^r_{A,V,\mathcal{O}} \theta^A_\gamma,$$

so the orbit sums descend. Their local splittings are the finite direct sums $\bigoplus_{i \in \mathcal{O}_U} A^r_{U,i}$; the direct sums of the $\beta$-maps, with the induced permutation of summands, provide their descent data. This proves (O1).

For (O2), a globally fixed label must return to itself after every loop, so $S_{U_0}$ is invariant under $H^r_A$. Every invariant subset of a finite group action is a union of orbits. Therefore every such globally labeled coarsening is coarser than the orbit partition. Statement (O3) is the singleton case.

The same path-independence argument on the pair-address set shows that a compatible support family is determined by an invariant base subset, and every invariant base subset is a union of pair orbits. A selector acts as the identity on compatible sections supported in its orbit and vanishes on the complementary support. It is therefore nonzero precisely when the orbit supports a nonzero compatible section. This proves (O4).

Finally, equivariance of $\rho_{sr}^{A}$ implies that the image of a fine orbit is the orbit of the image of any one of its points. Hence the preimage of a coarse orbit is a union of fine orbits. Summing the local projector-refinement identity over all addresses in the coarse orbit gives the formula in (O5). □

*Remark* 21.7 (Object orbits and matrix orbits differ). The orbit lanes on an object are controlled by $H_A^r \backslash I_{A,r}$. Transport selectors are controlled by the generally finer orbit set

$$H_{Y,X}^{u,r} \backslash (I_{Y,u} \times I_{X,r}).$$

Even when an object has only one transitive address orbit, its endomorphism matrices can have several pair orbits. Holonomy can therefore erase individual object labels while retaining a nontrivial global transport algebra.

## 21.4 Permutation modules and the orbital path algebra

The one-chart groupoid with automorphism group $H$ gives a concrete exact model. It also identifies the algebra carried by the pair-orbit selectors.

**Theorem 21.8** (Permutation-module orbital lane calculus)**.** *Let $\Bbbk$ be a commutative ring, let a finite group $H$ act on finite sets $I, J, K$, and let $\Bbbk[I], \Bbbk[J], \Bbbk[K]$ be the corresponding permutation modules. For an orbit $\mathcal{O} \subseteq J \times I$ under the diagonal action, let $B_{\mathcal{O}} : \Bbbk[I] \to \Bbbk[J]$ be the matrix whose $(j,i)$-entry is one when $(j,i) \in \mathcal{O}$ and zero otherwise. Then*

$$\mathrm{Hom}_{\Bbbk H}(\Bbbk[I], \Bbbk[J]) = \bigoplus_{\mathcal{O} \in H\backslash(J\times I)} \Bbbk B_{\mathcal{O}}.$$

*In particular, an equivariant matrix is exactly a matrix constant on every pair orbit.*

*Let*

$$\mathcal{P} \subseteq J \times I, \qquad \mathcal{Q} \subseteq K \times J, \qquad \mathcal{R} \subseteq K \times I$$

*be diagonal $H$-orbits. For any $(k,i) \in \mathcal{R}$, define*

$$c_{\mathcal{Q},\mathcal{P}}^{\mathcal{R}} := \#\{j \in J : (k,j) \in \mathcal{Q}, (j,i) \in \mathcal{P}\}.$$

*This integer is independent of the chosen $(k,i) \in \mathcal{R}$, and*

$$B_{\mathcal{Q}} B_{\mathcal{P}} = \sum_{\mathcal{R} \in H\backslash(K\times I)} c_{\mathcal{Q},\mathcal{P}}^{\mathcal{R}} B_{\mathcal{R}}.$$

*Thus the lane path law descends to an exact orbit basis with nonnegative integer structure constants.*

*Proof.* Write an arbitrary $\Bbbk$-linear map as a matrix $A = (A_{ji})$. The intertwining equations for the permutation actions are equivalent to

$$A_{hj,hi} = A_{ji} \qquad (h \in H).$$

Hence the entries are constant on diagonal orbits. The orbit-indicator matrices have disjoint supports, so they are linearly independent over every commutative ring and span all invariant matrices.

The $(k,i)$-entry of $B_{\mathcal{Q}} B_{\mathcal{P}}$ is the displayed cardinality. If $(k',i') = (hk, hi)$, then $j \mapsto hj$ is a bijection between the two sets being counted. The entry is therefore constant on $\mathcal{R}$, which gives the orbit-basis expansion. □

**Corollary 21.9** (Orbital endomorphism algebra)**.** *For one finite $H$-set $I$, the pair-orbit matrices form a basis of* $\mathrm{End}_{\Bbbk H}(\Bbbk[I])$*. Matrix multiplication in this basis is exactly the finite compatible-path contraction of theorem 21.3, with the preceding intersection numbers as structure constants.*

**Example 21.10** (The smallest nontrivial holonomy)**.** Let $H = C_2 = \{1, \sigma\}$ act on $I = \{1, 2\}$ by swapping the two addresses. On $X = \Bbbk^2$, let

$$S = \begin{pmatrix} 0 & 1 \\ 1 & 0 \end{pmatrix}, \qquad p_1 = \begin{pmatrix} 1 & 0 \\ 0 & 0 \end{pmatrix}, \qquad p_2 = \begin{pmatrix} 0 & 0 \\ 0 & 1 \end{pmatrix}.$$

The individual projectors do not descend because $Sp_1S^{-1} = p_2$, while their orbit sum $p_1 + p_2 = 1$ does descend. The pair-address set has two orbits,

$$\Delta = \{(1,1), (2,2)\}, \qquad \Omega = \{(1,2), (2,1)\}.$$

Accordingly,

$$\mathrm{End}_{\Bbbk C_2}(\Bbbk^2) = \left\{ \begin{pmatrix} a & b \\ b & a \end{pmatrix} : a, b \in \Bbbk \right\} = \Bbbk B_\Delta \oplus \Bbbk B_\Omega.$$

The singleton endpoint selector $\{(1,1)\}$ is not holonomy compatible and sends the equivariant identity matrix to $p_1$, which is not equivariant. The orbit selectors $C_\Delta$ and $C_\Omega$ are compatible and split every equivariant endomorphism into its diagonal-orbit and off-diagonal-orbit parts.

## 21.5 Cyclotomic orbit lanes over the rational field

The split cyclic group algebra supplies an arithmetic realization in which the address monodromy and its orbit coarsening are explicit.

**Proposition 21.11** (Rational descent of split cyclic Fourier lanes)**.** *Let $N \geq 1$, let $C_N = \langle g \rangle$, and let $K = \mathbb{Q}(\zeta_N)$. In $K[C_N]$, define*

$$e_j := \frac{1}{N} \sum_{\ell=0}^{N-1} \zeta_N^{-j\ell} g^\ell, \qquad j \in \mathbb{Z}/N\mathbb{Z}.$$

*These are the primitive split Fourier idempotents. For $\sigma_a \in \mathrm{Gal}(K/\mathbb{Q})$, where $\sigma_a(\zeta_N) = \zeta_N^a$,*

$$\sigma_a(e_j) = e_{aj}.$$

*The Galois orbits are indexed by divisors $q \mid N$, with*

$$\mathcal{O}_q = \left\{ j \in \mathbb{Z}/N\mathbb{Z} : \frac{N}{\gcd(N, j)} = q \right\}.$$

*Their orbit sums*

$$E_q := \sum_{j \in \mathcal{O}_q} e_j$$

*belong to $\mathbb{Q}[C_N]$ and satisfy*

$$E_q E_{q'} = \delta_{q,q'} E_q, \qquad \sum_{q \mid N} E_q = 1.$$

*More explicitly,*

$$\boxed{E_q = \frac{1}{N} \sum_{\ell=0}^{N-1} c_q(\ell) g^\ell,}$$

*where*

$$c_q(\ell) := \sum_{\substack{1\le a\le q\\ \gcd(a,q)=1}} e^{2\pi i a\ell/q} = \sum_{d\mid \gcd(q,\ell)} d\,\mu(q/d) \in \mathbb{Z}$$

*is the Ramanujan sum. The projectors $(E_q)_{q|N}$ form the finest $\mathbb{Q}$-rational coarsening obtainable by summing the split Fourier idempotents, and*

$$\mathbb{Q}[C_N]E_q \cong \mathbb{Q}(\zeta_q).$$

*Proof.* Character orthogonality gives the primitive idempotent relations for the $e_j$. Applying $\sigma_a$ to their coefficients gives $\sigma_a(e_j) = e_{aj}$. The unit group $(\mathbb{Z}/N\mathbb{Z})^\times$ acts transitively on elements of $\mathbb{Z}/N\mathbb{Z}$ having the same additive order, so its orbits are the sets $\mathcal{O}_q$.

Write every $j \in \mathcal{O}_q$ uniquely as $j = (N/q)a$ with $a \in (\mathbb{Z}/q\mathbb{Z})^\times$. The coefficient of $g^\ell$ in $E_q$ is then

$$\frac{1}{N}\sum_{a\in(\mathbb{Z}/q\mathbb{Z})^\times} \zeta_q^{-a\ell} = \frac{c_q(\ell)}{N},$$

where the last equality uses the integrality and evenness of the Ramanujan sum. Hence $E_q \in \mathbb{Q}[C_N]$. Orthogonality and completeness follow by grouping the primitive $e_j$ by their disjoint Galois orbits. Any rational sum of split primitive idempotents must be Galois invariant, so its support is a union of these orbits; this proves fineness. Finally,

$$\mathbb{Q}[C_N] \cong \mathbb{Q}[x]/(x^N-1) \cong \prod_{q|N}\mathbb{Q}[x]/(\Phi_q(x)) \cong \prod_{q|N}\mathbb{Q}(\zeta_q),$$

and $E_q$ is the identity projector of the $q$-th factor. □

*Boundary* 21.12 (Cyclic character lanes are not coefficient-residue lanes). The preceding proposition concerns primitive character idempotents in the split group algebra $K[C_N]$ and their rational Galois descent. The coefficient-residue projectors $\mathcal{P}_{N,j}$ on formal series from theorem 20.15 are defined coefficientwise over every commutative ring and already have fixed residue labels. A chosen rotation representation relates the two constructions after scalar extension, but their descent data are not identical and should not be conflated. Nothing in orbit descent turns the factorial step-product into an additive idempotent splitting.

## 21.6 Exact finite validation and scope

The accompanying verifier tests finite permutation actions, pair-orbit bases, equivariant matrix composition, orbit-compatible and deliberately incompatible selectors, equivariant refinement, and the exact Ramanujan-sum projectors in $\mathbb{Q}[C_N]$. It uses exact integer arithmetic after clearing the common cyclotomic denominators. These tests are an implementation regression for the displayed formulas, not a substitute for the proofs and not an external validation record.

**Holonomy-twisted lane transport result.** Finite nontrivial address holonomy does not invalidate exact lane transport. The complete global coordinate object is a matrix local system, and descended morphisms are exactly its compatible sections. Composition remains finite path contraction, complete resolution changes remain isomorphisms, and every holonomy-compatible selector retains an exact named residual. Monodromy orbits give the finest ordinary globally labeled coarsening of object lanes, while simultaneous pair orbits give the atomic global transport selectors. In permuta-

**Table 42:** Exact finite regression for selected holonomy-twisted lane clauses. The table is an implementation record, not a proof or external validation.

| Validation family | Exact assertions |
|---|---|
| Group actions and object-orbit descent | 7,780 |
| Pair-orbit partitions and intertwiner bases | 3,537 |
| Orbital path composition and structure constants | 1,212,963 |
| Compatible selectors and negative controls | 994 |
| Equivariant refinement and orbit-projector sums | 10,162 |
| Rational cyclotomic orbit projectors | 109,374 |
| Theorem-source contract | 13 |
| Total selected implementation assertions | 1,344,823 |
| Recorded failures | 0 |

tion modules these pair orbits form an exact basis of the intertwiner space with integer path-count structure constants.

*Boundary* 21.13 (Finite twisted scope). The theorem remains finite and profiled. It assumes invertible chart transitions, finite address sets, coherent address and splitting cocycles, and profile preservation of the operations used. It does not prove convergence for countably infinite lane sums, descent across noninvertible bridges, higher stack effectivity, or a canonical orbit system independent of the initially declared lane presentation. Orbit count is not identified with dimension, rank, entropy, information, or complexity. The permutation-module and cyclotomic formulas have classical algebraic antecedents; their role here is to provide exact native realizations of the twisted lane doctrine.

# Part IV

# Relative semantic quotients and changes of doctrine

## 22 Relative semantic quotients and behavioral cores

The preceding parts fix resolved signatures, profile-preserving realizations, normalized strata, typed bridges, and descent data. A second question remains inside each such setting: which distinctions must a representation retain for a declared family of future observations? This section formalizes that question without replacing the existing preservation-profile machinery. The central object is a behavioral quotient computed relative to a carrier doctrine, a continuation grammar, and an observation category.

### 22.1 Semantic slices and resolved observational systems

**Definition 22.1** (Semantic slice)**.** A *semantic slice* is a tuple

$$\Sigma = (\mathcal{A}, \mathcal{G}, \mathcal{V}, \mathcal{O})$$

consisting of:

(i) a carrier doctrine $\mathcal{A}$, which specifies how alternatives, routes, or packets combine;

(ii) a continuation grammar $\mathcal{G}$, presented here by a monoid $M$ or by a chosen generating family of admissible endomorphisms;

(iii) an observation category $\mathcal{V}$, such as **Set**, $R$-**Mod**, or $K$-**Vect**;

(iv) a declared family $\mathcal{O} = (o_j)_{j\in J}$ of observations in $\mathcal{V}$.

The slice belongs to the stratum passport. It does not replace the preservation profile $\Pi$. The profile specifies which constructions a bridge preserves, while the slice specifies which future distinctions define the current semantic task.

**Definition 22.2** (Resolved observational system)**.** Let $X$ be an object equipped with an action

$$\rho : M \longrightarrow \mathrm{End}(X)$$

of a continuation monoid and with observations

$$o_j : X \longrightarrow Y_j \qquad (j \in J).$$

The tuple

$$\mathsf{S} = (X, M, \rho, (o_j)_{j\in J})$$

is a *resolved observational system*. When the indicated product exists, its behavior map is

$$\mathrm{Beh}_{\mathsf{S}} : X \longrightarrow \prod_{(m,j)\in M\times J} Y_j, \qquad x \longmapsto \big(o_j(\rho(m)x)\big)_{m,j}.$$

The *relative behavioral object* is the coimage

$$Q_{\mathsf{S}} := \mathrm{Coim}(\mathrm{Beh}_{\mathsf{S}})$$

whenever that coimage exists.

In **Set**, the behavior map identifies states exactly when every declared future observation agrees. In a module category, the same object can be constructed directly from the intersection of kernels, without assuming that the possibly infinite product is part of the ambient profile.

**Definition 22.3** (Behavioral congruence and linear behavioral kernel)**.** In **Set** or a variety of algebras, put

$$x \equiv_{\mathsf{S}} y \quad\Longleftrightarrow\quad o_j(\rho(m)x) = o_j(\rho(m)y) \quad \text{for every } m \in M,\ j \in J.$$

Write $\Theta_{\mathsf{S}}$ for this relation. In $R$-**Mod**, define

$$N_{\mathsf{S}} := \bigcap_{m\in M}\bigcap_{j\in J} \ker(o_j\rho(m)).$$

Then

$$Q_{\mathsf{S}} = X/N_{\mathsf{S}}.$$

**Theorem 22.4** (Universal behavioral coimage)**.** *Assume the relevant effective quotient or module quotient exists. Then $Q_{\mathsf{S}}$ preserves every declared future observation. Moreover, if*

$$q : X \twoheadrightarrow Z$$

*is any surjective representation through which every map $o_j\rho(m)$ factors, there is a unique map*

$$\overline{q} : Z \longrightarrow Q_{\mathsf{S}}$$

*with $\overline{q}\,q : X \to Q_{\mathsf{S}}$ equal to the canonical quotient map. Thus $Q_{\mathsf{S}}$ is the coarsest exact representation for the declared semantic slice.*

*Proof.* In the relational setting, the kernel pair of $q$ is contained in $\Theta_S$, because equality under $q$ forces equality under every factorized future observation. The universal property of the quotient by $\Theta_S$ gives the unique map. In the module setting,

$$\ker q \subseteq \bigcap_{m,j} \ker(o_j \rho(m)) = N_S,$$

so the ordinary quotient universal property gives the same conclusion. □

*Boundary* 22.5 (No observer-independent minimum). The phrase "minimal representation" is meaningful only after the carrier, continuation grammar, observation category, and task have been declared. Changing any one of these data can change the quotient. In particular, equality of residual functions in **Set** and linear dependence of residual functions in $K$-**Vect** are different minimization problems.

## 22.2 The maximal stable invisible core

Let

$$K_0 := \bigcap_j \mathrm{KerPair}(o_j)$$

in the relational setting and

$$N_0 := \bigcap_j \ker(o_j)$$

in the linear setting.

**Theorem 22.6** (Behavioral core theorem)**.** *The behavioral relation $\Theta_S$ is the greatest continuation-stable congruence contained in $K_0$. In the module setting, $N_S$ is the greatest $\rho(M)$-invariant submodule contained in $N_0$.*

*Proof.* The identity continuation gives $\Theta_S \subseteq K_0$ and $N_S \subseteq N_0$. If $x \equiv_S y$, then for every $n, m \in M$ and every $j$,

$$o_j\rho(m)\rho(n)x = o_j\rho(mn)x = o_j\rho(mn)y = o_j\rho(m)\rho(n)y,$$

so the relation is stable. The same calculation proves invariance of $N_S$.

Conversely, let $R \subseteq K_0$ be continuation stable. If $xRy$, then $\rho(m)x\, R\, \rho(m)y$ for every $m$, and membership in $K_0$ forces

$$o_j\rho(m)x = o_j\rho(m)y$$

for every $j$. Hence $R \subseteq \Theta_S$. The submodule statement is identical with relations replaced by differences. □

*Remark* 22.7 (Comparison with holonomy). The maximal path-flat core in Section 4 intersects fixed spaces of closed transport words. The behavioral core intersects kernels of future observation words. Both constructions extract the greatest subobject on which a declared family of transformations becomes semantically invisible. They answer different questions and are not identified without a typed comparison map.

## 22.3 Greatest-fixed-point construction and finite recognition

Assume $M$ is generated by a family $A$. On congruences or submodules define

$$\Phi(R) := K_0 \cap \bigcap_{a \in A} \rho(a)^{-1}(R),$$

with the corresponding submodule formula in the linear setting.

**Theorem 22.8** (Coinductive characterization)**.** *The behavioral core is the greatest fixed point of* $\Phi$*:*

$$\Theta_S = \nu R.\Phi(R), \qquad N_S = \nu N.\Phi(N).$$

*Proof.* Every fixed point is invisible and stable under every generator, hence under the generated monoid, so it is contained in the behavioral core by theorem 22.6. Conversely, the behavioral core is a fixed point: stability gives its inclusion in its image under $\Phi$, while membership in $\Phi$ of that core makes the identity observation invisible and makes every first-generator successor behaviorally invisible, hence makes every continuation word invisible. Its maximality therefore proves the asserted greatest-fixed-point identities. □

**Corollary 22.9** (Finite certification)**.** *For finite $X$, descending partition refinement stabilizes after finitely many strict refinements. For finite-dimensional $X$ over a field, the chain*

$$N^{(0)} = N_0, \qquad N^{(r+1)} = N_0 \cap \bigcap_{a \in A} \rho(a)^{-1}(N^{(r)})$$

*stabilizes after at most* $\dim X$ *strict dimension drops. At stabilization it equals* $N_S$*.*

*Proof.* The iteration is descending and every strict inclusion of finite-dimensional subspaces lowers dimension by at least one. The behavioral core lies in $N^{(0)}$, and monotonicity of $\Phi$, together with its fixed-point property, preserves this inclusion at every stage. Thus the stabilized fixed point contains the behavioral core. Greatest-fixed-point maximality gives the reverse inclusion, proving equality. □

## 22.4 The task–congruence Galois connection

Fix a universe $\mathcal{Q}(X)$ of admissible queries on $X$. For $\mathcal{Q} \subseteq \mathcal{Q}(X)$, define

$$\mathrm{Ind}(\mathcal{Q}) := \bigcap_{q \in \mathcal{Q}} \mathrm{KerPair}(q).$$

For an equivalence relation or congruence $R$, define

$$\mathrm{Def}(R) := \{q \in \mathcal{Q}(X) : R \subseteq \mathrm{KerPair}(q)\}.$$

**Theorem 22.10** (Task–congruence Galois connection)**.** *For every query family $\mathcal{Q}$ and relation $R$,*

$$\mathcal{Q} \subseteq \mathrm{Def}(R) \quad \Longleftrightarrow \quad R \subseteq \mathrm{Ind}(\mathcal{Q}).$$

*Consequently,*

$$\mathrm{Cl}(\mathcal{Q}) := \mathrm{Def}(\mathrm{Ind}(\mathcal{Q}))$$

*is a closure operator on query families, and*

$$\mathrm{Sat}(R) := \mathrm{Ind}(\mathrm{Def}(R))$$

*is the observational saturation of $R$ relative to the admitted query universe.*

*Proof.* Both conditions say that every query in $\mathcal{Q}$ is constant on every $R$-class. The closure laws follow from the standard identities associated with an antitone Galois connection. □

**Definition 22.11** (Extensional task)**.** An *extensional task* is a closed query theory, equivalently a query family modulo equality of the closure Cl. When the admitted query universe separates the desired quotients, an extensional task can equivalently be represented by its observationally definable congruence.

**Corollary 22.12** (Task strengthening)**.** *Adding continuations or observations can only refine behavioral indistinguishability. Thus*

$$M \subseteq M', \qquad \mathcal{O} \subseteq \mathcal{O}' \quad \Longrightarrow \quad \Theta_{M',\mathcal{O}'} \subseteq \Theta_{M,\mathcal{O}},$$

*and there is a canonical forgetting map*

$$Q_{M',\mathcal{O}'} \longrightarrow Q_{M,\mathcal{O}}.$$

*Boundary* 22.13 (Definable tasks form a closure system). All continuation-stable congruences form a complete lattice. Congruences definable by the chosen query universe are always closed under arbitrary meets. Closure under joins requires an additional richness or quotient-completeness hypothesis on the query universe and is not asserted automatically.

## 22.5 Semantic quotient lattice

**Theorem 22.14** (Semantic quotient classification, classical)**.** *Let $X$ be an algebra in a variety. Surjective semantic maps*

$$q : X \twoheadrightarrow Q$$

*up to isomorphism of codomains are classified by congruences on $X$ through*

$$q \longmapsto \ker q.$$

*Moreover, a quotient $q$ maps to a quotient $r$ exactly when* $\ker q \subseteq \ker r$.

*Proof.* This is the first isomorphism theorem and the universal property of quotient algebras. It is included to fix the direction of the information order used below. □

**Corollary 22.15** (Combined and shared semantics)**.** *For semantic quotients with kernels $N$ and $M$:*

(i) *the least common refinement has kernel $N \cap M$;*

(ii) *the greatest common coarsening has kernel the generated congruence join $N \vee M$;*

(iii) *in a module category, $N \vee M = N + M$.*

## 22.6 The two-view semantic diamond

Let $X$ be an $R$-module and let

$$s : X \twoheadrightarrow S, \qquad t : X \twoheadrightarrow T$$

be surjective linear semantic maps. Put

$$N = \ker s, \qquad M = \ker t, \qquad J = X/(N \cap M), \qquad C = X/(N + M).$$

**Theorem 22.16** (Semantic diamond and exact compatibility sequence)**.** *The canonical square*

$$\begin{array}{ccc} J & \longrightarrow & T \\ \downarrow & & \downarrow \\ S & \longrightarrow & C \end{array}$$

*is a pullback in* $R$-**Mod**. *Equivalently,*

$$J \cong S \times_C T.$$

*There is also a canonical short exact sequence*

$$0 \longrightarrow X/(N \cap M) \xrightarrow{\alpha} X/N \oplus X/M \xrightarrow{\beta} X/(N+M) \longrightarrow 0,$$

*where*

$$\alpha(x + N \cap M) = (x + N, x + M)$$

*and*

$$\beta(a + N, b + M) = a - b + (N + M).$$

*Proof.* The map $\alpha$ is injective because its kernel is $N \cap M$. The formula for $\beta$ is well defined and surjective. Clearly $\beta\alpha = 0$. If $\beta(a + N, b + M) = 0$, then

$$a - b = n + m$$

for some $n \in N$ and $m \in M$. Set $x = a - n = b + m$. Then

$$(a + N, b + M) = (x + N, x + M) = \alpha(x + N \cap M).$$

Thus $\ker \beta = \operatorname{im} \alpha$, proving exactness. The kernel description of the fiber product is the same calculation. □

**Definition 22.17** (Relative semantic residual)**.** The information needed to augment $S$ so that it also retains $T$ is

$$R_{T|S} := \ker(J \to S) \cong N/(N \cap M) \cong (N + M)/M.$$

**Corollary 22.18** (Factorization criterion)**.** *The following are equivalent:*

$$t \text{ factors through } s, \qquad N \subseteq M, \qquad R_{T|S} = 0, \qquad J \to S \text{ is an isomorphism.}$$

*Moreover,*

$$0 \longrightarrow R_{T|S} \longrightarrow J \longrightarrow S \longrightarrow 0$$

*is exact.*

*Boundary* 22.19 (Residuals need not split). The exact sequence above does not canonically identify $J$ with $S \oplus R_{T|S}$. Vector-space extensions split noncanonically. Module, integral, semiring, filtered, or topological extensions may fail to split. A residual packet presented as an independent coordinate therefore requires an explicit splitting theorem or constructor passport.

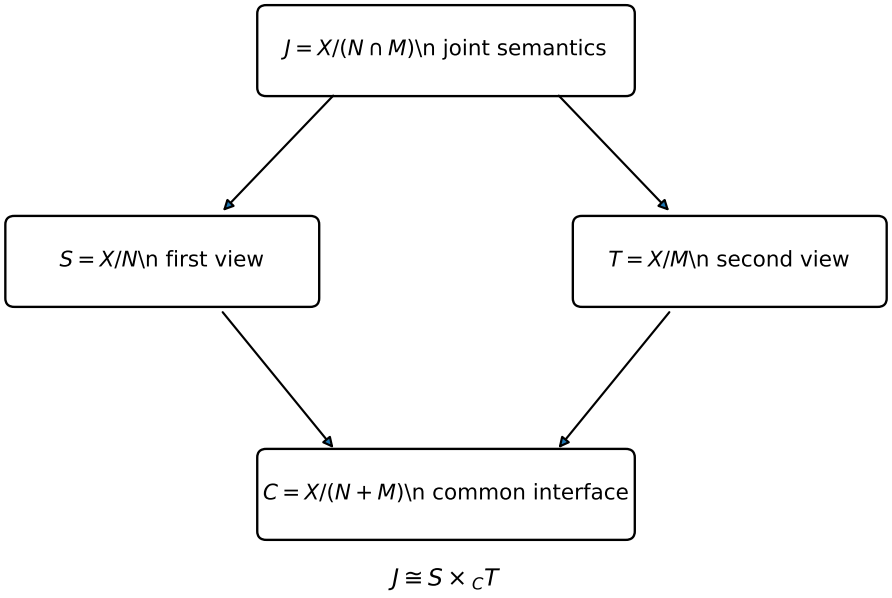



**Figure 57:** The semantic diamond. The joint representation $J$ retains both views. The common quotient $C$ is the compatibility interface over which the separate coordinates glue.

## 22.7 Exact change of task

**Theorem 22.20** (Task-change exact sequence)**.** *Let a stronger task have behavioral kernel $N_s$, and let a weaker task have behavioral kernel $N_w$, with*

$$N_s \subseteq N_w.$$

*Then*

$$0 \longrightarrow N_w/N_s \longrightarrow X/N_s \longrightarrow X/N_w \longrightarrow 0$$

*is exact. Thus $N_w/N_s$ is the exact semantic information discarded when the task is weakened.*

*Proof.* Apply the third isomorphism theorem to the chain $N_s \subseteq N_w \subseteq X$. □

**Corollary 22.21** (Composition of task loss)**.** *For*

$$N_1 \subseteq N_2 \subseteq N_3,$$

*there is an exact sequence*

$$0 \longrightarrow N_2/N_1 \longrightarrow N_3/N_1 \longrightarrow N_3/N_2 \longrightarrow 0.$$

*Hence task loss composes as extension data rather than as a canonically split sum.*

**Semantic quotient result.** Inside a fixed doctrine, declared future tasks are represented by continuation-stable congruences or subobjects. Behavioral minimization extracts the maximal stable invisible core. Task strengthening induces canonical forgetting maps, joint tasks form semantic diamonds, and relative task loss is measured by exact quotient objects. The construction is relative to the semantic slice and does not define an observer-independent minimum.

# 23 Carrier change, observer base change, and provenance

A behavioral quotient is computed inside an observation category, but the represented computation also has a carrier algebra. Additive convolution, Boolean support, max-plus aggregation, and convex support geometry do not combine routes by the same law. This section separates carrier translation from observer minimization and gives exact obstruction objects for both.

## 23.1 Carrier factorization and joint semantic completion

Let $\mathcal{R}$ be a raw algebra of expressions or histories for a fixed operation signature. Let

$$s : \mathcal{R} \longrightarrow S, \qquad t : \mathcal{R} \longrightarrow T$$

be homomorphisms into two semantic carriers.

**Theorem 23.1** (Carrier factorization gate)**.** *There is a unique homomorphism*

$$\varphi : \mathrm{im}(s) \longrightarrow T$$

*with $t = \varphi s$ if and only if*

$$\mathrm{KerPair}(s) \subseteq \mathrm{KerPair}(t).$$

*When the condition fails, any pair $x, y \in \mathcal{R}$ satisfying*

$$s(x) = s(y), \qquad t(x) \neq t(y)$$

*is an exact carrier-change obstruction witness.*

*Proof.* Factorization immediately implies constancy of $t$ on every fiber of $s$. Conversely, define

$$\varphi(s(x)) := t(x).$$

The fiber condition makes this well defined. Since both $s$ and $t$ preserve every primitive operation, so does $\varphi$. Uniqueness follows because $s$ is surjective onto its image. □

**Definition 23.2** (Joint semantic completion)**.** Define

$$j = (s, t) : \mathcal{R} \longrightarrow S \times T, \qquad J_{s,t} := \mathrm{im}(j).$$

The projection

$$p_s : J_{s,t} \longrightarrow \mathrm{im}(s)$$

is the *relative completion map* from the joint semantics to the source semantics.

**Theorem 23.3** (Universal joint completion)**.** *The object $J_{s,t}$ is the coarsest quotient of $\mathcal{R}$ preserving both $s$ and $t$. More precisely, if*

$$c : \mathcal{R} \twoheadrightarrow C$$

*admits maps $a : C \to S$ and $b : C \to T$ with $s = ac$ and $t = bc$, then there is a unique map*

$$C \longrightarrow J_{s,t}$$

*compatible with both semantics. Furthermore,*

$$t \text{ factors through } s \iff p_s \text{ is an isomorphism.}$$

*Proof.* The pair $(a, b)$ factors $j$ through $c$, and the image universal property gives the map to $J_{s,t}$. If $t = \varphi s$, then $J_{s,t}$ is the graph of $\varphi$, so $p_s$ is invertible. Conversely, if $p_s$ is invertible, define $\varphi = p_t p_s^{-1}$. □

## 23.2 Behavioral bridges and exact loss

Let $f : X \to Y$ be a linear bridge between observational systems, with behavioral kernels $N_X \subseteq X$ and $N_Y \subseteq Y$.

**Definition 23.4** (Task-compatible bridge)**.** The bridge is *task compatible* when

$$f(N_X) \subseteq N_Y.$$

Equivalently,

$$N_X \subseteq f^{-1}(N_Y).$$

Then there is a unique induced map

$$\overline{f} : X/N_X \longrightarrow Y/N_Y.$$

**Theorem 23.5** (Bridge-loss exact sequence)**.** *For every task-compatible linear bridge, there is an exact sequence*

$$0 \longrightarrow \frac{f^{-1}(N_Y)}{N_X} \longrightarrow \frac{X}{N_X} \xrightarrow{\overline{f}} \frac{Y}{N_Y} \longrightarrow \frac{Y}{N_Y + f(X)} \longrightarrow 0.$$

*Thus*

$$L_f := \frac{f^{-1}(N_Y)}{N_X}$$

*measures source distinctions collapsed by the bridge, while*

$$E_f := \frac{Y}{N_Y + f(X)}$$

*measures target semantic states outside the essential image.*

*Proof.* The kernel of $\overline{f}$ consists of classes $x + N_X$ for which $f(x) \in N_Y$, hence equals $f^{-1}(N_Y)/N_X$. The cokernel of $\overline{f}$ is the quotient of $Y/N_Y$ by $(f(X) + N_Y)/N_Y$, which is $Y/(N_Y + f(X))$. □

**Corollary 23.6** (Exact semantic equivalence gate)**.** *The induced bridge $\overline{f}$ is an isomorphism exactly when*

$$L_f = 0 \qquad \textit{and} \qquad E_f = 0.$$

*Faithfulness on the declared task and essential surjectivity on the declared task are therefore independent obligations.*

**Theorem 23.7** (Loss-composition extension)**.** *For induced quotient maps*

$$Q_X \xrightarrow{\overline{f}} Q_Y \xrightarrow{\overline{g}} Q_Z,$$

*there is a natural exact sequence*

$$0 \longrightarrow \ker \overline{f} \longrightarrow \ker(\overline{g}\,\overline{f}) \longrightarrow \ker \overline{g} \cap \operatorname{im} \overline{f} \longrightarrow 0.$$

*If $\overline{f}$ is surjective, this reduces to*

$$0 \longrightarrow L_f \longrightarrow L_{gf} \longrightarrow L_g \longrightarrow 0.$$

*Proof.* Map $x \in \ker(\overline{g}\,\overline{f})$ to $\overline{f}(x)$. Its image is exactly $\ker \overline{g} \cap \operatorname{im} \overline{f}$, and its kernel is $\ker \overline{f}$. Surjectivity of $\overline{f}$ identifies the intersection with $\ker \overline{g}$. □

*Boundary* 23.8 (Loss is extension data). The preceding sequence need not split. Consequently, composite information loss is not in general a scalar sum or a canonical direct sum of stagewise losses. A numerical loss budget may be useful, but it is a further invariant of the exact extension rather than a replacement for it.

## 23.3 Carrier-indexed observer packets

**Theorem 23.9** (Carrier-indexed observer packet theorem)**.** *Let $S$ be a finite continuation-state set, let $(A, \oplus, 0)$ be a commutative monoid, let $B$ be a finite branch alphabet, and let*

$$\delta : S \times B \longrightarrow S$$

*be a state transition. Suppose every branch $b \in B$ acts by a monoid homomorphism*

$$L_b : A \longrightarrow A.$$

*Take an empty aggregation to be $0$. For a state packet $a = (a_s)_{s \in S}$, define*

$$a'_t := \bigoplus_{\delta(s,b)=t} L_b(a_s).$$

*If a finite family of raw histories has already been aggregated by their state using $\oplus$, then this update gives exactly the same result as advancing every raw history separately and aggregating afterward.*

*Proof.* Expand the raw history update and group all terms by their predecessor state and new branch. Associativity and commutativity permit the regrouping. The identity

$$L_b\left(\bigoplus_i x_i\right) = \bigoplus_i L_b(x_i)$$

then moves aggregation through the branch action. The displayed formula is the resulting statewise sum. □

Two important realizations have the same state skeleton but different carriers.

1. For convex value semantics, $A$ is the family of compact convex sets, including the empty set, $\oplus$ is convex hull of union with identity $\varnothing$, and $L_b(C) = A_b^{\mathsf{T}} C$.
2. For linear polyphase routing, $A$ is an additive convolution algebra, $\oplus$ is coefficient addition, and $L_b$ multiplies route kernels by the declared filter or transition weight.

The theorem transports the observer skeleton only after the carrier law and the homomorphism obligations are specified.

## 23.4 Carrier no-go mechanisms

**Theorem 23.10** (Cancellation barrier)**.** *Let $R$ be a nonzero ring and let $S$ be a nontrivial zerosumfree semiring, so*

$$a + b = 0 \Longrightarrow a = b = 0.$$

*There is no unital semiring homomorphism $R \to S$.*

*Proof.* A unital homomorphism $\varphi$ would give

$$0 = \varphi(1 + (-1)) = 1_S + \varphi(-1).$$

Zerosumfreeness forces $1_S = 0$, contradicting nontriviality. □

**Theorem 23.11** (Idempotence barrier)**.** *Let $S$ be a nontrivial unital semiring with idempotent addition, and let $R$ be an additively cancellative nontrivial semiring. There is no unital semiring homomorphism $S \to R$.*

*Proof.* In $S$, $1 + 1 = 1$. Its image in $R$ would satisfy $1_R + 1_R = 1_R$, and additive cancellation would imply $1_R = 0$. □

**Example 23.12** (Haar cancellation)**.** For the normalized Haar bank,

$$\ell = \frac{x_0 + x_1}{\sqrt{2}}, \qquad d = \frac{x_0 - x_1}{\sqrt{2}},$$

and

$$x_0 = \frac{\ell + d}{\sqrt{2}}, \qquad x_1 = \frac{\ell - d}{\sqrt{2}}.$$

At $x = (1, 0)$, the two route contributions to $x_0$ are $1/2, 1/2$, while those to $x_1$ are $1/2, -1/2$. Additive reconstruction returns $(1, 0)$. Replacing route addition by maximum returns $(1/2, 1/2)$. The convex/max carrier is therefore not an exact replacement for the signed additive carrier.

## 23.5 Observer base change and the relation module

Let $E \subseteq K^M$ be the set of distinct residual future functions of a scalar series or observational system. Set minimization retains the elements of $E$ as distinct states. Free linearization produces the vector space $K^{(E)}$, while linear minimization retains only their span.

**Theorem 23.13** (Observer base-change exact sequence)**.** *The evaluation map*

$$\pi : K^{(E)} \longrightarrow \operatorname{span}_K(E), \qquad \sum_{e \in E} a_e [e] \longmapsto \sum_{e \in E} a_e e$$

*is surjective and fits into the exact sequence*

$$0 \longrightarrow \operatorname{Rel}_K(E) \longrightarrow K^{(E)} \xrightarrow{\pi} \operatorname{span}_K(E) \longrightarrow 0,$$

*where*

$$\operatorname{Rel}_K(E) := \ker \pi$$

*is the module of linear relations among distinct discrete residual states. Hence Set minimization commutes with free linearization exactly when $E$ is linearly independent.*

*Proof.* Surjectivity is the definition of the linear span. The sequence is the kernel-cokernel sequence of $\pi$. The kernel vanishes exactly when the basis symbols $[e]$ remain linearly independent after evaluation. □

**Theorem 23.14** (Exact polyphase separation)**.** *Fix $N \geq 1$ and $z \neq 0$. Let $S_z$ be the cyclic shift on $K^N$ satisfying*

$$S_z e_j = e_{j+1} \quad (j < N - 1), \qquad S_z e_{N-1} = z e_0,$$

*so $S_z^N = zI$. Put*

$$M_N = I + S_z, \qquad f_N(n) = e_0^{\mathsf{T}} M_N^n e_0.$$

*Then the $N \times N$ Hankel block*

$$H_{ij} = f_N(i + j), \qquad 0 \leq i, j < N,$$

*has determinant*

$$\det H = \pm z^{N-1}.$$

*Consequently its linear residual space has dimension $N$. If $z > 0$, the residual functions $k \mapsto f_N(n + k)$ are pairwise distinct, so the exact discrete future quotient is infinite while the linear continuation dimension is $N$.*

*Proof.* Factor $H = OC$, where row $i$ of $O$ is $e_0^{\mathsf{T}} M_N^i$, and column $j$ of $C$ is $M_N^j e_0$. For $j < N$, the binomial expansion of $(I + S_z)^j e_0$ is a unit upper-triangular change from $(e_0, \dots, e_{N-1})$, hence $\det C = 1$. The rows $e_0^{\mathsf{T}} S_z^k$, $0 \le k < N$, are $e_0^{\mathsf{T}}$ followed by $z e_{N-k}^{\mathsf{T}}$, so their determinant is $\pm z^{N-1}$. The binomial row change is also unit triangular, proving the determinant formula.

For positive $z$,

$$f_N(n) = \sum_{r=0}^{\lfloor n/N \rfloor} \binom{n}{Nr} z^r.$$

The sequence is strictly increasing from index $N-1$ onward. Prefixes below $N$ are distinguished by choosing the first suffix that crosses index $N$, and later prefixes differ already at suffix zero. Thus all residual functions are distinct. □

The interpretation of finite Hankel rank as minimal weighted-linear realization dimension is classical weighted-automata theory [20, 21]. The displayed family is retained here because it gives an exact internal example of an infinite discrete quotient and a finite linear quotient.

## 23.6 Observer-conditioned convex packets

Let $S$ be a finite observer-state set, let $B$ be a finite branch alphabet, and let $C_s \subseteq \mathbb{R}^d$ be a compact convex packet for each state, with empty packets allowed. Use the conventions

$$h_\varnothing(x) = -\infty, \qquad \operatorname{conv}(\varnothing) = \varnothing, \qquad \max \varnothing = -\infty.$$

For branch matrices $(A_b)_{b \in B}$ and a transition $\delta : S \times B \to S$, put

$$C'_t = \operatorname{conv} \bigcup_{\delta(s,b)=t} A_b^{\mathsf{T}} C_s.$$

**Theorem 23.15** (Observer-conditioned convex packet transport)**.** *For every state $t \in S$ and direction $x$,*

$$h_{C'_t}(x) = \max_{\delta(s,b)=t} h_{C_s}(A_b x).$$

*Repeated updates compose exactly with branch words. Within each fixed observer state, replacing a finite atom family by any other finite generating family of the same convex hull preserves all future value queries generated by linear branch actions.*

*Proof.* For a linear map $A$,

$$h_{A^{\mathsf{T}} C}(x) = h_C(Ax).$$

If the incoming fiber is empty, both sides of the formula are $-\infty$. Otherwise, the support function of the convex hull of a finite union is the maximum of the component support functions, with the same conventions for empty components. These identities give the formula. Finite unions of compact sets have compact convex hulls in finite dimension, so every updated packet stays in the declared carrier. Iteration follows from composition of the linear maps and of $\delta$. Equality of convex hulls is preserved by linear images and convex hull of union, proving future value equivalence. □

**Proposition 23.16** (Singular resurrection)**.** *A provenance state carried only by a strictly interior atom may be inactive for every current nonzero linear query and yet become active after an admissible singular continuation. In particular, if the zero map is admissible, every atom is sent to the same point and all provenance states tie.*

**Proposition 23.17** (Invertible hiding)**.** *Assume the total convex body is full-dimensional, query directions are nonzero, and every admissible branch matrix is invertible. A strictly interior atom remains strictly interior under every continuation and therefore cannot maximize a nonzero linear functional. Its provenance remains permanently hidden from the declared value query.*

*Proof.* Invertible linear maps preserve relative interior and full dimension. A nonzero linear functional cannot attain its maximum at a strict interior point of a compact full-dimensional convex body. □

*Boundary* 23.18 (Value, witness, and history are distinct tasks). Exact convex geometry determines value semantics and its derived normal-fan structure. It does not determine branch identity, maximizing multiplicity, or raw history. Value-only, one-witness, all-witness, and complete-history tasks therefore have different minimal quotients. No provenance deletion rule is valid without the admissible continuation class and the downstream query family.

**Carrier and observer result.** Exact carrier replacement is equivalent to semantic factorization. When it fails, the joint image is the universal completion preserving both semantics. Behavioral bridges carry independent kernel-loss and essential-image defects. Observer minimization then depends on the observation category: discrete residual equality and linear residual span are related by an exact relation module, not by automatic identification.

## 24 Admissibility change, geometric obstruction, and doctrine lifting

Task strengthening changes which distinctions must be retained. Enlarging an admissible realization class changes a different quantity: which completions or normal forms are allowed. The two variances should not be compressed into one undifferentiated order. This section formalizes admissibility monotonicity, separates gap from nonattainment, and places enrichment problems inside the existing bridge-passport architecture.

### 24.1 Admissible realization classes and optimized defect

**Definition 24.1** (Class-relative defect)**.** Let $X$ be a represented system, let $\Gamma$ be a declared class of admissible auxiliary structures, and let

$$d(X, g) \in [0, \infty]$$

be a defect functional. Define

$$\delta_\Gamma(X) := \inf_{g \in \Gamma} d(X, g).$$

The pair consisting of the infimum and its attainment status is the *class-relative defect profile*.

**Theorem 24.2** (Admissibility monotonicity)**.** *If* $\Gamma \subseteq \Gamma'$*, then*

$$\delta_{\Gamma'}(X) \leq \delta_\Gamma(X).$$

*Thus an obstruction in a restricted realization class need not remain an obstruction after the class is enlarged.*

*Proof.* The infimum on the left is taken over a superset of the candidates used on the right. □

**Definition 24.3** (Completion, gap, and escape)**.** Assume $d \geq 0$. The defect profile is:

(i) a *completion* when $\delta_\Gamma(X) = 0$ and the infimum is attained;

(ii) a *gap obstruction* when $\delta_\Gamma(X) > 0$;

(iii) an *escape obstruction* when $\delta_\Gamma(X) = 0$ but the infimum is not attained.

The trichotomy separates approximation from realization. A sequence of increasingly good coordinates may approach a missing completion only by leaving every compactly controlled part of the admissible parameter space.

**Proposition 24.4** (Compactness certificate for escape)**.** *Let $\Gamma$ be a Hausdorff parameter space, and let $d(X, -)$ be continuous. Suppose every sublevel set satisfying a declared conditioning bound is compact. If $\delta_\Gamma(X) = 0$ is not attained, then every near-minimizing sequence must eventually violate every such uniform conditioning bound.*

*Proof.* Fix a declared conditioning bound $c$, write $\Gamma_c$ for the parameters satisfying it, and let

$$K_c = \{g \in \Gamma_c : d(X, g) \le 1\}.$$

By hypothesis $K_c$ is compact. If $K_c$ is empty, every near-minimizing sequence eventually has defect below 1 and therefore lies outside $\Gamma_c$. Otherwise continuity gives an attained minimum

$$a_c = \min_{g \in K_c} d(X, g).$$

Since the zero infimum is not attained anywhere in $\Gamma$, $a_c > 0$. Every near-minimizing sequence eventually has defect below $\min\{1, a_c\}$, and therefore cannot belong to $\Gamma_c$. Since $c$ was arbitrary, each fixed conditioning bound is eventually violated; in particular no subsequence satisfying one fixed bound can be near-minimizing. □

## 24.2 Metric packets and intrinsic distortion

Let $T : (V, Q_s) \to (W, Q_t)$ be invertible between real or complex spaces of common finite dimension $n \ge 1$ with positive-definite metrics. Choose factors $Q_s = R_s^* R_s$ and $Q_t = R_t^* R_t$, and put

$$B_Q(T) := R_t T R_s^{-1}.$$

Define

$$D_Q(T) := \frac{\sigma_{\max}(B_Q(T))}{\sigma_{\min}(B_Q(T))} \ge 1, \qquad \Delta_Q(T) := \log D_Q(T).$$

**Proposition 24.5** (Coordinate covariance and composition)**.** *Simultaneous coordinate transport of $T, Q_s, Q_t$ leaves $D_Q(T)$ invariant. For composable invertible maps,*

$$D_Q(T_2 T_1) \le D_Q(T_2) D_Q(T_1),$$

*so*

$$\Delta_Q(T_2 T_1) \le \Delta_Q(T_2) + \Delta_Q(T_1).$$

*For a closed word $H$,*

$$D_Q(H) \ge \frac{\max_{\lambda \in \mathrm{spec}(H)} |\lambda|}{\min_{\lambda \in \mathrm{spec}(H)} |\lambda|}.$$

*Proof.* Coordinate transport changes $B_Q(T)$ by left and right unitary factors. Singular-value condition numbers are submultiplicative. The spectral lower bound follows because every eigenvalue modulus lies between the smallest and largest singular values. □

**Theorem 24.6** (Conformal metric-completion criterion)**.** *Let a connected finite graph carry real or complex vector spaces of common dimension $n \geq 1$ and invertible edge transports $T_e$. Reverse traversal of an edge uses $T_e^{-1}$. At a chosen root, determinant-normalized closed holonomy words are*

$$\widehat{H} := |\det H|^{-1/n} H.$$

*They form the determinant-normalized holonomy representation. Positive-definite vertex metrics and positive edge scales satisfying*

$$T_e^* Q_{t(e)} T_e = \lambda_e^2 Q_{s(e)}$$

*exist if and only if the determinant-normalized holonomy representation preserves a positive-definite metric at one root vertex. Equivalently, the normalized holonomy is unitarizable. In finite dimension, this is equivalent to relative compactness of its image.*

*Proof.* A compatible family makes every closed root holonomy $H$ conformal for the root metric $Q_o$. Taking determinants fixes its positive scale as $|\det H|^{1/n}$, so $\widehat{H}$ preserves $Q_o$.

Conversely, suppose every normalized root holonomy preserves $Q_o$. Choose spanning-tree maps $G_v$ from the root to each vertex and put

$$Q_v = (G_v^{-1})^* Q_o G_v^{-1}.$$

For an edge $e : u \to v$, the root word $H_e = G_v^{-1} T_e G_u$ satisfies

$$H_e^* Q_o H_e = |\det H_e|^{2/n} Q_o.$$

Consequently

$$T_e^* Q_v T_e = |\det H_e|^{2/n} Q_u, \qquad \lambda_e = |\det H_e|^{1/n} > 0.$$

This gives the required compatible family directly. A group preserving a positive-definite metric is conjugate into a compact orthogonal or unitary group. Conversely, averaging an inner product over the compact closure of a relatively compact image gives an invariant positive-definite metric. □

## 24.3 Exact convex-versus-quadratic separation

Consider

$$A_1 = \begin{pmatrix} 1 & 0 \\ 1 & 0 \end{pmatrix}, \qquad A_2 = \begin{pmatrix} 0 & 1 \\ 0 & -1 \end{pmatrix}.$$

**Theorem 24.7** (Sharp geometry-class separation)**.** *The norm $\|x\|_\infty$ satisfies*

$$\max\{\|A_1 x\|_\infty, \|A_2 x\|_\infty\} = \|x\|_\infty$$

*for every $x \in \mathbb{R}^2$. In contrast, for every positive-definite quadratic metric $Q$,*

$$\max\{\|A_1\|_Q, \|A_2\|_Q\} \geq \sqrt{2}.$$

*Equality holds for scalar multiples of the Euclidean metric. Hence the exact optimal convex/Finsler bound is 1, while the exact optimal quadratic bound is $\sqrt{2}$.*

*Proof.* The two images are

$$A_1(x_1, x_2) = (x_1, x_1), \qquad A_2(x_1, x_2) = (x_2, -x_2),$$

so the first identity is immediate.

Write

$$Q = \begin{pmatrix} a & c \\ c & b \end{pmatrix}, \qquad d = ab - c^2 > 0.$$

The squared induced norms are

$$u := \|A_1\|_Q^2 = \frac{b(a+b+2c)}{d}, \qquad v := \|A_2\|_Q^2 = \frac{a(a+b-2c)}{d}.$$

A direct calculation gives

$$ab\big((a+b)^2 - 4c^2\big) - 4(ab-c^2)^2 = ab(a-b)^2 + 4c^2(ab-c^2) \geq 0.$$

Thus $uv \geq 4$, and therefore

$$\max\{\sqrt{u}, \sqrt{v}\} \geq (uv)^{1/4} \geq \sqrt{2}.$$

Equality forces $a = b$ and $c = 0$, and then $u = v = 2$. □

This example is a sharp instance of the established gap between general extremal norms and common quadratic Lyapunov functions [24, 23]. Its role here is not a novelty claim. It proves that obstruction status must record the admissible geometry class.

## 24.4 Escape without positive gap

**Proposition 24.8** (Unipotent escape)**.** *Let*

$$H = \begin{pmatrix} 1 & 1 \\ 0 & 1 \end{pmatrix}.$$

*There is no positive-definite metric $Q$ with $H^*QH = Q$. Nevertheless, for*

$$Q_s = \mathrm{diag}(s^2, 1),$$

*we have*

$$D_{Q_s}(H) \longrightarrow 1 \qquad (s \downarrow 0),$$

*while*

$$\kappa_2(Q_s) = s^{-2} \longrightarrow \infty.$$

*Thus the metric-completion defect has zero infimum but is not attained.*

*Proof.* Writing $Q = \left(\begin{smallmatrix} a & c \\ c & b \end{smallmatrix}\right)$, the equation $H^*QH = Q$ forces $a = 0$, contradicting positive definiteness. For $Q_s$, the metric-normalized matrix is

$$\begin{pmatrix} s & 0 \\ 0 & 1 \end{pmatrix} H \begin{pmatrix} s^{-1} & 0 \\ 0 & 1 \end{pmatrix} = \begin{pmatrix} 1 & s \\ 0 & 1 \end{pmatrix},$$

whose singular-value condition number tends to one. The conditioning formula is immediate. □

## 24.5 Forgetful descent and enrichment lifting

Suppose richer categories $\widetilde{\mathcal{C}}$ and $\widetilde{\mathcal{D}}$ carry forgetful functors

$$U : \widetilde{\mathcal{C}} \to \mathcal{C}, \qquad V : \widetilde{\mathcal{D}} \to \mathcal{D}.$$

**Proposition 24.9** (Forgetful descent and enhancement lifting)**.** *A rich bridge*

$$\widetilde{B} : \widetilde{\mathcal{C}} \to \widetilde{\mathcal{D}}$$

*automatically determines an underlying bridge*

$$V\widetilde{B} : \widetilde{\mathcal{C}} \to \mathcal{D}.$$

*Given only a bare bridge $B : \mathcal{C} \to \mathcal{D}$, constructing $\widetilde{B}$ together with a comparison*

$$V\widetilde{B} \cong BU$$

*is a lifting problem. Its existence, uniqueness, and residual automorphisms are additional passport fields and may carry typed obstruction objects.*

*Proof.* The first statement is composition. The second is not an existence theorem but a precise reformulation of the enhancement problem: a lift is extra structure over the specified commutative square. Any failure must therefore be recorded relative to the chosen forgetful functors and comparison data. □

The pattern contains several earlier obstruction mechanisms:

| Underlying structure | Requested enrichment | Typed gate or obstruction |
|---|---|---|
| Projective semilinear cocycle | Linear semilinear descent | Relative Brauer class |
| Invertible transport graph | Compatible metric packet | Unitarizability of normalized holonomy |
| Faithful additive realization | Exact tensor fiber functor | Strong monoidal and exactness obligations |
| Max-plus value | Finite-temperature sum semantics | Residual partition mass |
| Bare quotient coordinates | Metric-decorated quotient | Compatible quotient metric and conditioning boundary |

No single obstruction object is asserted for all rows. The common statement concerns the shape of the lifting problem.

## 24.6 Two variances and the indexed architecture

Task changes and admissibility changes have opposite-looking effects. If a task is strengthened, its behavioral kernel shrinks and its quotient retains more information:

$$N_{\text{strong}} \subseteq N_{\text{weak}}, \qquad Q_{\text{strong}} \twoheadrightarrow Q_{\text{weak}}.$$

If an admissible realization class is enlarged, the optimized defect can only decrease:

$$\Gamma \subseteq \Gamma' \quad \Longrightarrow \quad \delta_{\Gamma'} \leq \delta_{\Gamma}.$$

These are different orders and should not be merged into one scalar notion of a stronger contract.

**Definition 24.10** (Doctrine-indexed task fiber)**.** For a doctrine $D$ and represented object $X$, let

$$\mathsf{Task}_D(X)$$

denote the ordered family of continuation-stable semantic quotients admitted by the declared query universe. Inside one fiber, kernel or congruence calculus governs task change. A change of doctrine

$$D \longrightarrow D'$$

requires a bridge passport specifying carrier transport, preserved constructions, comparison maps, and any lifting obstruction.

**Theorem 24.11** (Relative stratified semantic synthesis)**.** *Within the finite certified setting of this manuscript, the following statements hold.*

1. *Every declared semantic slice has a task-relative behavioral quotient whenever the required effective quotient exists.*
2. *Inside a module-valued slice, joint tasks, common coarsenings, bridge loss, essential-image failure, and task weakening are governed by the exact sequences of Sections 22 and 23.*
3. *Carrier changes are legal exactly on the factorization loci certified by theorem 23.1; otherwise the joint semantic image is the canonical exact completion preserving both views.*
4. *Observer changes may introduce additional relation objects such as* $\mathrm{Rel}_K(E)$*; they are not inferred from carrier compatibility alone.*
5. *Enlarging an admissible realization class weakens optimized defect but need not produce an attained completion.*
6. *Crossing to richer structure is a typed lifting problem and does not follow from the underlying bridge without an enhancement certificate.*

*Proof.* The clauses are respectively theorems 22.4, 22.16, 23.1, 23.5, 23.13 and 24.2 and proposition 24.9. No clause identifies distinct carriers, observer categories, or admissibility classes without the corresponding comparison data. □

*Boundary* 24.12 (Scope of the second-order calculus). The indexed architecture does not establish a complete double category of all mathematical doctrines, nor does it prove that every task quotient or enrichment is effectively recognizable. The fiberwise quotient and exact-sequence results are proved in the stated algebraic settings. Cross-doctrine coherence remains conditional on explicit carrier, topology, metric, tensor, convergence, or higher-categorical passports.

**Admissibility and lifting result.** Obstructions are relative to both the requested enrichment and the admissible realization class. Enlarging that class can remove a positive gap, while zero defect may still fail to be attained. Rich structure descends under forgetting, but reconstructing it from a bare representation is a lifting problem with its own typed gate. The resulting architecture is a family of task-quotient fibers connected only by certified doctrine bridges.

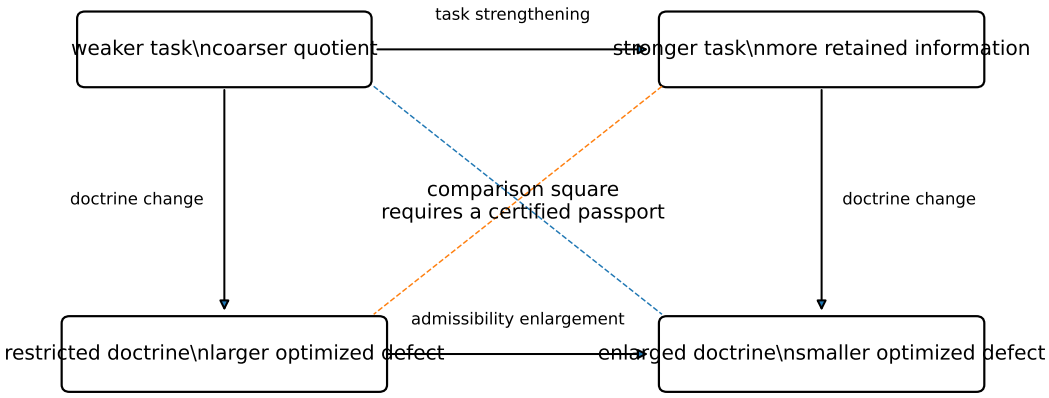



**Figure 58:** Two independent contract directions. Horizontal task strengthening retains more semantic information. Vertical admissibility enlargement allows more realizations and can weaken obstruction. A commuting square is a theorem-level comparison, not an automatic identification.

## 25 Scope, classification targets, and open boundaries

The global classification theorem is componentwise because the certified reversible core has five connected semantic components. The component tag is part of the invariant. Omitting it would compare objects for which no reversible semantic bridge has been proved.

The lane theorems have a different scope. The finite profiled Universal Lane Transport Theorem is exact inside a declared additive, idempotent-complete setting with complete split packet systems. Its realization, kernel, multilinear, fold, and descent clauses apply only under their additional hypotheses. Trivial address holonomy is required only for one fixed global address set. With a coherent finite address cocycle, complete matrices instead descend as sections of a matrix local system, and monodromy orbits give the finest ordinary global projector coarsening. The word “universal” refers to this formal lane calculus. It does not claim that every object has a finite lane presentation or that address count equals dimension, rank, entropy, information, or computational complexity.

The semantic quotient theorem is relative in another direction. It fixes a carrier doctrine, continuation grammar, observation category, and query family. The resulting quotient is universal only for that semantic slice. A different observation category can identify different linear combinations of residual states. A different carrier can change the legal aggregation law. A different continuation class can expose provenance that was previously invisible. There is therefore no observer-independent minimum hidden behind the notation.

The admissibility theory records a third boundary. A positive defect in a quadratic, integral, finite, or neutral class need not survive enlargement to a convex, rational, completed, or nonneutral class. Conversely, zero optimized defect does not imply that a completion exists. Attainment and conditioning remain part of the defect profile.

**Table 43:** Certified classification components and exact boundaries.

| Component | Semantic domain | Complete descended coordinates | Boundary |
|---|---|---|---|
| Digital–regular–linear–Mahler | Fixed-prime regular sequences with rational-mask and periodic subloci | Strict shortlex state, Cartier/mask data where defined, periodic linear data where defined | No all-radix or unrestricted functional/Newton-Mahler equivalence |
| Continuous local | $C(\mathbb{Z}_p, \mathbb{Z}_p)$ | Canonical Mahler coefficients and complete clopen branch packets | No universal local-analytic normal form or optimal mixed-radix tree |
| Marked Fuss | $U = z + \alpha U^q$ | Marked parameters $(q, \alpha)$, algebraic branch, recurrence, tree support and orbit data | Complete only on the marked nonlinear–algebraic–holonomic family |
| Euler–multiplicative | Fixed Euler basis and prime-uniform multiplicative locus | Euler exponent, divisor ghost, common local factor, multiplicative function | No arbitrary product-grammar or additive–multiplicative equivalence |
| Finite Galois | One finite semisimple Galois extension | Subgroup, fixed field, Reynolds projector, quotient and Mackey data | No modular/wild or nonneutral tensor reconstruction |

## 25.1 Directional satellites

Several useful constructions remain adjacent to the reversible core without becoming equivalences:

- reduction from integral section lattices to finite residue systems, with Smith–Tor ghosts and missing saturated coordinates;
- passage from a selected algebraic branch to a differential annihilator, which can forget the branch and its minimal polynomial;
- functional-Mahler masks and Newton–Mahler interpolation, which use different variables and require additional lifting and interpolation data;
- projective Galois descent, whose lift to an ordinary vector realization is governed by a relative Brauer class;
- faithful additive or Hilbert-space realizations that do not supply the exact tensor fiber functor required for Tannakian reconstruction;
- incomplete lane selections and noninjective folds, which retain explicit residuals or collision kernels;
- Boolean or max-valued summaries of signed additive computation, where cancellation obstructs carrier replacement;
- Set-valued future quotients and weighted-linear residual spaces, whose difference is measured by a relation module;
- geometric or provenance compactions that are valid only for the declared continuation class and downstream task.

These constructions remain in the directed transformation category with their exact loss, completion, or obstruction records.

## 25.2 Open mathematical obligations

The remaining foundational obligations are more sharply localized than in earlier editions.

1. Extend the certified atlases across radices, coefficient rings, semirings, and mixed local–global completions without losing normalization or effectivity.
2. Develop modular and wild analogues of finite semisimple Galois projector theory when Reynolds averaging fails.
3. Replace marked model-family results in the holonomic, algebraic, and nonlinear strata by broader native minimality and collision invariants.
4. Construct nonneutral and integral tensor-descent variants with their gerbe or torsor data retained explicitly.
5. Prove finite-data recognition theorems only on declared subgrammars where identifiability and certification are available.
6. Extend finite split and finite holonomy-twisted lane transport to infinite, completed, nonsplit, noninvertible, or genuinely nonadditive resolutions only after specifying the required convergence, exactness, and coherence doctrines.

7. Characterize which query universes are rich enough that every continuation-stable congruence is observationally definable, and determine when the definable task family is closed under joins.
8. Extend the module exact-sequence calculus to exact, regular, homological, enriched, and higher-categorical settings without silently importing additive arguments.
9. Develop effective algorithms for joint semantic completion, relation-module reduction, and task-relative bridge loss beyond finite matrices and finite automata.
10. Construct a fully coherent doctrine-indexed comparison object only after the required horizontal, vertical, and higher comparison cells have been verified.

**No global promotion.** Completion of the finite atlas, lane theorems, semantic quotient calculus, or class-relative defect theory does not promote absent bridges, incompatible carriers, noninjective folds, unresolved enrichments, or broad-stratum normal forms to equivalences. Every claimed transport remains relative to its grammar, profile, semantic slice, admissible realization class, and proof-status record. The detailed obligation and claim ledgers are retained in Appendices D and E.

## 26 Conclusion

The paper establishes a finite, typed, and auditable form of stratified universality. Its common object is not one formula and not one global coordinate system. It is a resolved syntax together with profile-preserving realizations, normalized local charts, typed bridges, task-relative quotients, and declared descent and enrichment doctrines.

The first proof architecture concerns representation. Packet and refinement data are literal in the additive–Karoubi envelope. Representation groupoids are separated from information-losing transformations. Bridge passports identify what is preserved, reflected, forgotten, or only partially defined. Holonomy, cokernel, Brauer, and higher-coherence defects record different failures of global trivialization. Effective descent turns compatible local presentations into global semantic objects. Compatible native invariants descend and become complete on the five declared normalized components.

The finite profiled Universal Lane Transport Theorem isolates the algebraic mechanism inside that architecture. Complete finite packet systems give exact analysis and synthesis. Every morphism becomes a unique lane-to-lane block matrix, composition becomes contraction over intermediate addresses, and certified coarsening aggregates fine blocks without changing the underlying morphism. Selectors split retained transport from named residuals. The holonomy-twisted extension shows that chart loops may permute lane labels without destroying the calculus. The matrices then form a local system, descended morphisms are its compatible sections, object-lane orbit sums give the finest ordinary global coarsening, and pair orbits carry exact path composition.

The second proof architecture concerns semantic sufficiency. For a fixed carrier, continuation grammar, observation category, and query family, the behavioral quotient is the coarsest representation preserving every future observation. Its kernel is the maximal stable invisible core. Task strengthening, joint semantics, common coarsening, relative residuals, bridge loss, essential-image failure, and task weakening become exact quotient constructions. This replaces an informal search for a universally smallest packet by a family of precise minima indexed by declared semantic tasks.

The third architecture concerns changes between those tasks and doctrines. Carrier replacement is a factorization theorem, not a vocabulary choice. Observer base change can introduce a relation module

even when the carrier is unchanged. Convex value, additive reconstruction, provenance, and weighted-linear state are therefore distinct semantic objects until a comparison theorem is supplied. Enlarging an admissible geometry can remove a positive obstruction, while zero infimum can still escape every well-conditioned realization. Rich structure descends under forgetting, but recovering it from a bare representation is a lifting problem.

The resulting theory is neither storage universality nor a claim that all mathematics is categorically equivalent. It is a calculus for asking, with explicit types, what survives a change of representation, what is lost, what obstructs reconstruction, what a declared task can safely forget, and what extra structure must be supplied to return. New strata, task fibers, or doctrines enter the theory only through normalizations, transport laws, effectivity proofs, comparison maps, exact loss records, and claim boundaries. Historical novelty and independent mathematical review remain separate from this internal formal synthesis.

## A Theorem concordance and proof-status index

The machine-readable concordance in the source package preserves, for all 75 components, the selected strongest source, exact theorem coordinate, hypotheses, proof class, imported input, and remaining obligation. The publication PDF retains the compact index below. This avoids duplicating the full theorem prose while preserving a complete auditable record in `Komorebi_Theorem_Concordance_Final_2026-10-06.json` and `final_generated/concordance_entries.tex`.

**Table 44:** Compact index to the theorem concordance. The detailed hypotheses and obligations appear in Appendix A.

| ID | Component | Status | Strongest source |
|---|---|---|---|
| FND-01 | Typed linear syntax and module semantics | proved internally | `PSC_I_Symbolic_Core.tex` |
| FND-02 | Finite free seed presentations | proved internally | `PSC_I_Symbolic_Core.tex` |
| FND-03 | Seed rank and functorial inequalities | proved internally | `PSC_I_Symbolic_Core.tex` |
| FND-04 | Closed seed-rank formulas | proved internally | `PSC_I_Symbolic_Core.tex` |
| FND-05 | Exact packet coordinates and reconstruction | proved internally | `PSC_I_Symbolic_Core.tex` |
| FND-06 | Block algebra and support calculus | proved internally | `PSC_I_Symbolic_Core.tex` |
| FND-07 | Coordinate transport and transfer naturality | proved internally | `PSC_I_Symbolic_Core.tex` |
| FND-08 | Subobject, quotient, and packet exactness | proved internally | `PSC_I_Symbolic_Core.tex` |
| FND-09 | Preservation profiles and theorem transport | proved internally | `PSC_I_Symbolic_Core.tex` |
| FND-10 | Finite resolved transfer and refinement calculus | proved internally | `Resolution_Theory_Final_Journal_Manuscript.tex` |

Continued on next page

| ID | Component | Status | Strongest source |
|---|---|---|---|
| FND-11 | Universal corner extension and faithful realization | proved internally | Resolution_Theory_Final_Journal_Manuscript.tex |
| FND-12 | Recognition and finite faithful dimension | proved internally | Resolution_Theory_Final_Journal_Manuscript.tex |
| FND-13 | Karoubi, countable, W*, and affiliated completion | proved internally | Resolution_Theory_Final_Journal_Manuscript.tex |
| FND-14 | Nonlinear packet operad and refinement coherence | proved internally | Resolution_Theory_Final_Journal_Manuscript.tex;Nonlinear_Transfer_Operad.texasspecializedsource |
| FND-15 | Local analytic nonlinear inversion | proved internally | Resolution_Theory_Final_Journal_Manuscript.tex |
| FND-16 | Universal Lane Transport Theorem, finite profiled form | proved internally | block15_section.tex,UniversalLaneTransportTheoremandcorollaries |
| FND-17 | Holonomy-Twisted Universal Lane Transport and Orbit Descent | proved internally | block16_section_final.tex,holonomy-twistedtransport,orbitdescent,orbitalcomposition,andcyclotomicrealization |
| CAT-01 | Representation groupoids separated from directional transformations | framework only | Abstraction_as_a_Resolved_Practice(1).tex;PSCPaperIcategoryofseededpacketsystems |
| GLU-01 | Finite graph holonomy and global-frame criterion | proved internally | PSC_Paper_III_Strengthened_Annals_Edition.tex |
| GLU-02 | Gauge classification of finite transports | proved internally | PSC_Paper_III_Strengthened_Annals_Edition.tex |
| GLU-03 | Maximal path-flat core | proved internally | Affine_Mahler_Packets_and_Periodic_Test_Sets.tex (Core-TransferAddendum04) |
| GLU-04 | Split analysis as a genuine two-chart atlas | proved internally | Affine_Mahler_Packets_and_Periodic_Test_Sets.tex (Addendum04) |
| GLU-05 | Exact affine Mahler chart composition and trivial CRT holonomy | proved internally | Affine_Mahler_Packets_and_Periodic_Test_Sets.tex (Addendum04) |
| DSC-01 | Descent commutes with complete resolution | proved conditionally | Projector_Calculus_Final_Current.tex |
| OBS-01 | Canonical obstruction relative to declared correction data | proved internally | PSC_Paper_III_Strengthened_Annals_Edition.tex |

Continued on next page

| ID | Component | Status | Strongest source |
|---|---|---|---|
| OBS-02 | Obstruction naturality and packet decomposition | proved internally | PSC_Paper_III_Strengthened_Annals_Edition.tex |
| OBS-03 | Relative/cohomological obstruction | proved internally | PSC_Paper_III_Strengthened_Annals_Edition.tex |
| OBS-04 | Nonlinear correction and complete filtered lifting | proved internally | PSC_Paper_III_Strengthened_Annals_Edition.tex |
| GAL-01 | Finite Galois projector realization | classical input | Resolution_Theory_Galois_Expanded_Journal_Manuscript.tex |
| GAL-02 | Effective linear semilinear descent | classical input | Resolution_Theory_Galois_Expanded_Journal_Manuscript.tex |
| GAL-03 | Brauer obstruction to projective descent | classical input | Resolution_Theory_Galois_Expanded_Journal_Manuscript.tex |
| GAL-04 | Tannakian reconstructed symmetry | classical input | Resolution_Theory_Galois_Expanded_Journal_Manuscript.tex |
| LIN-01 | C-finite recurrence $\leftrightarrow$ rational OGF $\leftrightarrow$ finite state | classical input | Projector_Seed_Calculus_for_Integer_Sequences_Local_Polyphase_Extension.tex |
| LIN-02 | Minimal linear dimension and similarity normalization | classical input | Projector_Seed_Calculus_for_Integer_Sequences_Local_Polyphase_Extension.tex |
| LIN-03 | Complete persistent C-finite packet invariant | proved internally | Projector_Seed_Calculus_for_Integer_Sequences_Local_Polyphase_Extension.tex |
| HOL-01 | P-recursive $\leftrightarrow$ D-finite coefficient translation | classical input | Projector_Seed_Calculus_for_Integer_Sequences_Local_Polyphase_Extension.tex |
| DIG-01 | Finite digit realization $\leftrightarrow$ finite k-kernel | proved internally | Projector_Seed_Calculus_for_Integer_Sequences_Local_Polyphase_Extension.tex |
| DIG-02 | Fixed-radix automaton normal form | classical input | Projector_Seed_Calculus_for_Integer_Sequences_Local_Polyphase_Extension.tex |

Continued on next page

| ID | Component | Status | Strongest source |
|---|---|---|---|
| ALG-01 | Selected algebraic branch → packet polynomial system | proved internally | `Projector_Seed_Calculus_for_Integer_Sequences_Local_Polyphase_Extension.tex` |
| TRN-01 | Invertible transform ↔ transported packet resolution | proved internally | `Projector_Seed_Calculus_for_Integer_Sequences_Local_Polyphase_Extension.tex` |
| PRD-01 | Euler-product exponents ↔ logarithmic-derivative recurrence | proved internally | `Projector_Seed_Calculus_for_Integer_Sequences_Local_Polyphase_Extension.tex` |
| MUL-01 | Prime-power seeds reconstruct multiplicative functions | proved internally | `Projector_Seed_Calculus_for_Integer_Sequences_Local_Polyphase_Extension.tex` |
| LOC-01 | Finite Newton–Mahler reconstruction and local transfer | proved internally | `Projector_Seed_Calculus_for_Integer_Sequences_Local_Polyphase_Extension.tex` |
| LOC-02 | Exact Mahler ↔ affine polyphase coordinate transport | proved internally | `Projector_Seed_Calculus_for_Integer_Sequences_Local_Polyphase_Extension.tex;Addendum04strengthensit` |
| LOC-03 | Sharp minimal integral packet and universal decoder | proved internally | `Affine_Mahler_Packets_and_Periodic_Test_Sets.tex (Addendum04)` |
| FMH-01 | Rational functional-Mahler mask → Cartier representation | proved internally | `Komorebi_Custom_GF_Cartier_Padic_Research_Report_0.3.pdf` |
| FMH-02 | Functional-Mahler finite state → automaton | proved internally | `Komorebi_Custom_GF_Cartier_Padic_Research_Report_0.3.pdf` |
| FMH-03 | Finite-mask Cartier transitions ↔ carry matrices | proved internally | `Komorebi_Custom_GF_Cartier_Padic_Research_Report_0.3.pdf` |
| ASM-01 | One explicit profile-indexed resolved envelope | conjectural | `ControllinghandoffÂğ4GapA;localingredientsinPaperI,ResolutionTheory,andnonlinearoperadsources` |

Continued on next page

| ID | Component | Status | Strongest source |
|---|---|---|---|
| ASM-02 | Authoritative declared stratum atlas | framework only | ControllinghandoffÂğ4GapB |
| ASM-03 | Bridge semantic, packet, refinement, and residual naturality | conjectural | ControllinghandoffÂğ4GapC;localnaturalityinputsFND-07/FND-09/OBS-02 |
| ASM-04 | Triple-overlap and quadruple coherence | conjectural | ControllinghandoffÂğ2.6andÂğ4GapC |
| ASM-05 | Effective descent for the heterogeneous atlas | conjectural | ControllinghandoffÂğ4GapD |
| ASM-06 | Native normalization and complete invariants beyond existing slices | conjectural | ControllinghandoffÂğ4GapE |
| ASM-07 | Coherent invariant descent and conditional global completeness | conjectural | ControllinghandoffÂğ4GapF |
| ASM-08 | Theorem concordance and edition control | proved internally | ThisWorkPackage0;Master_Theorem_Migration_Ledger.csv;latermigrationmaps |
| ASM-09 | Finite Profiled Resolved Atlas Assembly Theorem | proved conditionally | ThisWorkPackage0,Âğ6andcompanionLaTeXtheoremfile |
| SEM-01 | Universal behavioral coimage and task-relative minimum | proved internally | block17_semantic_quotients_final.tex |
| SEM-02 | Maximal stable invisible core | proved internally | block17_semantic_quotients_final.tex |
| SEM-03 | Greatest-fixed-point construction and finite certification | proved internally | block17_semantic_quotients_final.tex |
| SEM-04 | Task–congruence Galois connection | proved internally | block17_semantic_quotients_final.tex |
| SEM-05 | Semantic quotient classification by congruences | classical input | block17_semantic_quotients_final.tex |
| SEM-06 | Semantic diamond and exact compatibility sequence | proved internally | block17_semantic_quotients_final.tex |
| SEM-07 | Task-change exact sequence and extension-valued loss | proved internally | block17_semantic_quotients_final.tex |
| BRG-01 | Task-compatible bridge and five-term exact loss sequence | proved internally | block18_carrier_observer_change_final.tex |
| BRG-02 | Extension law for composite semantic loss | proved internally | block18_carrier_observer_change_final.tex |
| CAR-01 | Carrier factorization gate and joint semantic completion | classical input | block18_carrier_observer_change_final.tex |

Continued on next page

| ID | Component | Status | Strongest source |
|---|---|---|---|
| CAR-02 | Carrier-indexed observer packet theorem | proved internally | `block18_carrier_observer_change_final.tex` |
| CAR-03 | Cancellation and idempotence barriers | classical input | `block18_carrier_observer_change_final.tex` |
| OBC-01 | Observer base-change relation module | proved internally | `block18_carrier_observer_change_final.tex` |
| OBC-02 | Polyphase infinite-discrete versus finite-linear separation | proved internally | `block18_carrier_observer_change_final.tex` |
| CVX-01 | Observer-conditioned convex packet transport and provenance boundary | proved internally | `block18_carrier_observer_change_final.tex` |
| ADM-01 | Admissibility monotonicity and completion/gap/escape stratification | proved internally | `block19_admissibility_lifting_final.tex` |
| ADM-02 | Sharp convex-versus-quadratic packet separation | classical input | `block19_admissibility_lifting_final.tex` |
| DOC-01 | Forgetful descent, enhancement lifting, and doctrine-indexed task fibers | framework only | `block19_admissibility_lifting_final.tex` |

# B Edition-control ledger

**Table 45:** Edition-control ledger. Full hashes are retained so later strengthened editions can supersede specific rows without losing provenance.

| Source family | Selected file | SHA-256 | Decision |
|---|---|---|---|
| Paper I canonical symbolic core | `PSC_I_Symbolic_Core.tex` | `39c869f3bd16cbef102fe68dcad51125ab4511077cc45de6d91562c0748fa95c` | Primary theorem-ID and proof-status spine. Use the Expanded Clarified Edition for exposition, but preserve these stable labels/RecordIDs. |
| Paper I expanded clarified edition | `PSC_Paper_I_Expanded_Clarified_Edition.tex` | `e91239446e2e149bbf571c5bbc7e71a76a6f9a351d68963963cfe87f5fbf3c0f` | Co-primary expository edition, not a replacement for the canonical symbolic RecordID spine. |
| Resolution Theory final journal manuscript | `Resolution_Theory_Final_Journal_Manuscript.tex` | `3c0f37a5132c04d0715b0b85a88e34020ffdfc299bf6dd79b7fb4c4bdb32ecec` | Primary integrated source for finite resolved systems, corner representation/recognition, countable completion, and nonlinear operadic structure. |
| Paper III strengthened Annals edition | `PSC_Paper_III_Strengthened_Annals_Edition.tex` | `20452d11443835ca9c0e0484250c01fa51e0456574c7f7c7f5549fbd0f934c89` | Supersedes older Paper III status language on the relative universal obstruction: coker(D), naturality, quotient projectors, relative exact sequence, and mapping cones are theorem-level. The choice-free cross-problem assignment of D remains open. |
| Core-Transfer Addendum 04 | `Affine_Mahler_Packets_and_Periodic_Test_Sets.tex` | `d864bebe02eac16037f17dc677dee9078fbc02a093c7b491b31d2b0208bb91e1` | Strongest source for maximal directed cores and the exact finite Mahler/polyphase atlas, composite rank law, sharp channel minimum, and stabilization. |
| Resolution Theory Galois expanded manuscript | `Resolution_Theory_Galois_Expanded_Journal_Manuscript.tex` | `f3c89f23db5f6e1ee8da7c396c0b30d8274154b8d1fca25d18415ec5dfe54480` | Primary source for Galois projector strata and classical descent/reconstruction inputs. |

Continued on next page

| Source family | Selected file | SHA-256 | Decision |
|---|---|---|---|
| Sequence local/polyphase extension | `Projector_Seed_Calculus_for_Integer_Sequences_Local_Polyphase_Extension.tex` | `e310e5fbec56954e4490615acdeecb04122bad9bd9243e79d84a08174039038a` | Primary source for the broad sequence grammar, pairwise bridges, persistent C-finite complete packet invariant, and local/polyphase exact transfers. |
| Functional-Mahler/Cartier report 0.3 | `Komorebi_Custom_GF_Cartier_Padic_Research_Report_0.3.pdf` | `4480786c49abcb60fb39e07acf0e250c9a3af68c38ac7b4801f34bdaefd5a936` | Primary source for the rational functional-Mahler → Cartier → automaton direction and finite-mask Cartier/carry identification. |
| Nonlinear transfer operad specialized manuscript | `Nonlinear_Transfer_Operad.tex` | `051970594d8b34c2ec5af67e20e063963b7c8684b75a439f62ed2c5f0e70d3a8` | Specialized secondary source. Resolution Theory Final is the integrated primary source for overlapping operadic results. |
| Abstraction as a Resolved Practice | `Abstraction_as_a_Resolved_Practice(1).tex` | `78bad0bd370fec069f61b5b616dbc5898277229429213a227772a2df4f96861d` | Conceptual source for representation groupoids, broader directed categories, and atlas language; not the theorem source for heterogeneous effective descent. |
| Projector Calculus final current | `Projector_Calculus_Final_Current.tex` | `cc313296416b08ccbe73d893e1744ae840b6419fc5b6676805ef722ab0401b39` | Selected exact source for descent–limit interchange and cofinal resolution equivalence. |
| Master migration ledger | `Master_Theorem_Migration_Ledger.csv` | `dceabf345ac09e507a754a928ca716ed2f797ca9aff8d777e104b49ab73dbdd1` | Historical dependency/migration evidence only; it does not override a strengthened theorem edition. |
| Paper III migration/expansion map | `MIGRATION_AND_EXPANSION_MAP(1).md` | `5f42dc03e5989b8883ce934752c3885ce58ae923b900a02943c86c93e4ca2242` | Authoritative supersession note for the strengthened Paper III rewrite. |
| Remaining open questions after two resolutions | `Remaining_Open_Questions_and_Conjectures_After_Two_Resolutions.pdf` | `13e41d43b9bbeaf0d4e5ed6dd223f6adfaf46c63ebc51987a118d9ec40843c90` | Historical open-question snapshot. Every "open" entry must be checked against later strengthened editions before reuse. |
| Universal Lane Transport Theorem, finite profiled form | `block15_section.tex` | `c1ae8aa2472eda9df467bbbf20b3c861f1261333364af06ffaf1cd455b5ab026` | Selected controlling source for FND-16 and the finite lane-transport theorem family. |

Continued on next page

| Source family | Selected file | SHA-256 | Decision |
|---|---|---|---|
| Holonomy-Twisted Universal Lane Transport and Orbit Descent | `block16_section_final.tex` | `2b086cc6d806c3cf25b443a6ecefa871adba282d913deffaafabcadad2c0258a` | Selected controlling source for FND-17 and the finite nontrivial-address-holonomy extension. Final publication copy includes explicit 6 October 2026 local amendments; inherited source retained. |
| Part IV semantic quotient calculus | `block17_semantic_quotients_final.tex` | `ef408f87352057761b6bf55742f848612f585632691f71488d510393749b0735` | Primary source for behavioral cores, task congruences, semantic diamonds, residuals, and task-change exactness. Final publication copy includes the explicit 6 October 2026 coinduction proof clarification; inherited source retained. |
| Part IV carrier and observer calculus | `block18_carrier_observer_change_final.tex` | `6babbf13d884e5bdf86174ce89729ccf69feb694cf84e03c0f52c32038775157` | Primary source for carrier factorization, joint completion, bridge loss, observer base change, and provenance. Final publication copy includes explicit 6 October 2026 local amendments; inherited source retained. |
| Part IV admissibility and lifting calculus | `block19_admissibility_lifting_final.tex` | `038f352d1e9a82984963af0e90a14b104b8f17f7b2e8e4df2c8da627bc089799` | Primary source for optimized defect, completion/gap/escape, geometry-class separation, and enrichment lifting. Final publication copy includes explicit 6 October 2026 local amendments; inherited source retained. |
| Part IV exact symbolic validation | `results/block17_semantic_extension_validation.json` | `218123b49533a702126e8eea6f2e5f5172d4e9802902c6acb2460d39c0d334d1` | Finite exact implementation audit retained separately from universal proofs. |

# C Publication audit and development provenance

The consolidated edition retains a compact theorem-suite map and a development-provenance ledger so that editorial reordering does not erase proof dependencies or claim boundaries. The tables in this appendix are inherited records: their page counts and validation results refer to the original artifacts and the dated version 2.0.0 mathematical base. The final-edition build and publication checks are recorded separately in the release validation report.

**Table 46:** Publication-source audit for the Finite lane-transport theorem consolidated edition.

| Audit area | Record | Status |
|---|---|---|
| Source graph | 55 TeX files | PASS |
| Abstract length | 316 words | PASS |
| Labels and references | 519 labels; 131 references | PASS |
| Citation keys | 14 cited keys | PASS |
| Graphics | 57 included assets | PASS |
| Lane verifier | 197,099 exact assertions | PASS |
| Publication structure audit | 77 assertions | PASS |

**Table 47:** Publication-source and release-integrity audit for the Block 16 holonomy-twisted extension.

| Audit area | Record | Status |
|---|---|---|
| Source graph | 60 TeX files | PASS |
| Abstract | 346 words | PASS |
| Labels and references | 542 labels; 138 references | PASS |
| Citation keys | 14 cited keys | PASS |
| Graphics | 57 included assets | PASS |
| Block 16 verifier | 1,344,823 exact assertions | PASS |
| Concordance | 57 synchronized entries through FND-17 | PASS |
| Compiled PDF | 239 pages | PASS |
| Publication audit | 85 checks | PASS |

**Table 48:** Final formal-foundations publication audit.

| Audit surface | Recorded result |
|---|---|
| Source graph | 65 recursively included TeX files; 620 labels; 153 source references |
| Concordance | 75 components with synchronized status and domain counts |
| Inherited validation | Block 15 PASS; Block 16 PASS with 1,344,823 assertions |
| Part IV validation | 3,022 exact symbolic assertions; zero recorded failures |
| Compiled artifact | 247 pages; metadata, theorem-layer text, references, citations, and graphics checked |
| Audit result | 77 checks; 0 failures |
| Boundary | Internal publication integrity only; not independent peer review or historical-priority validation. |

**Table 49:** Development provenance retained after journal-facing reorganization.

| Stage | Mathematical contribution |
|---|---|
| Foundation | Typed resolved syntax, packet coordinates, preservation profiles, additive-Karoubi envelope |
| Atlas typing | Normalized strata, representation groupoids, bridge passports, information loss, obstruction types |
| Finite effectivity | Periodic and rational-mask heterogeneous atlases |
| Digital normalization | Fixed-radix regular, automatic finite-orbit, and integral prime-power layers |
| Product/local normalization | Euler–multiplicative and Newton-Mahler–polyphase atlases |
| Holonomic, algebraic, nonlinear | Marked model-family minimality, collision, and tree signatures |
| Symmetry | Finite Galois, Brauer, profinite, and neutral Tannakian slices |
| Global synthesis | Authoritative bridge matrix, higher coherence, invariant descent, tagged completeness |
| Lane transport | Complete finite-resolution analysis, synthesis, block transport, refinement, selection, residual accounting, and typed specializations |
| Holonomy transport | Matrix local systems, exact twisted synthesis, base-fiber invariants, monodromy-orbit coarsening, and orbital composition |
| Publication consolidation | Theorem spine, proof-order reorganization, scope compression, and source audit |

# D Detailed open-obligation ledger

## D.1 Correct dependency order

The remaining heterogeneous work has a strict topological order:

$$\boxed{\begin{array}{c}\text{profiled envelope} \longrightarrow \text{declared atlas} \longrightarrow \text{typed bridge laws} \\ \longrightarrow \text{higher coherence} \longrightarrow \text{effective descent} \longrightarrow \text{compatible invariants}\end{array}}$$

The first three arrows cannot be skipped. Pairwise formulas do not themselves define a pseudofunctor. Local completeness does not itself construct compatible global isomorphisms.

## D.2 What this manuscript closes

This paper closes the following finite parts of the program:

- the typed finite resolved signature, exact finite packet/refinement/residual calculus, preservation-profile gate, and additive split-idempotent resolved envelope;
- the formal finite atlas assembly theorem;
- explicit profiled stratum passports, normalized subcategories, representation groupoids, and the typed directed transformation category;
- bridge passports, bridge classes, information-loss profiles, overlap categories, bridge-law certificates, and a concrete higher-coherence defect;
- the split-bridge reversible-core theorem, the maximal holonomy-fixed path-flat core, and the exact obstruction-rank formula;
- the relative cokernel, coarsening exact sequence, mapping-cone extension, Hilbert-90 effectivity, Brauer obstruction, and Tannakian boundary in one typed comparison;
- a precise isomorphism-effectivity condition for global invariant completeness;
- two exact finite affine-Mahler atlas models;
- the normalized C-finite recurrence-rational-state atlas with effective object and morphism descent;
- cross-presentation descent of the exact C-finite packet-complexity profile;
- a four-chart atlas spanning linear, digital, and functional-Mahler strata on the unit purely periodic domain;
- complete bridge passports for that atlas, including the directional Cartier compiler lane and its exact loss profile;
- all four triple-overlap laws, the quadruple coherence equation, effective object and morphism descent, and a globally complete compatible invariant package;
- the Frobenius-radical characterization of rational canonical masks and the exact divisor-residue obstruction to rational collapse;
- the canonical finite Cartier module, its reachable-observable minimality theorem, and the exact identification of reachable compiler states with the $p$-kernel;

- effective descent across reduced mask, minimal Cartier-module, and minimal DFAO charts on the full unit rational-mask domain;
- a globally complete rational-mask invariant package and a strict negative control showing that the rational-mask atlas is a proper subatlas of the automatic stratum;
- the canonical section-module, strict shortlex, minimal digit-linear, and word-Hankel normalization theorem for every fixed-radix field-valued regular sequence;
- the automatic finite-orbit theorem over finite fields, including exact state-to-rank bounds and a strict compression corpus;
- the canonical raw and saturated integral section lattices for every integer-valued sequence of finite rational section rank;
- the digit-equivariant Smith–Tor reduction sequence, exact Smith and Fitting formulas, and good-prime criterion;
- finite minimal prime-power semantic section automata with explicit ambient module bounds and compatible reduction maps;
- the $p$-adic and profinite completion sequences, disappearance of finite ghost coordinates, persistence of the missing saturation quotient, and the separate integral and actual-section effectivity obstructions;
- the integral fixed-Euler-basis classification, divisor-ghost integrality locus, exact logarithmic-derivative recurrence, and finite-prefix triangular normalization;
- prime-power effective descent for integral multiplicative arithmetic functions, complete local Euler and ghost coordinates, valuation logarithmic derivatives, and multiplicative residue packets;
- the restricted divisor–ghost product–multiplicative atlas with effective object and morphism descent and a complete prime-power invariant;
- the continuous Newton–Mahler coefficient theorem as a normalized local chart, complete clopen branch analysis and synthesis, and strict nested branch coherence;
- exact affine Mahler coefficient transport, mixed-radix kernel composition, Chinese-remainder diamonds, and the complete branch-coefficient packet equivalence;
- the finite-degree bridge ladder, sharp integral and fixed-modulus packet sizes, explicit integer decoders, and prime-power rank-loss formulas;
- branchwise valuation ledgers, Frobenius sparsification, matrix Carmichael–Mahler state constructors, and principal-unit precision amplification;
- canonical monic minimal differential and tail-recurrence Ore charts, together with the finite transient ledger needed for exact reconstruction;
- the general arithmetic-multisection defect decomposition into orbit aliasing and address cancellation, with singularity-orbit and local-exponent passports;
- the exact hypergeometric packet equation, minimal differential-order phase diagram, orbit rank, and complete marked invariant for the binomial–Fuchsian model family;
- finite selected-branch algebraic normalization, exact residue-packet polynomial systems, the generic $d^N$ packet-degree theorem, and explicit tuple/stabilizer collision signatures;

- the marked polynomial fixed-point atlas across complete packet jets, colored operation trees, and exact packet equations;
- exact repeated-direction packet Faà di Bruno compression by colored integer-partition profiles;
- exact SCC elimination to the address-preserving cyclic nonlinear core;
- the finite arity-gcd tree signature controlling arithmetic packet support and the complete dominant-singularity orbit, together with the full $q$-ary phase theorem;
- the normalized finite subgroup–fixed-field–Reynolds atlas, exact normality and quotient-compression criterion, conjugate nonnormal atlas envelopes, and Mackey double-coset transition packets;
- nested ramification projectors and the weighted unresolved-rank formulas for Artin and Swan conductors;
- effective finite Galois vector descent, the framed Hilbert-90 chart, the exact relative Brauer obstruction, profinite finite-level reconstruction, and the neutral Tannakian tensor-fiber gate;
- an authoritative bridge matrix with named restricted equivalence loci, directional-loss entries, partial constructors, and explicit absent bridges;
- normalizer-induced triple and quadruple coherence for every reversible cycle in the certified finite atlas;
- coherent invariant comparison maps and effective invariant descent on five connected components;
- a complete tagged global invariant on the digital–regular–functional-Mahler, continuous Newton–Mahler, marked Fuss, Euler–multiplicative, and finite Galois semantic union;
- the weighted Fuss–Catalan nonlinear–algebraic–holonomic equivalence and its complete finite parameter invariant.
- the finite profiled Universal Lane Transport Theorem: exact analysis and synthesis, unique transfer blocks, compositional contraction, compatible coarsening, selectors and residuals, profiled realizations, conditional kernel and fold-loss clauses, factorial residue realization, and overlap-compatible descent under an explicit address cocycle.
- the finite holonomy-twisted lane extension: matrix-local-system analysis and synthesis, twisted path contraction, equivariant resolution change, holonomy-compatible selectors and residuals, the finest monodromy-orbit projector coarsening, pair-orbit transport atoms, orbital structure constants, and rational cyclic Fourier-orbit descent.

### D.3 What remains

**Table 50:** General extension obligations after the formal foundations v2.0 milestone.

| ID | Obligation | Current status | Remaining completion criterion |
|---|---|---|---|
| PO-01 | Extend the profile-indexed resolved envelope | proved conditionally | The additive-Karoubi core is proved. Add nonlinear, completion, monoidal, or integral doctrines only for newly selected strata and prove the corresponding profile-indexed universal property. |
| PO-02 | Freeze explicit finite atlases | proved internally | Closed for the unit-periodic, rational-mask, fixed-radix regular, product-multiplicative, continuous local Newton–Mahler, marked binomial–Fuchsian, selected algebraic, marked nonlinear-tree, and finite semisimple Galois atlases, and assembled into the five-component certified Block 13 atlas. Every further enlargement must again declare its semantic domain, chart categories, overlap categories, and component tag. |
| PO-03 | Define morphisms and normalized subcategories | proved internally | Closed for fixed-radix regular sequences, the canonical integral raw/saturated lattice record, fixed-basis Euler products, integral multiplicative functions, and continuous Newton–Mahler functions with complete branch packets. The marked binomial–Fuchsian holonomic chart, selected one-variable algebraic branch chart, marked polynomial fixed-point chart, finite semisimple subgroup chart, framed semilinear vector chart, and neutral Tannakian chart are closed; unrestricted holonomic, multivariate algebraic, unmarked nonlinear, semiring, cross-radix, unrestricted-product, modular, wild, and nonneutral enlargements remain separate passport obligations. |
| PO-04 | Type each bridge | proved internally | Closed for the authoritative Block 13 matrix on the certified domains, including equivalences on named overlaps, fully faithful inclusions, directional losses, constructors, partial bridges, and explicit absent cells. Every extension must retain the same bridge passport and information-loss discipline. |

Continued on next page

| ID | Obligation | Current status | Remaining completion criterion |
|---|---|---|---|
| PO-05 | Prove bridge naturality | proved internally | Closed for digit sections, behavior quotients, Hankel factorization, Smith reduction, Euler logarithmic derivatives, local Dirichlet products, divisor-ghost inversion, Mahler analysis and synthesis, affine polyphase transport, mixed-radix composition, valuation certificates, coefficient/Ore translation, hypergeometric packet synthesis, the marked alias/cancellation ledger, packet-polynomial residue reduction, Weil-restriction degree transport, the algebraic collision ledger, diagonal packet Faà di Bruno profile compression, SCC elimination, marked tree-address transport, subgroup inclusion, Reynolds averaging, normal quotient compression, Hilbert-90 gauge trivialization, and projective Brauer boundary transport on the declared overlaps. |
| PO-06 | Prove higher coherence | proved internally | Closed on every reversible cycle of the five-component certified atlas by the Block 13 normalizer-induced coherence theorem. Unframed vector descent retains intrinsic GL automorphisms, and broader atlases may have nontrivial comparison automorphisms or nonvanishing higher defects. |
| PO-07 | Prove object effectivity | proved internally | Closed for the verified digital, regular, integral, fixed-Euler-basis, multiplicative, divisor-ghost, and continuous Newton–Mahler domains, the marked binomial–Fuchsian domain, the selected algebraic branch domain, the marked nonlinear-system domain, the finite subgroup/projector domain, and framed finite Galois vector descent by explicit normalization from the represented semantic object and retained generator or symmetry data. |

Continued on next page

| ID | Obligation | Current status | Remaining completion criterion |
|---|---|---|---|
| PO-08 | Prove morphism effectivity | proved internally | Closed for the verified atlases because their normalized fibers are contractible or discrete; the complete clopen local packet also glues equality morphisms by explicit piecewise synthesis; the marked holonomic, selected algebraic, and marked nonlinear fibers are discrete; finite Galois vector morphisms descend by fixed points and scalar extension. Unframed symmetry groupoids retain intrinsic automorphisms and require genuine groupoid descent. |
| PO-09 | Construct native comparison maps | proved internally | Closed on the five certified components. Block 13 packages the digital-regular-mask-periodic, continuous Newton–Mahler, marked Fuss, Euler–multiplicative, and finite Galois native coordinates into coherent comparison families. Comparisons for unrestricted broad strata remain separate obligations. |
| PO-10 | Control isomorphism descent | proved internally | Closed for the five-component certified atlas: normalized fibers are discrete or contractible, comparison cells are coherent, and compatible local isomorphisms descend. In broader atlases identify or kill holonomy, cokernel, Brauer, nonneutral tensor, or higher-coherence obstructions. |
| PO-11 | Broaden automatic and regular invariants | proved conditionally | Fixed-radix field normalization, canonical integral saturation, Smith–Fitting reduction profiles, and compatible prime-power semantic towers are closed under the Block 06 hypotheses. Cross-radix comparison, arbitrary coefficient rings and semirings, and effective recognition from finite data remain open. |
| PO-12 | Normalize product and multiplicative strata | proved internally | Closed for the fixed integral Euler basis, integral multiplicative functions, and the multiplicative divisor-ghost overlap. Minimal compilers, unrestricted product grammars, monoidal closure of the overlap, and any global Cauchy-Dirichlet equivalence remain open. |

Continued on next page

| ID | Obligation | Current status | Remaining completion criterion |
|---|---|---|---|
| PO-13 | Broaden local Mahler theory | proved internally | Closed for continuous $\mathbb{Z}_p$-valued functions, canonical Newton–Mahler coefficients, complete clopen and coefficient packets, finite-degree affine channels, sharp standard packet sizes, and principal-unit precision ladders. Exact higher kernel valuations, optimal mixed-radix trees, nonlinear local systems, state recognition, and a combined spectral–local signature remain open. |
| PO-14 | Broaden holonomic packet minimality | proved conditionally | Canonical minimal Ore charts and the marked binomial–Fuchsian packet-order theorem are closed. General minimal multisection operators, canonical desingularization, monodromy-extension data, differential-module cyclicity, and a finite signature beyond the marked family remain open. |
| PO-15 | Broaden algebraic packet minimality | proved internally | Finite selected-branch normalization, exact packet polynomial systems, the generic $d^N$ Weil-restriction bound, and marked collision signatures are closed. Minimal multivariate system dimension, optimal symmetry-reduced degree bounds, ramified Puiseux passports, and universal branch-recognition algorithms remain open. |
| PO-16 | Broaden nonlinear and tree signatures | proved internally | Closed for marked polynomial fixed points, complete packet jets, repeated-direction Faà di Bruno profile compression, address-preserving SCC reduction, and positive simply generated tree support and dominant-orbit signatures. Arbitrary mixed directions, coordinate-free minimum nonlinear system dimension, sign-canceling tree weights, unmarked generators, noncontractive global dynamics, and a universal operadic normal form remain open. |
| PO-17 | Extend modular, wild, and nonneutral symmetry | proved conditionally | Finite semisimple Reynolds charts, framed Hilbert-90 descent, the projective Brauer obstruction, profinite finite-level reconstruction, and neutral Tannakian symmetry are closed. Derived fixed points, integral wild ramification, group-scheme torsion, nonneutral fiber functors, and gerbe-valued descent remain open. |
| PO-18 | Maintain theorem and edition provenance | proved conditionally | Ongoing. Every new claim must cite the selected strongest edition, exact theorem, hypotheses, imported input, and superseded predecessor. |

Continued on next page

| ID | Obligation | Current status | Remaining completion criterion |
|---|---|---|---|
| PO-19 | Separate internal proof from external validation | proved conditionally | Ongoing. Keep direct proof, exact computation, imported classical theorem, conjecture, and independent peer review in distinct status fields. |
| PO-20 | Extend the global invariant beyond the certified spine | proved conditionally | Work Package 6 is closed on the five-component finite atlas. Remaining targets are cross-radix comparison, semiring and all-ring normalization, unrestricted holonomic and multivariate algebraic invariants, unmarked nonlinear systems, modular and wild symmetry, nonneutral tensor descent, and any genuine bridges joining the current component tags. |
| PO-21 | Extend lane transport beyond the finite profiled theorem | proved conditionally | The complete finite split-idempotent calculus and its finite nontrivial-address-holonomy extension are closed under their printed hypotheses. Complete matrices descend as matrix-local-system sections, monodromy orbits give the finest ordinary projector coarsening, and pair orbits govern compatible selectors. Infinite resolutions, non-split decompositions, noninvertible transitions, general nonlinear doctrines, higher-stack effectivity, historical novelty, and unrestricted atlas globalization remain separate obligations. |
| PO-22 | Recognize task quotients effectively | proved conditionally | The fiberwise behavioral quotient and finite-dimensional stabilization theorems are proved. Effective recognition for infinite systems, symbolic query languages, enriched observations, and undecidable continuation grammars remains open. |
| PO-23 | Extend exact semantic loss beyond modules | proved conditionally | The semantic diamond, bridge-loss sequence, and extension law are proved in module categories. Exact, regular, homological, semiring, topological, and higher-categorical analogues require their own quotient and exactness doctrines. |
| PO-24 | Classify carrier and observer comparison maps | proved conditionally | Kernel factorization and the joint semantic completion are closed for algebraic carriers, and the relation module is closed over fields. Classification of lawful changes among noncommutative, measure-valued, completed, probabilistic, and nonlinear carriers remains open. |

Continued on next page

| ID | Obligation | Current status | Remaining completion criterion |
|---|---|---|---|
| PO-25 | Control admissibility and attainment | proved conditionally | Admissibility monotonicity and the completion/gap/escape trichotomy are proved. Effective optimal-geometry construction, attainment criteria, and conditioning rates remain doctrine-specific. |
| PO-26 | Build doctrine-level coherence only from certified cells | framework only | The doctrine-indexed task-fiber architecture is stated and several concrete lifting gates are proved. A complete double category, bicategory, or higher stack of doctrines is not yet constructed and must not be inferred from the fiberwise theorems. |

### D.4 Finite completion criterion

A rigorous first heterogeneous stratified-universality theorem should be declared complete only after the following finite milestone is met:

1. a profile-indexed envelope is constructed for every profile used by the selected atlas;
2. at least two genuinely different normalized strata are fully specified as categories;
3. every overlap bridge is typed and its information loss is stated;
4. every nonempty triple-overlap coherence equation is proved;
5. descent for objects and morphisms is effective;
6. one nontrivial native invariant family has coherent comparison maps and a proved global completeness theorem on the normalized descent category;
7. the theorem concordance and source-edition ledger are synchronized with the final manuscript.

The C-finite theorem completes a three-chart presentation atlas within one stratum. Theorems 9.10 and 9.12 meet all seven items for a restricted atlas spanning three strata. Theorems 10.11 and 10.12 enlarge the digital and functional-Mahler overlap from unit pure periodicity to every unit series with rational canonical mask. Theorems 11.6, 11.10 and 11.11 close fixed-base field-valued regular normalization. Theorems 12.3, 12.7 and 12.25 close the canonical integral saturation and prime-power reduction package for integer-valued sequences already known to have finite rational section rank. Theorems 13.4, 13.15, 13.23 and 13.24 now close fixed-basis product normalization, multiplicative prime-power normalization, and one explicit cross-stratum invariant overlap. Theorems 14.1, 14.3, 14.7, 14.9 and 14.13 now close the continuous Newton–Mahler chart, complete local polyphase descent, finite-degree collective recovery, and the principal-unit precision ladder. Theorems 15.8, 15.9, 15.12, 15.15 and 15.20 now close canonical Ore normalization, the general two-stage multisection defect ledger, and one exact marked regular-singular model case. Theorems 16.4 to 16.6 closes the selected one-variable algebraic chart. Theorems 17.4, 17.5, 17.9, 17.11, 17.13 and 17.15 now close the marked polynomial-system atlas, diagonal composition compression, address-preserving cyclic-core reduction, and one finite tree-signature family. Theorems 18.2, 18.12, 18.15 and 18.20 close the finite semisimple subgroup atlas, effective linear semilinear descent, exact projective obstruction, and the neutral tensor reconstruction gate. Theorems 19.2, 19.4,

19.7 and 19.11 now complete the finite global-invariant milestone: five certified connected components, coherent comparison maps, effective componentwise descent, and a complete tagged invariant on the declared semantic coproduct. The remaining program is therefore a cross-radix, semiring, modular and wild symmetry, nonneutral tensor, unrestricted holonomic, multivariate algebraic, general nonlinear, stronger local-valuation, optimal mixed-radix, and unrestricted product-grammar compatibility problem rather than a missing elementary Mahler-coordinate, Ore-normalization, rooted-tree expansion, finite Galois descent, or finite certified invariant-descent theorem.

Block 15 closes the common complete finite-resolution lane calculus under its printed hypotheses. Block 16 removes trivial address holonomy as a requirement for transport itself: complete coordinates descend as matrix-local-system sections and ordinary object lanes descend at monodromy-orbit resolution. Infinite or nonsplit lane doctrines, noninvertible transition theories, higher-stack effectivity, historical novelty review, and globalization over the unrestricted heterogeneous atlas remain open. The remaining mathematical program still includes cross-radix and semiring compatibility, modular and wild symmetry, nonneutral tensor descent, unrestricted holonomic and multivariate algebraic normalization, general nonlinear transport, stronger local valuations, optimal mixed-radix refinement, and unrestricted product grammars.

# E Detailed claim-boundary ledger

## E.1 Claims supported at manuscript level

The following statements are now supportable under the printed hypotheses:

- Komorebi Math has a substantial common resolved syntax and many proved local realization theories.
- The finite additive-Karoubi resolved envelope exists and has the stated universal property.
- Invertible representation changes and noninvertible transformations can be separated formally through representation groupoids, bridge passports, and a typed directed category.
- Information loss can be recorded separately as morphism collapse, object collapse, essential-image restriction, and loss of declared constructors or certificates.
- A finite profiled atlas has a descent, theorem-transport, and invariant-assembly theorem once its hypotheses are verified.
- Exact finite atlas models exist for graph holonomy, semilinear Galois descent, affine Mahler chart composition, split Mahler packet cores, and the normalized C-finite recurrence-rational-state triangle.
- Finite graph transport has a unique maximal path-flat core, while full frame trivialization is equivalent to identity fundamental holonomy.
- A canonical obstruction object exists relative to declared correction data; coarse vanishing can erase a nonzero fine obstruction.
- Under the stated classical hypotheses, Hilbert 90 gives effective vector descent and the Brauer class is the exact projective-to-linear lifting obstruction.
- Restricted complete invariants exist in several strata. The persistent C-finite slice has a complete global-to-packet minimality transfer theorem.
- The unit purely periodic atlas over $\mathbb{F}_p$ is a verified heterogeneous atlas across linear, digital, and functional-Mahler strata. Its objects and morphisms descend effectively, and its periodic resolved invariant package is complete on the declared normalized semantic category.
- The unit rational-mask atlas over $\mathbb{F}_p$ is a verified heterogeneous atlas across reduced functional-Mahler masks, minimal Cartier modules, and minimal digital automata. Its exact collapse obstruction separates the ultimately periodic locus from the genuinely non-C-finite automatic locus, and its descended invariant package is complete on the declared semantic category.
- For a fixed radix and field, every regular sequence has a canonical minimal section module, a strict shortlex coordinate record, and a word-Hankel rank certificate. These charts satisfy effective descent, and the pointed section module is complete on the declared regular category.
- Over a finite field, regularity is equivalent to automaticity and the minimal automaton is the finite section orbit. Over characteristic-zero fields, finite regular rank can coexist with an infinite kernel orbit.
- Every integer-valued fixed-radix sequence of finite rational section rank has a canonical finite free raw section lattice and a canonical finite free integer-valued saturation of the same rank.

- The Smith invariants and Fitting ideals of the finite saturation quotient determine the ghost kernel, semantic image size, missing quotient, good moduli, and prime-power generator profile exactly.
- Every prime-power coefficient reduction has a finite minimal semantic section automaton, and the compatible full module tower reconstructs the embedded $p$-adic raw lattice.
- $p$-adic completion, profinite completion, ordinary integral lifting, and actual section realization are distinct effectivity levels with explicit obstruction quotients.
- Every integral unit series has unique fixed Euler exponents and unique divisor ghosts, with exact Möbius integrality conditions and coefficient recurrence.
- Every integral multiplicative arithmetic function is reconstructed exactly from prime-power local series, and local Euler exponents and ghosts form complete additive coordinates for Dirichlet convolution.
- On the multiplicative exponent locus, the divisor–ghost transform gives an effective four-chart atlas and a complete prime-power descended invariant.
- Continuous $\mathbb{Z}_p$-valued functions, their canonical Mahler coefficients, complete clopen branch packets, and branchwise Mahler coefficients form an effective normalized local atlas.
- Affine Mahler kernels have finite triangular support, compose by exact mixed-radix substitution, and satisfy strict Chinese-remainder coherence.
- Finite-degree affine channels have distinct characteristic-zero, integral, modular, and collective-packet bridge passports, with sharp minimal packet sizes under the printed hypotheses.
- Declared monotone Mahler valuation profiles survive affine polyphase refinement, and principal-unit state packets acquire a certified linearly improving precision slope under $p$-power refinement.
- Every nonzero D-finite series and non-eventually-zero P-recursive sequence over a characteristic-zero field has a canonical monic minimal Ore annihilator; a finite transient ledger upgrades the tail operator to an exact semantic chart.
- Arithmetic multisection preserves holonomicity, and every fixed closure pipeline has an exact excess-order certificate relative to the unique minimal packet operator.
- In the marked binomial–Fuchsian family, nonintegral exponent gives minimal packet differential order $N$, positive integral exponent gives rational order one, and nonpositive integral exponent gives the exact finite-support alias/cancellation phase diagram.
- For a finite Galois extension in the semisimple setting, subgroups, fixed fields, and faithful Reynolds projectors form an order-reversing normalized atlas.
- Nonnormal intermediate fields form conjugate projector atlases with canonical core and normal-closure envelopes, while Mackey double cosets give exact induction–restriction transition packets.
- Ramification groups form a nested projector resolution, and the Artin and Swan conductors are weighted unresolved-rank sums.
- Finite Galois vector descent is effective on objects and morphisms; projective descent lifts to an ordinary vector packet exactly when its relative Brauer class vanishes.
- Every continuous finite-dimensional complex representation of a profinite group factors through a finite quotient, and shrinking open normal-subgroup projectors converge strongly to the identity.

- A faithful exact tensor fiber functor reconstructs an affine group scheme by neutral Tannakian duality; faithful corner realization alone does not cross this tensor boundary.
- The certified global-synthesis bridge matrix distinguishes reversible named overlaps from fully faithful inclusions, directional loss, partial constructors, and absent bridges.
- On the five declared connected components, local complete invariants have coherent comparison maps and descend to a complete tagged invariant that reflects isomorphisms.
- The marked weighted Fuss family gives a genuine reversible overlap among tree, selected algebraic, and P-recursive presentations, classified by the finite pair $(q, \alpha)$.
- At every declared complete finite resolution in an additive idempotent-complete category, analysis and synthesis are inverse, morphisms have unique lane-transfer matrices, composition is block contraction, and compatible refinement aggregates those matrices functorially.
- Finite lane selectors split retained transport from an exact residual. Under the separately printed abelian or strict-fold hypotheses, the discarded or collided part is measured by the corresponding kernel-exact sequence.
- Factorial residue lanes realize the formal theorem exactly, and the stated polyphase, Cartier, holonomic, local, nonlinear-tree, algebraic, and Galois cases are valid only with their declared native hypotheses.
- Finite nontrivial address holonomy does not obstruct complete lane transport when the address and splitting cocycles remain coherent: lane matrices descend as compatible sections of a matrix local system, and composition remains exact path contraction.
- Monodromy-orbit sums are the finest ordinary globally labeled coarsening obtainable from the original object-lane projectors, while simultaneous source-target pair orbits are the minimal nonempty holonomy-compatible Boolean transport supports; their selectors are nonzero only on orbits supporting nonzero compatible sections.
- For finite permutation modules, pair-orbit indicator matrices form an exact intertwiner basis with nonnegative integer path-count structure constants. For cyclic Fourier idempotents, rational Galois orbit sums are indexed by divisors and have exact Ramanujan-sum coefficients.

### E.2 Claims not established

The following statements are not proved here:

- every mathematical object has a finite Komorebi presentation;
- all strata are equivalent categories;
- every bridge is invertible;
- one global canonical minimal presentation exists across arbitrary grammars;
- one finite invariant classifies every stratum;
- equivalence of arbitrary presentations is decidable;
- the full eight-stratum heterogeneous atlas already satisfies effective descent, or the five certified global-synthesis components are reversibly connected to one another;

- every automatic sequence has a rational functional-Mahler mask, or functional Mahler equations and Newton-Mahler interpolation are unrestrictedly equivalent;
- one base-independent or all-ring canonical regular normal form, one minimal semiring realization theorem, or one cross-radix invariant compatible with every base;
- the integral lattice theorem automatically extends to arbitrary coefficient rings, non-Noetherian modules, semirings, all radices at once, or finite-data recognition of rational regularity;
- unique Euler coordinates imply finite structural complexity, a minimal product compiler, or a canonical factorization across arbitrary product grammars;
- ordinary Cauchy convolution and Dirichlet convolution are globally isomorphic, or prime-power seeds classify arithmetic functions without the multiplicativity axiom;
- the multiplicative Euler-exponent locus is closed under ordinary Euler-product multiplication;
- functional-Mahler coefficient equations and Newton–Mahler $p$-adic interpolation are canonically or unrestrictedly equivalent;
- every continuous $p$-adic function is locally analytic, every affine-kernel valuation lower bound is always sharp, or one optimal mixed-radix refinement tree has been constructed;
- the local atlas already carries a complete combined spectral–local invariant or a universal state-recognition theorem;
- arbitrary D-finite multisections have a proved finite torsion signature, a closed minimal-order formula, or a canonical apparent-singularity removal algorithm;
- local exponent eigenvalues alone determine the full monodromy representation, logarithmic extension data, or global differential Galois group;
- the marked binomial–Fuchsian invariant classifies unmarked holonomic series or recovers an algebraic branch from an annihilator;
- the $d^N$ algebraic packet bound is always minimal, or every resultant automatically selects the intended branch factor;
- selected algebraic branches admit one canonical minimal multivariate system dimension across arbitrary polynomial grammars;
- algebraic and D-finite presentations are equivalent without retained branch data;
- Reynolds averaging remains exact when the group order is not invertible, or finite semisimple Galois charts automatically extend to modular and wild integral representations;
- every projective cocycle descends to a vector space, or the Brauer class alone classifies the full central simple algebra without its remaining algebra data;
- every tensor category has a neutral fiber functor, or a faithful additive or corner representation automatically reconstructs a Tannakian group scheme;
- finite Galois effectivity proves effective descent for the unrestricted heterogeneous Komorebi atlas;
- internal manuscript proof status implies independent peer review;
- the name Universal Lane Transport establishes historical priority or novelty for classical residue filters, polyphase decompositions, Peirce block matrices, Cartier sections, or other imported ingredients;

- every object admits a complete finite split lane system, every useful resolution is additive, or the finite theorem and its finite holonomy-twisted extension automatically extend to infinite, completed, nonsplit, noninvertible, higher-stack, or arbitrary nonlinear settings;
- the number of lane addresses equals dimension, rank, minimal state size, entropy, independent information, or computational complexity without a separate theorem;
- an incomplete selector or noninjective fold is reversible, or its residual and collision kernel can be discarded without changing the represented transport.

**Final status of the present paper.** The project now has an explicit typed and packet-resolved common foundation, a proved additive-Karoubi envelope, profiled stratum and bridge passports, a directed information-loss calculus, a typed comparison of four obstruction theories, a proved finite assembly theorem, two exact affine-Mahler mechanisms, one fully effective normalized C-finite presentation atlas, and two fully effective heterogeneous digital/Mahler atlases. The fixed-radix regular stage adds the full fixed-radix field-valued regular atlas, a canonical word-Hankel and short-lex normal form, and the automatic finite-orbit theorem. The integral prime-power stage adds the canonical integral raw/saturated lattice pair, the exact Smith–Fitting reduction defect, finite prime-power semantic automata, and the $p$-adic/profinite effectivity hierarchy. The product-multiplicative stage adds canonical fixed-basis Euler and ghost coordinates, prime-power effective descent for multiplicative functions, and the complete restricted divisor–ghost atlas. The local Mahler-polyphase stage adds the normalized continuous Newton–Mahler atlas, strict complete polyphase descent, sharp finite-degree channel packets, valuation-profile transport, and principal-unit precision amplification. The holonomic stage adds canonical minimal Ore charts with finite transients, the general multisection alias/cancellation ledger, and an exact marked binomial–Fuchsian packet-minimality theorem. The algebraic stage adds finite selected-branch normalization, exact packet polynomial systems, a generic $d^N$ packet-degree theorem, and collision signatures with sharp Catalan and radical model cases. The nonlinear tree stage adds a marked polynomial fixed-point atlas, exact diagonal packet Faà di Bruno compression, an address-preserving cyclic-core dimension, and finite simply-generated-tree support and singularity signatures. The Galois-Tannakian stage adds the normalized finite subgroup–fixed-field–projector atlas, conjugate and Mackey transition packets, ramification details, effective Hilbert-90 descent, the exact relative Brauer obstruction, profinite finite-level resolution, and the neutral Tannakian tensor-fiber gate. The global synthesis stage adds the authoritative bridge matrix, normalizer-induced higher coherence, a five-component certified invariant atlas, the marked Fuss nonlinear–algebraic–holonomic triangle, and a complete tagged global invariant on the declared semantic union. The finite lane-transport stage adds the complete finite-resolution analysis, synthesis, block-composition, refinement, selector, residual, conditional fold-loss, factorial-realization, and certified-descent theorem family. The holonomy-twisted stage then removes global address triviality as a transport requirement, replacing fixed labels by matrix-local-system sections and recovering canonical ordinary lanes at monodromy-orbit resolution, with pair-orbit composition and rational cyclic orbit descent as exact realizations. The broad heterogeneous claim remains conditional on cross-radix and semiring compatibility, modular and wild symmetry, nonneutral tensor descent, unrestricted holonomic and multivariate algebraic normalization, general nonlinear normal forms and mixed-direction compression, stronger local valuation and optimal mixed-radix theory, unrestricted product grammars, and effective invariant comparison beyond the normalized domains proved here.

# F Validation record

The validation summarized below concerns internal package integrity and exact finite verification. It is not an external authenticity or peer-review certificate. The thematic verifiers record 39,805 checks for the unit-periodic atlas, 11,391 for rational masks, 89,055 for fixed-radix regular systems, 697,958 for integral saturation and prime-power towers, 595,964 for Euler-product and multiplicative coordinates, 229,743 for local Newton–Mahler and polyphase transport, 174,940 for holonomic packets, 73,088 for selected algebraic packets, 115,721 for nonlinear tree systems, and 11,195 for finite Galois and tensor models. The two global-synthesis suites execute 154,209 bridge assertions and 119,453 weighted Fuss and tagged-invariant assertions. They include 39,846 authenticated replay assertions already counted in the preceding records and contribute 233,816 new comparison, coherence, packet, and loss-control assertions. The nonduplicated cumulative record is 2,272,676 exact assertions with no failures; the raw executed total, including replay, is 2,312,522. The Block 15 verifier separately executes 197,099 exact finite regression assertions for selected lane-analysis, block-composition, refinement, fold, support, and factorial implementation clauses. The Block 16 verifier executes 1,344,823 exact assertions for finite group actions, object and pair orbits, orbital structure constants, compatible and incompatible selectors, equivariant refinement, rational cyclotomic orbit projectors, and theorem-source contracts, with 0 recorded failures. Detailed tables and machine-readable JSON records are included in the source package. The Part IV semantic-diamond audit additionally executes exact rational linear-algebra trials for quotient dimensions, factorization, relative residuals, and compatibility sequences. Its role is implementation validation; the universal statements are proved in the text.

**Table 51:** Internal validation record for Core-Transfer Addendum 04.

| Check | Recorded result |
|---|---|
| Package verifier | Overall pass: true; 383 ledger entries; 0 missing; 0 extra; 0 mismatched. |
| Exact theorem verifier | 48 of 48 gates passed; arithmetic used exact integers/fractions, finite-field elimination, integer/composite-modulus split decoding. |
| Full unit-test attempt | The full test script did not finish within two bounded runs (120 seconds and 600 seconds). The completed tests were passing when the second run timed out. No claim of a full-suite pass is made here. |
| Boundary | Internal consistency and exact finite verification only; no external authenticity or peer-review claim. |

**Table 52:** Exact finite and symbolic audit for the Part IV semantic quotient extension.

| Audit family | Assertions |
|---|---|
| Semantic diamond dimension | 1,000 |
| Relative residual dimension | 1,000 |
| Carrier factorization gate | 1,000 |
| Quadratic/convex symbolic identity | 1 |
| Polyphase Hankel determinants | 8 |
| Theorem-source contracts | 13 |
| **Total** | **3,022** |
| Recorded failures | 0 |

A legacy all-project unit-test script was attempted twice during an earlier consolidation stage, including a 600-second bounded run. The completed tests were passing when the second run timed out, but that

historical script did not finish within the bound. This statement does not qualify or replace the named thematic and Block 15 verifier records. No pass is claimed for that separate legacy all-project invocation.

## References


[1] Komorebi P., *Projector-Resolved Seed Calculus I: Typed Operator Systems, Seed Rank, and Exact Packet Coordinates*, Complete Symbolic Core Edition and Expanded Clarified Edition, 2026.

[2] Komorebi P., *Resolution Theory: Projector Corner Representations, Refinement Naturality, and Nonlinear Transfer*, final journal manuscript, 2026.

[3] Komorebi P., *Nonlinear Packet Calculus, Obstruction Complexes, and Holonomy*, strengthened Annals edition, 2026.

[4] Komorebi P., *Paper III Migration and Expansion Map*, 2026.

[5] Komorebi P., *Affine Mahler Packets and Periodic Test Sets: Core-Transfer Theorem Addendum 04*, 2026.

[6] Komorebi P., *Resolution Theory: Projector Geometry, Galois Descent, and Multiscale Realizations*, expanded journal manuscript, 2026.

[7] Komorebi P., *Projector-Seed Calculus for Integer Sequences: A Unified Realization Theory with Spectral, Local, Adelic, and Polyphase Transfer*, 2026.

[8] Komorebi P., *Custom Generating Functions III: Cartier Automata, Prime-Power Unit Kernels, Mixed-Radix q-Carries, and Cyclotomic Collapse*, research report 0.3, 2026.

[9] Komorebi P., *Nonlinear Transfer Operads and Projector-Resolved Jet Calculus*, 2026.

[10] Komorebi P., *Abstraction as a Resolved Practice: Mathematical Objects, Imagination, Bridges, and Human Reachability*, 2026.

[11] O. Ore, "Theory of non-commutative polynomials," *Annals of Mathematics* **34** (1933), 480–508.

[12] R. P. Stanley, "Differentiably finite power series," *European Journal of Combinatorics* **1** (1980), 175–188.

[13] F. Beukers and G. Heckman, "Monodromy for the hypergeometric function ${}_nF_{n-1}$," *Inventiones Mathematicae* **95** (1989), 325–354.

[14] K. Mahler, "An interpolation series for continuous functions of a $p$-adic variable," *Journal für die reine und angewandte Mathematik* **199** (1958), 23–34.

[15] P. Flajolet and R. Sedgewick, *Analytic Combinatorics*, Cambridge University Press, 2009.

[16] J.-P. Serre, *Local Fields*, Springer, 1979.

[17] J.-P. Serre, *Galois Cohomology*, Springer, 1997.

[18] P. Deligne and J. S. Milne, "Tannakian Categories," in *Hodge Cycles, Motives, and Shimura Varieties*, Lecture Notes in Mathematics 900, Springer, 1982.

[19] A. Nerode, "Linear automaton transformations," *Proceedings of the American Mathematical Society* **9** (1958), 541–544.

[20] J. W. Carlyle and A. Paz, "Realizations by stochastic finite automata," *Journal of Computer and System Sciences* **5** (1971), 26–40.

[21] T. Li, G. Rabusseau, and D. Precup, “Nonlinear weighted finite automata,” in *Proceedings of AISTATS 2018*, PMLR 84, 679–688, 2018.

[22] G. L. Litvinov, “The Maslov dequantization, idempotent and tropical mathematics: a brief introduction,” *Journal of Mathematical Sciences* **140** (2007), 426–444.

[23] F. John, “Extremum problems with inequalities as subsidiary conditions,” in *Studies and Essays Presented to R. Courant on His 60th Birthday*, Interscience, 1948, 187–204.

[24] T. Ando and M.-H. Shih, “Simultaneous contractibility,” *SIAM Journal on Matrix Analysis and Applications* **19** (1998), 487–498.

[25] R. Schneider, *Convex Bodies: The Brunn–Minkowski Theory*, second edition, Cambridge University Press, 2014.

[26] Komorebi P., *Projector Calculus: Resolution, Coordinate Atlases, Packet Arithmetic, Transfer Algebra, Residual Decomposition, and Infinite Completion*, final current edition, 2026.